# $CD4^+$ T Cell Mechanisms of Cross-Protective Rhinovirus Immunity and Rhinovirus-Induced Allergic Asthma

Lyndsey Marie Muehling
Lincoln, Nebraska

Master of Science, University of Virginia School of Medicine, 2014
Bachelor of Science, University of Nebraska-Lincoln, 2012

A Dissertation presented to the Graduate Faculty
of the University of Virginia in Candidacy for the Degree of
Doctor of Philosophy

Department of Microbiology, Immunology, and Cancer Biology

University of Virginia
October, 2018

## Abstract

Human rhinovirus (RV) is the major cause of the common cold, and poses a significant public health burden. RV infection also triggers acute wheezing episodes in patients with allergic asthma that often result in hospitalization. Despite this, there are no effective treatments or vaccines for RV infection. Little is known about $CD4^+$ T cell responses induced by RV or the T cell mechanisms underlying virus-induced asthma. The overarching objective of this thesis is to define the nature of $CD4^+$ T cell responses to RV in health and allergic asthma by precisely tracking T cells in a human experimental RV infection model using novel peptide/MHCII tetramers. The data show that circulating RV-specific $CD4^+$ T cells in healthy uninfected subjects recognize immunodominant epitopes of RV capsid proteins that are conserved across multiple RV strains. These cells bear an activated $T_H1$ effector memory signature, express CCR5, and respond rapidly to infection, consistent with cross-strain immunosurveillance. Moreover, increased numbers of RV-specific T cells prior to infection are linked to decreased infection rates. By contrast, higher numbers of circulating RV-specific $T_H1$ cells relate to worse lung function in uninfected allergic asthmatics. During infection, RV triggers an augmented RV-specific $T_H1$ response, along with other hallmark components of a type 1 response in the blood and airways. These findings challenge the prevailing views of deficient anti-viral responses in RV-induced asthma. We conclude that, although RV-specific $T_H1$ responses control infection in health, unconstrained $T_H1$ responses are linked to asthma pathogenesis despite underlying type 2 inflammation, even in the absence of infection. The findings support a model wherein repeated viral exposures increase the inflammatory set point in allergic asthma via $T_H1$-mediated processes.

## Acknowledgments

First, thank you to my mentor, Dr. Judith Woodfolk. Your patient guidance, knowledge, and advice have shaped me as a scientist, and I am so grateful for the many opportunities that you have offered me. Thank you to my co-mentor Dr. Engelhard and committee members Dr. Hahn, Dr. Braciale, and Dr. Erickson. Thank you to the members of the Woodfolk lab past and present—Rachana, Paul, Jake, Liesbeth, Marcia, Julia, Erin, & Marty—for your help and support, and our many wonderful undergrads and summer students. I am grateful to our many colleagues and collaborators at UVA and in the Allergy Division: Dr. Heymann, Dr. Platts-Mills, and Dr. Turner, for guidance, mentorship, and collaboration; Deb and Holly, who made the asthma trials possible; Lisa and Alex, for many IgE assays; and Cheree and Terri, for help acquiring specimens; and Dr. Ratcliffe, Dr. Conway, and Jim Patrie for assistance with statistical analyses. I am grateful for our amazing flow core facility led Joanne Lannigan, and to Brian, Mike, Claude, Alex, and Lesa for so much help over the years. Thank you to our collaborators at other institutions: Dr. Kwok and Duy at Benaroya Research Institute, and Dr. Irish and Cara at Vanderbilt.

Thank you to my Virginia friends, for bringing me out of the lab, blowing off steam, and connecting me to the community. Special thanks to my dearest friends from Lincoln (and beyond), who have brightened my days since as far back as elementary and middle school. My deepest gratitude is for my family: my parents, Brad and Linda, my sister Ellen, brother Justin, and brother-in-law Kenny, for unconditional love and belief, lighthearted diversions, and tireless care and sacrifice. Thank you to my grandparents, Judy Schutz and Nancy & Eldon Muehling, for your love, care, and constant support, and to my aunt, Dr. Amy Geschwender, for inspiration and encouragement. There aren't words to express how much you all mean to me.

———————

*Dedicated to the late Dr. Wilfred M. Schutz.*

## List of Abbreviations

| | |
|---|---|
| aa | Amino acid |
| ACT | Asthma Control Test |
| ANOVA | Analysis of variance |
| CBC | Complete blood count |
| CDHR3 | Cadherin-related family member 3 |
| CI | Confidence interval |
| CL | Confidence level |
| Comblib | Combinatorial peptide libraries |
| COPD | Chronic obstructive pulmonary disease |
| DC | Dendritic cell |
| DBPC | Double-blind placebo-controlled |
| ECP | Eosinophil cationic protein |
| ELISA | Enzyme-linked immunosorbent assay |
| $FEF_{25-75}$ | Forced expiratory flow between 25% and 75% of vital capacity |
| $F_{ENO}$ | Fractional exhaled nitric oxide |
| $FEV_1$ | Forced expiratory volume in one second |
| FMO | Fluorescence-minus-one |
| FVC | Forced vital capacity |
| GEE | Generalized estimating equations |
| GLM | Generalized linear models |
| GM | Geometric mean |
| HDAC | Histone deacetylase |
| HLA | Human leukocyte antigen |
| ICAM-1 | Intercellular adhesion molecule-1 |
| IDO | Indoleamine 2,3-dioxygenase |
| IEDB | Immune Epitope Database |
| IFN | Interferon |
| Ig | Immunoglobulin |
| IL | Interleukin |
| ILC | Innate lymphoid cell |

| | |
|---|---|
| IU | International units |
| KLF4 | Kruppel-like factor 4 |
| $LTC_4$ | Leukotriene $C_4$ |
| LDLR | Low-density lipoprotein receptor |
| MAML1 | Mastermind-like protein 1 |
| mDC | Myeloid dendritic cell |
| MFI | Mean fluorescence intensity |
| NA | Not applicable |
| NAT | Neutralizing antibody titers |
| n.d. | Not determined |
| NO | Nitric oxide |
| ns | Not significant |
| PBMC | Peripheral blood mononuclear cell |
| PBS | Phosphate buffered saline |
| $PC_{20}$ | Provocative concentration causing a 20% drop in $FEV_1$ |
| PCR | Polymerase chain reaction |
| pDC | Plasmacytoid dendritic cell |
| $peT_H2$ | Pathogenic effector $T_H2$ |
| $PGD_2$ | Prostaglandin $D_2$ |
| pMHCII | Peptide/MHC class II |
| POL | Polymerase |
| PRO | Protease |
| PRR | Pattern recognition receptor |
| RBPJ | Recombination signal binding protein for immunoglobulin kappa J region |
| RSV | Respiratory syncytial virus |
| RV | Rhinovirus |
| SD | Standard deviation |
| SEM | Standard error measurement |
| Sox4 | Sry-related high-mobility-group box 4 |
| TCF-1 | T cell factor 1 |
| $T_{CM}$ | T central memory |

| | |
|---|---|
| $T_{EM}$ | T effector memory |
| $T_{FH}$ | T follicular helper |
| TGEM | Tetramer-guided epitope mapping |
| $T_H$ | T helper |
| TJ | Tight junction |
| TLR | Toll-like receptor |
| TSLP | Thymic stromal lymphopoietin |
| t-SNE | t-distributed stochastic neighbor embedding |
| UTR | Untranslated region |
| VCAM-1 | Vascular cell adhesion molecule 1 |
| WBC | White blood cell |

# Table of Contents

## List of Figures

## List of Tables

# Chapter 1 — Introduction

Human rhinovirus (RV) plays a key role in both the common cold and allergic asthma. It is one of the leading causes of upper respiratory tract infections, and is known to trigger severe allergic asthma exacerbations. Little is known about the cellular immune response to RV, and RV-specific $CD4^+$ T cells are poorly characterized. Furthermore, the immune mechanisms of RV-induced allergic asthma have not been defined. In this chapter, we will provide an overview of rhinovirus infection, including viral structure, immune responses, and previous attempts at vaccine and drug development. Next, we will review allergic asthma and type 2 responses, before finally discussing the role of viruses in the inception and exacerbation of allergic asthma, including discussion of the proposed link to Immunoglobulin (Ig) E and the current theories about immune mechanisms of RV-induced asthma.

## Rhinovirus

Human rhinovirus is a common virus that is the major cause of the common cold. The common cold poses a significant health burden, resulting in 84 million ambulatory care visits in the United States each year, 20 million missed workdays, 22 million missed school days, and costing approximately $40 billion annually [1,2]. Multiple RV infections are contracted each year. Children experience 6-8 cases on average, with adults experiencing only 2-4 cases annually [3]. Typically, RV-induced mortality is not high in the general population, but increased morbidity and mortality has been reported among the elderly and those with chronic respiratory diseases such as asthma, chronic obstructive pulmonary disease (COPD), and cystic fibrosis [4–10].

Symptomatic rhinovirus infections are typically accompanied by rhinorrhea, nasal congestion, sore throat, headache, and malaise; however, many cases remain subclinical, including approximately 15-35% of cases in children [11–13]. Symptoms typically last for 7-14 days, but often persist for longer periods of time in those with chronic respiratory diseases [14,15]. The incidence of RV infections peak in the early fall and to a lesser extent in the spring, although the virus circulates year-round [16–18]. Rhinovirus is transmitted through shedding in nasal secretions by aerosolization and direct contact—especially to nasal and conjunctival mucosa—and can be recovered from finger pads after 1-2 hours of normal hand use, and from indoor surfaces for upwards of 3 hours [19,20]. Despite the ubiquitous nature and ready transmission of RV infection, there are no effective therapeutics or vaccines currently available.

### *Viral Structure and Classification*

Human rhinovirus is a picornavirus of the genus *Enterovirus*. Well over 150 serotypes of RV have been identified to date, and are classified into A-, B-, and C-species based on serology, sensitivity to antiviral compounds, and genome sequence [21–25]. Group C rhinoviruses, which cannot be cultured using conventional methods, were only recently described in 2009, following the development of MassTag PCR [26]. The majority of rhinovirus strains (~90% of RV-A and –B strains), often referred to as major group viruses, bind to intercellular adhesion molecule-1 (ICAM-1) as their cellular receptor [27–29]. Minor group RV-A and –B strains bind instead to the low-density lipoprotein receptor (LDLR)[28]. The cellular receptor for RV-C strains was recently reported to be cadherin-related family member 3 (CDHR3)—a transmembrane protein with an as-yet-undefined function [30]. In keeping with this, a coding SNP that increases cell-surface expression of CDHR3 was

previously identified within the asthma susceptibility locus chromosome 17q21, pointing to a potential link between RV-C infection and asthma exacerbation [30,31].

Human rhinovirus primarily infects epithelial cells of the nose and pharynx, and infection of bronchial epithelial cells has also been described [32–34]. In addition, RV binds to and enters other cell types, including monocytes, macrophages, eosinophils, and B- and T-lymphocytes; however, there is contradictory or incomplete evidence as to whether RV can replicate within these cell types [35–39]. Upon engagement with its cellular receptor, RV enters the host cell via endosomes and un-coats as the pH drops [14]. Viral RNA then exits the endosome to be translated by host ribosomes into a single polypeptide, which is cleaved into 11 proteins by virally-encoded proteases [14]. As a part of this process, the viral capsid polyprotein is cleaved into four individual proteins (VP1-4), which form protomers and assemble into an icosahedral capsid [14]. The virions are then released through cell lysis. Despite this, RV infection does not cause significant cytopathic effects due to the "patchy" pattern of epithelial cell infection [32,40].

Three of the RV capsid proteins are exposed on the capsid surface (VP1-3). The remaining capsid protein, VP4, is located on the interior of the capsid in close association with the viral genome (**Figure 1-1**)[14]. Of the capsid proteins, VP1 is the most surface-exposed, has high antigenic variability, and is a major target of antibody responses [41–43]. A "canyon" surrounding the vertices of the capsid contains the binding site for the major group receptor ICAM-1 [44]. The base of the canyon contains a hydrophobic binding pocket that is constitutively occupied, and displacement of the pocket factor by anti-viral compounds disrupts the capacity to infect host cells (**Figure 1-1**)[44]. As such, a number of these compounds have been explored as therapies for rhinovirus.

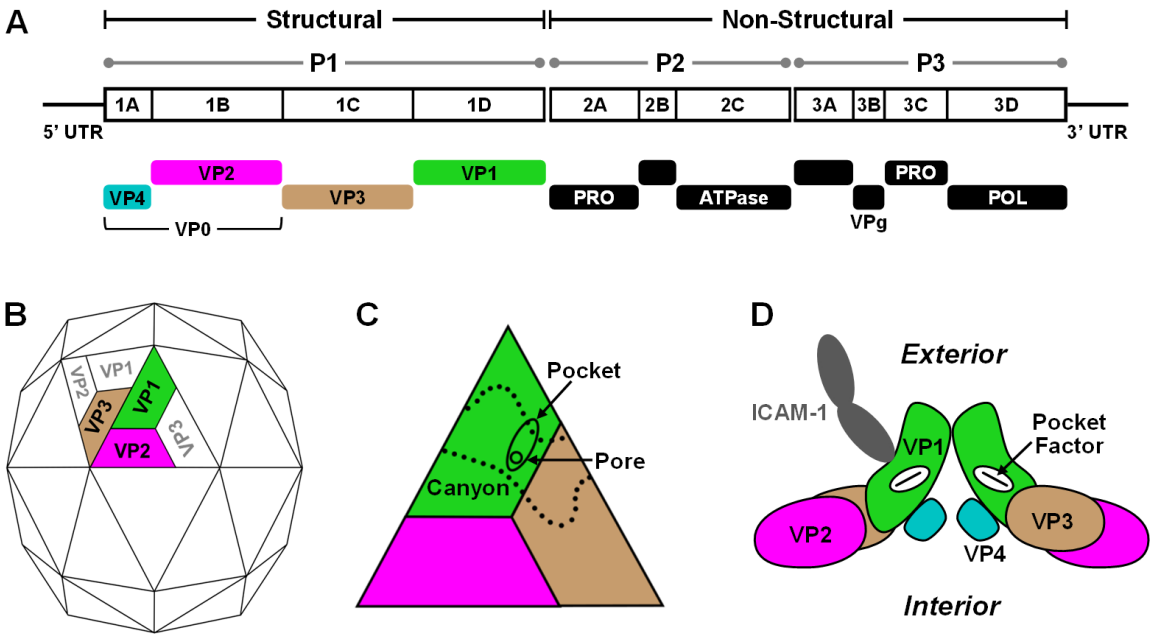


**Figure 1-1. Rhinovirus Polyprotein and Capsid Structure**

**(A)** Rhinovirus genome and polyprotein, including both structural and non-structural elements. Following translation, the virus polyprotein is cleaved into three subunits (P1-3), which are in turn further cleaved into their final forms. Adapted from [14] with permission. **(B)** Structure of rhinovirus capsid, with the external subunits of one protomer highlighted in color. **(C)** Depiction of the rhinovirus capsid face, including the canyon and drug-binding pocket with associated pore. Adapted from [45] with permission. **(D)** Cross-sectional depiction of viral capsid binding to the major group cellular receptor, ICAM-1. Adapted from [46] with permission. POL, polymerase; PRO, protease; UTR, untranslated region.

### *Immune Responses to Rhinovirus*

Perhaps the most well-defined aspect of the anti-RV immune response is the induction of protective neutralizing antibodies. Rhinovirus infection results in the development of strain-specific neutralizing antibodies over the course of 7-14 days, peaking over one month post-infection [47]. These antibodies prevent re-infection with the same strain, but are poorly cross-protective and typically wane after one year [47–50]. However, much remains to be discovered about the nature of these responses—including the class of antibody that provides neutralizing protection—and neutralizing antibodies are identified solely through a semi-quantitative culture-based neutralizing assay [51]. IgG antibodies capable of recognizing multiple strains have also been observed, although their function is currently unknown [43,52,53].

Little is known about the cellular immune response to RV. Immediately upon infection with RV, epithelial cells initiate an innate immune response, resulting in the induction of interferons (IFNs), the production of chemoattractants, and an increase in vascular permeability, all of which set the stage for the adaptive immune response [54–60]. Previous studies have observed T cell lymphopenia during the early days of experimental infection, as well as T cell infiltration of the respiratory tract, suggesting recruitment of T cells to the site of infection in addition to retention in local nodes [61,62]. Interestingly, peripheral blood lymphopenia during infection was most pronounced for $CD4^+$ T cells, and was strongly associated with increased symptom severity, implicating $CD4^+$ T cells in RV disease pathogenesis [62]. However, the characteristics of this T cell response are poorly defined.

Several *in vitro* studies have suggested a role for RV-specific T cells in protective immunity. Rhinovirus stimulation of $CD4^+$ T cells obtained from tonsillectomy samples demonstrated both proliferation and production of the hallmark T helper ($T_H$) 1-associated cytokine, IFN-γ [63]. In an experimental RV challenge study in humans, increased proliferation of PBMCs in response to *in vitro* RV stimulation was associated with reduced viral shedding, as was increased concentrations of IFN-γ in nasal secretions, suggesting a protective response mediated by $T_H1$ cells [64]. Furthermore, the majority of T cell clones generated by limiting dilution from peripheral blood mononuclear cells (PBMCs) derived from healthy subjects were found to proliferate to multiple RV strains *in vitro*, indicating that these responses might provide cross-strain protection [65]. Although T cells have been linked to both reduced viral shedding and elevated symptoms, these can be reconciled by considering research carried out for other respiratory viruses. In influenza, studies have shown that while pre-existing T cell immunity protects against infection, T cell responses during the acute phase contribute to symptomology [66,67]. Thus, early research hints at a role for $CD4^+$ T cells in both protection and pathology in RV infection, although these responses are poorly characterized. Protective $CD4^+$ T cell responses to RV infection will be explored in **Chapters 2** & **3**.

### *Treatments and Prevention Strategies for the Common Cold*

Despite the ubiquitous nature of rhinovirus infections, there are currently no approved treatments, and attempts at vaccine development have proven largely unsuccessful. This is in part due to the antigenic diversity of the rhinovirus species, with over 150 serotypes identified to date [68]. In the 1960s and 70s, several small-scale trials of inactivated RV vaccines showed some efficacy in preventing homotypic infections; however, these

strategies did not provide protection from heterologous infection, and thus were not pursued further [69–73]. Recent efforts at vaccine development continue to focus on inducing protective antibody responses, including a 50-valent inactivated RV-A vaccine that was recently tested in rhesus macaques [74]. However, the researchers stipulate that an 83-valent vaccine will be necessary to provide RV-A strain protection in humans, and would not provide protection from the RV-C strains implicated in asthma pathogenesis. In mouse models, recombinant RV polyprotein vaccination is capable of inducing cross-reactive IgG responses; however, the neutralizing capability of these IgG antibodies is unknown [52]. Further complicating matters, it appears that a large proportion of the antibody response in humans is misdirected toward a non-protective VP1 epitope [75]. As a result, no large-scale double-blind placebo-controlled clinical trials of vaccine candidates have been performed to date [76].

Given the limitations of vaccine strategies that induce neutralizing antibodies, recent attention has returned to antivirals [77]. As previously mentioned, anti-viral compounds that occupy the hydrophobic binding pocket in the RV capsid canyon can prevent infection; however, the use of capsid-binding agents as a treatment strategy for the common cold has as-yet proven unsuccessful, despite promising *in vitro* results. In the past several years, numerous capsid-binding drugs have failed to meet their primary study endpoints, including Pleconaril, Pirodavir, and its analog Vapendavir (ClinicalTrials.gov Identifiers: NCT00394914, NCT02367313)[78,79]. Other anti-viral strategies target the functional proteins of rhinovirus, including inhibition of proteases and polymerases. However, no such drugs have been approved for use in RV by the FDA, and the development of the protease

inhibitor Rupintrivir and an analogue have both been halted due to insufficient clinical benefit [80,81].

Numerous other pharmacologic treatment strategies have been tested in rhinovirus, including immune enhancement by inhaled IFNs and, in contrast, attempted limitation of inflammation through toll-like receptor (TLR) 3 blockade, although both of these methods failed to meet their primary endpoints when studied in asthmatics [82,83]. In addition, alternative treatments such as Echinacea, Vitamin D, and probiotic supplementation have also been investigated as novel therapeutics for the common cold, with mixed success [84–87]. Ongoing research indicates that these treatments might also have immunomodulatory effects, potentially through influencing T cell differentiation and effector activity [88]. Taken together, it is clear that new and improved strategies for the treatment of the common cold are needed, both for the general population and those with chronic respiratory diseases.

## Allergic Asthma

RV infection is one of the key triggers of allergic asthma exacerbations. Asthma is a chronic respiratory disorder characterized by periods of reversible airway hyperreactivity. This disease affects up to 300 million people worldwide, and costs in excess of $18 billion each year in the United States alone [89]. Asthma exacerbations often manifest as wheezing, shortness of breath, coughing, and tightness in the chest, and may result in hospitalization and/or death. Approximately 9% of children and 8% of adults have asthma in the United States, and asthma prevalence has grown by 15% over the past decade [90]. Importantly, one in five children with asthma visit the emergency department each year, and nine people die from asthma each day in the United States [90].

Asthma takes two main forms—allergic and non-allergic—of which there are many variations. Allergic asthma—characterized by the induction of IgE antibodies to otherwise innocuous allergens—is the most common form of asthma among children, and accounts for approximately 50% of asthma in adults [89]. This disease typically develops early in life—in contrast with non-allergic asthma, which is frequently adult-onset—and often progresses from initial allergic sensitization to the development of multiple allergic diseases, beginning with atopic dermatitis. While for many patients, standard treatment results in disease control, approximately 5-10% of patients have disease that is refractory to treatment, and these patients are frequent utilizers of healthcare resources [89,91]. Key areas for asthma research include better understanding the inception of disease in order to halt the rise in prevalence, as well as the development of new therapeutics in order treat those subjects for whom standard treatment fails.

### *$T_H2$ Immunity and the Allergic Response*

Allergic diseases have classically been associated with T helper ($T_H$) 2 inflammatory processes, also referred to as type 2 responses. While it is thought that $T_H2$ immune responses were evolved to protect against parasitic infections, in post-hygiene societies, $T_H2$ responses have been increasingly observed in response to otherwise innocuous antigens, such as food proteins, pollens, pet dander, dust mites, and molds [92]. These responses manifest in a number of diseases such as food allergy, atopic dermatitis, allergic rhinitis, and asthma. The prevalence of allergic diseases has dramatically increased over the last several decades [93]. The reasons for this phenomenon remain unknown; however, it is clear that these changes are occurring too quickly for the main drivers to be genetic, and it is commonly thought that reduced exposure to microbial products in post-hygiene

communities is a factor [92]. Given the ever-increasing issue of allergic disease and asthma, it is important to fully understand the immunological underpinnings of allergic processes in order to design more effective therapeutic and preventative strategies.

Classic $T_H2$ immunity is initiated by a primary exposure to an allergen (**Figure 1-2**). No symptoms manifest during this exposure, as the immune machinery is not yet in place to trigger a reaction. During primary exposures in the susceptible host, airway epithelial cells release innate $T_H2$-skewing cytokines, including thymic stromal lymphopoietin (TSLP), interleukin (IL)-25, and IL-33 [94]. These cytokines can in turn act on innate lymphoid cell (ILC) populations to promote an ILC2 program, as well as on antigen-presenting cells such as myeloid dendritic cells (mDCs). $T_H2$-primed DCs process and present allergen to naïve $CD4^+$ T cells, integrating numerous external stimuli and inducing a $T_H2$-skewing process (**Figure 1-3**). The resultant $T_H2$ cell population expresses the defining transcription factor GATA-3, Th2-associated chemokine receptors including CCR4 and CRTH2, and the hallmark $T_H2$ cytokines, IL-4, IL-5, and IL-13 [95]. In turn, IL-4 promotes B cell class-switching to produce allergen-specific IgE antibodies, whereas IL-5 drives eosinophil maturation and recruitment, and IL-13 promotes mucus production and airway hyperreactivity.

In the effector phase, allergen-specific IgE binds to its high-affinity receptor FcεRIα, which is expressed on basophils and mast cells, in addition to dendritic cells (**Figure 1-2)**. Upon secondary exposure to allergen, differentiated $T_H2$ effector cells are primed to respond rapidly via their recruitment to the airways and activation through T cell receptor (TCR) engagement. Memory T cells that express the central-homing marker CCR7 are sequestered in local nodes, where they are activated by antigen-presenting cells that have been primed at

the site of infection. This coincides with cross-linking of IgE receptor on mast cells by allergen. Upon cross-linking, these cells degranulate, releasing numerous inflammatory mediators including histamines, tryptase, leukotriene $C_4$ ($LTC_4$), prostaglandin $D_2$ ($PGD_2$), and cytokines including IL-4, ultimately triggering an acute reaction [96]. In addition, epithelial barrier integrity is compromised, both as the result of inflammatory mediators such as IL-31 and oncostatin M, as well as by the proteolytic activity of allergens such as Der p 1 [97–101]. These responses result in inflammation and smooth muscle contractility in the airways that manifests as wheeze, and the establishment of a "pro-allergic" $T_H2$ milieu in the respiratory tract that can persist even in the absence of allergen exposure.

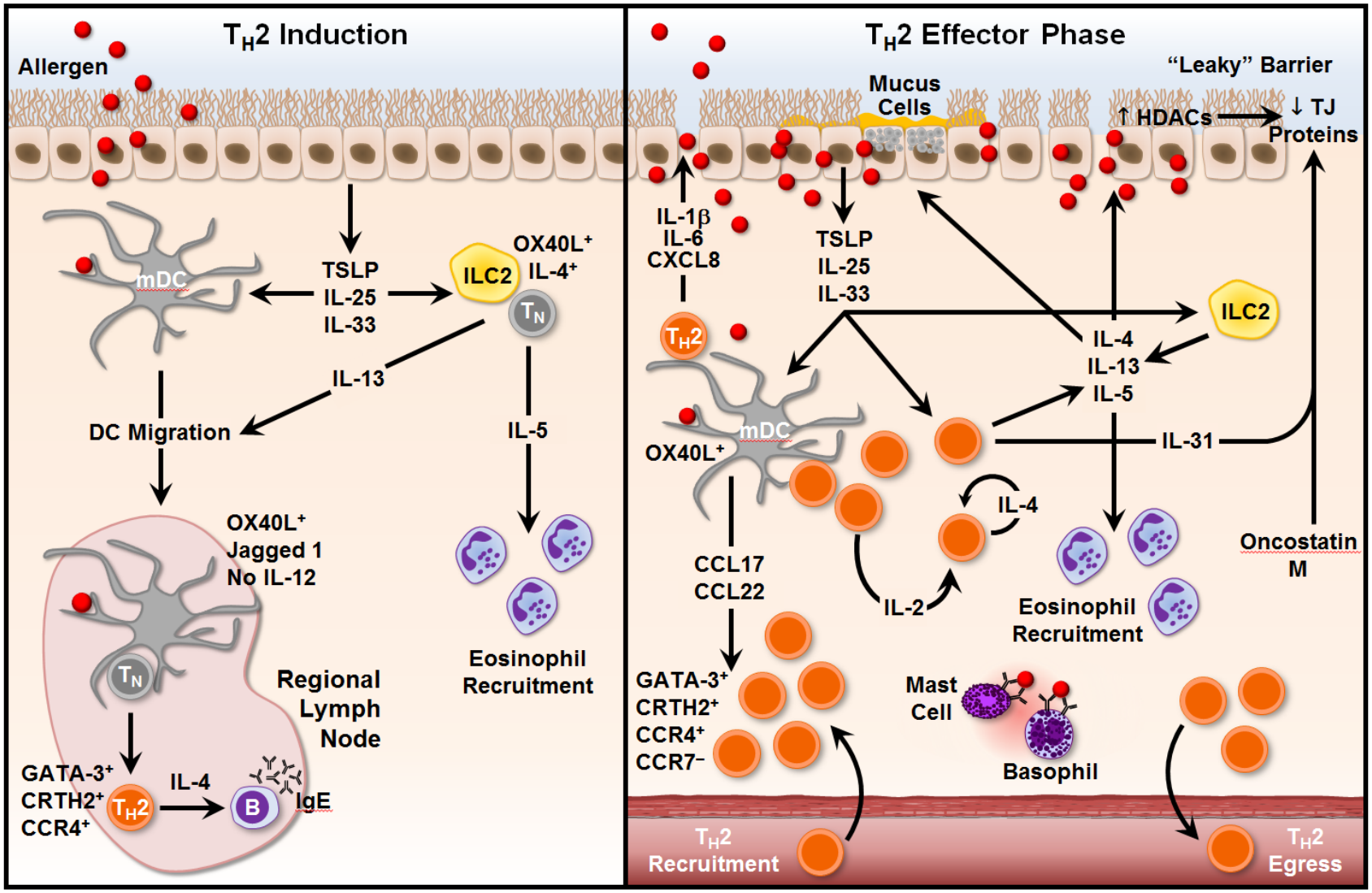
TH2 Induction
Allergen
mDC
TSLP
IL-25
IL-33
ILC2
OX40L+
IL-4+
TN
IL-13
DC Migration
IL-5
OX40L+
Jagged 1
No IL-12
TN
Regional
Lymph
Node
GATA-3+
CRTH2+
CCR4+
TH2
IL-4
B
IgE
Eosinophil
Recruitment
TH2 Effector Phase
"Leaky" Barrier
Mucus
Cells
↑ HDACs
↓ TJ
Proteins
IL-1β
IL-6
CXCL8
TSLP
IL-25
IL-33
ILC2
TH2
IL-4
IL-13
IL-5
mDC
OX40L+
IL-31
IL-4
Oncostatin
M
CCL17
CCL22
IL-2
Eosinophil
Recruitment
GATA-3+
CRTH2+
CCR4+
CCR7−
Mast
Cell
Basophil
TH2
Recruitment
TH2
Egress

**Figure 1-2. Type 2 Inflammatory Processes Involved in the Induction and Exacerbation of Allergic Asthma**

*(Left)* Initiation of a $T_H2$ response. Allergen exposure induces the release of innate cytokines at the epithelial barrier. This process which activates innate lymphoid cells and licenses DCs to migrate to regional lymph nodes, where they induce $T_H2$ cell differentiation and production of IgE. [94,102–108]

*(Right)* The $T_H2$ effector phase. Re-exposure to allergen cross-links surface-bound IgE on effector cells such as mast cells and basophils, resulting in degranulation and the release of inflammatory mediators such as histamine. Antigen-experienced $T_H2$ effectors ($CCR7^{-}$) respond rapidly via their recruitment in response to $T_H2$ chemoattractants produced in the respiratory tract (CCL17 & CCL22) and secretion of $T_H2$ cytokines. Egress or "spillover" of $T_H2$ cells from the inflamed respiratory tract results in recirculation, and possible reversion to a central-homing phenotype ($CCR7^{+}$). [98–101,109–118]

HDAC, histone deacetylase; TJ, tight junction.

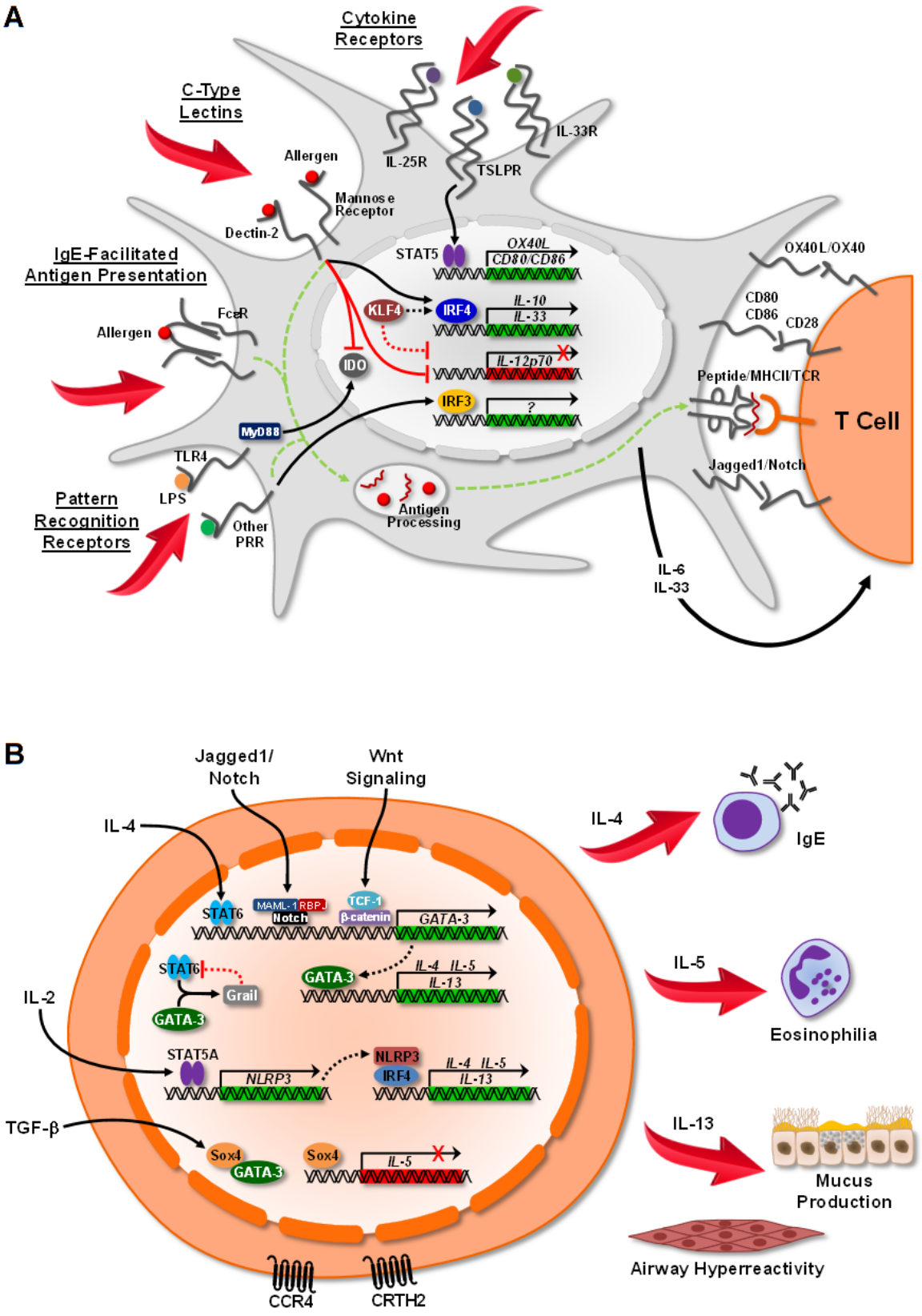
A
Cytokine Receptors
C-Type Lectins
IgE-Facilitated Antigen Presentation
Pattern Recognition Receptors
Allergen
Mannose Receptor
Dectin-2
IL-25R
TSLPR
IL-33R
FcεR
Allergen
TLR4
LPS
Other PRR
MyD88
IDO
KLF4
IRF4
IRF3
STAT5
OX40L
CD80/CD86
IL-10
IL-33
IL-12p70
?
Antigen Processing
OX40L/OX40
CD80
CD86
CD28
Peptide/MHCII/TCR
T Cell
Jagged1/Notch
IL-6
IL-33
B
Jagged1/ Notch
Wnt Signaling
IL-4
IL-2
TGF-β
STAT6
MAML-1
RBP-J
Notch
TCF-1
β-catenin
GATA-3
Grail
IL-4 IL-5 IL-13
STAT5A
NLRP3
IRF4
Sox4
IL-5
CCR4
CRTH2
IL-4
IgE
IL-5
Eosinophilia
IL-13
Mucus Production
Airway Hyperreactivity

**Figure 1-3. Molecular Events in $T_H2$ Differentiation**

**(A)** Myeloid dendritic cells act as a hub for $T_H2$ licensing. Dendritic cells integrate diverse external cues to generate a $T_H2$-permissive cytokine milieu. They also express an array of receptors and ligands that interact with $CD4^+$ T cells. In addition, c-type lectins and surface-bound IgE can facilitate increased allergen uptake for antigen presentation. [94,102,119–126]

**(B)** Within T cells, numerous molecular pathways—including IL-4-induced induction of GATA-3—orchestrate $T_H2$ differentiation and coordinate the accessibility of $T_H2$ loci for gene transcription. Regulatory signals, such as TGF-β, can counter $T_H2$-promoting signals and suppress $T_H2$ differentiation and function. [113,127–132]

IDO, indoleamine 2,3-dioxygenase; KLF4, Kruppel-like factor 4; MAML1, mastermind-like protein 1; PRR, pattern recognition receptor; RBPJ, recombination signal binding protein for immunoglobulin kappa J region; Sox4, Sry-related high-mobility-group box 4; TCF-1, T cell factor 1.

### *Asthma Heterogeneity and the T Cell Response*

Asthma is a highly heterogeneous disease, including many distinct types that are associated with their own unique immune profiles (**Figure 1-4**). As experimental techniques have advanced, it has become apparent that allergic asthma is characterized by more than simple $T_H2$ inflammation. Firstly, there are sub-phenotypes of $T_H2$ cells that express different combinations of $T_H2$ cytokines. $T_H2$ cells that produce high quantities of IL-5 are generally considered to be more pathogenic, and are sometimes referred to as "pathogenic effector $T_H2$ ($peT_H2$) cells" [133,134]. These $IL5^+$ $T_H2$ cells arise following multiple rounds of stimulation in parallel with the silencing of IFN-γ expression. Such cells express high levels of cytokines, are associated with eosinophilic inflammation, and have been described in numerous allergic diseases including eosinophilic gastrointestinal disease (EGID), atopic dermatitis, and eosinophilic airway inflammation [133,135–138]. Given the pathogenicity of $IL5^+$ $T_H2$ cells in multiple allergic diseases, they represent a key area for continuing research.

Interleukin-17, the characteristic cytokine of $T_H17$ cells, has been implicated in severe asthma, particularly neutrophilic asthma (**Figure 1-4**)[139]. Increased expression of IL-17 has been observed in the lungs of asthmatics, and levels correlate with disease severity [140–143]. Additionally, mouse models have implicated $T_H17$ cells in various aspects of the asthmatic response, including the promotion of neutrophilia, airway remodeling, and provocation of airway hyperreactivity through direct effects on airway smooth muscle [139,144,145]. $T_H2$ cells that co-express IL-17 have also been observed in subjects with allergic asthma [146]. Interestingly, in severe asthma these $IL\text{-}4^+IL\text{-}17^+$ produce more IL-4 than $IL\text{-}4^+IL\text{-}17^-$ cells, and are linked to more severe disease [146]. This is is in keeping with

studies that have implicated a mixed neutrophilic and eosinophilic response in the lung with increased asthma severity [147,148].

$T_H1$ cells were long considered to be counter-regulators of $T_H2$ responses, and vice-versa. However, recently a role for $T_H1$ cells in severe allergic asthma has been increasingly recognized (**Figure 1-4**)[149]. Mixed activation of $T_H1$ and $T_H2$ cells in the asthmatic lung has been observed during asthma exacerbations despite the dominance of $T_H2$ signatures at baseline [150]. Several studies of human cells obtained from the lungs of allergic asthmatics demonstrate enhanced $T_H1$ responses, including increased $T_H1$ cell infiltration into the airways and increased production of IFN-γ [151–157]. Other work has demonstrated relationships between higher levels of IFN-γ and increased asthma severity, thereby implicating $T_H1$ cells in asthma pathogenesis [151,158].

Mouse models of asthma provide contradictory evidence as to the role of $T_H1$ cells in allergic asthma. The spontaneous development of asthma-like disease in mice lacking the $T_H1$ lineage-specifying transcription factor T-bet is consistent with a regulatory role for $T_H1$ cells [159]. This is further bolstered by studies in which the adoptive transfer of $T_H1$ cells resulted in reduced $T_H2$ responses and suppressed airway hyperreactivity [160–162]. In contrast, other $T_H1$ adoptive transfer models demonstrated increased asthma responses, and in some instances also increased $T_H2$ inflammation [163–166]. One such $T_H1$ transfer study observed that $T_H1$ infiltration preceded $T_H2$ infiltration, and went on to demonstrate that $T_H1$ cells in the lung increase local expression of vascular cell adhesion molecule 1 (VCAM-1), perhaps through secretion of TNF-α, thereby facilitating the infiltration of additional T cells, including $T_H2$ cells [165,166]. Furthermore, several mouse models have implicated $T_H1$ cells in steroid-resistant severe asthma [167,168]. It is possible that these divergent responses

might be due to modulation by diverse inflammatory mediators, such as the IL-1 family cytokine IL-18, which has been shown to disrupt $T_H1/T_H2$ reciprocity in mice [167,169,170]. Given the varying and contradictory evidence for $T_H1$ responses in allergic asthma, further research is required to understand the interplay between $T_H1$ and $T_H2$ cells in severe asthma.

Advances in $CD4^+$ T cell research have led to the identification of numerous new T helper subsets. $T_H9$ cells are a distinct subset of IL-9-producing cells that share common molecular pathways with $T_H2$ cells [171–174]. IL-9 mediates a variety of processes that are often associated with $T_H2$ inflammation, including mast cell growth, goblet cell metaplasia, and IL-4-dependent antibody production by B cells [175]. High expression of IL-9 has been identified in the lungs of asthmatics, but the role of $T_H9$ cells in allergic asthma remains unclear due to their overlapping contributions with $T_H2$ cells, and the ability for ILC2s to produce IL-9 [175]. Also recently described, the $T_H22$ subset shares features with $T_H17$ cells including production of the characteristic cytokine IL-22, although they represent a distinct lineage [176]. The relevance of $T_H22$ cells to asthma has not been established; however, IL-22-expressing T cells have been implicated in other forms of allergic disease [177].

Regulatory T cells are also known to play a key role in modulating allergic disease. In health, tolerance to innocuous substances arises through the induction of $T_{REGS}$, a process believed to be disrupted in allergic disease. In humans, there is evidence that $T_{REG}$-mediated suppression of $T_H2$ activity is deficient in allergic disease, and reduced numbers of $T_{REGS}$ have been observed in bronchoalveolar lavage from children with asthma [178,179]. As such, many therapeutic strategies are focus on induction of functional $T_{REGS}$ in allergic patients. There is evidence that conventional allergen immunotherapy, which is clinically efficacious, induces $T_{REG}$ populations [180].

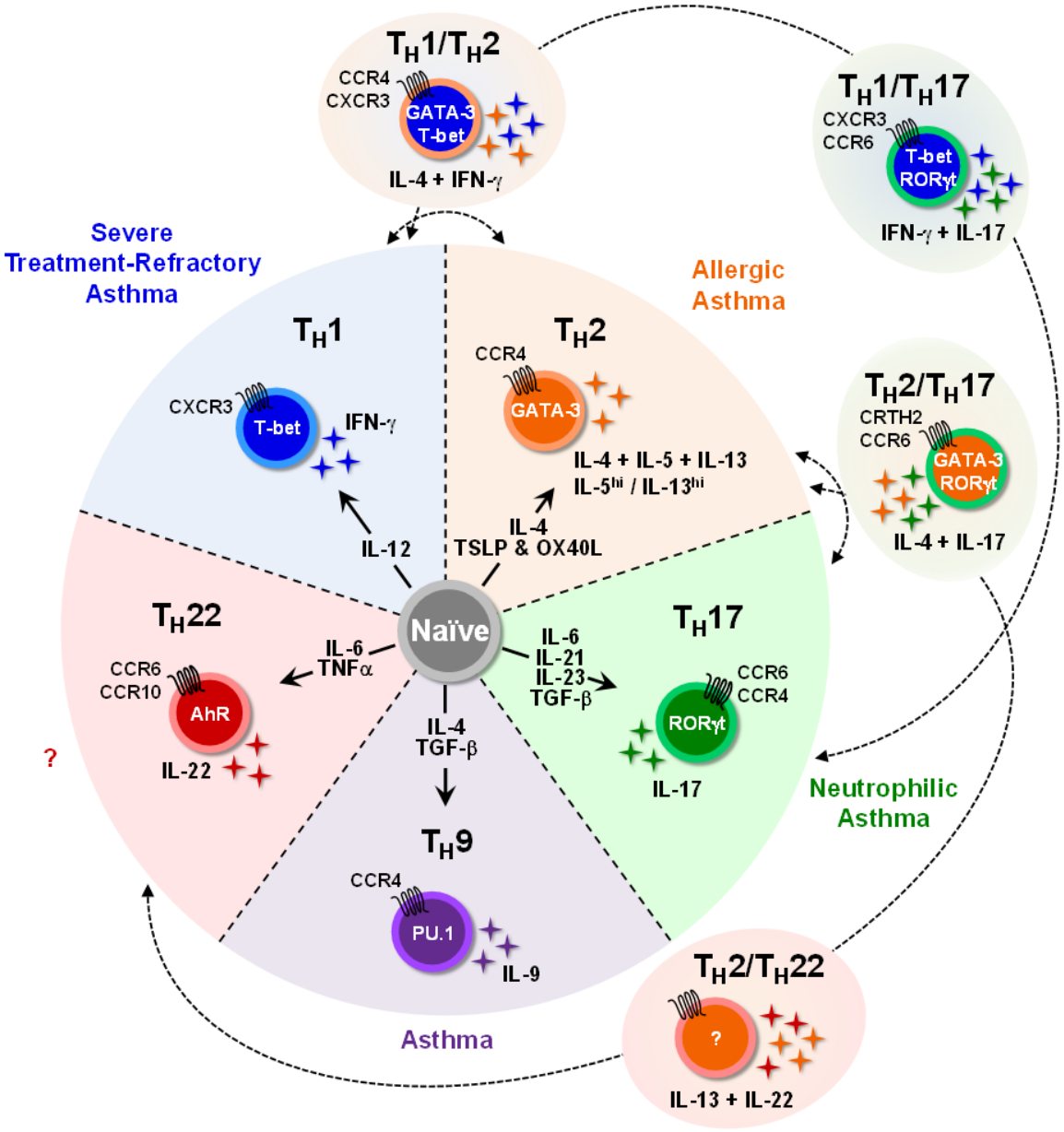


**Figure 1-4. CD4⁺ T Cell Subsets Linked to Asthma**

Distinct T helper subsets differentiate in response to specific cytokines. Each subset bears a unique molecular signature, including lineage-specifying transcription factors, surface chemokine receptors, and cytokines.

### *Treatments and Strategies for the Prevention of Asthma*

Standard treatments for severe asthma include inhaled and systemic corticosteroids, bronchodilators such as albuterol and long-acting beta agonists (LABAs), and leukotriene inhibitors. However, a subset of severe asthmatics continues to have uncontrolled asthma despite receiving therapy, and these patients utilize the highest levels of healthcare resources [91,181]. As such, additional therapeutics are needed to address this unmet need.

The majority of asthma drugs under development are biologics that target the $T_H2$ inflammatory axis. The first biologic approved by the FDA for use in asthma was omalizumab (anti-IgE), which received approval for treatment of patients aged 12 and older in 2003, and for children six years and older in 2016 [182,183]. When used as an add-on therapy for severe allergic asthma, omalizumab decreases the rate of asthma exacerbations, provides a steroid-sparing effect, and decreases use of rescue medication [184]. In addition, omalizumab is thought to provide benefit in allergic asthmatics with respiratory viral infections, an aspect that will be discussed later in this chapter.

Omalizumab acts by binding to the Fc region of IgE, both in its soluble and B-cell membrane-bound forms. This results in the formation of IgE aggregates, which are unable to bind to FcεRIα on mast cells and basophils, and reduces the production of IgE by B cells [185–187]. Importantly, omalizumab does not recognize receptor-bound IgE. Instead, FcεRIα is decreased on mast cells and basophils due to natural receptor turnover and the lack of free IgE to bind and stabilize new IgE receptors [187,188]. It is also possible that omalizumab might indirectly impact other aspects of the $T_H2$ immune response, whether through a reduction of IgE-facilitated antigen presentation by dendritic cells to T cells, or by reducing the inflammatory milieu via prevention of mast cell activation (**Figure 1-5**). The

impact of omalizumab on T cell responses has not been well-studied. Several studies have shown decreased $CD4^+$ T cell numbers in the airway mucosa following omalizumab administration; however, a more recent study of allergen-specific cells demonstrated no decrease in IL-13 expression or increase of $T_{REG}$ numbers post-treatment [189–191]. Further study is required to fully characterize the indirect effects of anti-IgE on T cell responses, and this aspect is addressed in **Chapter 4**.

Newer biologics in development for allergic asthma are generally focused on blocking $T_H2$-associated cytokines of both the innate and adaptive immune response. Several biologics aim to disrupt the actions of $T_H2$ cytokines. Biologics targeting IL-5 have been approved for use since 2015. Mepolizumab, reslizumab, and benralizumab are all IL-5 antagonists approved as add-on therapies for severe asthma. Mepolizumab and reslizumab both target IL-5 directly, whereas benralizumab targets the IL-5Rα [192]. Most recently, in 2018 the FDA approved dupilumab for use as an add-on therapeutic in adults with moderate-to-severe asthma. Dupilumab acts by disrupting both IL-4 and IL-13 pathways through the targeting of their shared receptor chain, IL-4Rα [193]. Monoclonal antibodies targeting IL-13 alone (lebrikizumab and tralokinumab) have proven to be less effective, and have not received FDA approval [194,195].

Biologics targeting the initiating events of allergic $T_H2$ inflammation are also in development. Neutralization of TSLP has shown promise in mouse models of allergic asthma, and an anti-TSLP monoclonal (tezepelumab) has been shown to reduce asthma exacerbations in early studies in patients [196,197]. Similarly, disruption of IL-33 by anti-IL-33 and anti-IL-33R monoclonal antibodies is another avenue for drug development [198]. Other emerging drugs include CRTH2 antagonists (which target $T_H2$ memory cells and

CRTH2$^{+}$ eosinophils, basophils, and ILC2s), and an inhaled DNAzyme that cleaves and inactivates *GATA3* mRNA (SB010) [199–202]. Importantly, all these drugs target allergic asthmatics with "$T_H2^{high}$" inflammatory profiles. However, the development of biologics for other $T_H$ profiles associated with asthma is lacking.

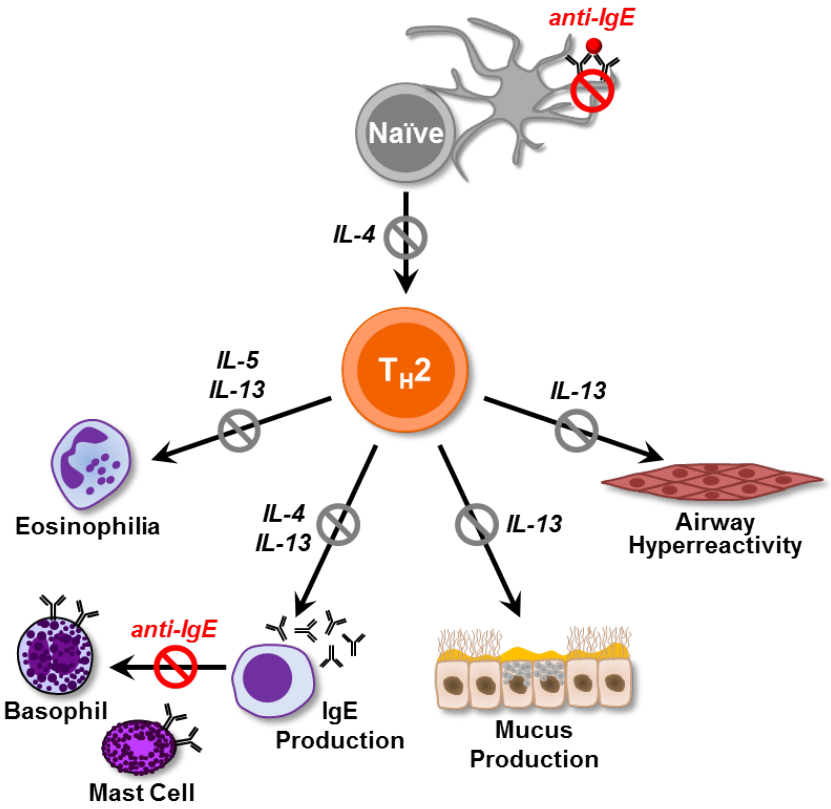


**Figure 1-5. Potential Effects of Omalizumab (Anti-IgE) on T Cell-Mediated Type 2 Inflammatory Processes**

Red symbols denote known direct effects of anti-IgE on surface expression of IgE receptors on dendritic cells, mast cells, and basophils. Gray symbols denote potential indirect effects of anti-IgE treatment, possibly mediated by decreased IgE antibody-facilitated presentation of allergen and consequent decreased $T_H2$ differentiation and activation.

## Viruses and Allergic Asthma

It has long been appreciated that respiratory viral infections are major triggers of exacerbations in patients with allergic asthma; in fact, this interaction was documented in the 12th century by the physician Moses Maimonides in his "Treatise on asthma" [203,204]. However, it was not until the 1960's, with the improvement of molecular diagnostics, that human rhinovirus was specifically implicated in asthma exacerbation [205,206]. In addition to exacerbating asthma, respiratory viral infections in early life play a role in the development of allergic asthma, although the mechanisms remain unknown. A greater understanding of virus-induced allergic asthma is essential for the development of improved therapeutics for the prevention of virus-induced exacerbations, as well as to halt the progression of asthma in infancy and early childhood.

One of the key risk factors for the development of asthma is wheezing in response to respiratory viral infections during the first three years of life [207–209]. Respiratory syncytial virus (RSV) was long considered to be the main virus implicated in these infections within the first year of life, with RV predominating in older children and adults [208,210,211]; however, RV has also been implicated in early life wheeze and the subsequent development of asthma [209,212,213]. There is continuing debate as to whether viral infections in early life influence the development of allergy and asthma, or rather reflect a pre-existing asthma predisposition [214]. Recent studies have given mixed results: a twin birth cohort study by Thomsen and colleagues concluded that pre-existing asthma predisposition results in severe RSV infections requiring hospitalizations [215]. By contrast, a Tennessee birth cohort, it was found that infants born in the months before the winter virus peak had increased risk for the subsequent development of asthma, implying a causative role

for RSV and other winter viruses [216]. While it is clear that early life virus-induced wheeze might lead to the development of allergic asthma, it is likely that asthma arises from a confluence of multiple factors, including genetic predisposition of the host, viral infections, and environmental exposures to allergens and other immune stimuli [217].

Approximately 80% of acute wheezing episodes in allergic asthmatics are caused by respiratory viral infections, of which the majority can be attributed to rhinovirus [218,219]. Furthermore, the severity and duration of symptoms induced by RV are typically increased in these patients [220]. Both RV-A and RV-C species are linked to severe asthma exacerbations, whereas RV-B are not [217]. Decreased rates of replication of RV-B species have been observed within epithelial cells, as well as reduced induction of cytokines and chemokines including IP-10, RANTES, and IFN-λ [221]. Thus, the magnitude of anti-viral immune responses might be a factor in the propensity to induce asthma exacerbations.

### *Associations with IgE*

Numerous studies have suggested a link between rhinovirus infections and IgE. One key indicator of a role for IgE, or else its associated inflammation, is the synergistic effect of RV infection and allergen exposure on asthma exacerbations. The risk of severe episodes requiring hospitalization in asthmatics with RV infection significantly increases with allergen exposure [222,223]. Other work echoes this finding. In a study of allergic rhinitics, segmental bronchoprovocation with allergen and experimental RV infection synergistically enhanced histamine release and eosinophil recruitment [224]. By contrast, other studies found that prior allergen exposure did not enhance RV symptom severity, and even delayed and shortened cold symptoms [225,226]. Thus, the interaction between allergen and RV and the involvement of IgE within this process warrants further investigation.

The *in vivo* elimination of IgE in asthmatic patients also implies a role for IgE during RV infection. A double-blind placebo-controlled study of omalizumab in inner city asthmatic children found that anti-IgE treatment attenuated the seasonal peaks in asthma exacerbations that coincide with RV infections [227]. In a follow-up study, those asthmatic children who were randomized to receive anti-IgE for 90 days experienced shorter infections with decreased viral shedding and reduced risk of developing illness during RV infection as compared with patients who received standard treatment [228,229].

Several studies at the University of Virginia have bolstered the link between IgE and virus-induced asthma. In cross-sectional studies of wheezing and control children who attended the emergency department, the strongest odds for wheezing were found in those children with both RV infection and a $T_H2$-inflammatory biomarker—specifically IgE to aeroallergens, nasal eosinophilia, or increased nasal eosinophil cationic protein (ECP), a product released by eosinophils [211,230]. In a subsequent pediatric cross-sectional case-control study performed in children attending the Hospital Nacional de Niños in Costa Rica, the risk of wheeze was greatest among patients with the highest levels of serum IgE to dust mite coupled with RV positivity [231]. Work from the same group using an RV experimental infection model found that acute cold symptoms were increased in allergic asthmatics with high total serum IgE versus those with lower IgE (**Figure 1-6**)[232]. Asthmatics with high IgE also exhibited increased airway inflammation based on elevated airway nitric oxide (NO) and high concentrations of ECP [232]. These collective studies establish a link between IgE and RV-induced asthma. It remains unclear whether IgE plays a direct role, or whether it provides a marker of underlying inflammatory processes that promote the pathogenicity of RV in asthma. The role of IgE in RV-induced asthma is investigated in **Chapter 4**.

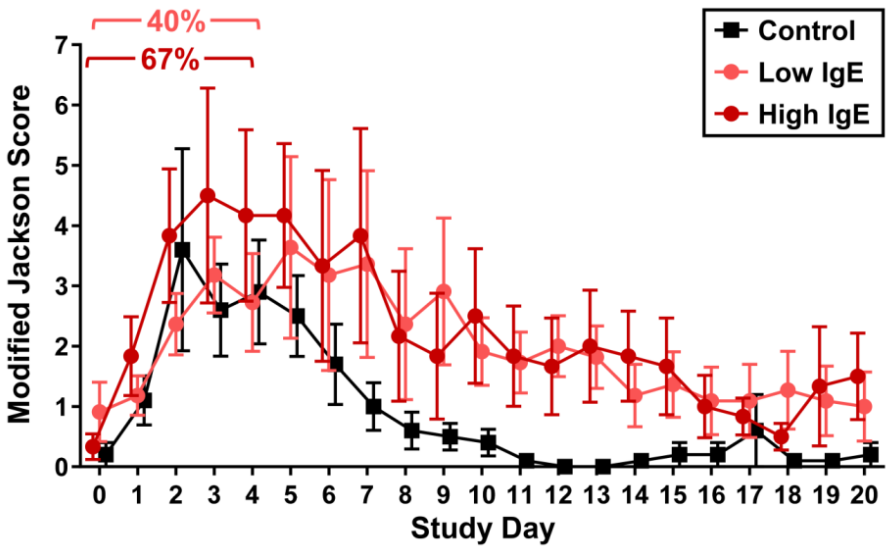


**Figure 1-6. Increased RV Symptoms in Allergic Asthmatics with High IgE**

Upper respiratory symptom scores as assessed by the modified Jackson criteria [233], including sore throat, sneezing, rhinorrhea, and nasal congestion. Total serum IgE: Low IgE, 29.2-124 IU/mL; High IgE, 371-820 IU/mL. Numbers denote the percent of allergic asthmatic subjects experiencing peak symptoms during acute infection, as opposed to delayed symptoms. Symbols denote means ± SEM. Data courtesy of Dr. Peter Heymann. Adapted with permission from [232].

### *Mechanisms of RV-Induced Asthma*

RV has been linked to seasonal peaks in asthma exacerbations, particularly in the fall when children return to school, although RV circulates throughout the year [234]. This may be due to other environmental factors, including increased allergen exposure. Although the precise mechanisms through which RV triggers allergic asthma are not known, several mouse models have demonstrated the involvement of $T_H2$-like immune responses in RV infection, and the relative contributions of $T_H1$ and $T_H2$ immunity in RV-induced asthma is a major area for continuing research [235–239].

A prevailing theory for virus-induced allergic asthma is that anti-viral immunity is deficient. There have been several reports of deficient interferon production (namely IFN-β and IFN-λ) by bronchial epithelial cells from asthmatic subjects following *in vitro* stimulation with virus, as compared with healthy controls [240,241]. Decreased production of IFN-α by plasmacytoid dendritic cells (pDCs) has also been reported following both IgE cross-linking and viral stimulation *in vitro* [242]. Similarly, reduced production of IFN-γ by cultured PBMCs from asthmatics has also been reported, in addition to decreased levels of secreted IFN-γ in bronchoalevolar lavage during experimental RV infection [243,244]. Given the counter-regulatory relationship between $T_H1$ and $T_H2$ inflammation, it has been suggested that deficient $T_H1$ responses might enable robust $T_H2$ inflammation, and that $T_H2$ inflammation might itself suppress $T_H1$ responses [245–249]. This is supported by a mouse model in which T-bet deficient mice that cannot produce $T_H1$ cells develop $T_H2$-skewed responses to RV infection, including airway eosinophilia and $T_H2$ cell infiltration into the lung [250].

Given the reported link between IgE and RV infection, it has been suggested that

IgE crosslinking counter-regulates IFN production, especially IFN-α production by pDCs [251–253]. In a trial of omalizumab in allergic asthma, researchers reported increased production of IFN-α by PBMC cultures co-stimulated with IgE crosslinking antibody and RV in those subjects receiving anti-IgE [229]. In keeping with this, Gill et al. found that reductions in the high affinity IgE receptor FcεRIα on pDCs following omalizumab were associated with reduced exacerbation rates and increased IFN-α [254]. However, a molecular mechanism has not been identified for IgE-mediated downregulation of IFNs in pDCs, or any other cell type. Indeed, several lines of evidence support a link between IgE signaling and increased IFN production. These include increased IFN-α production following IgE cross-linking in a mouse model of lupus, and a requirement for IgE signaling intermediates Lyn and Fyn for TLR-mediated IFN production [255,256].

Despite reports of IFN deficiency in asthmatics, this remains controversial due to contradictory evidence and a lack of reproducibility. Allergic asthmatics and healthy controls have similar viral titers both in natural and experimental infections, suggesting a similar capacity to control infection [257]. The notion of IFN deficiency is further challenged by the failure of inhaled IFN-β to prevent the worsening of asthma symptoms when administered to asthmatics at the inception of cold symptoms [82]. As previously discussed, several studies support a pathogenic role for $T_H1$ cells and IFN-γ in certain types of asthma [151–157]; in keeping with this, neither subcutaneous nor nebulized IFN-γ for the treatment of allergic asthma provided clinical benefit [258,259].

Additional studies show equivalent IFN production in allergic asthmatics and healthy subjects in response to RV [260–262]. Furthermore, enhanced IFN networks have been

linked to asthma development, exacerbations, and increased disease severity in both humans and mice. Increased IFN-β and IFN-λ have been reported in the sputum of asthmatics—particularly those with neutrophilic disease—as compared with controls [263,264]. Similarly, increased levels of IFN-γ and IFN-$\gamma^+$ T cells have been observed in the lower airways of allergic asthmatics, including those experiencing active exacerbation, as compared with controls [265,266]. Importantly, increased levels of IFN-α, IFN-β, and IFN-γ in the airways correlated with asthma severity [266]. Similar observations have been made in RSV infection, including an association between increased type I and III interferons and interferon stimulated genes in RSV-stimulated bronchial epithelial cells and reduced lung function [267]. Observations of increased IFNs in asthma have even been made in studies that also report an innate IFN deficiency. A recent study describing deficient IFN production by epithelial cells during experimental infection also observed increased numbers of IFN-$\alpha^+$ subepithelial cells, which correlated with symptom severity [268]. The same group also observed increased IFN-γ and IFN-λ concentrations in the nose of asthmatics versus controls in a different RV infection study. Moreover, RV only induced IFNs in the lower airways of asthmatics [269].

Conflicting reports of IFN deficiency in allergic asthma may be impacted by subject selection and disease heterogeneity. For example, it was recently reported that the induction of $IFN^{low}$ cytokine signatures by RV-stimulated PBMCs was associated with early-onset exacerbation-prone asthma, while the $IFN^{high}$ signatures were associated with later-onset asthma [270]. Thus, the role of IFNs in allergic asthma is not clearly defined, and requires further study with careful consideration of both experimental model and subject characteristics.

## Limitations of Current Research Models

At the cellular level, much of the immune response to RV remains undefined, in part due to the limitations of mouse models of RV infection. RV is not a natural pathogen of mice, and mouse ICAM-1 does not bind to RV [271]. In order to address this, many mouse studies have utilized minor group RV strains, or else adopted the use of a mouse-human ICAM-1 chimeric BALB/c strain [272]. While an inflammatory response is induced in these models, they fail to reproduce human disease. Although an inflammatory response is induced, it is localized to the lungs of mice, which is not the principal site of infection and inflammation in humans [272]. Furthermore, viral titers in mouse models rapidly decline after only 12-24 hours, in contrast with the more protracted infection observed in humans [272,273]. This limits the study of viral replication and calls into question whether these models establish a productive infection. These factors, coupled with the limitations of mouse models of allergic asthma, necessitate alternative models for investigation [273,274].

In order to address these issues, many studies of RV infection utilize *in vitro* methods, including both cell lines and human specimens. *In vivo* models pose a greater challenge due to issues of the timing of naturally occurring infections, diversity of RV strains, and heterogeneity within the general population. For this reason, experimental RV challenge in human subjects is such a vital tool. Experimental rhinovirus challenge has been performed in human subjects since the 1960's, and played a key role in understanding the transmission of RV infection and the induction and protective effects of neutralizing antibodies [50,275–277]. Previous experimental infection studies have analyzed cellular responses at only a superficial level. Hence, the major focus of this thesis was to apply these models to interrogate RV-specific $CD4^+$ T cell responses in health and RV-induced allergic asthma.

## Thesis Rationale

Rhinovirus is an important viral pathogen in the etiology of the common cold and allergic asthma exacerbations. There are currently no effective treatments or vaccines. Much of the cellular immune response to RV remains poorly defined; however, $T_H1$ cells are known to promote cellular immune responses against intracellular pathogens, including viruses, whereas $T_H2$ cells promote allergic inflammation. Thus, $CD4^+$ T cells likely play a key role in virus-induced allergic asthma, and provide a crucial avenue for research. This thesis aims to characterize the $CD4^+$ T cell response to rhinovirus infection in the context of health and allergic asthma. We hypothesized that $CD4^+$ T cells mediate cross-strain protection in healthy subjects, but that an exaggerated T cell response in subjects with allergic asthma promotes disease pathogenesis.

In this thesis, we first identify T cell targets within RV capsid proteins, and assess their utility for the potential development of a cross-protective T cell-targeted vaccine (**Chapter 2**). Next, we define $CD4^+$ T cell immune responses to RV in healthy subjects during experimental infection by using novel peptide/MHC class II tetramers to track RV-specific $CD4^+$ T cells in the circulation (**Chapter 3**). Finally, we characterize RV-specific $CD4^+$ T cell responses in infected allergic asthmatics, and weigh the relative contributions of $T_H1$ versus $T_H2$ cells using tetramer-based methods. In this chapter, we also probe the role of IgE in RV-induced asthma and its associated T cell responses by studying allergic asthmatics with a range of IgE titers, and by testing the effects of IgE blockade in a double-blind placebo-control study of anti-IgE treatment during RV infection (**Chapter 4** & **Appendix I**).

Overall, this thesis significantly expands the knowledge of RV-specific $CD4^+$ T cell responses, including identifying novel epitopes that provide potential vaccine targets, establishing proof-of-concept for cross-strain T cell immunity, and identifying CCR5 as a signature of RV-specific immune responses. Finally, we demonstrate augmented $T_H1$ responses in allergic asthmatics infected with RV, and present evidence of disease pathogenicity. Our findings challenge the existing paradigms of deficient anti-viral responses in asthma. Moreover, they raise important questions about how IgE blockade may influence the T cell response to RV. Taken together, these studies advance our understanding of adaptive immunity and immune pathology during RV infection, and provide a major stepping stone towards the development and improvement of new treatments for RV infection.

*Portions of this chapter were adapted from: L Muehling*, M Lawrence*, J Woodfolk. "Pathogenic $CD4^+$ T cells in patients with asthma." J Allergy Clin Immunol (2017). *Equal contribution.*

# Chapter 2 — Circulating Rhinovirus-Specific CD4+ T Cells Recognize Conserved Epitopes of Viral Capsid Proteins

## Introduction

Infection with RV is the main cause of the common cold, and typically runs a benign course, but can induce severe disease exacerbations resulting in hospitalization or death in those with chronic respiratory diseases [5–7,224,278,279]. There are currently no effective treatments for RV infection, and attempts to develop a vaccine have failed [76,280]. It is known that RV infection induces a neutralizing antibody response that prevents re-infection with the same strain; however, this response is transient and is highly strain-specific due to antigenic variability [21,47–49,275,277,281]. There is mounting evidence to support a protective role for $CD4^+$ T cells in respiratory viral immune responses, including RV [52,64,67,282,283]. Despite the numerous reports of T cell epitopes within capsid proteins of diverse viruses, no studies have explored RV. The RV capsid is composed of four proteins (VP1-4) that assemble to form an icosahedral structure [14]. Exposure of VP1 and VP2 on the capsid surface makes them attractive targets for an immune response, as evidenced by the ability to readily detect anti-VP1 antibodies, including IgG, in the serum [41–43]. In a mouse model, immunization with conserved capsid proteins of RV-A16 induced cross-reactive immune responses driven by $CD4^+$ T cells, which were associated with more rapid viral clearance [52]. These studies suggest that capsid proteins warrant further evaluation as T cell targets in humans.

We hypothesized that circulating memory $CD4^+$ T cells capable of recognizing different RV strains are readily detectable in adults due to repeat priming by previous RV infections. In this chapter, we describe the identification of $CD4^+$ T cell epitopes of RV

capsid proteins, the development of peptide/MHC class II (pMHCII) tetramers displaying these epitopes, and the characterization of circulating $CD4^+$ T cells specific for VP1 and VP2. Furthermore, by integrating *in vitro* and *in silico* epitope mapping, we validate and interrogate the immunodominant epitopes recognized by circulating $CD4^+$ T cells in healthy subjects, and establish their cross-reactive potential.

## Materials and Methods

### *Human Subjects*

Experiments were carried out in 61 healthy subjects (aged 18-45 years), who reported no cold symptoms at the time of participation. Written informed consent was obtained from all subjects, and all studies were approved by the University of Virginia Human Investigation Committee and Benaroya Research Institute Institutional Review Board.

### *HLA Typing*

Venous blood was collected in BD Vacutainer® Sodium Citrate Tubes (BD Biosciences, San Jose, CA), followed by genomic DNA extraction using the Gentra Puregene Blood Kit (Qiagen, Germantown, MD). Human leukocyte antigen (HLA) typing was performed using DRB1 SSP Unitray Kits (Invitrogen, Carlsbad, CA), according to the manufacturer's instructions.

### *PBMC Isolation*

Venous blood samples were collected in heparinized syringes, and PBMCs were isolated by Ficoll gradient centrifugation. Cells were either used fresh for tetramer-guided epitope mapping (TGEM) experiments, or else viably cryopreserved in FBS + 10% DMSO and stored in liquid nitrogen.

### *Tetramer-Guided Epitope Mapping*

Tetramer-guided epitope mapping was used to identify $CD4^+$ T cell epitopes of RV capsid proteins, and to generate pMHCII tetramers. These experiments were performed by the laboratory of Dr. William Kwok at the Benaroya Research Institute. Briefly, peptide libraries (20mer peptides with 12 aa overlap) were generated to span the length of the RV-A16 and RV-A39 VP1, VP2, and VP4 capsid protein sequences (UniprotKB accession #Q82122, Q5XLP5)[284]. Peptide/MHC class II tetramers for different commonly-expressed HLA molecules (HLA-DRB1*0101, *0301, *0401, *0404, *0701, 1101, 1501, and DRB5*0101 for RV-A16; HLA-DRB1*0401 for RV-A39) were then assembled, and displayed either pooled or individual peptides [285]. Biologically relevant pMHCII tetramers were identified as follows: (1) PBMC cultures established from healthy donors with known HLA-DR types were stimulated with RV peptide pools for 14 days, and then stained with pMHCII tetramer pools; (2) positive pMHCII signals were de-convoluted by repeat staining with single-peptide tetramers; (3) tetramers giving strong signals (≥1% of total $CD4^+$ T cells) in multiple subjects in the single-peptide tetramer screen were then retested for their ability to detect RV-specific $CD4^+$ T cells directly *ex vivo*. All experiments were performed in subjects expressing the relevant HLA-DR allele.

### *Ex Vivo Flow Cytometry Analysis of Tetramer⁺ Cells*

PBMCs from subjects expressing relevant HLA-DR alleles were stained with PE-conjugated rhinovirus pMHCII tetramers, without *in vitro* stimulation. When available, tetramers displaying an irrelevant peptide ($GAD_{555-567}$) were used as a negative staining control [286]. Cells were then labeled with anti-PE magnetic beads and enriched using an AutoMACS separator (Miltenyi Biotec, Auburn, CA). Cells were then stained for cell viability

and surface markers of interest, and then analyzed using a BD LSR Fortessa (BD Biosciences, San Jose, CA). The precursor frequencies of circulating tetramer$^+$ cells were calculated using an unenriched sample, according to established methods (Frequency=n/N, where n is the number of tetramer$^+$ cells in the enriched sample, and N is the total number of CD4$^+$ T cells in the sample)[287].

### *Sequence Alignment Analyses*

The sequences of VP1 and VP2 epitopes were compared with other RV strains using a protein BLAST search (National Center for Biotechnology Information)[288]. Multiple sequence alignments of BLAST results were performed using Jalview version 2.8.2 [289]. Graphs depicting sequence percent identity were generated using GraphPad Prism 7 (GraphPad Software, Inc., La Jolla, CA).

### *In Silico Prediction of HLA Binding and Epitope Prediction*

MHC class II binding predictions for RV capsid polyproteins were performed using the Immune Epitope Database (IEDB) consensus method. This method integrates three different epitope prediction methods— SMM-align, NN-align, and the combinatorial peptide scanning library (Comblib)—to identify a 15mer consensus epitope [290–293]. In cases where Comblib was not available for a given allele, the Sturniolo method was used instead [294]. MULTIPRED2, an epitope prediction program that uses the NetMHCpan and NetMHCIIpan algorithms, was used to predict 9mer core epitopes for numerous alleles corresponding to HLA class I and II supertypes [295–298]. This analysis was performed for the major HLA class II DR supertypes containing alleles used in TGEM (DR1, DR3, DR4, DR7, DR11, and DR15), as well as minor class II DR supertypes and class I supertypes. NetMHCIIpan was used to predict 19mer class II epitopes for single HLA alleles.

### *Location of T Cell Epitopes Within the Three-Dimensional RV Capsid Structure*

The locations of $CD4^+$ T cell epitopes within the three-dimensional structure of the virus capsid were visualized using PyMol, based on the X-ray crystal structure of native RV-A16 at 2.15-Å resolution (PDB code 1aym)[299,300].

### *Assay to Assess T Cell Cross-Reactivity*

The capacity for RV-specific $CD4^+$ T cells to expand and produce cytokines in response to RV-derived peptide epitopes was assessed using established methods [285]. Briefly, PBMCs from healthy HLA-DRB1*$0401^+$ subjects were stimulated with RV-A39 peptides ($VP2_{60}$: SDDNWLNFDGTLLGNLLIFP, >90% purity) (New England Peptides, Gardner, MA), or else left unstimulated, for 14 days. Supplemental recombinant human IL-2 was added on day 7 (10 U/mL, Life Technologies, Carlsbad, CA). Cells were then stained with both RV-A16 and RV-A39 pMHCII tetramers and re-stimulated with PMA and ionomycin in the presence of Brefeldin A, followed by staining for viability, cell surface markers and intracellular cytokines. Cells were analyzed using a BD LSR Fortessa, and data was analyzed using FlowJo (Tree Star, Ashland, OR). Complex cytokine signatures were analyzed using SPICE version 5.3, downloaded from http://exon.niaid.nih.gov [301].

### *Flow Cytometry Antibodies and Reagents*

Fluorochrome-conjugated monoclonal antibodies for flow cytometry included: anti-CD3 (clone SK7), anti-CD4 (L200), anti-CD14 (MϕP9), anti-CD19 (SJ25C1), anti-CD45RA (HI100), anti-CXCR5 (RF8B2), anti-PD-1 (EH12.1), anti-IL-4 (8D4-8) (BD Biosciences, San Jose, CA); anti-CD4 (clone SK3), anti-CD25 (BC96), anti-CD45RO (UCHL1), anti-IL-7Rα (A019D5), anti-CXCR3 (G025H7), anti-CXCR5 (J252D4), anti-CCR7 (G043H7), anti-IFN-γ (B27), IL-17A (BL168), anti-IL-21 (3A3-N2) (Biolegend, San Diego, CA); anti-CCR4 (clone

205410)(R&D Systems, Minneapolis, MN); anti-CD3 (clone UCTH1), anti-CD4 (OKT4), anti-CD14 (61D3), anti-CD19 (SJ25C1), anti-CD25 (BC96) (eBioscience, San Diego, CA). Aqua viability dye was obtained from Invitrogen (Carlsbad, CA), and compensation beads were obtained from BD Biosciences (San Jose, CA). Anti-PE MicroBeads were obtained from Miltenyi Biotec (Auburn, CA). Fix & Perm solution and Alexa Fluor® 568 Protein Labeling Kits were purchased from Life Technologies (Carlsbad, CA).

### *Statistical Methods*

Percentages of T cells with discrete phenotypes were compared using the Wilcoxon matched-pairs signed rank test for paired analyses, and the Mann-Whitney *U* test for unpaired analyses.

## Results

### *RV Epitopes Bind Multiple HLA Molecules and Are Conserved*

We first sought to identify $CD4^+$ T cells in the blood of healthy subjects, and to interrogate their epitope specificity by TGEM. Two external (VP1 & VP2) and one internal (VP4) capsid protein of RV were selected for analysis. TGEM of RV-A16 was performed in 24 subjects in the context of 8 common HLA-DR molecules that provide ≥80% coverage of the US population, using PBMCs from 24 subjects. This process yielded 45 pMHCII tetramers displaying 30 candidate epitopes from VP1 and VP2 (**Table 2-1**). No epitopes for VP4 were identified. Twelve tetramers provided reliable signals when used for direct *ex vivo* staining of PBMCs (≥2 $tetramer^+$ cells per $10^6$ $CD4^+$ T cells in ≥3 subjects), yielding frequencies up to 247 per $10^6$ $CD4^+$ T cells (**Table 2-1**). Four of these validated tetramers displayed VP1 epitopes (three unique), and eight displayed VP2 epitopes (seven unique). Two of these epitopes ($VP1_{P23}$ and $VP2_{P21}$) bound two different MHC molecules each,

indicating HLA promiscuity. In addition, TGEM of RV-A39 was performed for the common HLA-DR molecule, HLA-DRB1*0401 (HLA-DR4) alone, yielding one epitope each of RV-A39 VP1 and VP2.

All epitopes mapped to regions of VP1 and VP2 that were highly conserved across the 77 strains belonging to RV species A. Specifically, 8 of the 12 RV-A16 and RV-A39 epitopes had ≥85% amino acid sequence identity with ≥88% of all RV-A strains, including three were identical to >50% of RV-A strains (**Table 2-2**)[302]. Although sequence identity was lower with RV-B strains, seven epitopes had 65-95% identity across ≥72% of RV-B strains. As expected, RV-A epitopes had the lowest identity with RV-C strains, which diverge in sequence from RV-A and RV-B species. Nonetheless, sequence similarities of ≥50% were observed for nine of the epitopes. Together, these results confirm that circulating epitope-specific $CD4^+$ T cells detected at the highest frequencies in HLA-diverse subjects recognize conserved epitopes of external capsid proteins, including both species-specific and pan-species varieties.

## Table 2-1. Peptides Containing Candidate Epitopes of RV-A16 VP1 and VP2

| HLA Allele | Epitope | | *In vivo* Frequency (% CD4)* | *Ex vivo* Frequency (# per $10^6$ CD4)† | Validated |
|---|---|---|---|---|---|
| 1*0101 | $VP1_{P18}$ | HIVMQYMYVPPGAPIPTTRN | 3.51, 0, 0 | NA | N |
| | $VP1_{P20}$ | TTRNDYAWQSGTNASVFWQH | 18.7, 0, 0 | NA | N |
| | **$VP1_{P23}$** | **PRFSLPFLSIASAYYMFYDG** | **8.37, 0.35, 2.37** | **6, 15, 6** | **Y** |
| | $VP2_{P12}$ | GIFGENMFYHFLGRSGYTVH | 0.63, 0, 1.23 | NA | N |
| | $VP2_{P22}$ | NWLNFDGTLLGNLLIFPHQF | 0.35, 0, 0 | NA | N |
| | $VP2_{P23}$ | LLGNLLIFPHQFINLRSNNS | 1.6, 3.19, 1.58 | NA | N |
| | **$VP2_{P24}$** | **PHQFINLRSNNSATLIVPYV** | **2.82, 3.17, 11.3** | **17, 148, 26** | **Y** |
| 1*0301 | **$VP2_{P21}$** | **NEKQPSDDNWLNFDGTLLGN** | **1.57, 0.87** | **29, 4, 6** | **Y** |
| | $VP2_{P22}$ | NWLNFDGTLLGNLLIFPHQF | 2.61, 0.75 | NA | N |
| 1*0401 | $VP1_{P14}$ | QIRRKFEMFTYARFDSEITM | 0.59, 0.96 | 4 | N |
| | $VP1_{P18}$ | HIVMQYMYVPPGAPIPTTRN | 0, 0.65 | 2 | N |
| | **$VP2_{P21}$** | **NEKQPSDDNWLNFDGTLLGN** | **5.13, 0.89** | **9, 63, 3** | **Y** |
| | $VP2_{P22}$ | NWLNFDGTLLGNLLIFPHQF | 3.38, 0.89 | 1 | N |
| | $VP2_{P25}$ | SNNSATLIVPYVNAVPMDSM | 0, 0.46 | NA | N |
| 1*0404 | $VP1_{P17}$ | AAKDGHIGHIVMQYMYVPPG | 2.00, 2.99, 2.60 | 112 | N |
| | **$VP1_{P18}$** | **HIVMQYMYVPPGAPIPTTRD** | **1.84, 4.22, 2.76** | **247, 10, 52, 5** | **Y** |
| | **$VP2_{P3}$** | **RGDSTITSQDVANAVVGYGV** | **6.86, 1.61** | **36, 1, 38, 5** | **Y** |
| | $VP2_{P8}$ | TSSNRFYTLDSKMWNSTSKG | 0.77, 1.82 | 2 | N |
| | $VP2_{P15}$ | ASKFHQGTLLVVMIPEHQLA | 0.98, 0.81 | NA | N |
| | $VP2_{P21}$ | NEKQPSDDNWLNFDGTLLGN | 0, 0.65 | NA | N |
| 1*0701 | $VP1_{P15}$ | FTYARFDSEITMVPSVAAKD | 0.26, 0 | NA | N |
| | $VP1_{P16}$ | EITMVPSVAAKDGHIGHIVM | 0.60, 0 | NA | N |
| | **$VP1_{P23}$** | **PRFSLPFLSIASAYYMFYDG** | **1.84, 0.74** | **3, 8, 13, 2** | **Y** |
| | $VP1_{P27}$ | VVTNDMGTLCSRIVTSEQLH | 0, 0.13 | NA | N |
| | $VP1_{P32}$ | RPPRAVQYSHTHTTNYKLSS | O.53, 0 | NA | N |
| | **$VP2_{P26}$** | **VPYVNAVPMDSMVRHNNWSL** | **1.57, 0.84** | **4, 16, 14, 5** | **Y** |
| 1*1101 | $VP1_{P29}$ | EQLHKVKVVTRIYHKAKHTK | 3.35, 2.79 | 0, 3, 0 | N |
| | $VP2_{P1}$ | PSVEACGYSDRIIQITRGDS | 1.59, 1.16, 0.66 | NA | N |
| | **$VP2_{P2}$** | **SDRIIQITRGDSTITSQDVA** | **2.18, 1.22, 2.28** | **8, 11, 15** | **Y** |
| | $VP2_{P8}$ | TSSNRFYTLDSKMWNSTSKG | 0, 0, 0.26 | NA | N |
| | $VP2_{P9}$ | LDSKMWNSTSKGWWWKLPDA | 0.22, 0, 0 | NA | N |
| | $VP2_{P12}$ | GIFGENMFYHFLGRSGYTVH | 1.55, 0, 0.38 | NA | N |
| | $VP2_{P22}$ | NWLNFDGTLLGNLLIFPHQF | 0, 1.31, 0 | NA | N |

| | | | | | |
|---|---|---|---|---|---|
| 1*1501 | VP1$_{P23}$ | PRFSLPFLSIASAYYMFYDG | 0.28, 0.78, 0 | NA | N |
| | VP1$_{P24}$ | SIASAYYMFYDGYDGDTYKS | 0.31, 0, 0 | NA | N |
| | VP2$_{P15}$ | ASKFHQGTLLVVMIPEHQLA | 0.55, 0.53 | NA | N |
| | VP2$_{P16}$ | LLVVMIPEHQLATVNKGNVN | 0, 3 | NA | N |
| | **VP2$_{P25}$** | **SNNSATLIVPYVNAVPMDSM** | **9.02, 2.26** | **31, 5, 13, 71** | **Y** |
| | VP2$_{P30}$ | ISNIVPITVSISPMCAEFSG | 0.46, 0 | NA | N |
| | VP2$_{P31}$ | ITVSISPMCAEFSGARAKTV | 0.37, 0 | NA | N |
| DRB5 | **VP1$_{P21}$** | **QSGTNASVFWQHGQPFPRFS** | **3.91, 0.95** | **11, 28, 20** | **Y** |
| | VP1$_{P22}$ | FWQHGQPFPRFSLPFLSIAS | 3.52, 0.74 | 10, 4 | N |
| | VP1$_{P23}$ | PRFSLPFLSIASAYYMFYDG | 2.03, 2.90 | 11 | N |
| | **VP2$_{P10}$** | **TSKGWWWKLPDALKDMGIFG** | **3.93, 4.49, 0.38** | **60, 24, 136** | **Y** |
| | VP2$_{P24}$ | PHQFINLRSNNSATLIVPYV | 0, 0.67, 0 | NA | N |

Validated epitopes are shown in bolded font. *Based on percentage of $CD4^+$ T cells that were $tetramer^+$ in PBMC cultures stimulated with corresponding peptide pools (n=24). †Based on frequency of $tetramer^+$ $CD4^+$ T cells stained directly *ex vivo*, without peptide culture (n=29). NA, not applicable.

## Table 2-2. Sequence Similarity Between RV Epitopes and RV Strains Belonging to Species A, B, and C

| | Epitope | RV-A | | | | | RV-B | | RV-C | |
|---|---|---|---|---|---|---|---|---|---|---|
| | | 100% | 99-95% | 94-90% | 89-85% | Sum | Total | Range | Total | Range |
| RV-A16 | $VP2_{P3}$ RGDSTITSQDVANAVVGYGV | 40/77 (51.9%) | 17/77 (22.1%) | 10/77 (13.0%) | 7/77 (9.1%) | 74/77 (96.1%) | 10/29 (34.5%) | 72-67% | 1/51 (2.0%) | 72% |
| RV-A16 | $VP2_{P2}$ SDRIIQITRGDSTITSQDVA | 50/77 (64.9%) | 8/77 (10.4%) | 13/77 (16.9%) | 2/77 (2.6%) | 73/77 (94.8%) | 23/29 (79.3%) | 65% | 21/51 (41.2%) | 78-72% |
| RV-A16 | $VP1_{P23}$ PRFSLPFLSIASAYYMFYDG | 39/77 (50.6%) | 14/77 (18.2%) | 3/77 (3.9%) | 17/77 (22.1%) | 73/77 (94.8%) | 21/29 (72.4%) | 74-68% | 7/51 (13.7%) | 70-65% |
| RV-A16 | $VP2_{P26}$ VPYVNAVPMDSMVRHNNWSL | 8/77 (10.4%) | 53/77 (68.8%) | 5/77 (6.5%) | 6/77 (7.8%) | 72/77 (93.5%) | 23/29 (79.3%) | 82-71% | 7/51 (13.7%) | 76-70% |
| RV-A16 | $VP2_{P10}$ TSKGWWWKLPDALKDMGIFG | 31/77 (40.3%) | 33/77 (42.9%) | 1/77 (1.3%) | 7/77 (9.1%) | 72/77 (93.5%) | 21/29 (72.4%) | 95-84% | 4/51 (7.8%) | 89-79% |
| RV-A16 | $VP2_{P24}$ PHQFINLRSNNSATLIVPYV | 7/77 (9.1%) | 43/77 (55.8%) | 12/77 (15.6%) | 8/77 (10.4%) | 70/77 (90.9%) | 23/29 (79.3%) | 85-70% | 7/51 (13.7%) | 75-70% |
| RV-A16 | $VP2_{P25}$ SNNSATLIVPYVNAVPMDSM | 7/77 (9.1%) | 59/77 (76.6%) | 4/77 (5.2%) | 0/77 (0.0%) | 70/77 (90.9%) | 22/29 (75.9%) | 84-68% | 7/51 (13.7%) | 74-68% |
| RV-A16 | $VP1_{P21}$ QSGTNASVFWQHGQPFPRFS | 2/77 (2.6%) | 16/77 (20.8%) | 21/77 (27.3%) | 29/77 (37.7%) | 68/77 (88.3%) | 0/29 (0.0%) | NA | 0/51 (0.0%) | NA |
| RV-A16 | $VP2_{P21}$ NEKQPSDDNWLNFDGTLLGN | 17/77 (22.1%) | 5/77 (6.5%) | 20/77 (26.0%) | 9/77 (11.7%) | 51/77 (66.2%) | 6/29 (20.7%) | 89% | 0/51 (0.0%) | NA |
| RV-A16 | $VP1_{P18}$ HIVMQYMYVPPGAPIPTTRD | 1/77 (1.3%) | 3/77 (3.9%) | 8/77 (10.4%) | 28/77 (36.4%) | 40/77 (51.9%) | 3/29 (10.3%) | 79-54% | 0/51 (0.0%) | NA |
| RV-A39 | $VP1_{P14}$ AQVRRKFEMFTYVRFDSEIT | 1/77 (1.3%) | 10/77 (13.0%) | 24/77 (31.2%) | 27/77 (35.1%) | 62/77 (80.5%) | 8/29 (27.6%) | 80-75% | 5/51 (9.8%) | 90-80% |
| RV-A39 | $VP2_{P60}$ SDDNWLNFDGTLLGNLLIFP | 5/77 (6.5 %) | 13/77 (16.9%) | 20/77 (26.0%) | 17/77 (22.1%) | 55/77 (71.4%) | 24/29 (82.8%) | 70-5-% | 6/51 (11.8%) | 60-50% |

Values denote the number of RV-A types with the given amino acid sequence identities, with percentages in parentheses. For species B and C, the total number of strains within the top 5000 hits and their corresponding range of amino acid identities are given. Peptides are listed from highest to lowest sum sequence identity for RV-A. The total number of RV types within each species is based on classification of McIntyre et al. [302]. NA, not applicable.

### *HLA Class I and II Binding Hotspots Localize to Conserved Regions of VP1 and VP2*

There was good agreement between $CD4^+$ T cell epitopes identified by TGEM and those predicted by *in silico* methods. At least one consensus 15mer epitope was predicted for each TGEM epitope in the context of its relevant HLA molecule using the IEDB consensus method (**Table 2-3**). This algorithm accounts for the contribution of flanking residues to HLA binding [290–294]. Furthermore, 13 of the 14 predicted consensus epitopes had a percentile rank in the top 10% of results, indicating strong predicted binding. Predicted 9mer core epitopes localized to molecular regions that were conserved across RV-A strains (**Figure 2-1**). Core epitopes of $VP1_{P23}$ and $VP2_{P10}$ were the most highly conserved within the picornavirus family (**Figure 2-1**).

To assess the contribution of peptide length to $CD4^+$ T cell epitopes, we used an algorithm that predicts 9mer core epitopes for HLA supertypes encompassing 1077 class I and class II molecules without accounting for the contribution of flanking residues (MULTIPRED2)[295]. By this method, only two 9mer $CD4^+$ T cell epitopes corresponding to any TGEM epitope were identified. These epitopes were nested within $VP1_{P23}$ (aa 187-195) and $VP2_{P24}$ (aa 189-197), and were predicted to bind to those HLA molecules displaying the corresponding TGEM epitopes (i.e. *0101 and *0701 for $VP1_{P23}$, and *0101 for $VP2_{P24}$), as well as >80% of molecules of the corresponding HLA supertype (**Table 2-3** & **Figure 2-2**). No 9mer epitopes for VP4 were predicted by this method (*data not shown*). By contrast, 12 of the 14 epitopes predicted by TGEM were predicted using a 19mer input for the same algorithm (**Table 2-3**).

Because $CD8^+$ T cells are central to anti-viral immunity, we next queried whether RV-A16 epitopes might also provide a target for $CD8^+$ T cells. Using MULTIPRED2, we predicted a high density of MHC class I binding motifs for HLA-A, -B, and –C supertypes spanning two regions, designated A (VP1 aa 140-200) and B (VP2 aa 160-200) (**Figure 2-2**). Regions A and B also contained multiple $CD4^+$ T cell epitopes identified by TGEM and predicted binding motifs for common and less common HLA-DR supertypes (**Figure 2-2**). Motifs were predicted for molecules belonging to all HLA class I supertypes, including >55% of all molecules within most HLA-A and HLA-B supertypes. Together, these results confirm the potential for conserved epitopes of RV capsid proteins to bind a broad array of HLA molecules, and to activate both $CD4^+$ and $CD8^+$ T cells.

**Table 2-3. Predicted MHCII Binding of TGEM Epitopes of RV VP1 & VP2**

| | HLA Allele | Epitope | | Amino Acid Position | Consensus Rank | NetMHCIIpan 9mer $IC_{50}$ | NetMHCIIpan 19mer $IC_{50}$ |
|---|---|---|---|---|---|---|---|
| RV-A16 | 1*0101 | $VP1_{P23}$ | PRFSLPFLSIASAYYMFYDG | 181-200 | **1.58** | **172.97** | **5.67** |
| | | $VP2_{P24}$ | PHQFINLRSNNSATLIVPYV | 186-205 | **3** | **181.55** | **8.98** |
| | 1*0301 | $VP2_{P21}$ | NEKQPSDDNWLNFDGTLLGN | 162-181 | **1.03** | 4370.08 | **302.6** |
| | 1*0401 | $VP2_{P21}$ | NEKQPSDDNWLNFDGTLLGN | 162-181 | **3.81** | 5426.27 | 549.54 |
| | 1*0404 | $VP1_{P18}$ | HIVMQYMYVPPGAPIPTTRD | 141-160 | **0.17** | 6965.00 | **151.24** |
| | | $VP2_{P3}$ | RGDSTITSQDVANAVVGYGV | 18-37 | 12.10 | 10711.98 | **459.38** |
| | 1*0701 | $VP1_{P23}$ | PRFSLPFLSIASAYYMFYDG | 181-200 | **1.41** | **475.46** | **14.74** |
| | | $VP2_{P26}$ | VPYVNAVPMDSMVRHNNWSL | 202-221 | **3.75** | 6153.57 | **287.34** |
| | 1*1101 | $VP2_{P2}$ | SDRIIQITRGDSTITSQDVA | 10-29 | **1.33** | 3995.77 | 696.30 |
| | 1*1501 | $VP2_{P25}$ | SNNSATLIVPYVNAVPMDSM | 194-213 | **6.64** | 9592.89 | **298.16** |
| | DRB5 | $VP1_{P21}$ | QSGTNASVFWQHGQPFPRFS | 165-184 | **1.02** | 2664.32 | **38.55** |
| | | $VP2_{P10}$ | TSKGWWWKLPDALKDMGIFG | 74-93 | **2.85** | 1218.18 | **91.2** |
| RV-A39 | 1*0401 | $VP1_{P14}$ | AQVRRKFEMFTYVRFDSEIT | 105-124 | **2.36** | 4512.74 | **364.91** |
| | | $VP2_{P60}$ | SDDNWLNFDGTLLGNLLIFP | 169-188 | **3.81** | 5426.27 | **222.37** |

Epitopes were identified and validated by TGEM, and predicted 9mer cores and binding constants were generated using *in silico* approaches (IEDB Consensus, NetMHCIIpan). Predicted 9mer binding cores are underlined. Bolded values meet defined criteria for predicted MHCII binding (IEDB Consensus Rank ≤10; NetMHCIIpan $IC_{50}$ >500).

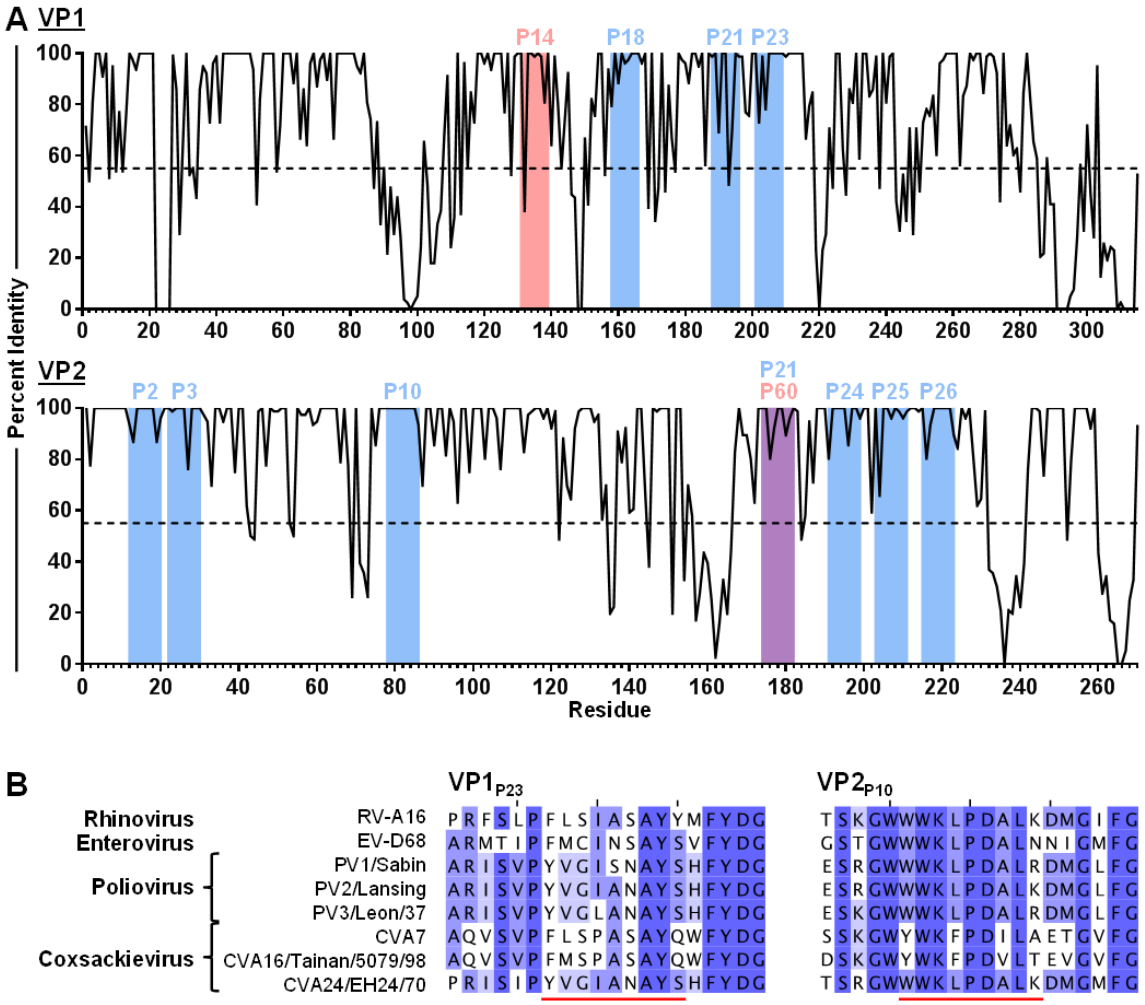


**Figure 2-1. Core Epitopes Displayed by Validated RV pMHCII Tetramers Map to Conserved Regions of Capsid Proteins**

**(A)** Location of predicted core epitopes within RV VP1 and VP2 amino acid sequences. The sequence identity for all 77 RV-A strains is depicted by the solid black line, while blue shading denotes the location of RV-A16 core epitopes, and red the RV-A39 core epitopes.

**(B)** Sequence alignment of RV-A16 $VP1_{P23}$ and $VP2_{P10}$ with non-RV picornavirus family members. Shading denotes degree of sequence identity, while red lines denote the predicted core epitopes.

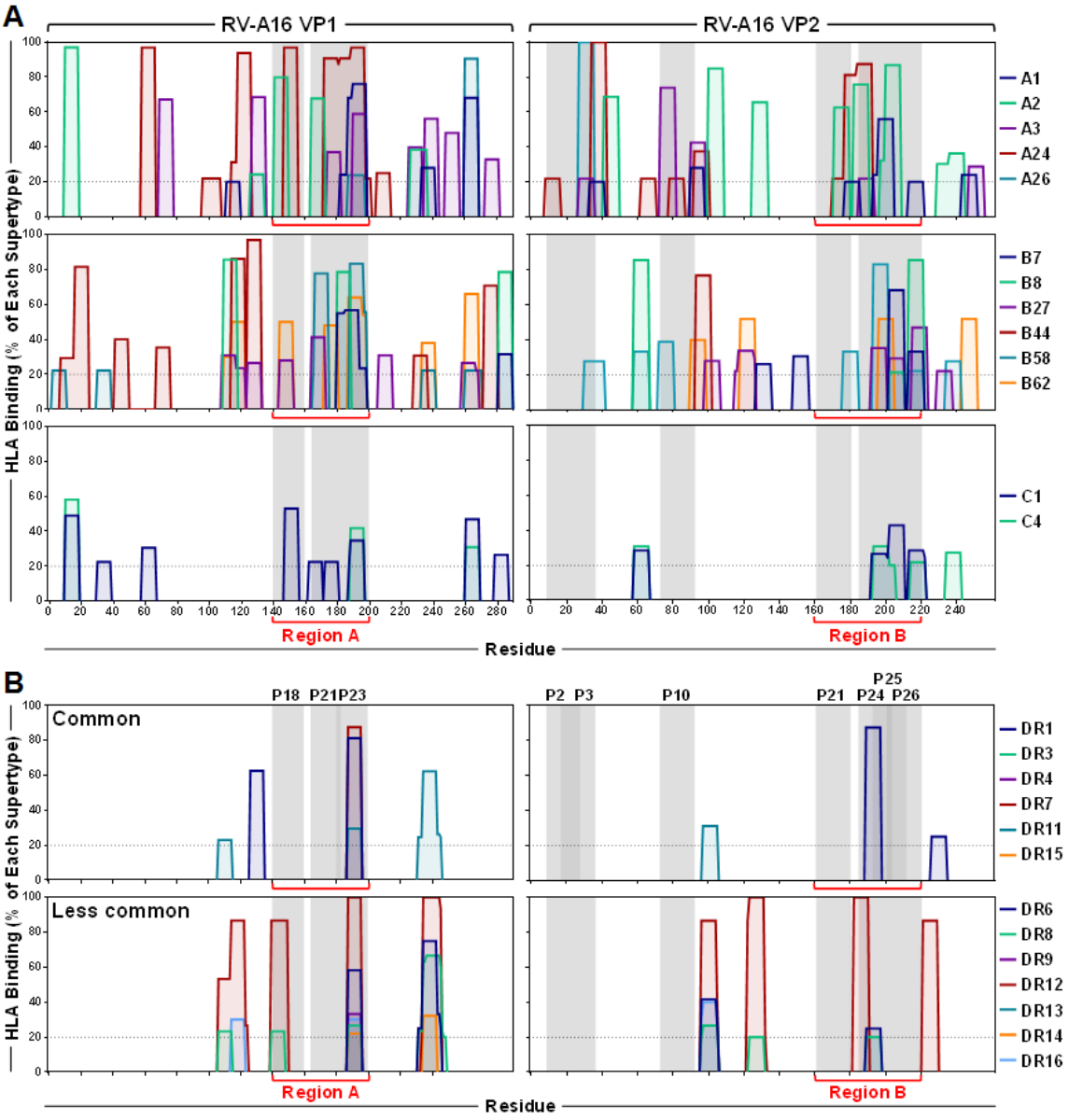


**Figure 2-2. HLA Class I and II Binding Hotspots Localize to Conserved Regions of VP1 and VP2 Capsid Proteins**

Epitope binding to HLA class I and II supertypes was analyzed for RV-A16 VP1 and VP2 using MULTIPRED2. The percentage binding is shown for **(A)** the major MHC class I supertypes, HLA-A, -B, and –C; and **(B)** common MHC class II DRB1 supertypes used in TGEM studies, and less common DRB1 supertypes. Epitopes with predicted binding to ≥20% of molecules from each supertype (dotted line) are shown. $IC_{50}$ threshold ≤500nM.

### *VP1 Epitopes of RV-A16 Map to the Hydrophobic Binding Pocket*

The existence of conserved T cell epitopes might seem to contradict the selective pressures that drive antigenic diversity of RV species. Thus, we explored whether T cell epitopes mapped to regions of functional significance for the virus. Analyses in the context of the oligomeric subunit formed by the capsid proteins VP1-4 revealed that all T cell epitopes contained residues exposed on the external and/or internal surfaces of the viral capsid (**Figure 2-3**). In addition, most epitopes mapped to the interface of adjacent oligomeric subunits.

Most RV-A and RV-B strains gain entry into host cells via surface ICAM-1, whereas RV-C uses an alternate mode of entry [30,44,303,304]. ICAM-1 binds in a canyon within VP1 containing a hydrophobic binding pocket, which is occupied by a pocket factor that regulates viral entry, uncoating, and assembly [300]. Positional analyses in the context of the three-dimensional structure of VP1-4 revealed that each VP1 epitope mapped to the hydrophobic binding pocket of RV-A16, with two residues of the $VP1_{P18}$ core epitope ($Pro^{1146}$ and $Tyr^{1144}$) residing close to the pocket factor (**Figure 2-3**)[300,305].

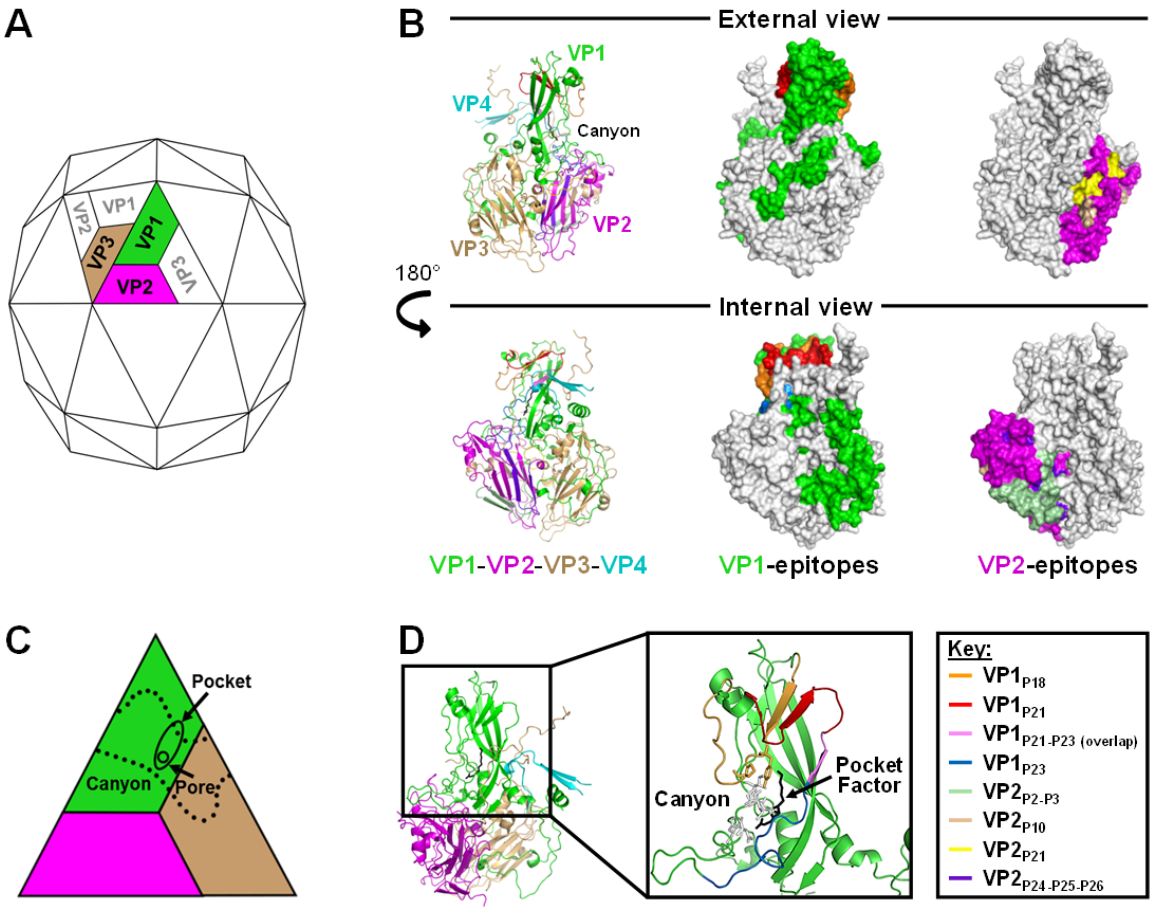


**Figure 2-3. Position of RV-A16 T Cell Epitopes Within the Capsid Structure**

**(A)** Assembly of protomers to form the RV capsid. VP1, 2, and 3 are external, while VP4 is internal. **(B)** Position of epitopes on the external and internal aspects of the RV capsid protomer. T cell epitopes are colored according to the given key. **(C)** Footprint of the canyon within a triangular capsid subunit composed of VP1+VP2 from one protomer and VP3 from the adjacent protomer. Schematic adapted from [45]. **(D)** Location of canyon and pocket binding factor within one protomer viewed from the capsid interior. Expanded view depicts VP1 only for simplicity. Residues with an atom within 4 Å of the pocket factor are depicted as white sticks (Ile$^{1098}$, Asn$^{1099}$, Leu$^{1100}$, Asn$^{1212}$, Met$^{1214}$, His$^{1260}$)[300]. Residues associated with the binding pocket are shown in orange (Tyr$^{1144}$ & Pro$^{1146}$). Lauric acid, a representative pocket factor, is shown as a black stick model.

### *Pre-Existing Epitope-Specific CD4⁺ T Cells Display $T_H$1 Signatures*

Repeated T cell priming by previous RV infections caused by different strains would be expected to induce circulating memory $CD4^+$ T cell populations that preferentially target conserved RV epitopes at higher numbers than those recognizing less well-conserved regions of capsid proteins. Consistent with this theory, direct *ex vivo* analysis of untouched $tetramer^+$ cells in 29 healthy revealed robust frequencies of up to 247 $tetramer^+$ cells per $10^6$ $CD4^+$ T cells (**Figure 2-4**). These cells had a predominant memory phenotype (>60% $CD45RA^-$) and displayed a $T_H1$ signature ($CXCR3^+$, $CCR4^-$) that was uniform across all epitope specificities. $Tetramer^+$ cells included a $CXCR5^+$ subset, suggesting the presence of T follicular helper ($T_{FH}$) cells with lymph node-homing capabilities (**Figure 2-4**).

### *Evidence of T Cell Cross-Reactivity at the Epitope Level*

Finally, we sought to identify cross-reactive T cell epitopes between different RV strains. As previously stated, TGEM yielded T cell epitopes for both RV-A16 and RV-A39 VP2 capsid proteins for HLA-DR4 (RV-A16: $VP2_{P21}$; RV-A39: $VP2_{P60}$), which contain corresponding core epitopes (**Table 2-3** & **Figure 2-1**). By contrast, no RV-A16 counterpart was identified for the RV-A39 VP1 epitope. Stimulating cells from $HLA\text{-}DR4^+$ subjects with RV-A39 $VP2_{P60}$ induced expansion of T cells specific for RV-A16 $VP2_{P21}$, despite different flanking residues (**Figure 2-5**). Expanded RV-specific T cells were predominantly $IFN\text{-}\gamma^+$ $IL\text{-}4^-$, consistent with a dominant $T_H1$ subset. Minor populations expressing the $T_H17$-associated cytokine IL-17A, and the $T_{FH}$-associated cytokine IL-21, were also identified (**Figure 2-5**). These findings establish proof-of-concept for cross-reactive $CD4^+$ T cell determinants between different strains.

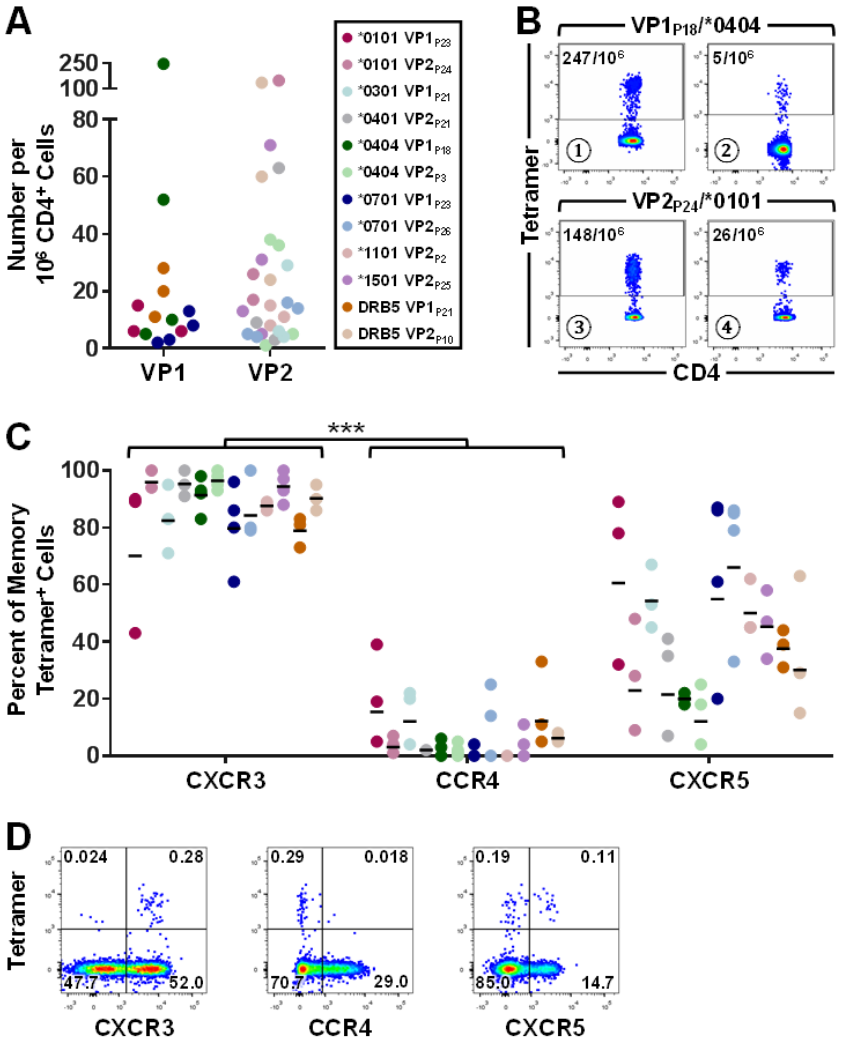


**Figure 2-4. Pre-Existing Epitope-Specific Memory Cells Display $T_H1$ and $T_{FH}$ Signatures**

**(A)** Frequencies of RV-specific $CD4^+$ T cells determined by direct *ex vivo* staining with tetramer for each TGEM epitope (n=29, 3-4 subjects per tetramer). **(B)** Representative data showing tetramer$^+$ T cells within the $CD4^+$ T cell gate stained with $VP1_{P18}$/*0404 and $VP2_{P24}$/*0101 tetramers in four subjects with high and low T cell frequencies. **(C)** Surface phenotype of tetramer$^+$ memory ($CD45RA^-$) $CD4^+$ T cells analyzed directly *ex vivo*. Bars denote geometric means. **(D)** Representative data from one subject showing expression of surface markers on memory $CD4^+$ T cells. ***$p \leq 0.001$.

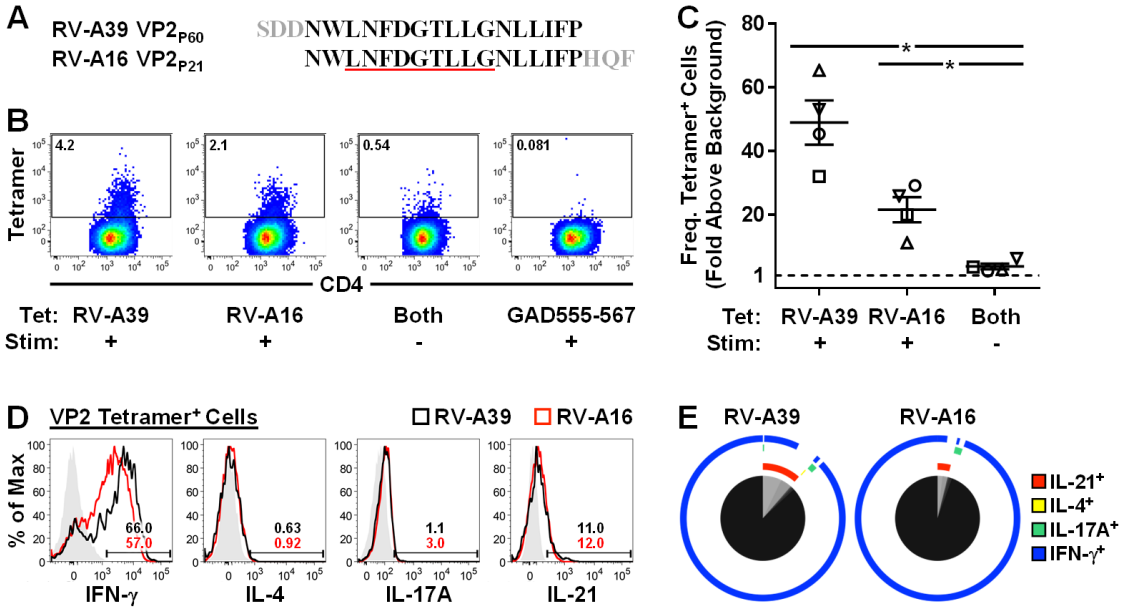


**Figure 2-5. Proof-of-Concept of T Cell Cross-Reactivity at the Epitope Level**

**(A)** Alignment of corresponding RV-A39 and RV-A16 HLA-DR4-restricted epitopes of VP2. Predicted core epitopes are underlined. Gray residues denote different flanking residues. **(B)** Scatterplots showing representative tetramer staining. **(C)** Cells from four HLA-DR4$^{+}$ seronegative subjects were either stimulated with RV-A39 VP2$_{P60}$ (+) or unstimulated (–) for 14 days. Cells were then stained with tetramers displaying RV-A39 VP2$_{P60}$ or RV-A16 VP2$_{P21}$. Stimulated cells stained with tetramers displaying an irrelevant peptide (GAD$_{555\text{-}567}$) provided a negative control. Frequencies of tetramer$^{+}$ T cells are shown relative to numbers obtained using the control tetramer. Bars denote means ± SEM. *p≤0.05. **(D)** Representative histograms showing cytokine expression in RV-A39 and RV-A16 VP2-specific CD4$^{+}$ T cells after culture. Shaded histograms denote fluorescence-minus-one (FMO) controls. **(E)** Average cytokine profiles for RV-A39 and RV-A16 VP2-specific CD4$^{+}$ T cells after stimulation with RV-A39 VP2$_{P60}$ analyzed by SPICE (n=4). Each pie slice denotes a discrete T cell phenotype, and colored arcs denote each cytokine in relation to each phenotype.

## Discussion

By integrating *in vitro* and *in silico* epitope mapping approaches, we have constructed a comprehensive map of $CD4^+$ T cell epitopes of the RV capsid proteins VP1 and VP2. Our strategy allowed the identification of immunologically relevant epitopes in the context of multiple HLA molecules and characterization of cognate $CD4^+$ T cells. We report that those circulating RV-specific memory $CD4^+$ T cells present at the highest frequencies in HLA-diverse subjects recognize a limited set of species-specific and pan-species epitopes. Our ability to readily identify circulating virus-specific memory T cells in healthy subjects supports the view that these T cells arise from repeated previous infections with homotypic or heterotypic RV strains or related viruses. Pre-existing cells included $T_H1$ effectors and $T_{FH}$ cells, both of which would be expected to contribute to viral clearance through cytolysis and by helping B cells produce antibodies [306–308].

TGEM provides a sensitive and comprehensive approach for identifying T cell epitopes restricted to a specific HLA molecule [309]. Our study design involved several analytical steps, including identification of T cell epitopes *in vitro* using peptide-stimulated cultures established from subjects with known HLA type, followed by validation by direct *ex vivo* staining of cells in additional subjects. The immunodominance of these epitopes was supported by the reliable detection of RV-specific $CD4^+$ T cells specific for each of the validated epitopes in the context of 8 HLA-DR molecules, covering >80% of the general population. Indeed, RV-specific T cells targeting the same HLA-DR4-restricted epitope were readily detected in 11 HLA-$DR4^+$ subjects included in our study. The ability for computer algorithms to predict those $CD4^+$ T cell epitopes identified by TGEM further supported their significance. Moreover, enrichment of a broad array of class I HLA binding motifs

within TGEM epitopes highlighted their potential to activate $CD8^+$ T cells in tandem with $CD4^+$ T cells. A major advantage of our approach as compared with other epitope mapping methods—such as ELISPOT, intracellular cytokine assays, or proliferation assays—is that the identified epitopes identified by TGEM are proven to bind to specific MHC molecules. In addition, TGEM is highly sensitive based on its ability to detect cell frequencies as low as 1 in 300,000 $CD4^+$ T cells [309,310]. Assay sensitivity is critical, given the low precursor frequency of antigen-specific $CD4^+$ T cells in the T cell repertoire and their random distribution in tissue culture wells. Thus, less-sensitive methods such as ELISPOT often warrant the use of statistical modeling to confirm immunodominance [311]. Subsequent to the publication of our results, Gaido et al. confirmed two of our four TGEM epitopes using proliferation assays [312].

The T cell frequencies observed in this chapter were within the range of those reported using pMHCII tetramers for other viral epitopes in the absence of current exposure, including those present several years after vaccination [313,314]. Because TGEM preferentially selects for T cell epitope specificities that exist at the highest frequencies, our results imply selective persistence of T cells directed against conserved epitopes. This is consistent with iterative priming of specific memory T cells by epitopes common to multiple RV strains. In line with this theory, we provided proof-of-concept for shared T cell epitopes among different RV strains. This observation was significant given that corresponding HLA-DR4-restricted epitopes were identified in separate TGEM experiments using different peptide libraries, spanning VP2 of RV-A16 and RV-A39. Our inability to identify a match from RV-A16 for an HLA-DR4-restricted VP1 epitope of RV-A39 is likely explained by differences in sequence within the 9mer core epitope.

Positioning of T cell epitopes within structural elements that interact with ICAM-1 and at protein interfaces that are likely involved in capsid protein assembly might provide a structural basis for the conservation of RV epitopes. Interestingly, no T cell epitopes of the small capsid protein VP4 were identified by TGEM, and this was borne out by *in silico* analyses. VP4 is highly conserved across different RV strains and is the only capsid protein that resides completely on the internal aspect of the capsid [315]. Although it would seem that VP4 should provide an attractive target for cross-reactive T cells based on its sequence conservation, its lack of MHCII binding motifs likely precludes MHC binding and the induction of cognate T cells. Recent work has shown that VP4 separates from the capsid during viral cell entry to form multimeric pores within the host cell membrane that facilitate transmembrane transport of the viral genome [316]. This aspect, which is presumably critical to viral pathogenesis, might explain its highly conserved nature. Regardless, failure to detect VP4 epitopes lends credence to the importance of the external capsid proteins VP1 and VP2 as immunogenic antigens that promote durable $CD4^+$ T cell responses.

It has been known for decades that serum neutralizing antibodies induced by RV infection protect against re-infection with the same strain [48,49,275,277]. However, attempts to develop cross-protective antibody-based vaccines have been disappointing due to the high degree of antigenic among the numerous identified RV serotypes [76,280]. By contrast, recent work in mice immunized with conserved capsid protein antigens has provided proof-of-concept for the capacity to induce cross-reactive immune responses driven by $CD4^+$ T cells [52]. There are several lines of evidence to support a protective role for $CD4^+$ T cells in RV infections in humans. For example, RV-specific $CD4^+$ T cell clones produce IFN-γ and proliferate in response to stimulation with multiple RV serotypes

[65,317]. Moreover, higher proliferation and IFN-γ responses before RV infection have been linked to reduced viral shedding after inoculation [64].

In this chapter, we have identified conserved $CD4^+$ T cell epitopes of RV capsid proteins that cluster into HLA binding hotspots. These peptides, which span narrow molecular regions, will not only provide a valuable tool for evaluating T cell responses to RV in humans, but could also inform the design of peptide vaccines designed to boost T cell immunity to multiple RV strains. Further elucidation of the complexity and function of RV-specific T cells and their relationship to clinical and immune outcomes following infection is warranted.

*This chapter was adapted from: L Muehling*, D Mai*, W Kwok, P Heymann, A Pomés, J Woodfolk. "Circulating memory $CD4^+$ T cells target conserved epitopes of rhinovirus capsid proteins and respond rapidly to experimental infection in humans." J Immunol (2016). *Equal contribution.*

*&*

*L Muehling, R Turner, K Brown, P Wright, J Patrie, S Lahtinen, M Lehtinen, W Kwok, J Woodfolk. "Single-cell tracking reveals a role for pre-existing $CCR5^+$ memory $T_H1$ cells in the control of rhinovirus-A39 after experimental infection in humans." J Infect Dis (2018).*

# Chapter 3 — A Role for Pre-Existing CCR5$^+$ Memory $T_H1$ Cells in the Control of Rhinovirus-A39 in Healthy Individuals

## Introduction

As previously discussed, although the common cold poses a significant public health and economic burden, there are currently no effective treatments for rhinovirus infection, and attempts at vaccine development have failed [76,280]. Despite several decades of study, knowledge of adaptive immunity to RV remains nascent. Neutralizing antibody responses are known to prevent re-infection with the same strain; however, they are not cross-protective [21,23,47,48,50,275]. The induction of neutralizing antibodies during infection and the presence of serum IgG antibodies specific for RV capsid proteins each indicate a requirement for T cell help [41,53]. This is bolstered by identification of RV-specific CD4$^+$ T cell clones that secrete IFN-γ and the presence of IFN-γ$^+$ CD4$^+$ T cells in the bronchoalveolar lavage of asthmatics undergoing experimental RV challenge [65,244]. In **Chapter 2**, we report the identification of immunodominant CD4$^+$ T cell epitopes of RV capsid proteins, VP1 and VP2.

In this chapter, we describe the use of pMHCII tetramers to precisely track RV-specific CD4$^+$ T cells and assess their relationship to infection profiles after intranasal challenge with RV-A39. Owing to inherent variability in the response to RV in humans, we sought to monitor only those T cells with identical epitope specificities. To accomplish this, we recruited HLA-DR4$^+$ subjects within a large cohort of subjects who participated in a clinical trial of probiotic supplementation for the common cold [318,319]. Our findings support a key role for CCR5$^+$ $T_H1$ effectors in the control of RV infection.

## Materials and Methods

### *Human Subjects and RV-A39 Experimental Challenge Study*

Subjects expression the common allele HLA-DR4 were identified by HLA typing a large cohort enrolled in a randomized double-blind placebo-controlled trial of probiotic supplementation for common cold using *Bifidobacterium animalis* subsp. *lactis* (Bl-04) at the University of Virginia Medical Center (NCT01669603) (**Table 3-1** & **Figure 3-1**). All subjects were healthy with no history of allergic or respiratory diseases, and were seronegative for the challenge strain (RV-A39, serum neutralizing antibody titer [NAT] ≤1:4). Informed consent was obtained from all study participants, and research was approved by the UVA Human Investigation Committee.

Details of the parent challenge study have previously been published [319]. Briefly, subjects were randomized to receive either Bl-04 probiotic or placebo daily for 28 days prior to RV inoculation, continuing for 4 days post-inoculation. Subjects were inoculated 100 $TCID_{50}$ RV-A39 split between both nostrils (FDA-BB-IND #12934), and subjects were followed for 21 days following inoculation. Sixteen healthy HLA-$DR4^+$ subjects (ages 18-60 years) completed RV challenge. Blood was obtained from study subjects before treatment (day -28), before RV-A39 challenge (day 0), and during acute and convalescent infection (days 5 and 21) (**Figure 3-1**). Nasal wash specimens for T cell studies were analyzed from an additional eight HLA-diverse subjects on day 5 of RV-A39 challenge, and additional healthy HLA-$DR4^+$ subjects not undergoing RV challenge were recruited for functional studies.

**Table 3-1. Characteristics of Study Subjects**

| | HLA-DR4$^+$ Subjects (n=16) |
|---|---|
| **Female Gender [n (%)]** | 12 (75%) |
| **Race [n (%)]** | |
| **Asian** | 0 (0%) |
| **Black** | 0 (0%) |
| **White** | 15 (94%) |
| **Other** | 1 (6%) |
| **Ethnicity [n (%)]** | |
| **Hispanic** | 1 (6%) |
| **Non-Hispanic** | 14 (88%) |
| **Unknown** | 1 (6%) |
| **Age [yrs, mean (SD)]** | 21.25 (3.7) |

**[Next] Figure 3.1. Study Design and Subject Enrollment**

**(A)** Schematic depicting the experimental model of probiotic supplementation with RV-A39 challenge. **(B)** Consort diagram depicting the enrollment of HLA-DR4$^+$ subjects who tested seronegative for RV-A39 at screening and completed a double-blind placebo-controlled study of probiotic supplementation for the common cold.

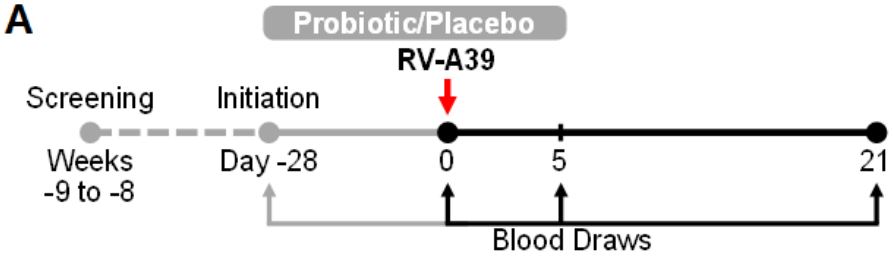
A
Probiotic/Placebo
RV-A39
Screening
Initiation
Weeks
-9 to -8
Day -28
0
5
21
Blood Draws

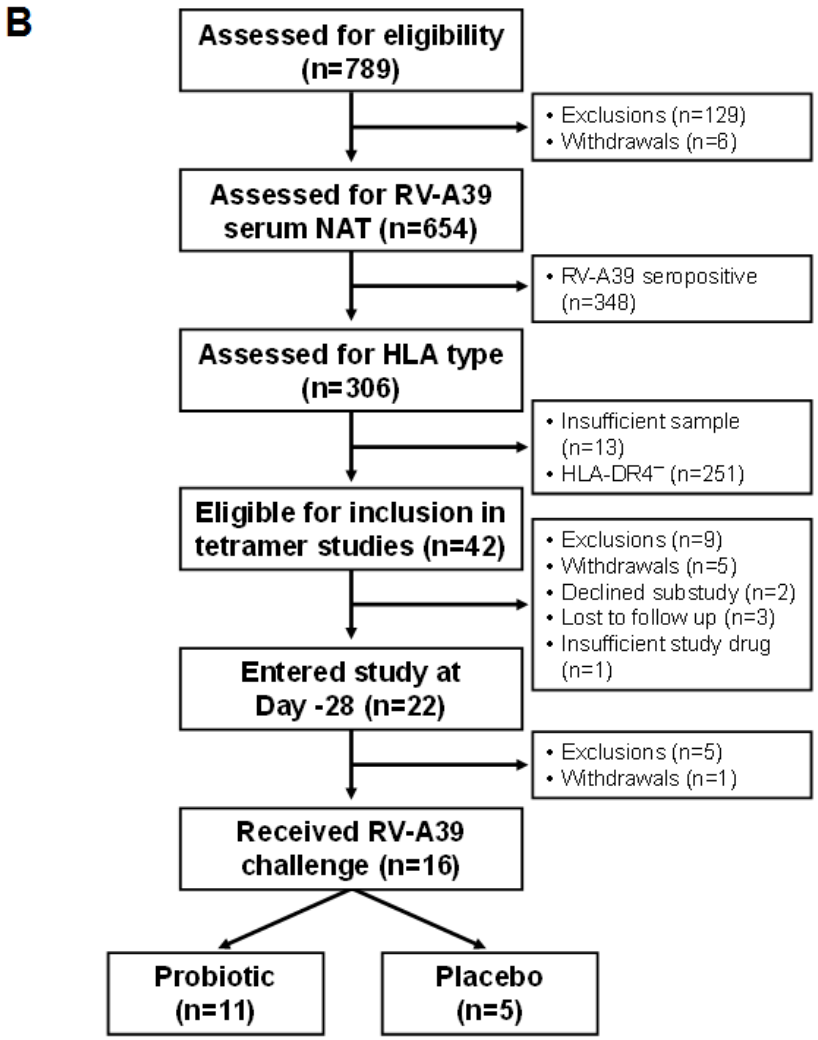
B
Assessed for eligibility (n=789)
• Exclusions (n=129)
• Withdrawals (n=6)
Assessed for RV-A39 serum NAT (n=654)
• RV-A39 seropositive (n=348)
Assessed for HLA type (n=306)
• Insufficient sample (n=13)
• HLA-DR4⁻ (n=251)
Eligible for inclusion in tetramer studies (n=42)
• Exclusions (n=9)
• Withdrawals (n=5)
• Declined substudy (n=2)
• Lost to follow up (n=3)
• Insufficient study drug (n=1)
Entered study at Day -28 (n=22)
• Exclusions (n=5)
• Withdrawals (n=1)
Received RV-A39 challenge (n=16)
Probiotic (n=11)
Placebo (n=5)

### *Assessment of Viral Exposure and Infection Status*

As a component of the parent study screening process, serum was obtained during subject screening (8-9 weeks prior to RV challenge), as well as at days 0 and 21. RV-A39-specific serum NAT were determined using standard microtiter assays [51]. Nasal washes were performed on days 1-5 of infection, and were assessed for RV-A39 viral titer using a semi-quantitative culture assay [51]. Subjects were considered to be infected if they had a ≥4-fold increase in RV-A39 NAT at day 21 as compared with day 0, and/or if RV-A39 was identified in at least one nasal wash. Natural exposure to respiratory viruses including related rhinovirus/enterovirus species prior to RV challenge was assessed in day 0 nasal washes by polymerase chain reaction (PCR) (Luminex xTag® Respiratory Virus Panel, Austin, TX).

### *Flow Cytometric Analysis of Tetramer⁺ Cells*

Tetramer staining was performed as described in **Chapter 2**, both for direct *ex vivo* staining and for intracellular cytokine staining following *in vitro* peptide culture. Virus-specific cells were identified using two RV-A39 tetramers displaying conserved epitopes of VP1 and VP2 (see **Chapter 2**).

Unsupervised high-dimensional analysis of flow cytometry data was performed using a t-distributed stochastic neighbor embedding (t-SNE) algorithm via ACCENSE and Cytobank (http://cytobank.org) [320,321]. Expression of CD45RO, CCR7, CCR5, CD25, and IL-7Rα were used to generate t-SNE plots. Complex cytokine signatures were analyzed using SPICE version 5.3, as described in **Chapter 2** [301].

### *Analysis of Cytokines and CD4+ T Cells in Nasal Wash Specimens*

Cytokines were analyzed in day 0 and 4 nasal washes by multiplex assay (TGFβ, G-CSF, GM-CSF, IFN-γ, IL-1α, IL-12p70, IL-15, MIP-3α, IL-1β, IL-6, IP-10, MCP-1, MIP1α, and TNFα; Aushon BioSystems, Inc., Billerica, MA). IL-8 was assessed by an enzyme-linked immunosorbent assay (ELISA) (R&D Systems, Minneapolis, MN).

To analyze nasal T cells in day 5 nasal washes, mucus was gently dissociated with warm phosphate-buffered saline (PBS) and filtered through a 35-μm nylon mesh filter (Corning Life Sciences, Corning, NY). Cells were stained for viability and surface markers as described in **Chapter 2**, before analysis by an LSRFortessa (BD Biosciences, San Jose, CA).

### *Flow Cytometry Antibodies and Reagents*

Fluorochrome-conjugated monoclonal antibodies were used for flow cytometry, and were as follows: anti-CD3 (clone SK7), anti-CD14 (MφP9), anti-CD19 (SJ25C1), anti-CD183/CXCR3 (1C6/CXCR3), anti-CD195/CCR5 (2D7/CCR5), anti-CD279/PD-1 (EH12.1), anti-IL-4 (8D4-8) (BD Biosciences, San Jose, CA); anti-CD4 (SK3), anti-CD25 (BC96), anti-CD45RO (UCHL1), anti-CD127/IL-7Rα (A019D5), anti-CD185/CXCR5 (J252D4), anti-CD194/CCR4 (L291H4), anti-CD197/CCR7 (G043H7), anti-IFN-γ (B27), anti-IL-17A (BL168), anti-IL-21 (3A3-N2) (Biolegend, San Diego, CA). Compensation beads were purchased from BD Biosciences, and aqua viability dye was purchased from Invitrogen (Carlsbad, CA). Anti-PE microbeads were purchased from Miltenyi Biotec (Auburn, CA). Fix & Perm solution was purchased from Life Technologies (Carlsbad, CA).

### *Statistical Methods*

Within-group comparisons of T cell frequencies and phenotypes at each time point were performed using the Wilcoxon signed rank test. Within-subject comparisons of cell subpopulations were performed using the Kruskal-Wallis test with Dunn's multiple comparisons correction. Comparisons between probiotic and placebo groups were performed using mixed-effects analysis of variance (ANOVA) on log-transformed values with Bonferroni correction. Between-group comparisons of time to viral shedding were performed using the log-rank chi-square test of Kaplan Meier survival data. Between-group comparison of viral titers was performed using repeated-measures ANOVA. Comparisons of stimulated and unstimulated cells were performed using the Mann-Whitney rank sum test. $p<0.05$ was considered statistically significant.

## Results

### *Experimental RV-A39 Model.*

To attain sufficient subjects to rigorously characterize and track virus-specific $CD4^+$ T cells with identical epitope specificities in an *in vivo* RV infection model, HLA-$DR4^+$ subjects were identified by screening 789 subjects enrolled in a double-blind placebo-controlled (DBPC) trial of probiotic supplementation for common cold [319]. The seven-week trial involved a four-week period of probiotic supplementation followed by intranasal challenge with RV-A39 and three weeks of subsequent monitoring (**Figure 3-1**). Forty-two subjects were identified who tested negative for serum neutralizing antibodies to RV-A39 and who expressed HLA-DR4. Of these, 16 subjects completed the seven-week trial (probiotic, n=11; placebo, n=5) (**Figure 3-1**).

### *Baseline Assessment of Virus-Specific CD4⁺ T Cell Numbers and Memory Status*

Circulating RV-specific $CD4^+$ T cells were analyzed at days -28 and 0 before RV challenge to assess basal T cell numbers and phenotype. $Tetramer^+$ T cells were identified in PBMCs using a mixture of two HLA-DR4 tetramers displaying conserved immunodominant peptide epitopes from the viral capsid proteins VP1 and VP2 ($VP1_{P14}$ & $VP2_{P60}$), as described in **Chapter 2** (**Figure 3-2**). Analysis of the data for probiotic effects identified no difference in the numbers of RV-specific cells between or within probiotic and placebo groups at each time point ($p>0.05$), consistent with a recent report of a lack of effect of Bl-04 supplementation on circulating $CD4^+$ T cells (**Figure 3-3** & **Table 3-1**)[322]. Virus-specific T cells were present in all subjects on days -28 and 0 at frequencies between 2 and 79 per $10^6$ $CD4^+$ T cells. In *post hoc* analyses, three subjects were either seropositive to RV-A39 (n=2) or had positive PCR for RV/enterovirus in nasal wash specimens (n=1) at day 0, indicating natural exposure to RV-A39 or related viral species before inoculation (**Figure 3-1**). Two of these subjects had high frequencies of RV-specific $CD4^+$ T cells (30 and 70 per $10^6$ $CD4^+$ T cells), which decreased during the four-week pre-challenge period (**Figure 3-3**). The majority of pre-existing RV-specific cells were central ($T_{CM}$: $CCR7^+CD45RO^+$) or effector memory phenotypes ($T_{EM}$: $CCR7^-CD45RO^+$) (**Figure 3-3**). Although $T_{EM}$ numbers decreased within the probiotic group from days -28 to 0 ($p=0.037$), this effect was not significant when naturally exposed subjects were excluded ($p=0.148$).

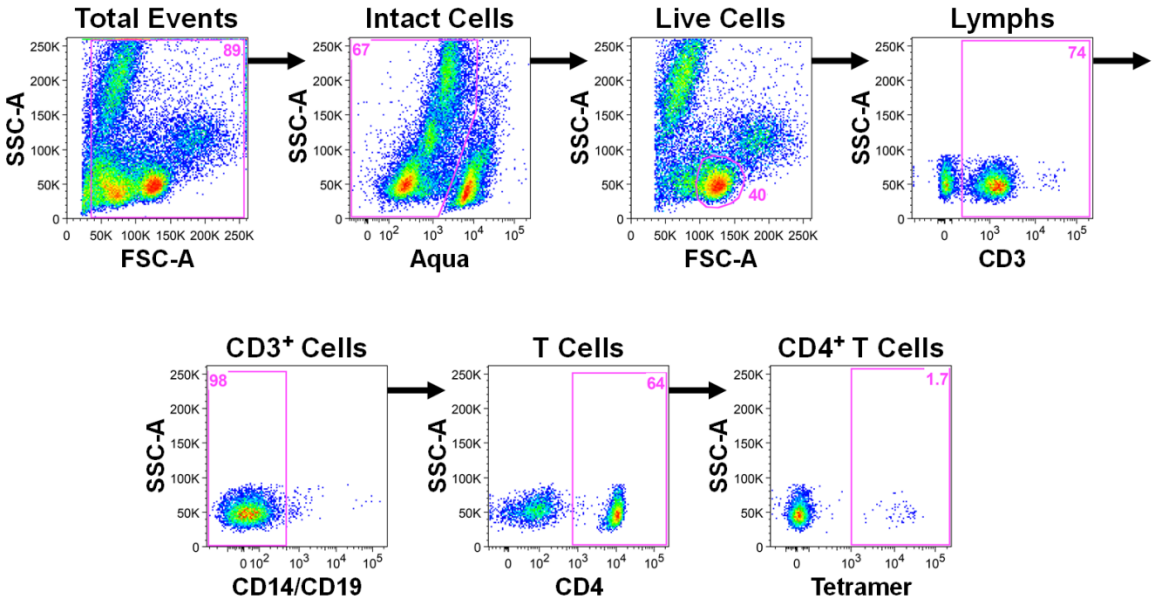


**Figure 3-2. Gating Strategy for the Identification of Tetramer⁺ CD4⁺ T Cells**

PBMCs were stained with PE-labeled RV tetramers, and then enriched using an anti-PE magnetic column prior to flow cytometry analysis.

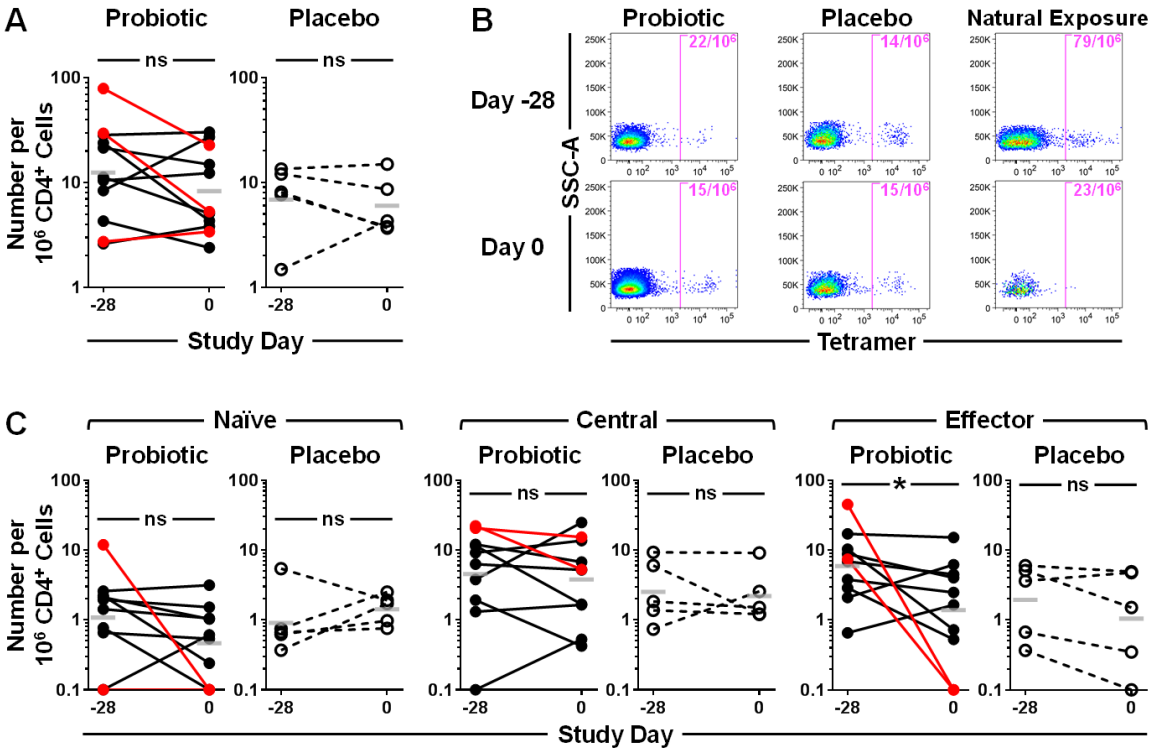


**Figure 3-3. Numbers of Pre-Existing Circulating RV-Specific CD4⁺ T Cells and Their Memory Signature**

**(A)** Comparison of the numbers of circulating RV tetramer$^+$ cells at day -28 (pre-supplementation) and day 0 (post-supplementation, immediately before RV inoculation) in HLA-DR4$^+$ subjects (probiotic, n=11; placebo, n=5). **(B)** Representative flow plots from three subjects. **(C)** Numbers of RV tetramer$^+$ cells with naïve (CCR7$^+$CD45RO$^-$), central memory (CCR7$^+$CD45RO$^+$), or effector memory (CCR7$^-$CD45RO$^+$) signatures in each group. One subject receiving placebo was excluded from phenotypic analyses owing to technical limitations. Subjects shown in red have evidence of natural exposure to RV-A39 or a related viral species. Bars denote geometric means. *p≤0.05. ns, not significant.

## Table 3-2. Comparison of RV-Specific CD4+ T Cell Frequency and Phenotype Between Probiotic and Placebo Groups

| Study Day | GM Ratio (Probiotic: Placebo) | Lower 95% CL | Upper 95% CL | Unadjusted P value | Bonferroni Lower 95% CL | Bonferroni Upper 95% CL | Bonferroni Corrected P Value |
|---|---|---|---|---|---|---|---|
| **RV-Specific Cell Precursor Frequency (# per $10^6$ $CD4^+$ T Cells)** | | | | | | | |
| -28 | 1.82 | 0.64 | 5.18 | 0.255 | 0.47 | 7.03 | 1.000 |
| 0 | 1.34 | 0.47 | 3.81 | 0.579 | 0.35 | 5.17 | 1.000 |
| 5 | 2.18 | 0.76 | 6.19 | 0.141 | 0.56 | 8.41 | 0.566 |
| 21 | 0.66 | 0.23 | 1.87 | 0.425 | 0.17 | 2.55 | 1.000 |
| **Naïve Cell Frequency (% of Tetramer+ Cells)** | | | | | | | |
| -28 | 0.73 | 0.16 | 3.40 | 0.677 | 0.10 | 5.45 | 1.000 |
| 0 | 0.29 | 0.06 | 1.34 | 0.107 | 0.04 | 2.14 | 0.429 |
| 5 | 0.64 | 0.14 | 3.00 | 0.561 | 0.09 | 4.81 | 1.000 |
| 21 | 0.83 | 0.18 | 3.88 | 0.808 | 0.11 | 6.22 | 1.000 |
| **Central Memory Cell Frequency (% of Tetramer+ Cells)** | | | | | | | |
| -28 | 0.74 | 0.30 | 1.80 | 0.497 | 0.23 | 2.33 | 1.000 |
| 0 | 1.14 | 0.47 | 2.77 | 0.769 | 0.36 | 3.59 | 1.000 |
| 5 | 1.38 | 0.57 | 3.35 | 0.471 | 0.44 | 4.34 | 1.000 |
| 21 | 1.21 | 0.50 | 2.95 | 0.665 | 0.38 | 3.82 | 1.000 |
| **Effector Memory Cell Frequency (% of Tetramer+ Cells)** | | | | | | | |
| -28 | 1.38 | 0.57 | 3.32 | 0.464 | 0.44 | 4.30 | 1.000 |
| 0 | 0.94 | 0.39 | 2.27 | 0.895 | 0.30 | 2.94 | 1.000 |
| 5 | 1.41 | 0.58 | 3.39 | 0.439 | 0.45 | 4.38 | 1.000 |
| 21 | 1.39 | 0.58 | 3.36 | 0.451 | 0.45 | 4.35 | 1.000 |
| **CD45RO+ Cell Frequency (% of Tetramer+ Cells)** | | | | | | | |
| -28 | 1.11 | 0.71 | 1.75 | 0.634 | 0.61 | 2.01 | 1.000 |
| 0 | 1.10 | 0.70 | 1.73 | 0.665 | 0.61 | 1.99 | 1.000 |
| 5 | 1.24 | 0.78 | 1.95 | 0.346 | 0.68 | 2.24 | 1.000 |
| 21 | 1.41 | 0.89 | 2.22 | 0.133 | 0.78 | 2.55 | 0.531 |
| **CCR7+ Cell Frequency (% of Tetramer+ Cells)** | | | | | | | |
| -28 | 0.87 | 0.49 | 1.55 | 0.636 | 0.41 | 1.84 | 1.000 |
| 0 | 0.95 | 0.54 | 1.70 | 0.872 | 0.45 | 2.01 | 1.000 |
| 5 | 0.92 | 0.52 | 1.64 | 0.781 | 0.44 | 1.95 | 1.000 |
| 21 | 0.87 | 0.49 | 1.56 | 0.639 | 0.41 | 1.84 | 1.000 |

**IL-7Rα$^+$ Cell Frequency (% of Tetramer$^+$ Cells)**

| | | | | | | | |
|---|---|---|---|---|---|---|---|
| -28 | 0.98 | 0.56 | 1.71 | 0.940 | 0.48 | 2.00 | 1.000 |
| 0 | 0.77 | 0.44 | 1.34 | 0.353 | 0.38 | 1.58 | 1.000 |
| 5 | 0.68 | 0.39 | 1.19 | 0.177 | 0.33 | 1.40 | 0.706 |
| 21 | 1.04 | 0.60 | 1.81 | 0.891 | 0.51 | 2.12 | 1.000 |

**CCR5$^+$ Cell Frequency (% of Tetramer$^+$ Cells)**

| | | | | | | | |
|---|---|---|---|---|---|---|---|
| -28 | 0.94 | 0.46 | 1.89 | 0.849 | 0.38 | 2.34 | 1.000 |
| 0 | 0.99 | 0.49 | 1.99 | 0.969 | 0.40 | 2.47 | 1.000 |
| 5 | 1.24 | 0.62 | 2.50 | 0.529 | 0.50 | 3.10 | 1.000 |
| 21 | 1.84 | 0.91 | 3.71 | 0.085 | 0.74 | 4.60 | 0.341 |

GM, Geometric Mean; CL, Confidence Limit. *p≤0.05.

### *Pre-Existing RV-Specific T Cells Are Activated and Armed to Home to the Respiratory Tract*

Because additional statistical analyses revealed no T cell differences between probiotic and placebo groups at any time point, including after RV infection, phenotypic data for RV-specific cells are analyzed together from here on (**Table 3-2**). Both $T_{CM}$ and $T_{EM}$ cell types were enriched within RV-specific cells as compared with total $CD4^+$ T cells before RV challenge (**Figure 3-4**). Moreover, expression of the T cell activation marker CD25 was higher on RV-specific cells ($p=0.042$), whereas expression of IL-7Rα, which decreases upon activation, was lower ($p\leq0.002$) (**Figure 3-4**). It is notable that a higher proportion of RV-specific expressed CCR5, a $T_H1$-associated receptor that permits homing to the respiratory tract ($p<0.001$)[323,324].

Analysis of cytokine expression in four uninfected HLA-$DR4^+$ subjects showed that pre-existing RV-specific $CD4^+$ T cells were predominantly IFN-$\gamma^+$, but they also included IL-$17A^+$IFN-$\gamma^-$, IL-$21^+$IFN-$\gamma^-$, and IL-$21^+$IFN-$\gamma^+$ cells, indicating a mixture of $T_H1$, $T_H17$, and T follicular helper ($T_{FH}$) cells (**Figure 3-5**). The presence of circulating RV-specific cells displaying the characteristic $T_{FH}$ surface signature ($CXCR5^+PD\text{-}1^{lo/-}$) was confirmed directly *ex vivo* (*data not shown*). Collectively, these features confirm enhanced activation and tissue migratory potential of pre-existing virus-specific $T_H1$ cells.

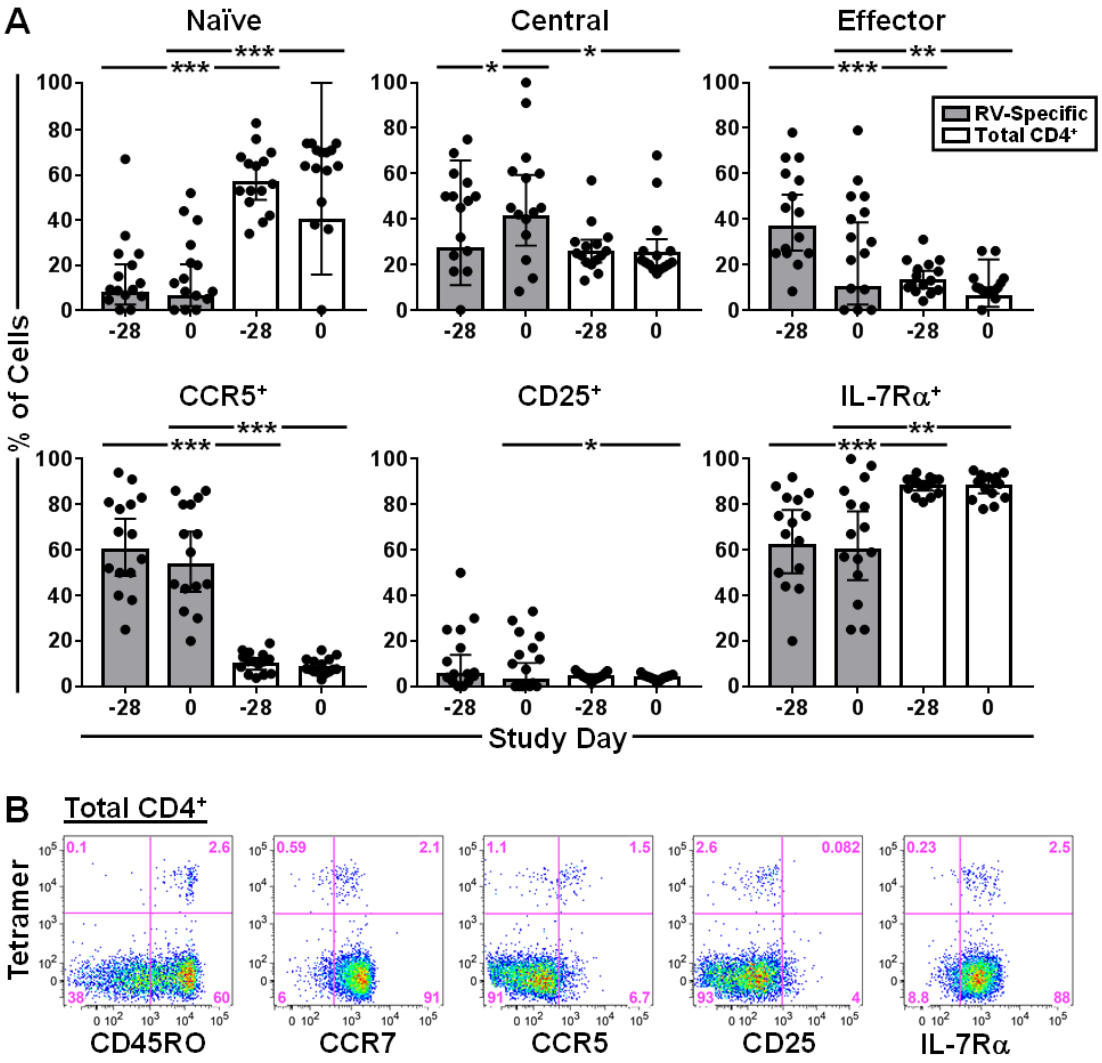


**Figure 3-4. Comparison of the Surface Phenotype of RV-Specific Cells and Total CD4⁺ T Cells**

**(A)** Percentage of cells with surface phenotypes of cells analyzed on days -28 and 0 before RV challenge (n=15). Bars denote geometric means ± 95% CI. *p≤0.05, **p≤0.01, ***p≤0.001. **(B)** Representative dot plots from one subject, depicting expression of surface markers on tetramer$^+$ cells within the CD4$^+$ T cell gate.

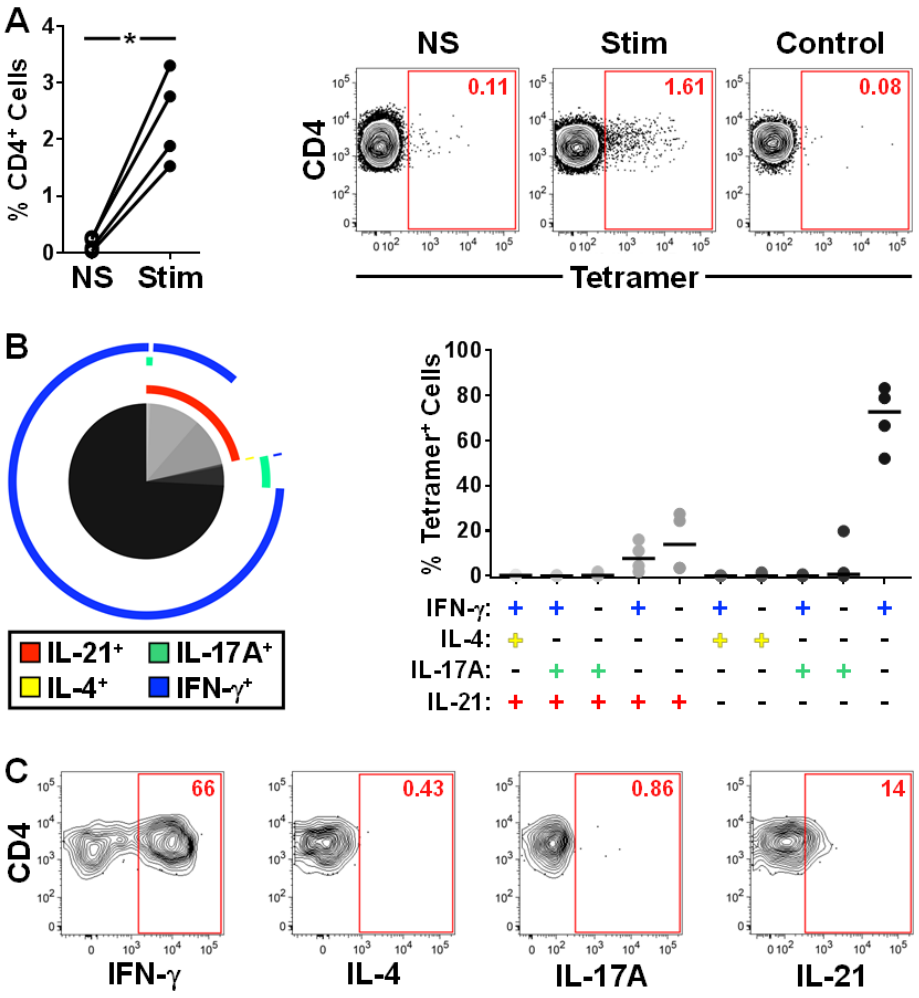


**Figure 3-5. RV-Specific CD4⁺ T Cells Produce $T_H1$ and $T_{FH}$ Cytokines**

**(A)** Percentage of RV tetramer$^+$ cells in stimulated and unstimulated PBMC cultures (n=4). Representative data from one subject are shown to the *right*. **(B)** Averaged cytokine profile of RV tetramer$^+$ cells from 4 subjects (*left*). Pie slices denote T cell subsets, and colored arcs depict cytokine production. The percentage of cells with each cytokine signature for each subject are shown to the *right*. Bars denote medians. **(C)** Representative contour plots of RV tetramer$^+$ cell cytokine staining from one subject.

### *Numbers of RV-Specific T Cells Link to a Rise in Serum Neutralizing Antibodies and Delayed Viral Shedding During Infection*

Intranasal challenge with RV-A39 resulted in infection in 12 of 16 subjects (probiotic, n=7; placebo, n=5) (**Figure 3-6**). All infected subjects developed positive nasal cultures for RV-A39 on days 1-5, with peak viral titers at day 3 (*data not shown*). Eight of these had a rise in serum neutralizing antibody titers (NAT) by day 21, two showed no rise, and the remaining two were those who tested seropositive for RV-A39 at day 0, but nonetheless had positive cultures following inoculation (**Figure 3-6**). Four subjects remained uninfected, of whom all received probiotic, including one who had positive viral PCR on day 0. There was a trend towards decreased viral titers and longer time to viral shedding in the probiotic versus placebo group, similar to that observed in the parent probiotic study (**Figure 3-7**)[319].

Among all infected subjects who had a rise in NAT, numbers of circulating RV-specific cells increased (1.2- to 16-fold change) during acute and/or convalescent infection (day 5 and/or 21) compared with day 0 ($p \leq 0.014$) (**Figure 3-6**). By contrast, RV-specific cells remained relatively constant in uninfected subjects and infected subjects with no rise in NAT. Using an arbitrary threshold of 10 cells per $10^6$ $CD4^+$ T cells, subjects who had higher numbers of RV-specific cells on day 0 ($\geq$10 $tetramer^+$ cells/$10^6$ $CD4^+$ T cells) had a longer time to viral shedding, and a lower proportion of subjects shed virus versus those who had lower T cell numbers (<10 $tetramer^+$ cells/$10^6$ $CD4^+$ T cells) ($p=0.039$) (**Figure 3-7**). This effect was diminished after correcting for probiotic effect ($p=0.126$).

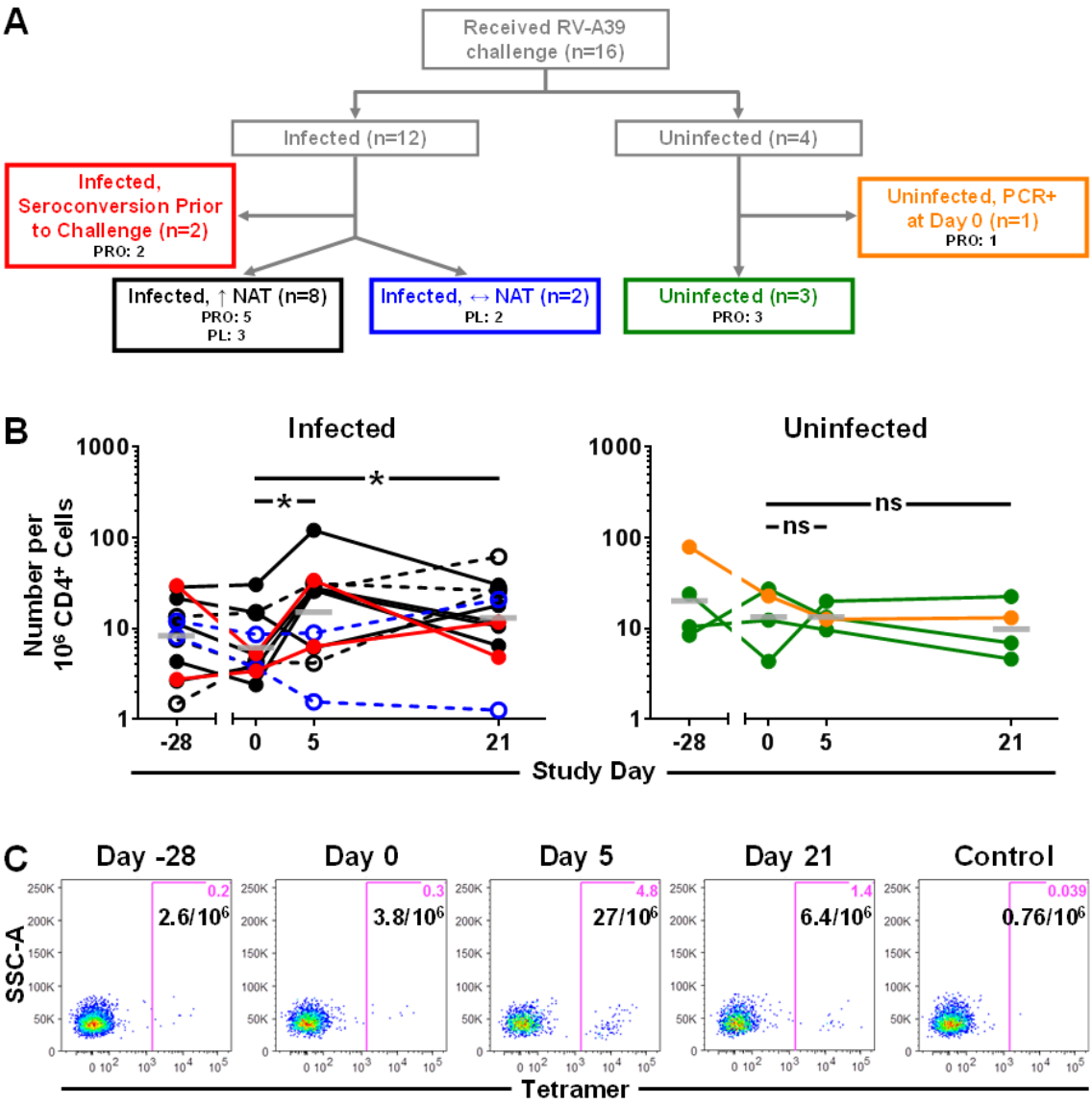


**Figure 3-6. Numbers of RV-Specific CD4⁺ T Cells in Relation to Infection Status During RV Challenge**

**(A)** Diagram of infection outcomes in 16 HLA-DR4$^+$ subjects. Colored boxes denote heterogeneous infection profiles. **(B)** Change in frequencies of RV tetramer$^+$ cells during the 7-week study period, color coded according to the diagram in **A**. Open symbols with dashed lines denote subjects receiving placebo. Bars depict geometric means. *p≤0.05.

**(C)** Representative flow plots from one infected subject.

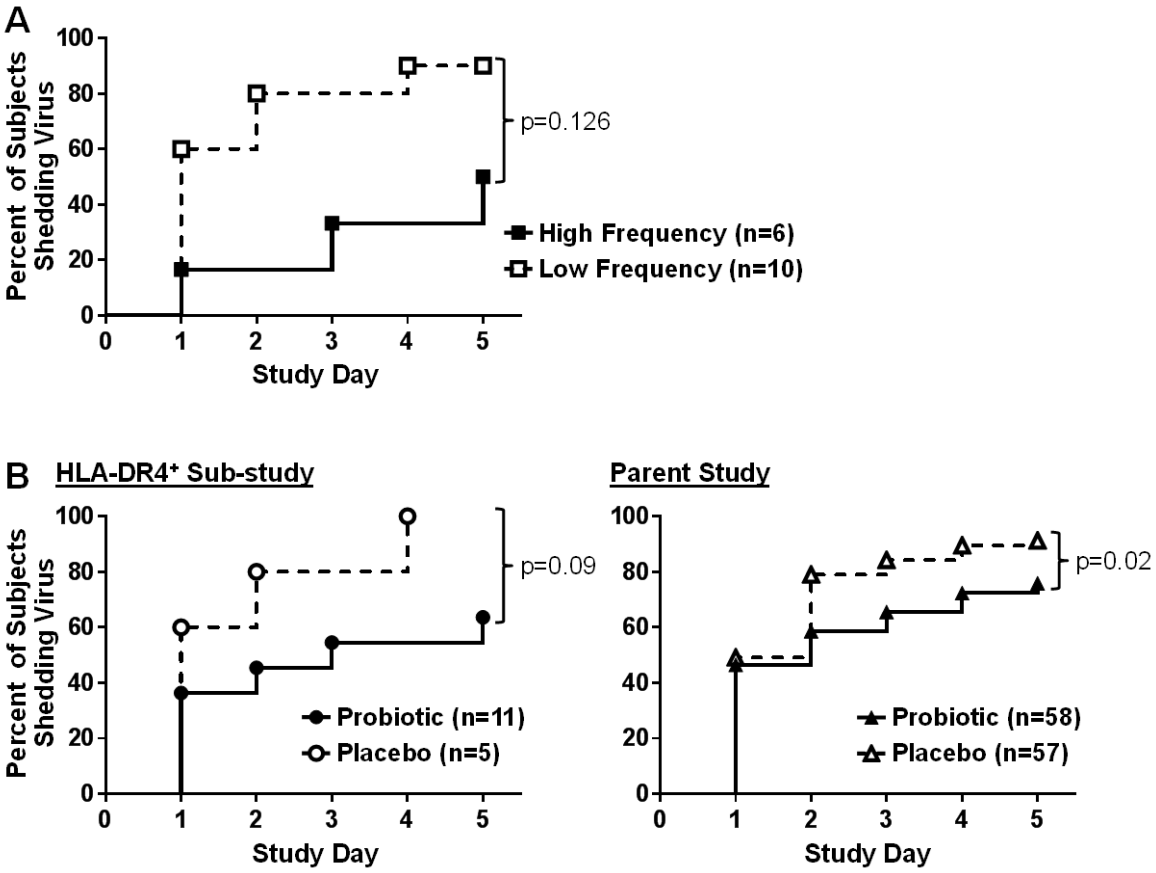


**Figure 3-7. Viral Shedding is Delayed in Subjects with High Pre-Existing Frequencies of RV-Specific Cells and Those Receiving Probiotic**

**(A)** Time to viral shedding in HLA-DR4$^+$ subjects, according to pre-existing RV tetramer$^+$ CD4$^+$ T cell frequencies at day 0. Subjects with classified as "high frequency" had ≥10 tetramer$^+$ cells per $10^6$ CD4$^+$ T cells, whereas those classified as "low frequency" had <10 tetramer$^+$ cells per $10^6$ CD4$^+$ T cells. **(B)** Time to viral shedding according to probiotic supplementation group in both the HLA-DR4$^+$ substudy (*left*) and the larger parent study (*right*).

### *Virus-Specific Effector Memory CD4⁺ T Cells Respond to RV Infection*

T cell phenotyping of RV-specific cells after challenge revealed a sharp decrease in the percentage of naïve T cells on day 5 in all infected subjects who had a rise in NAT, concurrent with an increase in the percentage of $T_{EM}$ cells, loss of IL-7Rα, and increased expression of CD25 (**Figures 3-8** & **3-9**). Conversely, IL-7Rα levels increased on RV-specific cells in infected subjects who had no increase in NAT. In uninfected subjects, RV-specific cells displayed a shift towards effector memory type, despite no overall change in numbers or activation status (**Figures 3-8** & **3-9**).

### *CCR5 is a Marker for Effector Memory T Cells That Respond to RV Infection*

To assess the relevance of circulating RV-specific effector memory T cells to the respiratory tract, expression of CCR5, a marker of respiratory-homing potential, was analyzed in relation to RV infection [323,324]. Levels of CCR5 were markedly increased on RV-specific cells after challenge in infected subjects, and $CCR5^+$ RV-specific cells were enriched for $T_{EM}$ cells (**Figure 3-10**). To better visualize the complex phenotypes of $CCR5^+$ RV-specific cells within the broader $CD4^+$ T cell compartment, unsupervised high-dimensional analysis was performed using t-SNE [320,321]. This method maps single cells onto a two-dimensional plot based on their expression of all tested markers. This analysis confirmed that in infected subjects who had a rise in NAT, RV-specific cells mapped to a population of $CCR5^+$ $T_{EM}$ cells that contained activated cells ($CD25^+$ and/or IL-7Rα$^-$) (**Figure 3-10**). Moreover, $CCR5^+$ cells comprised a major subset of total $CD4^+$ T cells at baseline (Geo. mean= 8.6%; 95% CI= 6.9-11.8%; n=11), that was modulated in a similar manner to $CCR5^+$ RV-specific cells during infection. $CCR5^+$ T cells, including those that were RV tetramer$^+$, were also modulated in uninfected subjects after RV challenge

(**Figure 3-10**). By contrast, t-SNE analysis confirmed a lack of modulation of RV-specific and CCR5$^+$ T cells (*data not shown*).

**[Next] Figure 3-8. Transitions in Memory Status During Rhinovirus Infection**

**(A)** Representative contour plots from one infected subject, depicting RV tetramer$^+$ cells overlaid on total CD4$^+$ T cells, analyzed for expression of CCR7 and CD45RO. **(B)** Memory status of RV tetramer$^+$ and total CD4$^+$ T cells at each time point (n=11). One subject receiving placebo was excluded owing to technical limitations. **(C)** Memory status of RV tetramer$^+$ cells in uninfected subjects (n=4). Open symbols with dashed lines denote subjects who received placebo. Bars denote medians. *$p \leq 0.05$, **$p \leq 0.01$ for infected subjects with a rise in NAT post-challenge.

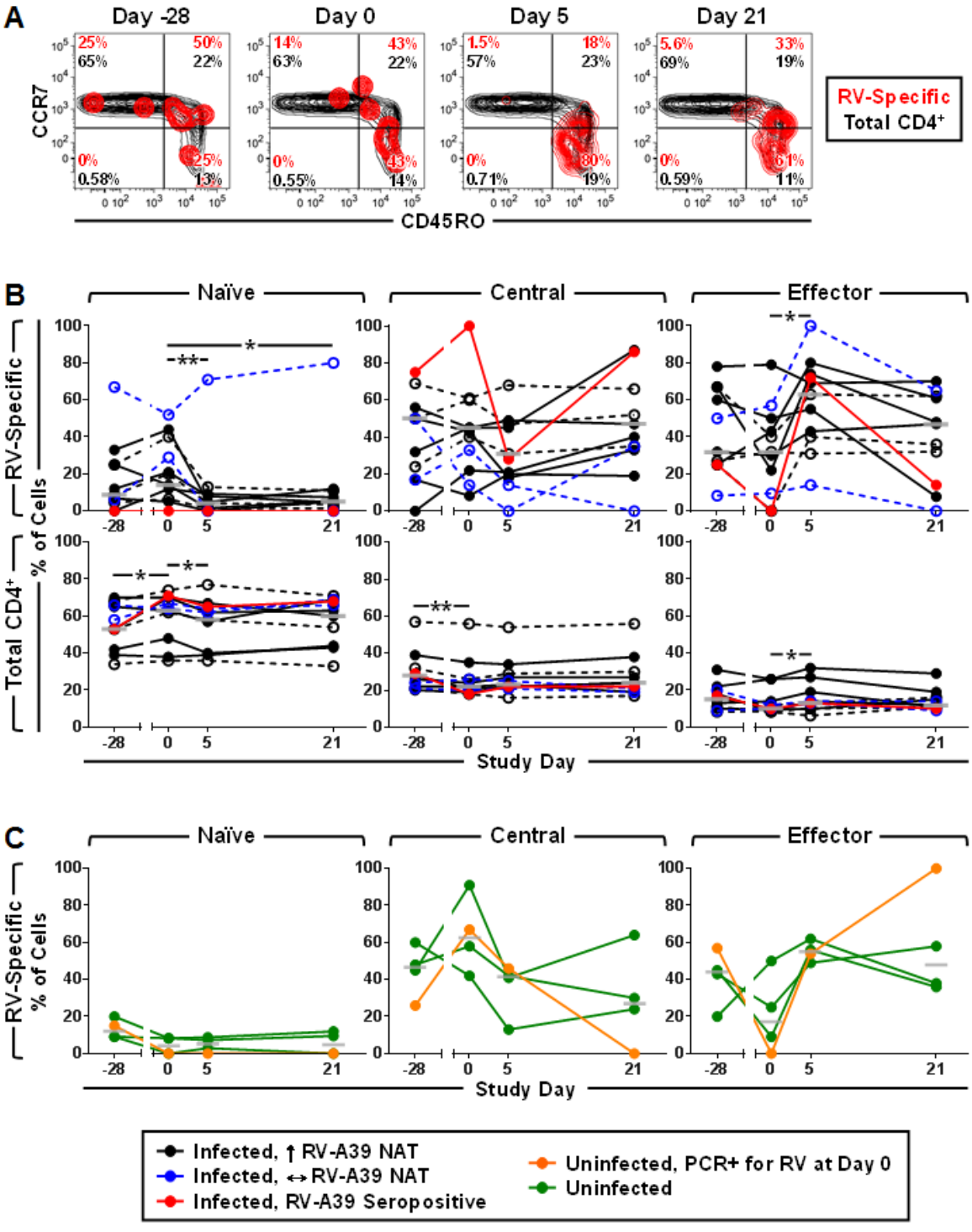
A
Day -28
Day 0
Day 5
Day 21
CCR7
CD45RO
25%
65%
50%
22%
0%
0.58%
25%
13%
14%
63%
43%
22%
0%
0.55%
43%
14%
1.5%
57%
18%
23%
0%
0.71%
80%
19%
5.6%
69%
33%
19%
0%
0.59%
61%
11%
RV-Specific
Total CD4+
B
Naïve
Central
Effector
RV-Specific
% of Cells
Total CD4+
% of Cells
Study Day
C
Naïve
Central
Effector
RV-Specific
% of Cells
Study Day
Infected, ↑ RV-A39 NAT
Infected, ↔ RV-A39 NAT
Infected, RV-A39 Seropositive
Uninfected, PCR+ for RV at Day 0
Uninfected

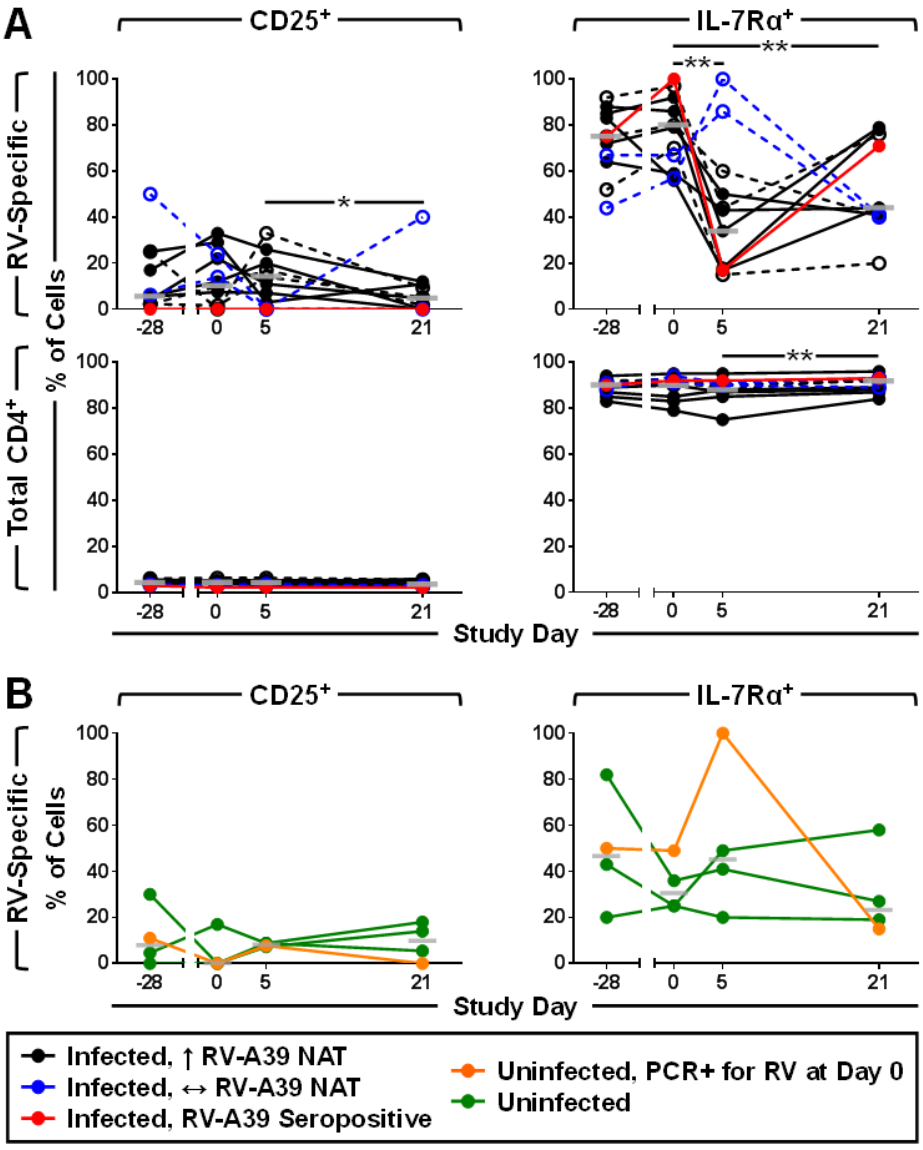


**Figure 3-9. Activation of RV-Specific CD4⁺ T Cells During Infection**

Expression of CD25 and IL-7Rα by RV tetramer$^+$ and total CD4$^+$ T cells at each time point in **(A)** infected, and **(B)** uninfected subjects. Data are shown for 11 infected and 4 uninfected subjects. One infected subject receiving probiotic was excluded from analysis owing to technical limitations. Open symbols with dashed lines denote subjects who received placebo. Bars denote medians. **p≤0.01, for infected subjects with a rise in NAT post-challenge.

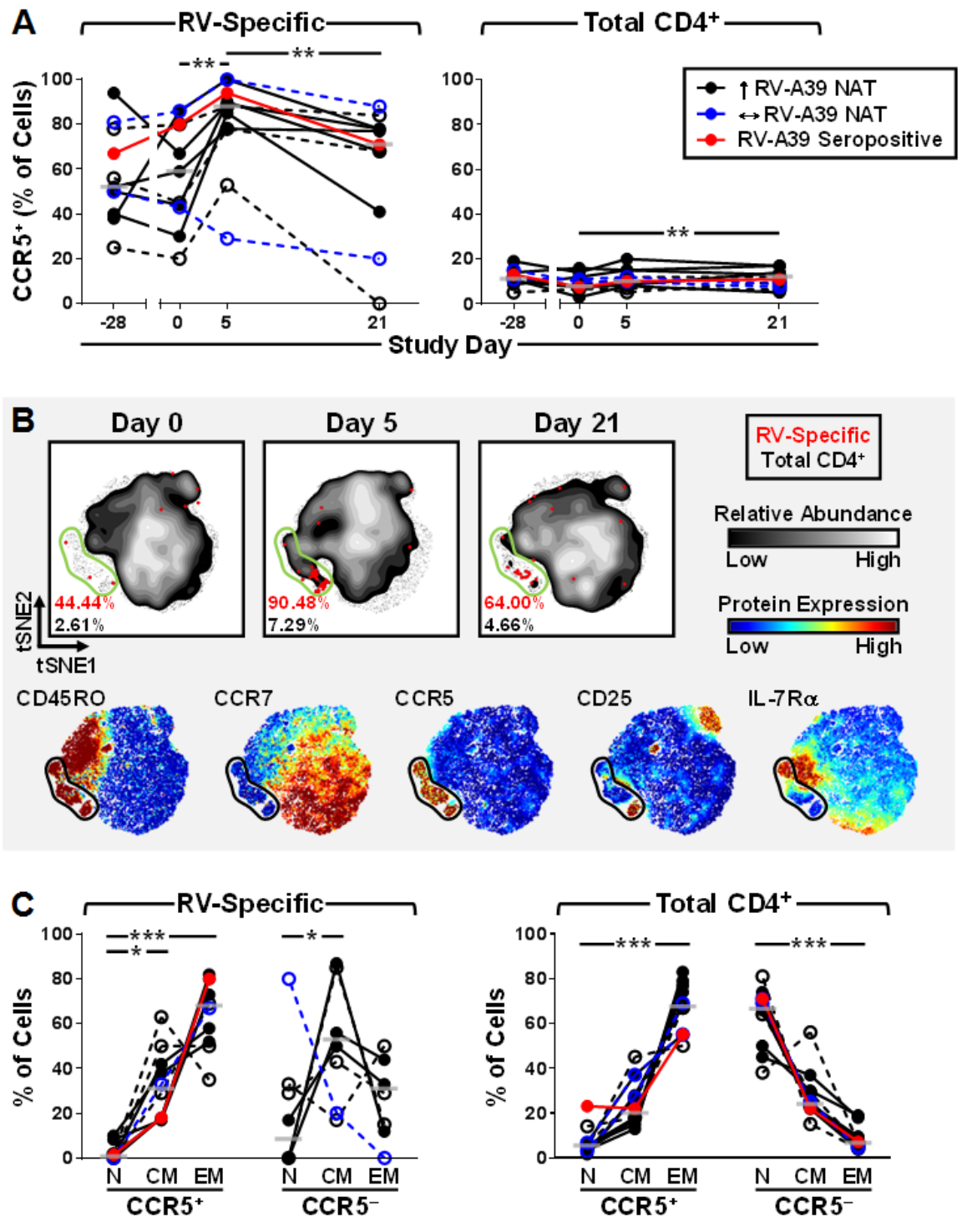
A
RV-Specific
Total CD4+
CCR5+ (% of Cells)
↑ RV-A39 NAT
↔ RV-A39 NAT
RV-A39 Seropositive
Study Day
B
Day 0
Day 5
Day 21
RV-Specific
Total CD4+
Relative Abundance
Low
High
Protein Expression
Low
High
tSNE2
tSNE1
44.44%
2.61%
90.48%
7.29%
64.00%
4.66%
CD45RO
CCR7
CCR5
CD25
IL-7Rα
C
RV-Specific
Total CD4+
% of Cells
N CM EM
CCR5+
CCR5−

**Figure 3-10. Modulation of CCR5$^+$ CD4$^+$ T Cells During RV Infection**

**(A)** Percentage of RV-specific and total CD4$^+$ T cells expressing CCR5 at each time point, as determined using traditional gating methods. Infected, n=11. **(B)** High-dimensional mapping of RV-specific and total CD4$^+$ T cells from one representative subject using t-SNE. Rainbow-colored t-SNE plots depict the intensity of expression for each marker tested, and drawn gates denote CCR5$^+$ subsets.

**(C)** Percentage of CCR5$^+$ and CCR5$^-$ cells with naïve [N], central memory [CM], or effector [EM] phenotypes at day 5. Subjects with limited cell numbers were excluded. Open symbols with dashed lines denote subjects who received placebo. Bars denote medians. *$p \leq 0.05$, **$p \leq 0.01$, ***$p \leq 0.001$, for infected subjects with a rise in NAT post-challenge.

### *Nasal CD4⁺ T Cells Isolated During Acute Infection Display RV-Specific Signatures*

Analysis of nasal wash specimens obtained during early infection (day 4) revealed an increase in cytokine levels versus day 0 for CXCL10/IP-10 (ligand for the $T_H1$-associated receptor CXCR3), as well as IL-6 and G-CSF (both of which modulate CCR5 expression on T cells) ($p \leq 0.01$) (**Figure 3-11**)[325–328]. Among those CCR5 ligands measured (CCL2/MCP-1, CCL3/MIP-1α, and CCL5/RANTES), MCP-1 was most abundant before RV challenge, and levels generally increased after challenge (**Figure 3-11**)[329]. MIP-1α and RANTES were not consistently detectable in either this or the parent study (*data not shown*). Changes in IL-8, which have been linked to symptom severity, were variable (**Figure 3-11**)[330].

Nasal wash specimens obtained from HLA-diverse infected subjects at day 5 contained $CD4^+$ T cells, which comprised 0.4-2.5% of total live cells in these specimens (*data not shown*). Assessment of T cell surface signatures in the nose confirmed a dominant $T_H1$ signature based on expression of CXCR3 and CCR5 (**Figure 3-12**). Whereas $CXCR3^-$ $CCR5^+$ cells were predominantly $T_{EM}$ type, the majority of cells expressing CXCR3 ($CXCR3^+$, $CXCR3^+CCR5^+$) were $T_{CM}$ cells. Moreover, subtypes that expressed CCR5 had loser levels of IL-7Rα compared with $CCR5^-$ cells (**Figure 3-12**). These collective observations strongly support the recruitment of $CCR5^+$ $T_H1$ effectors, including activated RV-specific cells, from the blood to the upper respiratory tract during RV infection.

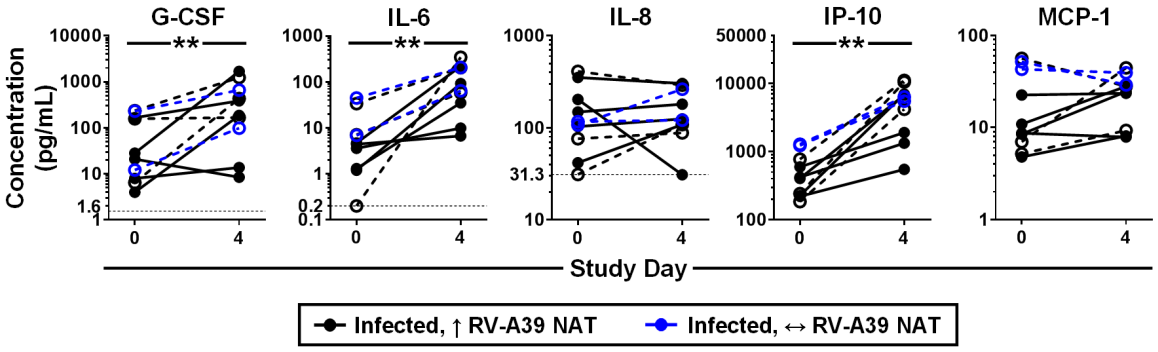


**Figure 3-11. Nasal Cytokine Levels During Early RV Infection**

Cytokine levels immediately prior to RV challenge (day 0), and 4 days post-challenge in infected subjects (n=10). MIP-1α and RANTES were detectable in only 2 and 3 subjects, respectively, and are not shown. Open symbols with dashed lines denote subjects who received placebo. Symbols below the dotted lines denote samples concentrations below the assay limit of detection. **p≤0.01.

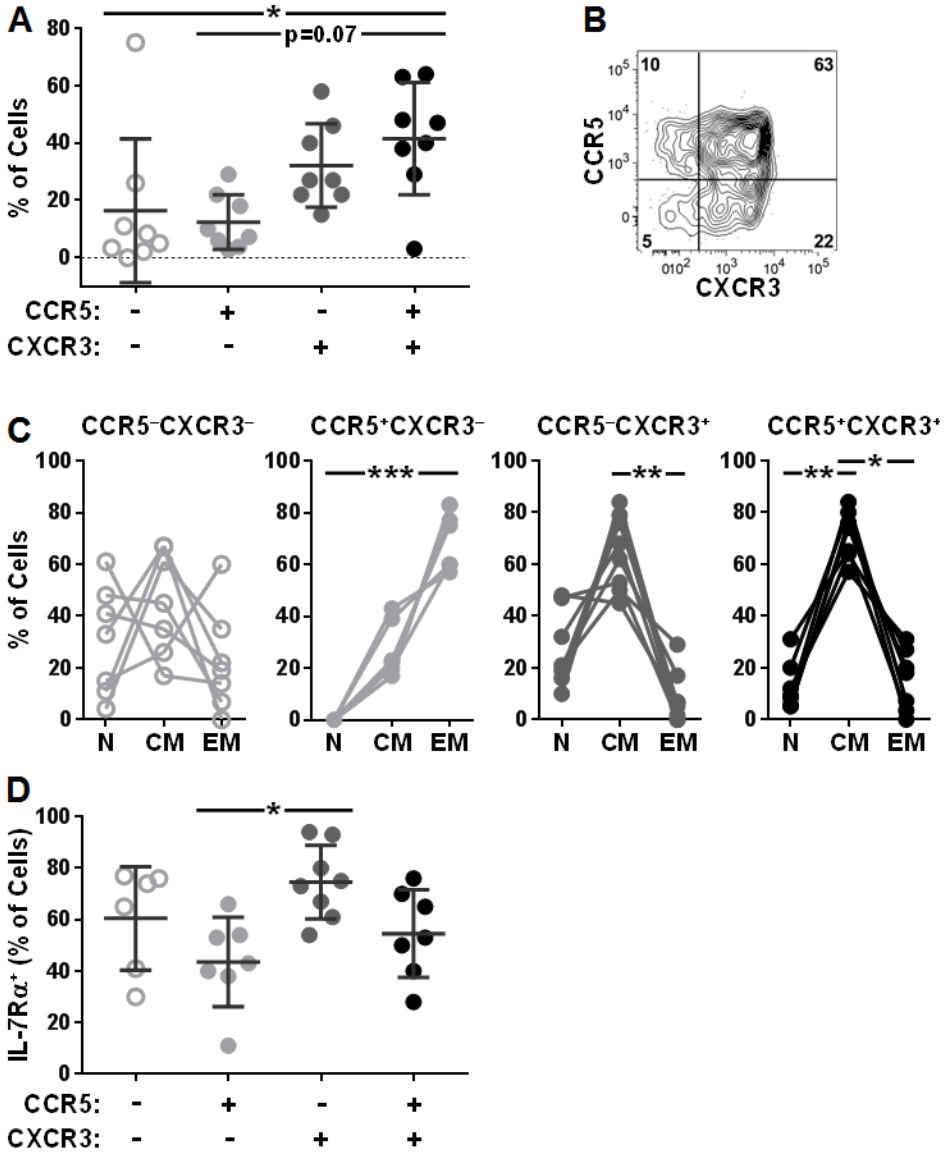


**Figure 3-12. Nasal CD4⁺ T Cell Signatures During Acute RV Infection**

Phenotype of $CD4^+$ T cells in nasal washes obtained 5 days after RV challenge, from 8 HLA-diverse subjects. **(A)** Percentage of nasal $CD4^+$ T cells that express CCR5 and/or CXCR3. **(B)** Representative contour plot from one subject. **(C)** Percentage of nasal $CD4^+$ T cells with naïve [N] central memory [CM], or effector memory [EM] phenotypes, according to expression of CCR5 and CXCR3. Bars denote the mean ± SD. *p≤0.05, **p≤0.01, ***p≤0.001.

## Discussion

For the first time, we provide formal evidence of a role for circulating $CCR5^+$ memory $T_H1$ effectors in the control of RV infection. By monitoring RV-specific $CD4^+$ T cells for an extended period of time, we provide multiple lines of evidence to support their role before and after RV inoculation. This includes the following: (1) T cell molecular signatures and numbers consistent with immune surveillance in the absence of infection; (2) a relationship between increased numbers of pre-existing RV-specific $CD4^+$ T cells and increased time-to-viral shedding among healthy subjects; (3) T cell expansion, activation, and enhanced homing ability in tandem with the production of neutralizing antibodies; and (4) the presence of T cell signatures in the nose during acute infection that match activated RV-specific T cells in the blood.

Although previous *in vitro* studies have inferred a role for $CD4^+$ T cells in RV infection, none have used tetramers to systematically enumerate and characterize responding T cells directly *ex vivo* [64,65,312]. A major limitation of tetramer studies is the requirement to match each tetramer to the HLA type of the test subject; thus, recruiting sufficient subjects with the same HLA type to analyze identical T cell specificities can be problematic. We circumvented this limitation by recruiting HLA-$DR4^+$ subjects from a much larger cohort of subjects who were challenged with RV-A39. This enabled us to apply a precise and uniform approach to analyze the quantity and quality of the $CD4^+$ T cell response to RV, its kinetics, and its relationship to infection status.

In **Chapter 2**, we reported that immunodominant $CD4^+$ T cell epitopes of RV are conserved, and that T cells recognizing these epitopes are cross-reactive among RV-A species. In this chapter, higher numbers of RV-specific T cells were detected before

challenge among subjects who had evidence of recent natural viral exposure, and RV tetramer$^{+}$ cells were present in all seronegative subjects. Given the conserved nature of HLA-DR4-restricted RV-A39 epitopes, such pre-existing memory T cells likely arise from iterative priming by related viruses during previous exposures. The enrichment of effector memory cells within the RV tetramer$^{+}$ subset at baseline, coupled with their enhanced activation and expression of the tissue-homing marker CCR5, supports a role for pre-existing RV-specific T cells in immune surveillance. This was borne out by their rapid expansion, augmented activation, and increased migratory potential in the blood after RV challenge, which may reflect egress of primed T cells from lymph nodes and/or "spillover" from inflamed tissues.

In further support of a protective role for T cells, those subjects who had higher numbers of pre-existing RV-specific cells had longer time to viral shedding following inoculation, and a lower proportion of subjects shed virus. Although this effect was no longer significant after correcting for probiotic effects, statistical analysis supported a trend despite the small sample size. Although no effect of probiotic on T cells was observed in this study, we acknowledge the administration of probiotic supplementation as a limitation. Nonetheless, our findings are in line with previous studies of Bl-04 supplementation, which also failed to identify probiotic modulation of T cell populations or broader immune signatures [322,331]. Thus, further work is required in a larger sample to examine the relationship between pre-existing T cell numbers and infection.

Expansion of RV-specific T cells after challenge was restricted to those subjects who had a rise in serum NAT. Virus-specific cells produced both $T_H1$ and $T_{FH}$-associated cytokines, suggesting that these cells are equipped to promote viral clearance and provide

help for antibody responses [63–65,67,244,332]. It is notable that no T cell expansion or evidence of activation was observed in two infected subjects who had no rise in NAT. This might reflect the ability to clear virus locally, independent of circulating T cells and perhaps through innate mechanisms or the involvement of other cell types. We were surprised to find that, in subjects who remained uninfected after RV challenge, enrichment of $T_{EM}$ cells and increased expression of CCR5 was evident for RV-specific cells, despite no change in T cell numbers. Whether such "covert" T cell responses reflect successful local regulation of virus warrants further exploration.

The RV-specific T cells identified in this chapter represent only two epitope specificities: one each for the capsid proteins VP1 and VP2. Although recent work suggests that these structural proteins are major antigenic targets for $CD4^+$ T cells (see **Chapter 2**), additional epitopes may reside within the RV capsid or else within functional proteins [312]; thus, RV-specific T cells are likely more abundant than reported here. In addition, relatively rare RV specificities are unlikely to account for the observed fluxes in a major $CCR5^+$ $T_{EM}$ subset after RV challenge. These likely reflect a bystander T cell response involving rerouting of $CCR5^+$ T cells between the blood and upper respiratory tract. The presence of T cells in the nose of infected subjects that bear a molecular signature that akin to circulating RV-specific cells strongly supports the notion of active T cell migration between these sites. In addition to CCR5, nasal T cells were analyzed in the context of the canonical $T_H1$ marker CXCR3. Although nasal $CXCR3^-CCR5^+$ cells were predominantly $T_{EM}$ type ($CCR7^-$ $CD45RO^+$) analogous to RV-specific cells in the blood, $CXCR3^+$ cells maintained expression of CCR7. Moreover, $CCR5^+$ subtypes in the nose expressed lower levels of IL-7Rα compared with $CCR5^-$ subtypes, suggesting an increased state of activation. Together, our

results support the view that CCR5 is a marker for $T_{EM}$ cells that respond locally to RV infection.

In summary, our findings demonstrate a pivotal role for $CCR5^+$ memory $T_H1$ cells primed by past exposure to related viruses in the control of RV. Our results provide an important stepping stone to future work aimed at understanding T cell-mediated protective and pathogenic mechanisms in RV infection that could guide the design of new treatments.

*This chapter was adapted from: L Muehling, R Turner, K Brown, P Wright, J Patrie, S Lahtinen, M Lehtinen, W Kwok, J Woodfolk. "Single-cell tracking reveals a role for pre-existing CCR5$^+$ memory $T_H1$ cells in the control of rhinovirus-A39 after experimental infection in humans." J Infect Dis (2017).*

*&*

*R Turner, J Woodfolk, L Borish, J Steinke, J Patrie, L Muehling, S Lahtinen, M Lehtinen. "Effect of probiotic on innate inflammatory response and viral shedding in experimental rhinovirus infection – a randomised controlled trial." Benef Microbes (2017).*

# Chapter 4 — Rhinovirus Infection Induces Enhanced $T_H1$ Responses That Promote Chronic Inflammation in Allergic Asthma

## Introduction

As previously discussed, RV infections are major triggers of allergic asthma exacerbations, including severe exacerbations that can result in hospitalization and death, although the mechanisms of these responses remain unknown [218,219]. A prevailing view is that pre-existing type 2 inflammation in the lower airways is a key contributor. In accord with this notion, increased levels of IgE antibodies, including IgE specific for dust mite allergens, are associated with worse cold symptoms and increased risk and severity of wheeze during RV infection [211,230,232]. The ability for anti-IgE to reduce the number of asthma exacerbations coincident with peak allergen exposure and seasonal RV infections lends further credence to this theory [227,229].

Studies of the mechanisms of RV-induced asthma have generally addressed the question based on the mutually inhibitory actions of type 1 and type 2 responses. Several studies have reported the deficient production of interferons by bronchial epithelial cells and plasmacytoid dendritic cells in allergic asthmatics in response to RV or else toll-like receptor ligands that bind RV-sensing innate receptors [240–242,251–254]. Such observations, which arise from patients with mild-to-moderate disease, imply attenuation of type 1 anti-viral responses by pre-existing type 2 disease [245,247]. However, other studies have failed to corroborate these findings, or else observed enhanced IFNs in the asthmatic airways, and there is no evidence of a reduced ability to clear virus in asthmatic subjects [257,260–266]. Approaching the topic from a different angle, other work has reported the ability for RV infection to augment the $T_H2$-promoting cytokines TSLP and IL-33 in bronchial epithelial

cells from asthmatic patients [333,334]. These collective studies infer that RV infection modulates downstream T cell responses and consequent allergic inflammation by inhibiting virus-specific $T_H1$ responses, enhancing $T_H2$ responses, or both. Despite this, no studies have rigorously tested T cell outcomes *in vivo*, or more specifically, the relative contributions of virus-specific $T_H1$ cells and allergen-specific $T_H2$ cells. This aspect is critical to reconciling existing data, understanding asthma pathogenesis, and optimizing treatments for RV-induced asthma.

Here, we describe the simultaneous analysis of antigen-specific $T_H1$ and $T_H2$ cells in asthmatics before and after experimental RV infection. Our development of RV pMHCII tetramers (**Chapter 2**) enabled us, for the first time, to precisely track the number and function of circulating virus-specific T cells in parallel with allergen-specific $T_H2$ cells in infected asthmatics. By integrating T cell data with parallel assessments of pro-inflammatory cytokines, clinical parameters, and *in vivo* IgE blockade, we report a paradoxical amplification of anti-viral $T_H1$ responses linked to high IgE levels and worse lung function in patients with asthma. Our findings support a role for type 1 responses in driving chronic inflammation in asthmatic patients who are highly allergic.

## Materials and Methods

### *Human Subjects and RV-A16 Experimental Challenge Model*

Details about the screening and enrollment of subjects, experimental RV-A16 challenge, and clinical procedures are found in **Appendix I**. Briefly, allergic asthmatic and healthy control subjects were enrolled in an experimental RV-A16 infection study. Allergic asthmatics with total serum IgE levels within the dosing range for anti-IgE (omalizumab, see **Appendix I**) were included in a DBPC study of anti-IgE (range 133-493 IU/mL), with

treatment initiating eight weeks prior to RV challenge. Those asthmatics with IgE levels too high for anti-IgE treatment (≥596 IU/mL) underwent RV challenge only, along with healthy controls. For the purposes of this study, the term "baseline" will be used to refer to study time points prior to both RV challenge and anti-IgE intervention (day 0: controls and high IgE asthmatics; day -56: mid IgE asthmatics).

### *Flow Cytometric Analysis of Cell Populations*

Intermediate resolution HLA-DRB1 typing was performed by the Blood Center of Wisconsin (Milwaukee, WI, USA). Peripheral blood specimens were collected for PBMC isolation by density grade centrifugation at days -56, 0, 4, 7, and 21. PBMCs were viably cryopreserved for later analysis by flow cytometry. Peptide/MHCII tetramer staining was performed as described in **Chapter 2**, with one modification: cells were also stained with allergen-specific tetramers labeled with the PE conjugate, PE-CF594. Cell enrichment and flow cytometry analysis then proceeded as previously described.

Additional peripheral blood specimens were obtained at days -56, 0, 4, and 21 for the analysis of circulating dendritic cell populations. Fresh whole blood specimens were stained with a cocktail of fluorescent antibodies directed against surface markers. Red blood cells were then lysed with BD FACS Lysis Solution (BD Biosciences, San Jose, CA), followed by permeabilization and antibody staining for intracellular markers (FIX & PERM Cell Permeabilization Kit, Invitrogen, Carlsbad, CA). Specimens were then run on a BD LSR Fortessa (BD Biosciences, San Jose, CA). All flow cytometry data was analyzed using Flow Jo (Tree Star, Ashland, OR) and SPICE version 5.3, as previously described in **Chapter 2** [301].

### *Flow Cytometry Antibodies and Reagents*

Fluorochrome-conjugated monoclonal antibodies for flow cytometry included: anti-CD3 (clone SK7), anti-CD14 (MφP9), anti-CD19 (SJ25C1), anti-CD123/IL-3R (6H6), anti-CD183/CXCR3 (1C6/CXCR3), anti-CD195/CCR5 (2D7/CCR5), anti-CD279/PD-1 (EH12.1), anti-HLA-DR (G46-6), Lin1 cocktail (anti-CD3, -CD14, -CD16, -CD19, -CD20 and -CD56) (BD Biosciences, San Jose, CA); anti-CD4 (SK3), anti-CD41 (HIP8), anti-CD45RO (UCHL1), anti-CD127/IL-7Rα (A019D5), anti-CD185/CXCR5 (J252D4), anti-CD194/CCR4 (L291H4), anti-CD197/CCR7 (G043H7), anti-CD294/CRTH2 (BM16), anti-FcεRIα (AER-37) (Biolegend, San Diego, CA). Aqua viability dye was obtained from Invitrogen (Carlsbad, CA), and compensation beads were obtained from BD Biosciences (San Jose, CA) and eBiosciences (San Diego, CA). Anti-PE MicroBeads were obtained from Miltenyi Biotec (Auburn, CA).

### *Multiplex Cytokine Bead Assays*

Nasal wash and nasal lining fluid specimens were procured according to the procedures outlined in **Appendix I**. Specimens were frozen for analysis at a later date, when all study time points could be analyzed together. Cytokines and chemokines were analyzed using commercially available multiplex bead kits (EMD Millipore, Burlington, MA). Those analytes expected to be abundant were analyzed in nasal wash (IL-6, IL-8, IP-10, MIP-1β), whereas T cell-derived cytokines were assessed in the more highly concentrated nasal lining fluid (IFN-γ, IL-4, IL-5, IL-13, IL-17A).

### *Statistical Methods*

For T cell numbers, between-group comparisons at baseline and within-group comparisons across time were performed using generalized linear models (GLM) for normal data, and the Kruskal-Wallis test for non-normal data. Comparisons between groups over time were performed using generalized estimating equations (GEE). Differences between fold changes were performed using the Mann-Whitney test. Multiple comparisons adjustments were performed for RV- and allergen-cell frequency analyses using the Holm-Sidak adjustment for 37 comparisons. Given the exploratory nature of these studies, figures reflect unadjusted p values. The complete statistical comparisons of antigen-specific cell frequencies, including adjusted and unadjusted p values, can be found in **Appendix II**. For other parameters, between-group comparisons at single time points and within-group comparisons over time were performed using the Kruskal-Wallis test. Between-group comparisons of fold change were performed using the Mann-Whitney test. Cytokine concentrations over time were compared using 2-way ANOVA. $p \leq 0.05$ was considered statistically significant.

## Results

### *Increased Numbers of Circulating RV-Specific CD4⁺ T Cells Are Linked to Worse Lung Function in Uninfected Asthmatics*

As a first step, the numbers of circulating RV- and allergen-specific $CD4^+$ T cells were analyzed in all allergic asthmatics and healthy controls in the absence of RV infection (asthma, n=28; control, n=12). Antigen-specific T cells were identified using pMHCII tetramers, including both RV tetramers (see **Chapter 2**) and allergen tetramers (**Table 4-1**). Allergen tetramers were selected based on serum IgE profiles (see **Table 4-2** & **Appendix**

**I**). Asthmatics were sensitized to two or more inhalant allergens, including those from perennial (dust mite, cat) and seasonal (birch, timothy grass) sources (see **Appendix I** for more details). Priority was given to tetramers displaying epitopes of the major dust mite allergen, Der p 1, given the IgE dominance of dust mites in asthmatics (64.5% sensitized), its importance in asthma pathogenesis, and for uniformity [231]. To optimize cell detection, up to three tetramers from a single antigen source were used when available, based on the subject's HLA type (**Table 4-2**).

Dual tetramer staining of PBMCs from subjects who tested seronegative for RV-A16 demonstrated higher numbers of RV-A16-specific and allergen-specific $CD4^+$ T cells in asthmatics versus controls (RV: Geo. mean= 16 per $10^6$ $CD4^+$ T cells vs. 8 per $10^6$, p=0.013; Allergen: 10 per $10^6$ vs. 2 per $10^6$, p=0.002) (**Figures 4-1** & **4-2**). As expected, asthmatics had worse lung function compared with controls (p=0.04, see **Appendix I** for additional details). Increased numbers of RV-specific cells—and to a lesser extent, allergen-specific cells—correlated with worse lung function as defined by $FEV_1$/FVC ratio (r=-0.51, p=0.0008; and r=-0.36, p=0.02, respectively) (**Figure 4-2**). Furthermore, the numbers of RV-specific cells—but not allergen-specific cells—were markedly higher in asthmatics with an abnormal $FEV_1$/FVC ration of <80% (p=0.003) (**Figure 4-3**). This finding was not influenced by the number or type of tetramers used (*data not shown*). Analysis of the T cell markers PD-1 and CCR5—which are expressed in the airways of children with severe asthma and in subjects infected with RV, as described in **Chapter 3**—revealed higher expression on RV-specific T cells in asthmatics with reduced lung function, suggesting T cell transit to and from the inflamed airways [335,336]. These data support a link between higher

numbers of pathogenic RV-specific cells and airway inflammation in asthmatics, even in the absence of infection.

**Table 4-1. Allergen Tetramers: Peptide Epitopes and Corresponding HLA-DRB1 Restriction**

| Peptide | Epitope | HLA-DRB1 Restriction |
|---|---|---|
| *Dust Mite (Der p 1)* | | |
| Der p $1_{P2}$ | SLLALSAVYARPSSIKTFEE | *0101 |
| Der p $1_{P7}$ | NFLESVKYVQSNGGAINHLS | *0701 |
| Der p $1_{P14}$ | NGNAPAEIDLRQMRTVTPIR | *0301 |
| Der p $1_{P24}$ | GVVQESYYRYVAREQSCRRP | *1101 |
| Der p $1_{P30}$ | HSAIAVIIGIKDLDAFRHYD | *0401 |
| Der p $1_{P34}$ | PNYHAVNIVGYSNAQGVDYW | *1501 |
| Der p $1_{P39}$ | YFAANIDLMMIEEYPYVVIL | *0701 |
| *Cat Dander (Fel d 1)* | | |
| Fel d $1_{P2}$ | IFYDVFFAVANGNELLLDLS | *0701 |
| Fel d $1_{P3}$ | VANGNELLLDLSLTKVNATE | *0301 |
| Fel d $1_{P13}$ | TPDEYVEQVAQYKALPVVLE | *1501 |
| Fel d $1_{P14}$ | VAQYKALPVVLENARILKNC | *0101 |
| *Silver Birch (Bet v 1)* | | |
| Bet v $1_{P14}$ | VATPDGGSILKISNKYHTKG | *1101 |
| Bet v $1_{P18}$ | KEMGETLLRAVESYLLAHSD | *1501 |
| Bet v $1_{P27}$ | NFKYNYSVIEGGP | *0701 |
| Bet v $1_{P38}$ | GSILKISNKYHTK | *0301 |
| Bet v $1_{P48}$ | ETLLRAVESYLLA | *0701 |
| *Timothy Grass (Phl p 1)* | | |
| Phl p $1_{P13}$ | EEPIAPYHFDLSGHAFGAMA | *0401 |
| Phl p $1_{P20}$ | KGSNPNYLALLVKYVNGDGD | *0101 |
| Phl p $1_{P24}$ | KWIELKESWGAIWRIDTPDK | *1101 |

Tetramers previously developed by Dr. William Kwok, Benaroya Research Institute.

## Table 4-2. RV and Allergen Tetramers Selected for Study Subjects

| RV-A16 Tetramer Selection | Allergen Tetramer Selection | Specific IgE ($kU_A/L$) |
|---|---|---|
| *Controls, n=12* | | |
| $VP1_{P23}$/*0101, $VP2_{P24}$/*0101 | Der p $1_{P2}$/*0101 | ≤0.1 |
| $VP2_{P21}$/*0401 | Der p $1_{P30}$/*0401 | ≤0.1 |
| $VP2_{P21}$/*0301 | Bet v $1_{P38}$/*0301 | ≤0.1 |
| $VP2_{P25}$/*1501 | Der p $1_{P34}$/*1501 | ≤0.1 |
| $VP2_{P25}$/*1501 | Der p $1_{P34}$/*1501 | ≤0.1 |
| $VP1_{P23}$/*0701, $VP2_{P26}$/*0701 | Der p $1_{P7}$/*0701, Der p $1_{P39}$/*0701 | ≤0.1 |
| $VP2_{P21}$/*0401 | Der p $1_{P30}$/*0401 | ≤0.1 |
| $VP2_{P21}$/*0401 | Der p $1_{P30}$/*0401 | ≤0.1 |
| $VP2_{P21}$/*0401, $VP1_{P23}$/*0701, $VP2_{P26}$/*0701 | Der p $1_{P30}$/*0401, Der p $1_{P7}$/*0701, Der p $1_{P39}$/*0701 | ≤0.1 |
| $VP2_{P25}$/*1501 | Der p $1_{P34}$/*1501 | ≤0.1 |
| $VP2_{P2}$/*1101 | Der p $1_{P24}$/*1101 | ≤0.1 |
| $VP2_{P21}$/*0401 | Der p $1_{P30}$/*0401 | 0.31 |
| *Asthmatics, n=28* | | |
| $VP1_{P23}$/*0701, $VP2_{P26}$/*0701 | Fel d $1_{P2}$/*0701 | 0.77 |
| $VP1_{P23}$/*0101, $VP2_{P24}$/*0101, $VP2_{P21}$/*0301 | Der p $1_{P2}$/*0101, Der p $1_{P14}$/*0301 | 1.36 |
| $VP2_{P21}$/*0301 | Der p $1_{P14}$/*0301 | 2.92 |
| $VP2_{P21}$/*0401, $VP2_{P2}$/*1101 | Phl p $1_{P13}$/*0401, Phl p $1_{P24}$/*1101 | 6.34 |
| $VP1_{P23}$/*0701, $VP2_{P26}$/*0701 | Fel d $1_{P2}$/*0701 | 6.74 |
| $VP2_{P21}$/*0401 | Der p $1_{P30}$/*0401 | 10.4 |
| $VP2_{P21}$/*0401, $VP2_{P25}$/*1501 | Der p $1_{P30}$/*0401, Der p $1_{P34}$/*1501 | 10.6 |
| $VP1_{P23}$/*0701, $VP2_{P26}$/*0701 | Der p $1_{P7}$/*0701, Der p $1_{P39}$/*0701 | 11.5 |
| $VP1_{P23}$/*0101, $VP2_{P24}$/*0101 | Der p $1_{P2}$/*0101 | 11.9 |
| $VP1_{P23}$/*0101, $VP2_{P24}$/*0101 | Fel d $1_{P14}$/*0101 | 14.6 |
| $VP2_{P2}$/*1101, $VP2_{P25}$/*1501 | Bet v $1_{P14}$/*1101, Bet v $1_{P18}$/*1501 | 15.4 |
| $VP1_{P23}$/*0101, $VP2_{P24}$/*0101 | Phl p $1_{P20}$/*0101 | 15.9 |
| $VP2_{P21}$/*0301, $VP2_{P25}$/*1501 | Der p $1_{P14}$/*0301, Der p $1_{P34}$/*1501 | 18.4 |
| $VP2_{P21}$/*0301, $VP2_{P2}$/*1101 | Bet v $1_{P38}$/*0301, Bet v $1_{P14}$/*1101 | 19.2 |
| $VP1_{P23}$/*0701, $VP2_{P26}$/*0701 | Der p $1_{P7}$/*0701, Der p $1_{P39}$/*0701 | 19.4 |
| $VP1_{P23}$/*0101, $VP2_{P24}$/*0101 | Phl p $1_{P20}$/*0101 | 20.2 |
| $VP2_{P21}$/*0301 | Der p $1_{P14}$/*0301 | 21.7 |
| $VP2_{P21}$/*0401 | Phl p $1_{P13}$/*0401 | 23.9 |
| $VP2_{P21}$/*0301, $VP2_{P25}$/*1501 | Fel d $1_{P3}$/*0301, Fel d $1_{P13}$/*1501 | 24.0 |

| | | |
|---|---|---|
| VP2$_{P21}$/*0301 | Der p 1$_{P14}$/*0301 | 26.5 |
| VP2$_{P21}$/*0301, VP1$_{P23}$/*0701, VP2$_{P26}$/*0701 | Fel d 1$_{P3}$/*0301, Fel d 1$_{P2}$/*0701 | 26.9 |
| VP2$_{P21}$/*0401 | Der p 1$_{P30}$/*0401 | 33.4 |
| VP2$_{P21}$/*0301 | Der p 1$_{P14}$/*0301 | 33.7 |
| VP1$_{P23}$/*0101, VP2$_{P24}$/*0101, VP2$_{P25}$/*1501 | Der p 1$_{P2}$/*0101, Der p 1$_{P34}$/*1501 | 36.3 |
| VP1$_{P23}$/*0701, VP2$_{P26}$/*0701, VP2$_{P2}$/*1101 | Der p 1$_{P7}$/*0701, Der p 1$_{P39}$/*0701, Der p 1$_{P24}$/*1101 | 39.2 |
| VP2$_{P21}$/*0401, VP1$_{P23}$/*0701, VP2$_{P26}$/*0701 | Bet v 1$_{P18}$/*0401, Bet v 1$_{P27}$/*0701, Bet v 1$_{P48}$/*0701 | 51.4 |
| VP2$_{P21}$/*0301, VP2$_{P2}$/*1101 | Der p 1$_{P14}$/*0301, Der p 1$_{P24}$/*1101 | 56.4 |
| VP2$_{P25}$/*1501 | Der p 1$_{P34}$/*1501 | 66.5 |

Each row represents one subject.

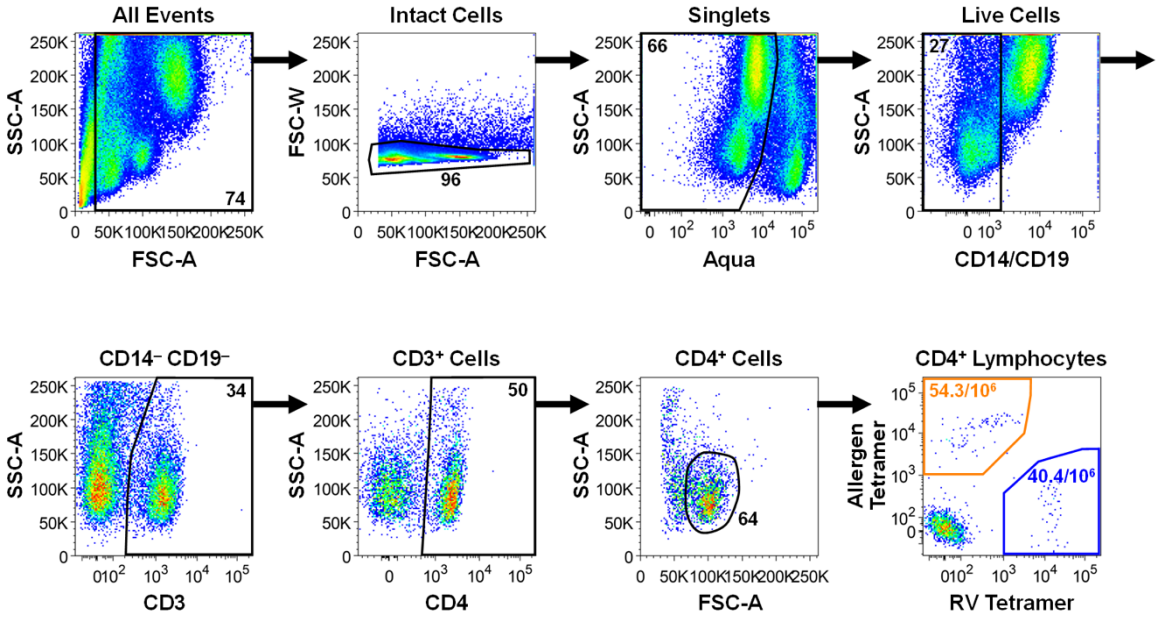


**Figure 4-1. Gating Strategy for the Identification of Rhinovirus- and Allergen-Specific CD4⁺ T Cells**

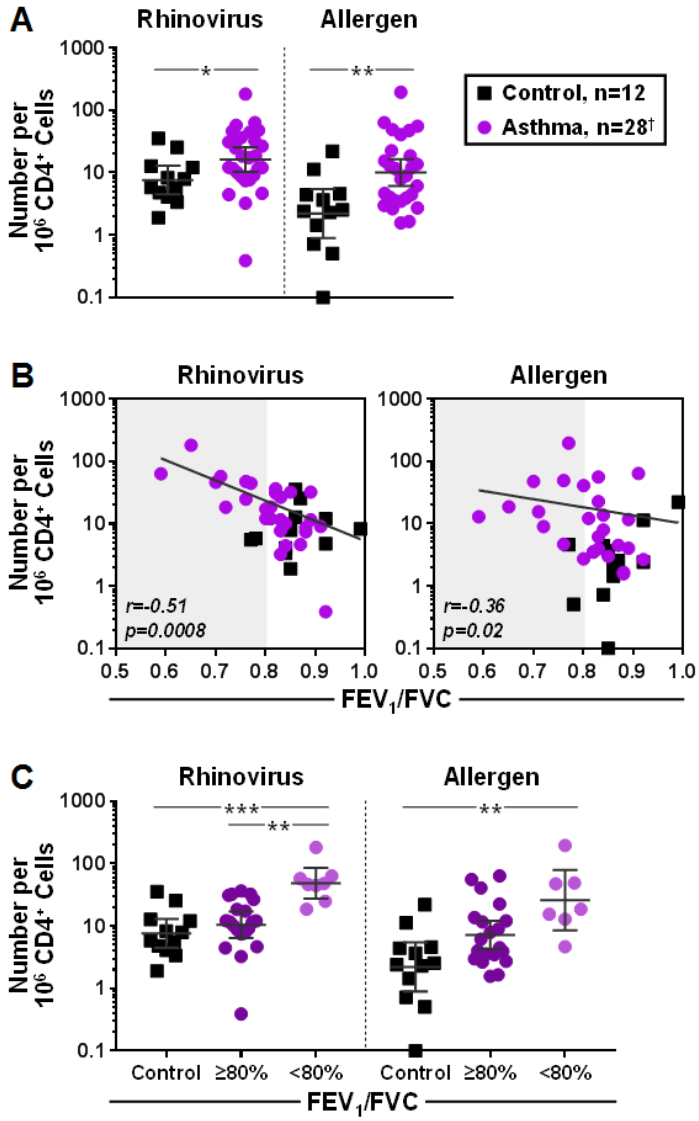


**Figure 4-2. Higher Numbers of Circulating RV-Specific CD4⁺ T Cells Are Linked to Worse Lung Function in Uninfected Asthmatics**

Cells were analyzed in all subjects prior to any intervention (baseline). **(A)** Frequencies of RV- and allergen-specific $CD4^+$ T cells. **(B)** Correlation between numbers of antigen-specific T cells and $FEV_1/FVC$ at baseline. Lines depict semi-logarithmic regressions. Shaded regions denote reduced lung function [337]. **(C)** Antigen-specific $CD4^+$ T cell numbers, classified according to asthmatic lung function. Bars denote geometric means ± 95% CI. †n=27 for allergen-specific cells. *p≤0.05, **p≤0.01.

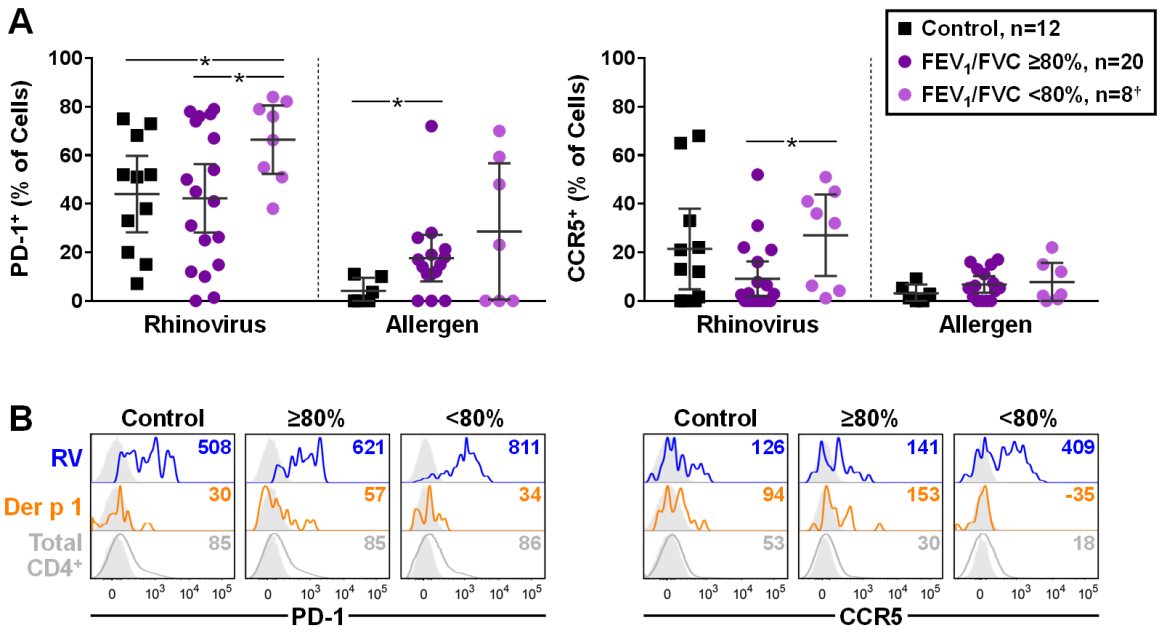


**Figure 4-3. Expression of PD-1 and CCR5 on Antigen-Specific CD4⁺ T Cells in Relation to Lung Function**

**(A)** Percentage of antigen-specific cells expressing PD-1 and CCR5. Bars denote geometric means ± 95% CI. **(B)** Representative histograms depicting expression of PD-1 and CCR5 in asthmatic and control subjects. Shaded histograms depict FMO controls, and values denote corrected geometric mean fluorescence intensity (MFI). †n=7 for allergen-specific cells. *p≤0.05, **p≤0.01, ***p≤0.001.

### *Armed RV-Specific $T_H1$ Effectors Co-Exist with $T_H2$ Cells in Uninfected Asthmatics*

In **Chapters 2** & **3** we reported that in healthy uninfected subjects, the majority of circulating RV-specific T cells that recognize conserved epitopes bear memory phenotypes consistent with priming by previous exposures to related RV strains. Here, we report the same finding for RV-specific T cells in asthmatics. In asthmatics, RV-specific T cells contained a similarly high percentage of memory ($CD45RO^+$) cells as controls (Geo. mean= 79.8% vs. 80.9%); moreover, this was markedly higher compared with the percentage of allergen-specific memory T cells (38.2%, p=0.0013) (**Figure 4-4**). Assessment of tissue-homing effector memory cells ($T_{EM}$: $CCR7^-CD45RO^+$) revealed similar percentages within RV-specific and allergen-specific cells of asthmatics; however, the percentage of lymphoid-homing central memory cells ($T_{CM}$: $CCR7^+CD45RO^+$) was higher in RV-specific cells versus allergen-specific cells, consistent with active immune surveillance of re-circulating virus-specific cells (**Figure 4-4**). Analysis of complex signatures confirmed a $T_H1$ phenotype of RV-specific $T_{CM}$ and $T_{EM}$ cells based on expression of the characteristic chemokine receptors CXCR3 and CCR5 (**Figure 4-5**). While RV-specific $T_{CM}$ contained $CXCR3^+$ cells that lacked CCR5, the inverse was true of RV-specific $T_{EM}$ (**Figure 4-5**). Of note, $CXCR3^-CCR5^+$ $T_{EM}$ cells were found to be preferentially activated in the nose during RV infection (**Chapter 3**). RV-specific T cells also contained $T_{CM}$ and $T_{EM}$ cells that lacked any of the surface markers tested. In contrast, allergen-specific memory cells bore predominantly $T_H2$-associated surface markers (CCR4, CRTH2), and the signatures of $T_{CM}$ and $T_{EM}$ subsets did not differ (**Figure 4-5** & *data not shown*). These data confirm the presence of RV-specific $T_H1$ effectors armed to home to the lung in uninfected subjects, and their co-existence with type 2 responses.

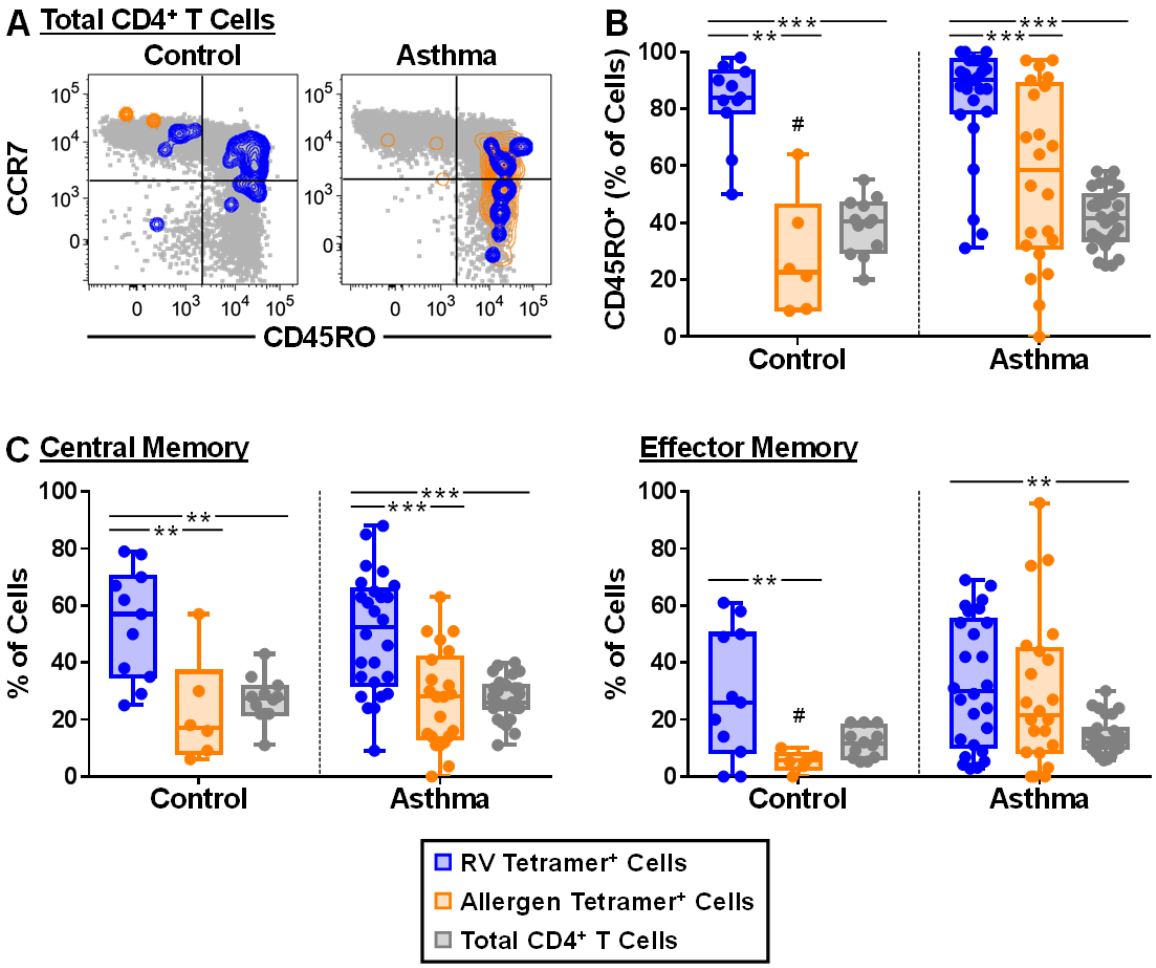


**Figure 4-4. Memory Signatures of Antigen-Specific T Cells in Uninfected Asthmatics and Controls**

**(A)** Representative plots showing expression of CCR7 and CD45RO on RV-specific and allergen-specific cells relative to total $CD4^+$ T cells. **(B & C)** Percentage of cells expressing **(B)** total memory cells ($CD45RO^+$), and **(C)** central ($CCR7^+$) and effector ($CCR7^-$) memory subsets at baseline. *differences between cell types; #differences between groups. **$p \leq 0.01$, ***$p \leq 0.001$.

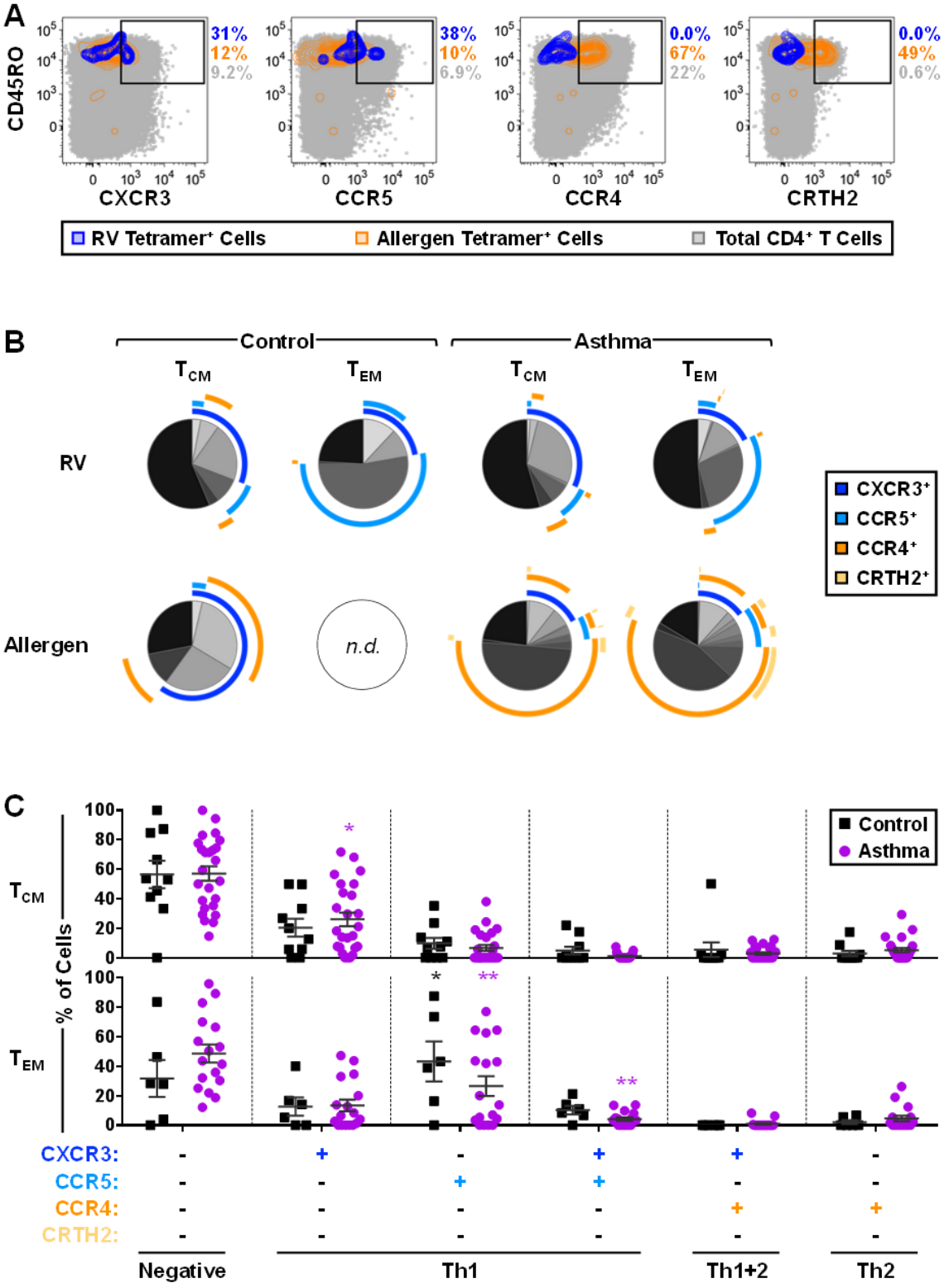
A
CD45RO
CXCR3
CCR5
CCR4
CRTH2
31%
12%
9.2%
38%
10%
6.9%
0.0%
67%
22%
0.0%
49%
0.6%
RV Tetramer+ Cells
Allergen Tetramer+ Cells
Total CD4+ T Cells
B
Control
Asthma
TCM
TEM
RV
Allergen
n.d.
CXCR3+
CCR5+
CCR4+
CRTH2+
C
% of Cells
Control
Asthma
CXCR3:
CCR5:
CCR4:
CRTH2:
Negative
Th1
Th1+2
Th2

**Figure 4-5. Expression of $T_H1$- and $T_H2$-Associated Markers on Antigen-Specific T Cells in Uninfected Subjects**

**(A)** Representative plots depicting expression of $T_H1$ and $T_H2$ surface markers on RV- and allergen-specific cells for one asthmatic subject. **(B)** SPICE plots displaying the average signatures of central and effector memory cells in asthmatic and healthy control subjects. **(C)** Percentage of RV-specific $T_{CM}$ and $T_{EM}$ cells displaying discrete surface signatures. *difference between central and effector memory cell types. Bars denote means ± SEM. *$p \leq 0.05$, **$p \leq 0.01$. n.d., not determined

### *Asthmatics with High IgE Mount an Exaggerated T Cell Response to Rhinovirus*

Next, to assess T cell responses during infection, asthmatics and controls were experimentally infected with RV-A16, as described in **Appendix I**, and shown in the schematic in **Figure 4-6**. This study design also enabled evaluation of the relationship between T cell responses and IgE by stratifying asthmatics based on IgE levels and assessing the effect of IgE blockade *in vivo*. Asthmatics with high IgE (≥596 IU/mL) received RV challenge only, whereas those with lower IgE levels within the dosing range for omalizumab (133-493 IU/mL) were enrolled in a DBPC trial of anti-IgE treatment beginning 8 weeks prior to RV challenge (**Figure 4-6**, see **Appendix I** for full details on the clinical study).

Following RV challenge, asthmatics with high IgE mounted a more rapid and robust T cell response to RV compared with controls, based on higher numbers of circulating RV-specific $CD4^+$ T cells during acute infection (day 4, $p \leq 0.001$) and the peak effector phase (day 7, $p=0.003$), as well as increased fold induction from baseline (**Figure 4-7**. See **Appendix II** for complete statistical tables). In asthmatics with high IgE, but not controls, the numbers of allergen-specific $CD4^+$ T cells also increased during acute infection, but to a lesser degree than the RV-specific response (day 7, mean fold change [day 0]: RV=39.5; allergen=5.1)(**Figures 4-7** & **4-8, Appendix II**). Asthmatics with high IgE also had worse symptoms in both the upper and lower airways, but had similar viral clearance compared with controls (see **Appendix I**).

In those asthmatics with lower IgE who received anti-IgE, T cell responses to RV were weaker during the effector phase than in asthmatics with higher IgE, (Geo. mean= 18 per $10^6$ $CD4^+$ T cells vs 45 per $10^6$, $p=0.028$), and numbers of allergen-specific cells did not change (**Figures 4-7** & **4-8, Appendix II**). Randomized allocation in the anti-IgE trial

resulted in a disproportionately large number of asthmatics in the placebo group who had normal lung function at study entry, and $FEV_1/FVC$ was significantly increased as compared with the treatment group ($p=0.005$) (see **Appendix I** for additional details). RV-specific T cell numbers remained unchanged during the effector phase in subjects receiving placebo, and the numbers tracked lower as compared with subjects receiving anti-IgE (**Figure 4-7** & **Appendix II**). Numbers of RV-specific T cells, but not allergen-specific cells, remained elevated three weeks post-infection, coincident with a "late" symptom phase in asthmatics (**Figure 4-7** & **Appendix I**). Thus, RV-specific T cells responses are amplified after infection in asthmatics with high IgE, and remain elevated for several weeks. By contrast, allergen-specific T cells revert to baseline numbers despite their initial expansion in asthmatics with high IgE only.

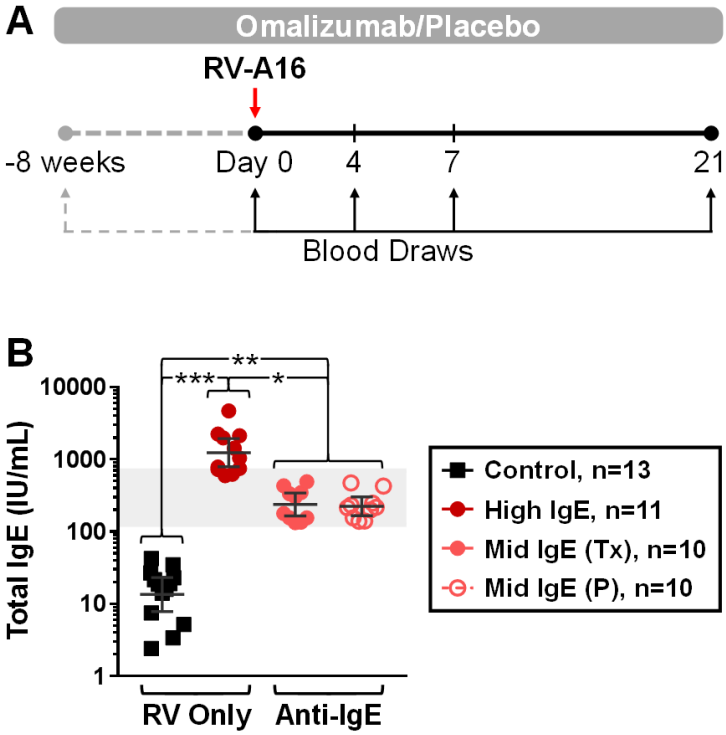


**Figure 4-6. RV-A16 Experimental Challenge Model and IgE Levels in Study Subjects**

**(A)** Study design schematic. All subjects received RV-A16 challenge. A subset of asthmatic subjects was enrolled in a DBPC trial of anti-IgE treatment that started eight weeks prior to RV challenge (gray). **(B)** Total IgE in study subjects at screening. Shaded region denotes anti-IgE dosing range. Bars denote geometric means ± 95% CI. *p≤0.05, **p≤0.01, ***p≤0.001.

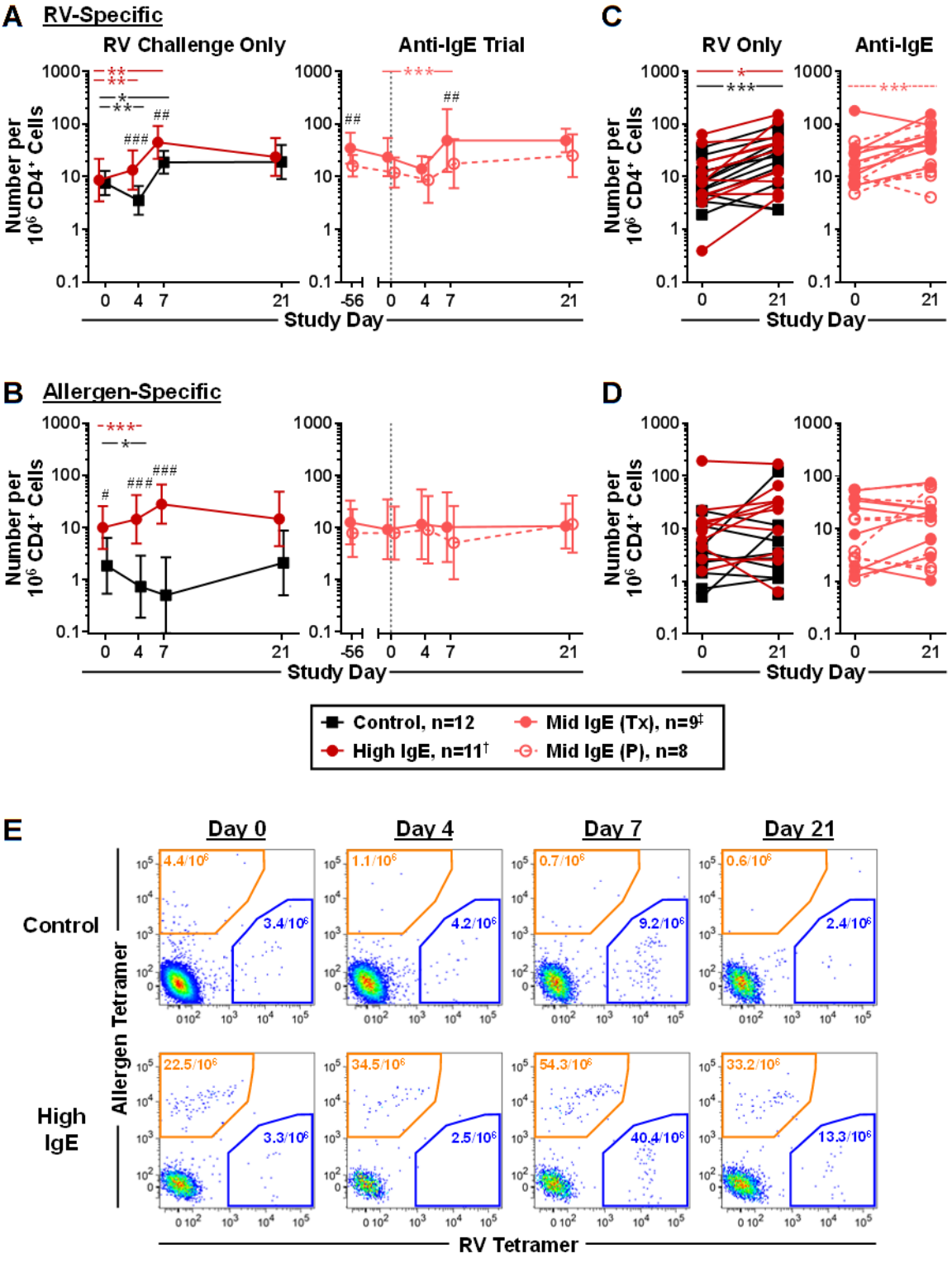
A RV-Specific
RV Challenge Only
Anti-IgE Trial
C
RV Only
Anti-IgE
B Allergen-Specific
D
Number per 10^6 CD4+ Cells
Study Day
Control, n=12
High IgE, n=11†
Mid IgE (Tx), n=9‡
Mid IgE (P), n=8
E
Day 0
Day 4
Day 7
Day 21
Control
High IgE
Allergen Tetramer
RV Tetramer
4.4/10^6
3.4/10^6
1.1/10^6
4.2/10^6
0.7/10^6
9.2/10^6
0.6/10^6
2.4/10^6
22.5/10^6
3.3/10^6
34.5/10^6
2.5/10^6
54.3/10^6
40.4/10^6
33.2/10^6
13.3/10^6

**Figure 4-7. Changes in Numbers of Antigen-Specific T Cells During Infection in Asthmatics and Controls**

**(A & B)** T cell numbers immediately before RV challenge (day 0) and at days 4, 7, and 21 post-challenge. In the anti-IgE trial, cells were also analyzed immediately before the first administration of anti-IgE (day -56). **(C & D)** Change in T cell numbers in the convalescent phase (day 21 vs. 0) for each subject. **(E)** Representative flow plots depicting RV and allergen tetramer staining in one high IgE asthmatic and one control during infection. Symbols denote geometric means ± 95% CI. *denotes within-group comparisons with day 0; #denotes between-group comparisons. †n=10 for allergen-specific cells; ‡n=8 on days 0-7 due to sample limitations. *$p \leq 0.05$, **$p \leq 0.01$, ***$p \leq 0.001$.

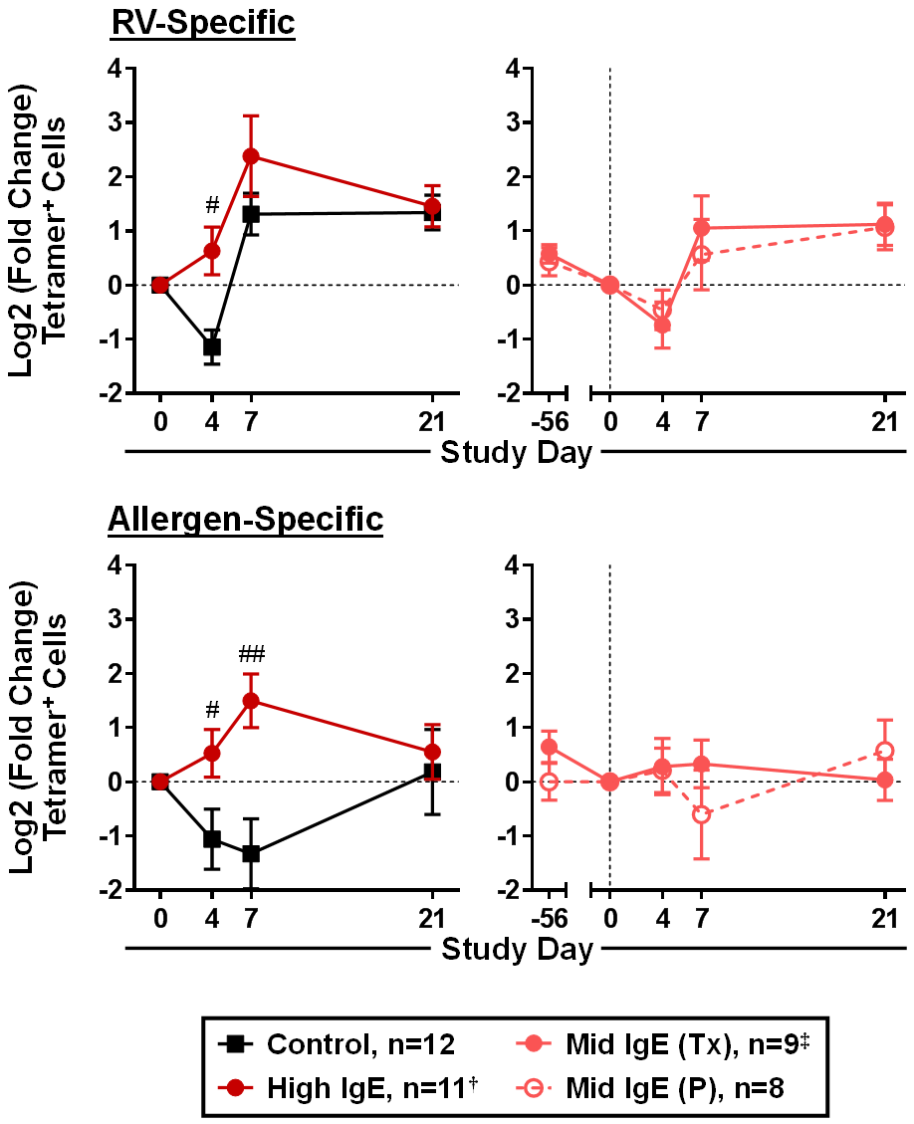


**Figure 4-8. Augmented Induction of Antigen-Specific T Cells in Asthmatics with High IgE During RV Infection**

Fold change values are Log2-transformed. Symbols denote means ± SEM. #denotes between-group comparisons. †n=10 for allergen-specific cells; ‡n=8 on days 0-7 due to sample limitations. *p≤0.05, **p≤0.01, ***p≤0.001.

### *Circulating $T_H1$ Cells, But Not $T_H2$ Cells, Are Activated During Infection in Asthmatics*

Further analysis confirmed that $T_H1$ and $T_H2$ signatures were maintained in RV- and allergen-specific $T_{CM}$ and $T_{EM}$ cells, respectively, over the course of infection in both asthmatics with high IgE and controls (**Figure 4-9** & *data not shown*). On day 4, the percentage of circulating RV-specific T cells expressing PD-1 decreased, indicating egress of PD-$1^+$ cells from the periphery during the acute phase (**Figure 4-10**). Additionally, RV-specific cells alone were activated during the effector phase, as judged by downregulation of IL-7Rα, coincident with increased levels of PD-1 and CCR5. Similar profiles were observed for RV-specific T cells in asthmatics with lower IgE regardless of treatment group, although RV-specific T cells expressed lower IL-7Rα and higher PD-1 at the start of the study in the anti-IgE group that also had worse lung function (**Figure 4-10**). T cell activation during infection was most pronounced for RV-specific subsets that expressed CXCR3 and CCR5 either alone or in combination (**Figure 4-10**). Together, these data confirm the selective activation of circulating RV-specific $T_H1$ cells in asthmatics during infection, as well as the maintenance of RV-induced $T_H1$ activation in asthmatics who received anti-IgE.

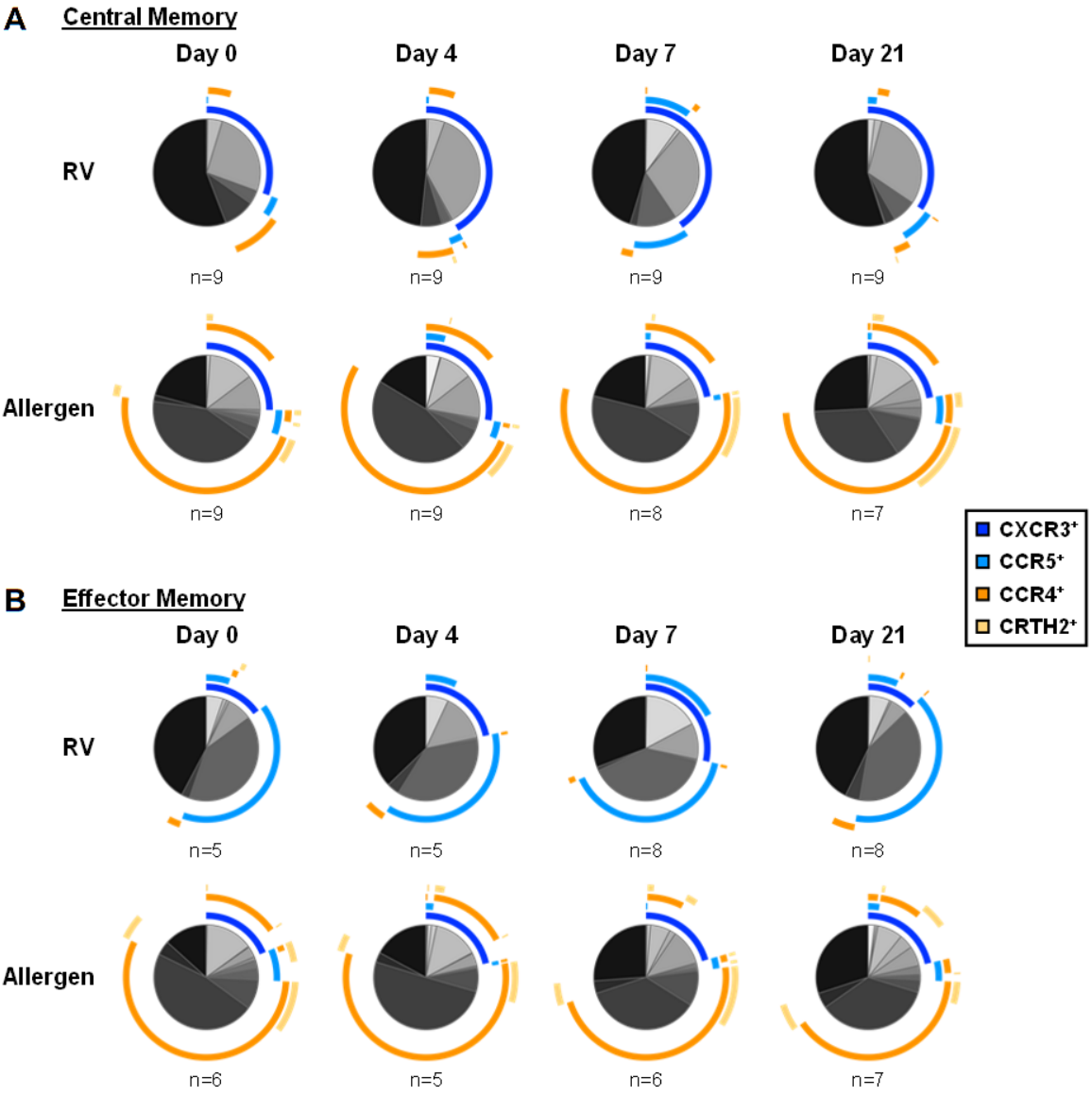


**Figure 4-9. RV- and Allergen-Specific Cells Maintain $T_H1$ and $T_H2$ Surface Phenotypes During RV Infection**

SPICE charts displaying the averaged surface signature for RV- and allergen-specific **(A)** central memory, and **(B)** effector memory cell populations in asthmatics with high IgE.

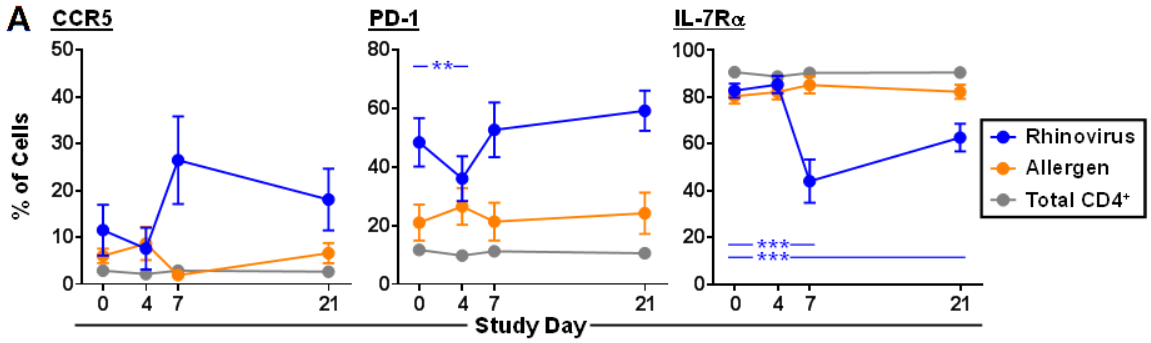
A
CCR5
PD-1
IL-7Rα
% of Cells
Study Day
Rhinovirus
Allergen
Total CD4+

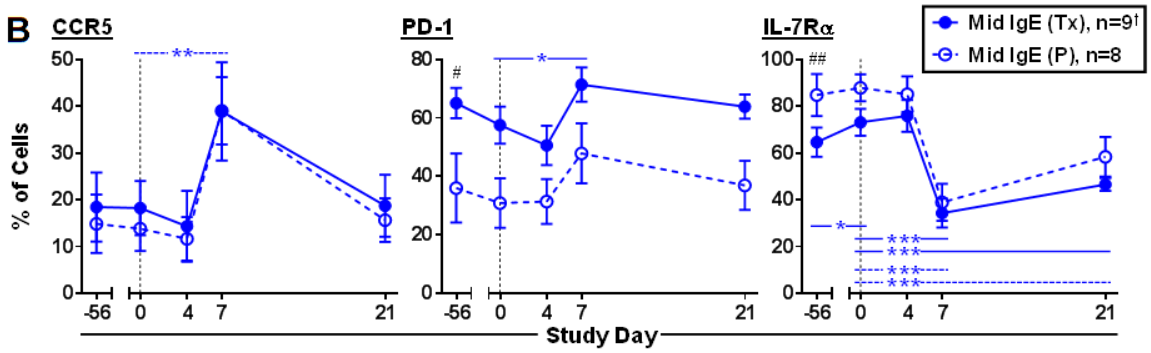
B
CCR5
PD-1
IL-7Rα
% of Cells
Study Day
Mid IgE (Tx), n=9†
Mid IgE (P), n=8

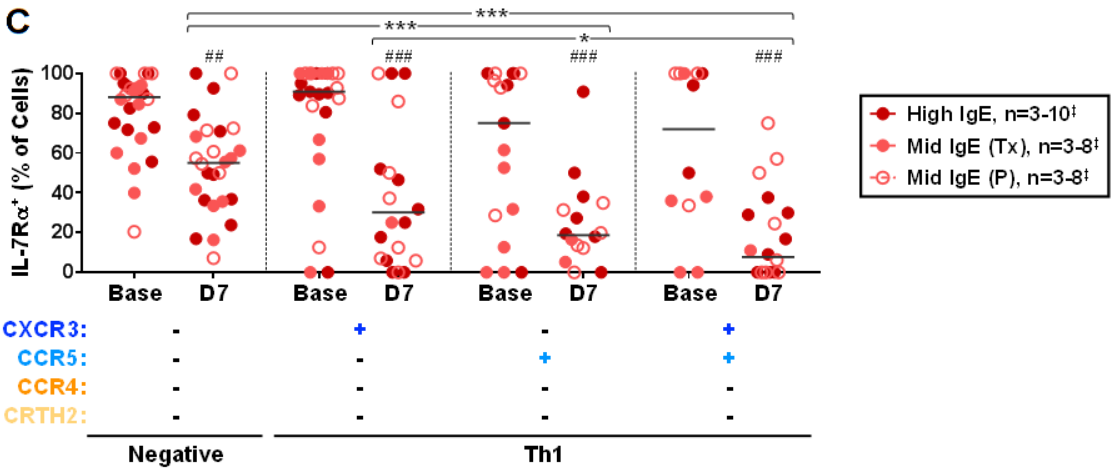
C
IL-7Rα+ (% of Cells)
Base
D7
CXCR3:
CCR5:
CCR4:
CRTH2:
Negative
Th1
High IgE, n=3-10‡
Mid IgE (Tx), n=3-8‡
Mid IgE (P), n=3-8‡

**Figure 4-10. RV-Specific T Cells Are Preferentially Activated in Asthmatics During RV Infection**

**(A)** Change in the percentage of cells expressing markers of respiratory homing potential and activation in asthmatics with high IgE during infection. *denotes differences across time. Symbols and bars denote means ± SEM. **(B)** Change in the percentage of RV-specific cells expressing markers of respiratory homing potential and activation in asthmatics with lower levels of IgE that are enrolled in a trial of anti-IgE during infection. *denotes differences across time; #denotes between-group differences. Symbols and bars denote means ± SEM. **(C)** Percentage of RV-specific cells in asthmatics expressing IL-7Rα at baseline and during the effector phase (day 7) according to surface signature. *denotes differences between signatures at day 7; #denotes differences between time points. Bars denote medians. †n=8 on days 0-7 due to sample limitations; ‡subjects with low cell counts within each subpopulation were excluded. *$p \leq 0.05$, **$p \leq 0.01$, ***$p \leq 0.001$.

### *RV Infection Induces a Robust Type 1 Response in the Upper Airways of Asthmatics*

Interferons are critical to anti-viral responses and facilitate $T_H1$ differentiation. Deficient production of IFN-α by cells isolated from the blood and airways of asthmatics has been attributed, at least in part, to an inhibitory IgE pathway operating in plasmacytoid DCs (pDCs)[251–254]. Such a deficit might be expected to manifest as an attenuated $T_H1$ responses at the site of RV infection; thus, we performed a comprehensive analysis of $T_H1$-associated cytokines at all levels of the $T_H1$ axis in the noses of infected subjects. Using nasal lining fluid to optimize the detection of low-level cytokines revealed a marked induction of IFN-α during acute infection in asthmatics with high IgE, and was comparable to controls (**Figure 4-11**). Additionally, the $T_H1$ effector cytokine IFN-γ peaked during the acute phase and remained detectable up to three weeks following infection (**Figure 4-11**). Notably, for asthmatics in the anti-IgE trial, IFN-α and IFN-γ levels were significantly higher in the anti-IgE group during acute infection than those receiving placebo. By contrast, $T_H2$ cytokine levels did not change significantly during infection in asthmatics, although asthmatics had higher levels at baseline as compared with controls (**Figure 4-11**).

Assessments of more abundant $T_H1$-promoting cytokines and chemokines that are produced by pDCs—including IL-6, IL-8, IP-10, and MIP-1β—were performed using nasal washes [338–340]. High levels of the $T_H1$ chemoattractants IP-10 and MIP-1β—the chemokine ligands of CXCR3 and CCR5, respectively—were induced at high levels in all asthmatics, in conjunction with the pro-inflammatory cytokines IL-6 and IL-8 (**Figure 4-12**). Moreover, there was a higher fold increase in IP-10 levels in asthmatics with high IgE

compared with controls (**Figure 4-12**). Together, these cytokine profiles indicate a robust type 1 response at all levels of the $T_H1$ axis in the upper airways of infected asthmatics, despite high IgE and a pre-existing $T_H2$ milieu.

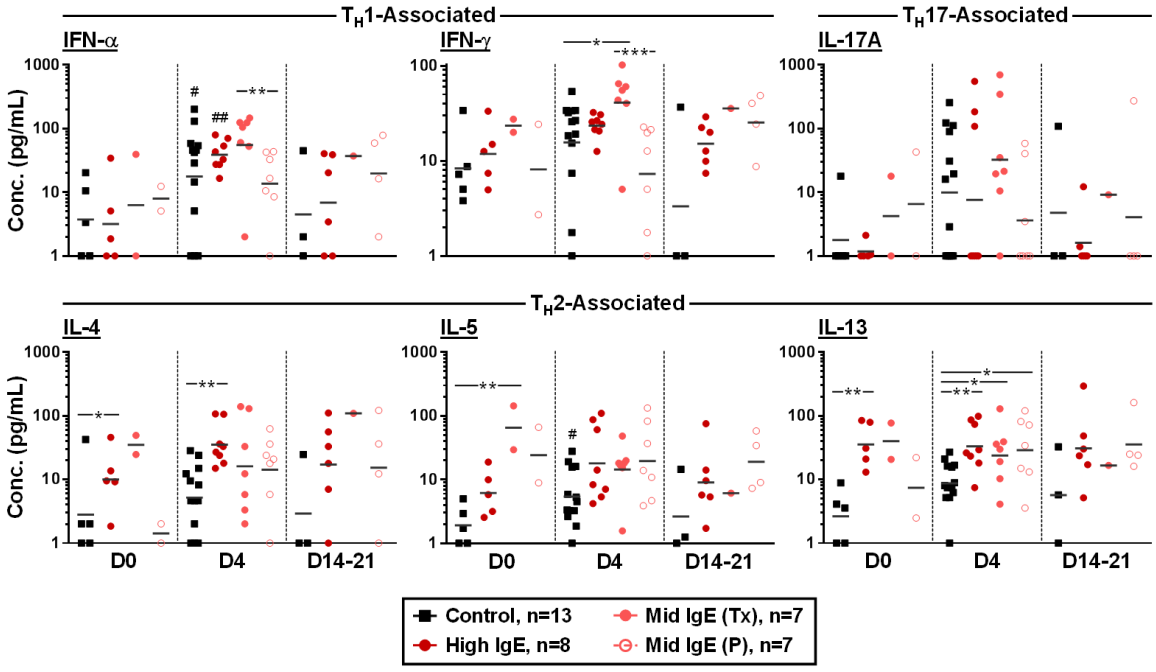


**Figure 4-11. Levels of $T_H$ Cytokines in the Nose During RV Infection**

Cytokines were analyzed in nasal lining fluid specimens during RV infection. Sample sizes varied over time, owing to the inability to perform analyses in "dry" samples. Statistics were performed in sample sizes ≥3. Bars denote geometric means. *denotes between-group comparisons; #denotes within-group difference compared with day 0. *p≤0.05, **p≤0.01, ***p≤0.001.

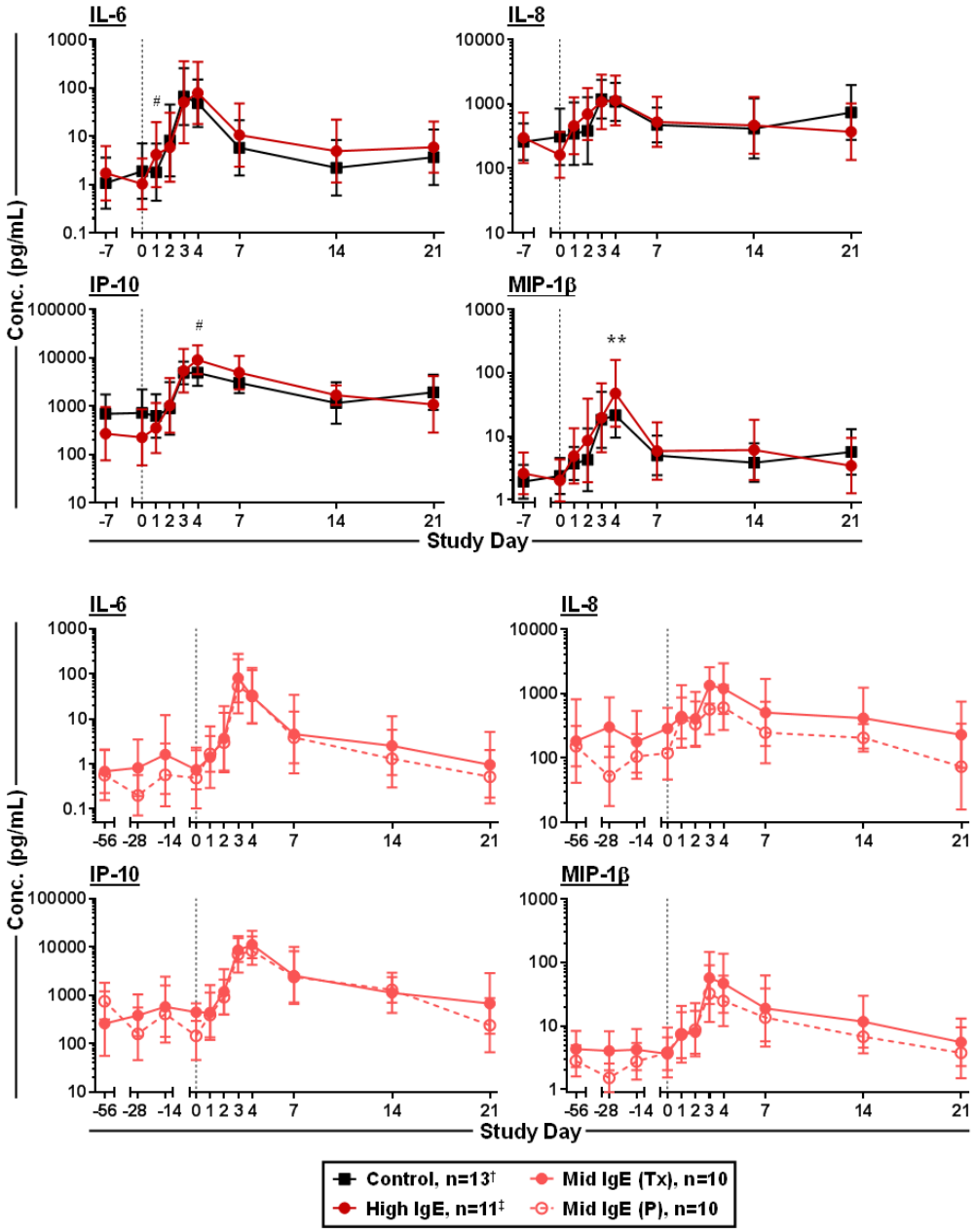


**Figure 4-12. Levels of Type 1-Associated Pro-Inflammatory Cytokines in the Nose**

Cytokines were assayed in nasal wash specimens in all subject groups. Symbols denote geometric means ± 95% CI. *denotes between-group comparison of concentrations; #denotes between-group comparison of fold change from day 0. †n=11 for IL-6 and MIP-1β; ‡n=10 for IL-6 and MIP-1β. *p≤0.05, **p≤0.01.

### *Anti-IgE Preferentially Abolishes IgE Receptor on Plasmacytoid Dendritic Cells Compared with Other Cell Types*

During RV infection, circulating pDCs—but not myeloid DCs (mDCs)—were expanded in the blood of asthmatics with high IgE, but not in controls or asthmatics with moderate IgE enrolled in the anti-IgE trial (**Figure 4-13**). Analyses of the three principal cell types in the blood that express the high-affinity IgE receptor performed prior to study initiation revealed that pDCs have the strongest correlation between FcεRIα expression and IgE levels (**Figure 4-14**). Although FcεRIα was reduced on all cell types following anti-IgE treatment, its expression was maintained on ~55% of basophils and ~30% of mDCs, but was almost completely abolished on pDCs (**Figure 4-14**). Moreover, while receptor levels partially rebounded on mDCs after infection, this did not occur in pDCs. Thus, pDCs are more sensitive to *in vivo* IgE blockade compared with FcεRIα$^+$ cell types involved in type 2 inflammation.

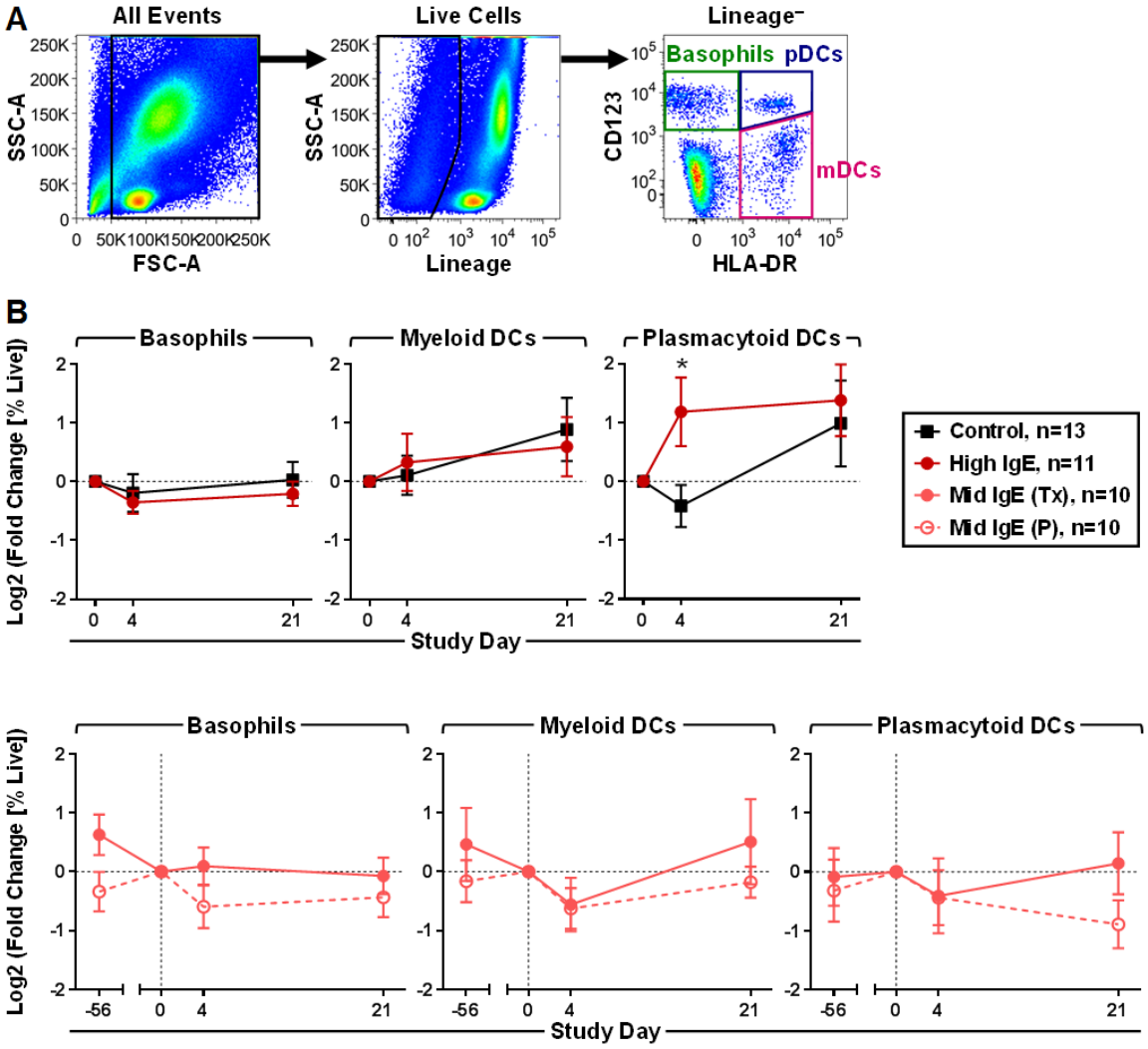


**Figure 4-13. Circulating Plasmacytoid Dendritic Cells Increase During Acute Rhinovirus Infection**

**(A)** Gating strategy for the identification of dendritic cell populations and basophils from whole blood. **(B)** Fold change in percentages of basophils, mDCs, and pDCs from day 0 for all subject groups. Fold change values are Log2-transformed. Symbols represent means ± SEM. *p≤0.05.

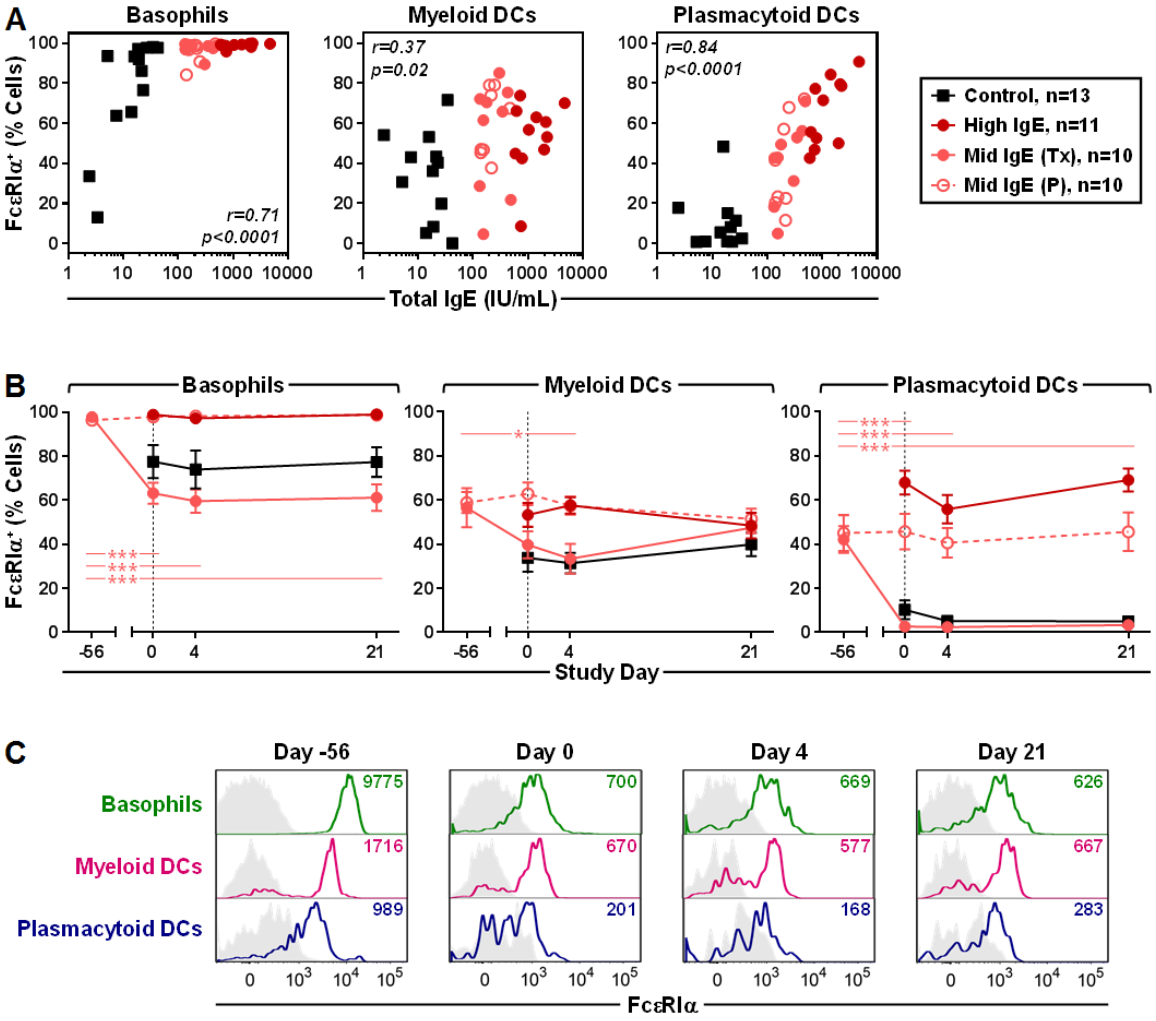


**Figure 4-14. IgE Receptor and its Relationship to Serum IgE and Anti-IgE Treatment**

**(A)** Spearman correlation of FcεRIα expression on cell populations versus total IgE at baseline. **(B)** Percentage of cells expressing FcεRIα over the course of RV infection. Symbols represent means ± SEM. **(C)** Representative histograms depicting expression of FcεRIα in one asthmatic subject receiving anti-IgE. Shaded histograms depict FMO controls. Values denote the corrected MFI for FcεRIα. *p≤0.05, **p≤0.01, ***p≤0.001.

## Discussion

Allergic asthma is commonly thought to be driven by type 2 inflammatory responses. Here, by precisely tracking antigen-specific $T_H1$ and $T_H2$ cells in parallel and analyzing multiple immune and clinical parameters during RV infection, we find a paradoxical amplification of anti-viral $T_H1$ responses in asthmatics with high IgE. Specifically, we observed increased numbers of RV-specific $T_H1$ cells compared with healthy controls during infection, as well as preferential activation of $T_H1$ versus $T_H2$ cells in the blood despite a rise in $T_H2$ cell numbers. Furthermore, we provide evidence of the recruitment of $T_H1$ cells to the airways based on transitions in functional markers on cells in the circulation coupled with the induction of $T_H1$ chemoattractants and a robust $T_H1$ signature in the nose.

Analysis of RV-specific T cells in uninfected subjects prior to virus inoculation also yielded new insight into their role in maintaining inflammation in the absence of infection. While higher numbers of allergen-specific T cells were expected in uninfected asthmatics compared with non-allergic subjects, the increased numbers of RV-specific memory cells in uninfected asthmatics and their link to worse lung function were novel findings. Those RV-specific T cells identified in this study target conserved peptide epitopes, as described in **Chapter 2**; as such, these cells are poised to respond rapidly as a result of priming by previous RV infections. This is borne out in their tissue-homing and memory signatures, and their rapid expansion and activation following RV inoculation. Such traits of immune surveillance would also be expected to elicit T cell effector functions in the inflamed airways. In contrast to allergen-specific T cells, numbers of RV-specific T cells remained elevated several weeks after virus was cleared, coincident with sustained secretion of $T_H1$-associated mediators in the nose, and a late symptom phase in asthmatics (**Appendix I**). Together,

these observations support the view that a single RV exposure agitates and sustains airway inflammation by promoting $T_H1$ inflammation in allergic asthmatics. Given that younger asthmatics typically experience 6-8 colds annually, we propose a model wherein repeated RV infections occurring in close succession and in the context of pre-existing type 2 inflammation induce a paradoxical amplification of anti-viral $T_H1$ responses that drive chronic airway inflammation and recurrent disease exacerbations. This process, which disrupts T cell homeostatic mechanisms that regulate $T_H1$ responses, raises the inflammatory set point, thereby reprogramming subsequent responses to viral exposures.

Robust anti-viral $T_H1$ responses following infection were associated with an uptick in numbers of circulating allergen-specific T cells that lacked an activated phenotype. While this might reflect a bystander response resulting in the proliferating of allergen-specific cells, the failure for these cells to downregulate IL-7Rα was intriguing. Recent work in a mouse model established a requirement for IL-7 in homeostasis of allergen-specific T cells in the airways, supporting its relevance to these cells [341]. Nevertheless, to our knowledge, nothing is known about the mechanisms of trafficking and activation of allergen-specific cells in humans *in vivo*, or bystander responses of these cells. It is possible that the increase in allergen-specific cells in the periphery during RV infection reflects mobilization of pre-existing allergen-specific cells from inflamed sites or anatomical niches in the absence of proliferation. Alternatively, it may arise from IL-7-independent bystander activation and proliferation, possibly mediated via IL-2 and IL-15 [342,343]. Whether allergen recognition is required remains unknown. Given that the majority of allergen-specific cells were dust mite-specific, concomitant exposure to this perennial allergen would be expected during RV infection. The elevated levels of $T_H2$ cytokines in the nose in the absence of infection align

with this notion. On the other hand, a robust $T_H2$ response during infection might be suppressed, at least in part, by anti-viral responses owing to the weaker receptor affinity for allergen versus RV epitopes, inhibition by the $T_H1$ axis, and cell competition for activating factors [246,248,249,344,345].

Emerging data on asthma endotypes has revealed a role for $T_H1$ cells in asthmatics with severe disease, including our own work in asthmatic children [151,158,336]. These findings solidify the concept of "$T_H1$ on $T_H2$" inflammation that is borne out by our recent work linking type 1 mediators to sensitivity to inhalant allergens in patients with $T_H1$-associated asthma [336]. Nonetheless, a key question remains regarding the mechanisms of $T_H1$ amplification in allergic asthma, and specifically the link between IgE and the $T_H1$ axis. With this in mind, it is noteworthy that $T_H1$ responses were less robust in untreated asthmatics that had lower levels of IgE and normal lung function versus those with higher IgE.

Although current dosing guidelines precluded us from testing the capacity for anti-IgE to modulate anti-viral $T_H1$ responses in asthmatics with high IgE, we did gain important new insight into the actions of anti-IgE on pDCs relative to other cell types that express IgE receptor, as well as the relationship between IgE receptor and serum IgE across a broad range of IgE levels. Specifically, expression of surface IgE receptor on pDCs and serum IgE were found to be tightly linked. Moreover, the IgE receptor was efficiently downregulated in pDCs of subjects who received anti-IgE, thereby potentiating the disruption of IgE networks in these cells. A key question is whether this might be clinically beneficial. Treatment of asthmatic children with omalizumab has been reported to enhance RV-induced IFN-α responses in pDCs *in vitro*, suggesting that IgE blockade might rectify

deficient IFN responses [254]. In the present study, the trend towards increased IFNs in the nose of asthmatics in the anti-IgE group compared with untreated asthmatics with high IgE agrees with this theory, although this did not transpire as an amplified $T_H1$ response during infection, as one might have predicted. This aspect also raises the important question of whether increased IFNs are a desirable outcome in asthmatic patients infected with RV. This may be the case for those who have IgE levels that fall within the lower range specified for anti-IgE treatment, and within whom re-programming of the inflammatory set point may be limited; however, in those asthmatics with higher IgE levels or more severe disease, enhanced IFNs might prove detrimental owing to a loss of T cell homeostasis and consequent re-programming of $T_H1$ responses. Moreover, it is possible that pDCs are refractory to IgE blockade in patients with higher IgE. Given that IgE receptor is maintained at the cell surface by its interactions with IgE and that pDCs provide a sensitive barometer of allergic sensitization, our data are consistent with the notion that pDCs are the last to load as IgE levels rise, and the first to lose IgE in the presence of IgE blockade [187,188,346]. This concept of "sequential loading" of various IgE-receptor-bearing cell types introduces an important variable and raises the question of whether the susceptibility of pDCs to IgE modulation falls within a specified range of IgE [346]. Regardless of the direct involvement of IgE, our data support pDCs as a viable drug target for "normalizing" $T_H1$ responses based on their increased numbers in infected asthmatics with high IgE and the robust induction of $T_H1$-related cytokines, of which pDCs are a major source.

While we cannot make any firm assertions regarding the T cell modulatory effects of anti-IgE in the present study, several compelling lines of evidence support the potential for anti-IgE to impact the $T_H2$ axis. These include decreased expression of IgE receptor on

basophils and myeloid DCs, and the lack of a discernable $T_H2$ response based on change in numbers of allergen-specific $T_H2$ cells; however, we cannot exclude the possibility that decreased $T_H2$ responses in asthmatics treated with anti-IgE occurred by virtue of their lower IgE levels. Nonetheless, the removal of type 2 components that can also promote $T_H1$ responses may prove beneficial within a low range of IgE. One such example is IL-33. This cytokine is arguably a strong candidate for driving $T_H1$ responses owing to its high expression in the inflamed airways of asthmatic patients, its induction by RV, and its ability to directly promote $T_H1$ cell responses in inflamed settings via its receptor ST2 [347]. Similarly, a broad array of pro-inflammatory cytokines, including those detected in the present study, might maintain increased numbers of RV-specific $T_H1$ cells after infection resolves. From a more controversial standpoint, there is intriguing new evidence to indicate that IgE itself can drive IFN production by pDCs, and that IgE signaling elements are required for pDC responses [255,256]. However, these responses are likely to be highly context-dependent. Hence, our findings highlight the need to elucidate the relationship between IgE and $T_H1$ responses, and in particular to assess how inhibition of the $T_H2$ axis in asthmatics with high IgE might influence $T_H1$-mediated inflammation.

There are several limitations of our study. First, all RV challenges were performed in young adults, since children cannot be challenged for safety and ethical reasons. Nonetheless, several features point to commonalities between children with acute asthma and adults in our model. These include (1) similar mediator profiles, RV receptor (ICAM-1) profiles, and viral loads in the nose during infection, and (2) increased RV-induced symptoms with higher total IgE [231,232,257]. Also, as previously mentioned, our study precluded a definitive conclusion regarding the influence of anti-IgE on anti-viral $T_H1$

responses *in vivo* owing to the lower IgE levels in subjects enrolled in the anti-IgE trial and the discrepant lung function and baseline T cell profiles between groups. Finally, it was not feasible to collect T cells from the lower airways owing to regulatory constraints at the time the study was initiated. However, this caveat is offset by the strong type 1 cytokine signature present in the nose, and previous verification of the relevance of circulating RV-specific T cells to acute events in the airways, as described in **Chapter 3**.

In summary, our findings establish a key role for $T_H1$ responses to RV in promoting inflammatory processes that govern allergic asthma. The results challenge existing paradigms related to type 2-mediated processes, and shift the spotlight to $T_H1$ cells as an integral component of asthma pathogenesis.

*This chapter was adapted from: L Muehling, R Agrawal, P Wright, H Carper, D Murphy, L Workman, J Eccles, S Ratcliffe, B Capaldo, R Turner, TAE Platts-Mills, P Heymann, W Kwok, J Woodfolk. "Rhinovirus infection in allergic asthmatics induces a paradoxical boost in anti-viral $T_H1$ responses that drives chronic inflammation" (Manuscript in preparation).*

# Chapter 5 — Conclusions and Future Directions

## Synopsis

In this thesis, we aimed to define the $CD4^+$ T cell response to RV infection in both healthy subjects and those with allergic asthma. Furthermore, we sought to examine how IgE relates to T cell responses to RV. In order to accomplish this, we first identified a discrete panel of immunodominant peptides that are presented by an array of commonly expressed HLA molecules (**Chapter 2**). These peptide epitopes localized to highly conserved regions of capsid proteins likely associated with viral assembly and infectivity. Tetramer staining of PBMCs from healthy subjects directly *ex vivo* confirmed that RV-specific $T_H1$ cells targeting conserved epitopes were readily detectable in uninfected healthy subjects and displayed cross-protective attributes. Together, these findings led us to propose that these peptides provide vaccine candidates that are capable of inducing cross-strain immunity.

Next, we sought to define the $CD4^+$ T cell response to RV in healthy subjects during experimental infection (**Chapter 3**). An important feature of this study was the use of a uniform experimental approach in HLA semi-matched subjects, which provided important information on the degree of heterogeneity of the T cell response in humans. In our model, we observed robust activation and expansion of circulating $CCR5^+$ RV-specific memory T cells during the acute phase in infected subjects only. A key finding was that those subjects with higher numbers of RV-specific $CD4^+$ T cells prior to infection had reduced rates of infection and delayed viral shedding. We concluded that $CCR5^+$ RV-specific $CD4^+$ T cells primed by previous RV infections are armed for immunosurveillance against multiple RV strains in healthy subjects. These cells rapidly respond upon RV exposure and are pivotal to controlling infection.

Finally, we probed the T cell mechanisms of virus-induced asthma (**Chapter 4**). A novel link was observed between increased numbers of RV-specific $CD4^+$ T cells and worse lung function in asthmatics before RV challenge, suggesting a pathogenic role even in the absence of infection. During infection, asthmatics with high IgE mounted an enhanced $T_H1$ response to RV compared with healthy controls and asthmatics with lower IgE, in addition to increased frequencies of circulating pDCs and the robust induction of IFNs and $T_H1$-associated mediators in the nose, despite a pre-existing $T_H2$ milieu. Although our study precluded any definitive conclusions about the role of IgE in cellular mechanisms of RV pathogenesis, we did observe a failure to mount an allergen-specific $T_H2$ response during RV infection in subjects receiving anti-IgE, as well as increased nasal IFN-$\alpha$ levels during infection. Plasmacytoid DCs were highly responsive to anti-IgE. Together, these findings suggest that disruption of IgE networks can redress the $T_H1/T_H2$ balance in RV-infected asthmatics. We propose that augmented $T_H1$ responses contribute to RV-induced asthma pathogenesis both during acute infection and in the absence of infection.

Given that the majority of work was performed using peripheral blood specimens, it was important to confirm the relevance of RV-specific $T_H1$ effectors to disease in the respiratory tract. Extensive analysis of cytokine signatures in the nose during RV infection confirmed the robust production of $T_H1$ chemoattractants in both asthmatics and controls, including CCR5 ligands and other type 1 mediators (**Chapter 4**). This is bolstered by preliminary observations in a separate study showing robust $T_H1$ signatures in the nose of children presenting to the emergency department with acute wheeze with or without RV infection (**Figure 5-1**)[231]. At the cellular level, we also identified $CCR5^+$ effector T cells in the noses of healthy control subjects, and confirmed their activation during acute RV

infection (**Chapter 3**). Although isolation of T cells from the respiratory tract of asthmatics during RV infection was not feasible, our group recently reported a dominant $CCR5^+$ $T_H1$ signature in the lower airways of children with severe asthma, including those who were highly allergic (**Figure 5-2**). Together, these studies support a pathogenic role for $T_H1$ responses in the development and persistence of allergic asthma, thereby challenging the current paradigm of type 2-driven disease.

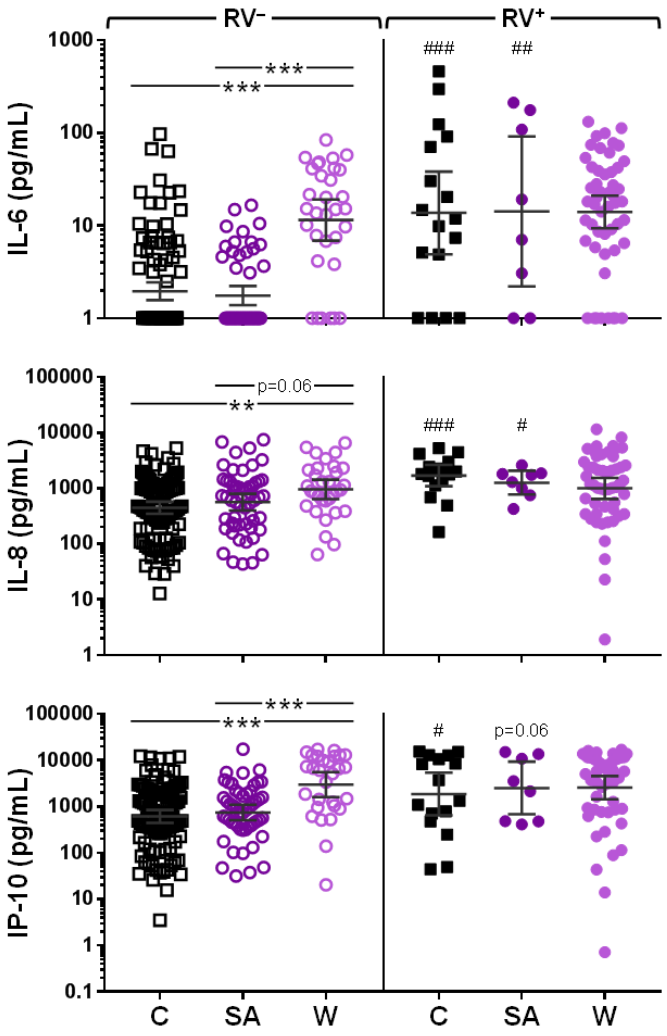


**Figure 5-1. Nasal Cytokine Production in a Case-Control Emergency Department Study of Wheeze and Rhinovirus Infection**

Subjects were recruited as described in [231]. Briefly, children presenting to the emergency department with acute wheeze were classified accordingly. Those presenting for non-wheezing issues were classified as either stable asthmatics (hospitalized or received drugs for asthma in the past year) or healthy controls. C, control; SA, stable asthma; W, wheeze. IL-6 values below the limit of detection are denoted as 1 pg/mL. Symbols represent geometric means ± 95% CI. *denotes between-group comparisons; #denotes within-group comparisons between $RV^+$ and $RV^-$ subjects. *p≤0.05, **p≤0.01, ***p≤0.001.

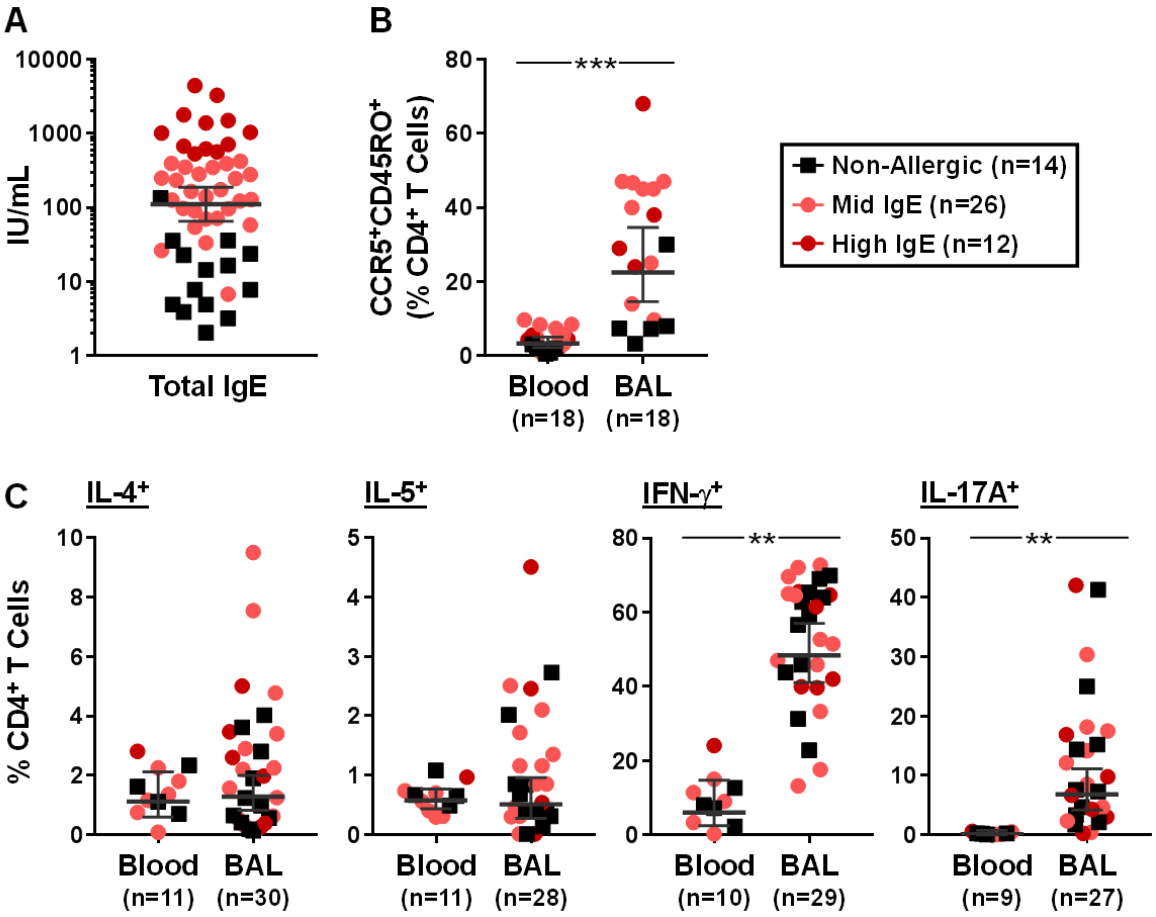


**Figure 5-2. Enrichment of CCR5$^+$ and IFN-γ$^+$ CD4$^+$ T Cells in the Lungs of Children with Severe Asthma**

**(A)** Total serum IgE of children with severe asthma undergoing clinically indicated bronchoscopy (mid IgE≤500 IU/mL; high IgE>500 IU/mL). **(B)** Percentage of CCR5$^+$ memory CD4$^+$ T cells in paired blood and BAL specimens. **(C)** Percentage of CD4$^+$ T cells expressing intracellular cytokines in paired blood and BAL specimens. Symbols denote geometric means ± 95% CI. *p≤0.05, **p≤0.01, ***p≤0.001. Adapted from [336]. Symbols were re-colored based on IgE levels, consistent with **Chapter 4**.

## Future Directions

### *Demonstrate Cross-Strain T Cell Immunity in a Sequential Challenge Model*

We have demonstrated a link between increased numbers of circulating RV-specific $CD4^+$ T cells in uninfected subjects and reduced viral load, as well as the cross-reactive potential of these cells (**Chapters 2** & **3**). Next, the ability of pre-existing cells to protect against both homotypic and heterotypic infections needs to be formally tested *in vivo* in a sample size powered to address this question. Our study was limited by the small number of subjects and the confounding effect of probiotic. Moreover, it will be important to confirm our observations in subjects with a broad repertoire of HLA molecules. Also, while our *in vitro* and *in silico* work supported the cross-reactive potential of RV-specific T cells that target conserved epitopes (**Chapter 2**), this needs to be confirmed *in vivo*.

With this in mind, we have initiated a study that involve monitoring T cell responses in healthy subjects sequentially challenged with different RV strains. A targeted total enrollment of 80 seronegative subjects will be infected with RV-A16 and then re-challenged after 15 weeks with either RV-A16 or RV-A39. This study design allows us to assess RV-A16-specific $CD4^+$ T cells both before and during the primary and secondary challenges (30-week period) in order ascertain whether increased numbers of RV-A16-specific $CD4^+$ T cells induced by primary challenge protect from subsequent RV-A39 infection. The use of a 25-marker panel for spectral flow cytometry will enable deep phenotyping of RV-specific T cells, in order to interrogate the development and evolution of T cell memory responses in a setting that mimics repeated natural infection.

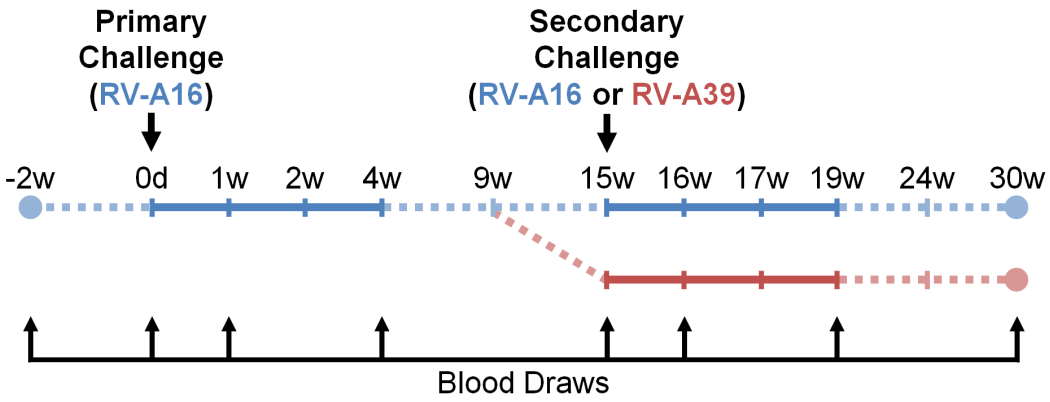


**Figure 5-3. Future Directions: Rhinovirus Double Challenge Study**

Schematic depicting an ongoing clinical study of heterotypic and homotypic secondary rhinovirus challenges in healthy control subjects. Solid lines denote the infection phase, whereas dashed lines denote run-in and follow-up periods.

### *Assess "Global" Immune Responses to Rhinovirus Using High-Dimensional Experimental Methods*

The advent of new high-dimensional single-cell analytical methods provides new avenues for research and discovery in rhinovirus infection and allergic asthma. While we have characterized RV- and allergen-specific $CD4^+$ T cells using 15-parameter multicolor flow cytometry, in-depth analysis of T cells and assessment of the contribution of other cell types was not performed.

In **Chapter 2**, we described different infection profiles in healthy subjects undergoing experimental RV challenge. Of particular interest were two groups of subjects, one that became infected but did not mount a neutralizing antibody response or T cell responses in the periphery, and the other that remained uninfected despite RV inoculation. Given our inability to detect T cell responses in these subjects, we hypothesized that RV was controlled by local immune responses and/or other circulating cell types, possibly including $CD8^+$ T cells and innate immune cells. Such "covert" responses could be studied using high-dimensional technologies such as mass cytometry (cytometry by time-of-flight, CyTOF). This technology, which utilizes antibodies labeled with discrete heavy metal isotypes in lieu of fluorochromes, can be used to measure over 40 markers simultaneously [348]. In a pilot study using PBMC specimens from two allergic asthmatics undergoing RV challenge, we used a 33-marker panel to monitor a broad range of lymphocyte responses, including $CD4^+$ T cells, $CD8^+$ T cells, γδ-T cells and B cells (**Table 5-1**). We observed fluxes in a discrete population of cells during the acute phase, which expressed CCR5 and the $T_H1$-defining transcription factor T-bet (**Figure 5-4**). Notably, this population comprised both $CD4^+$ T cells and B cells. This opened a new avenue of research on the various B cell populations responding to RV infection, their associated antibodies, and the characterization of a unique T-$bet^+$ B-cell subset that may be involved in viral clearance [349,350]. CyTOF also revealed a marked expansion of circulating γδ-$TCR^+$ cells three weeks post-challenge (*data not shown*). Little is known about the role of γδ-T cells in asthma; however, several studies of human lung cells suggest that γδ-T cells contribute to allergic $T_H2$ inflammation [351–353]. On the other hand, mouse models of asthma describe contradictory roles, with γδ-T cells suggested to both suppress allergic inflammation, as well as provide an essential contribution to late

asthmatic responses [354–356]. We plan to include γδ-T cells in future immunophenotying panels in order to determine what, if any, role they play in RV-induced asthma.

**Table 5-1. Marker Panel for "Global" Analysis of Cellular Responses to RV**

| | | | | |
|---|---|---|---|---|
| CD3 | CD33 | CD27 | CXCR5 | CCR7 |
| CD4 | CD57 | CD44 | ICOS | CXCR3 |
| CD45 | HLA-DR | CD45RA | PD-1 | CCR5 |
| CD7 | TCRγδ | CD45RO | APC-Bcl6 (APC) | CCR4 |
| CD8 | CD25 | ckit | GATA3 | CCR6 |
| CD14 | CD69 | CD43 | PE-RORγt (PE) | |
| CD19 | IL-7Rα | IgD | T-bet | |

Markers are colored as follows: White (gating); Orange (activation); Green (memory); Blue (B cell-associated markers); Purple ($T_{FH}$-associated markers); Orange (lineage-specifying transcription factors); Teal (homing receptors, including characteristic $T_H$ chemokine receptors). In instances where an anti-fluorophore mass-tagged antibody was used, the mass-tagged secondary antibody is given in parentheses.

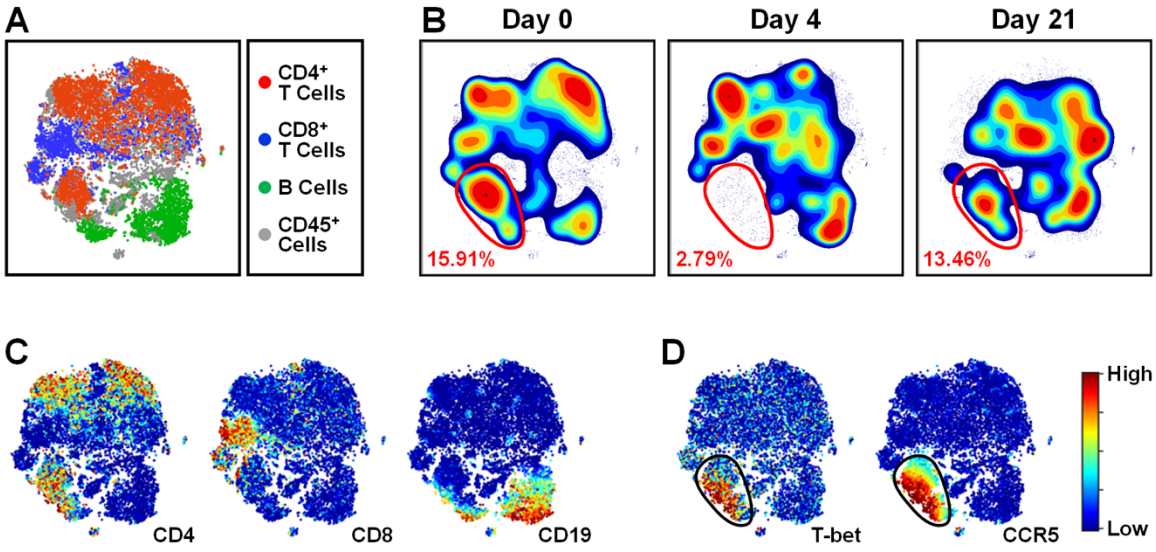


**Figure 5-4. Mass Cytometric Analysis Reveals Dynamic Flux in CCR5$^+$ T-bet$^+$ Lymphocytes in Allergic Asthmatics During Acute Infection**

**(A)** viSNE map of CD45$^+$ cells, including definition of T and B cell populations. **(B)** Time course of viSNE maps depicting cell density. The red outline defines a major population comprised of CD4$^+$ T cells and B cells that "disappears" from the blood during acute infection. **(C & D)** Maps depicting the expression of **(C)** B and T lymphocyte populations, and **(D)** expression of T-bet and CCR5 within the major populations of circulating lymphocytes during RV infection.

### *Exploring the Heterogeneity and Stability of RV-Specific CD4+ T Cells*

Our work highlights the need for an in-depth analysis of RV-specific $CD4^+$ T cells. Although the signature of $T_H1$ cells appeared stable during RV infection in both asthmatics and controls, we tested only a limited number of surface markers. Moreover, a large proportion of virus-specific T cells in asthmatics lacked expression of any marker (**Chapter 4**). A future major objective will be to identify pathogenic $T_H1$ signatures in patients with asthma. Such signatures may arise *de novo*, or else by subversion in the inflamed milieu of chronic asthma. Preliminary data obtained by CyTOF identified a "$T_H1$ + $T_H2$" signature in $CCR5^+$ $CD4^+$ T cells, based on co-expression of T-bet and GATA-3, and the emergence of a $CCR5^+$T-bet$^-$GATA-$3^+$ population after RV infection in asthmatics. These signatures might reflect transitions within $CCR5^+$ T cells during infection. In order to address T cell stability and identify pathogenic $T_H1$ signatures, single cell gene expression profiling of RV-specific $CD4^+$ T cells is planned in the near future. This technique can be applied to the whole transcriptome, or else to a targeted set of genes. By combining this technique with index fluorescence-activated cell sorting (FACS), we will be able to identify and sort single tetramer$^+$ cells using comprehensive antibody panels for fluorescence flow cytometry, and link each transcriptome signature to its corresponding protein signature. Putative pathogenic T cell signatures can then be sorted for *in vitro* assays of effector function.

### *Elucidate Mechanisms of Interaction Between $T_H1$ and $T_H2$ Pathways*

One major outstanding question is how a pre-existing $T_H2$ milieu might promote an augmented $T_H1$ response to RV in allergic asthmatics. This might occur as follow: (1) IgE and anti-viral signaling networks interact in dendritic cells to boost anti-viral responses; and (2) induction of $T_H2$-promoting cytokines boosts $T_H1$ responses either through the priming

of dendritic cells, including plasmacytoid dendritic cells, or else direct interaction with $CD4^+$ $T_H1$ cells.

There are several possible points of intersection between IgE and anti-viral (i.e. TLR) signaling pathways. For example, recent work in DCs has demonstrated a role for the IgE signaling components Lyn and Fyn in TLR signaling, and induction of IFN production by IgE receptor crosslinking, albeit in the context of autoimmune disease (**Figure 5-5**)[255,256]. This paradigm is complicated by our findings that nasal levels of IFNs were actually highest in asthmatics who received anti-IgE. This is consistent with previous reports of an inhibitory role for IgE in the modulation of IFN production. However, IFNs are not the only type 1 cytokines capable of mediating $T_H1$ responses. Indeed, increased IFNs in asthmatics who received anti-IgE did not translate to augmented $T_H1$ responses in those subjects compared to those with high levels of IgE. Thus, further work on the link between IgE and IFN production is warranted.

In our model of experimental RV infection, whole blood specimens were obtained at four time points (days -56, 0, 4, and 21) for fixation and preservation with SmartTube reagents (SmartTube, Inc., San Carlos, CA), and stored either unstimulated or following direct *ex vivo* IgE crosslinking. This method of specimen storage allows for the preservation of intracellular signaling events including phosphorylation of signaling molecules, and provides a valuable resource for the future probing of IgE and TLR signaling networks operating during RV infection by phosphor-flow cytometry.

As mentioned briefly in **Chapter 4**, IL-33 provides another candidate for $T_H1$ amplification. Although classically considered to be a $T_H2$-skewing cytokine, its capacity for inducing $T_H1$ responses via both the modulation of dendritic cells and direct effects on

$CD4^+$ T cells is well-described [347,357,358]. Although IL-33 was not detected in nasal washes in our model (*data not shown*), another group has reported IL-33 in nasal lining specimens from asthmatics infected with RV [269]. This provides a more sensitive method of cytokine detection. Continuing research is focused on the potential synergy between IL-33 and virus in promoting RV-specific $T_H1$ responses in culture in highly allergic asthmatics. The ability for IL-33 to act directly versus indirectly (i.e. via DCs) on $CD4^+$ T cells will be tested.

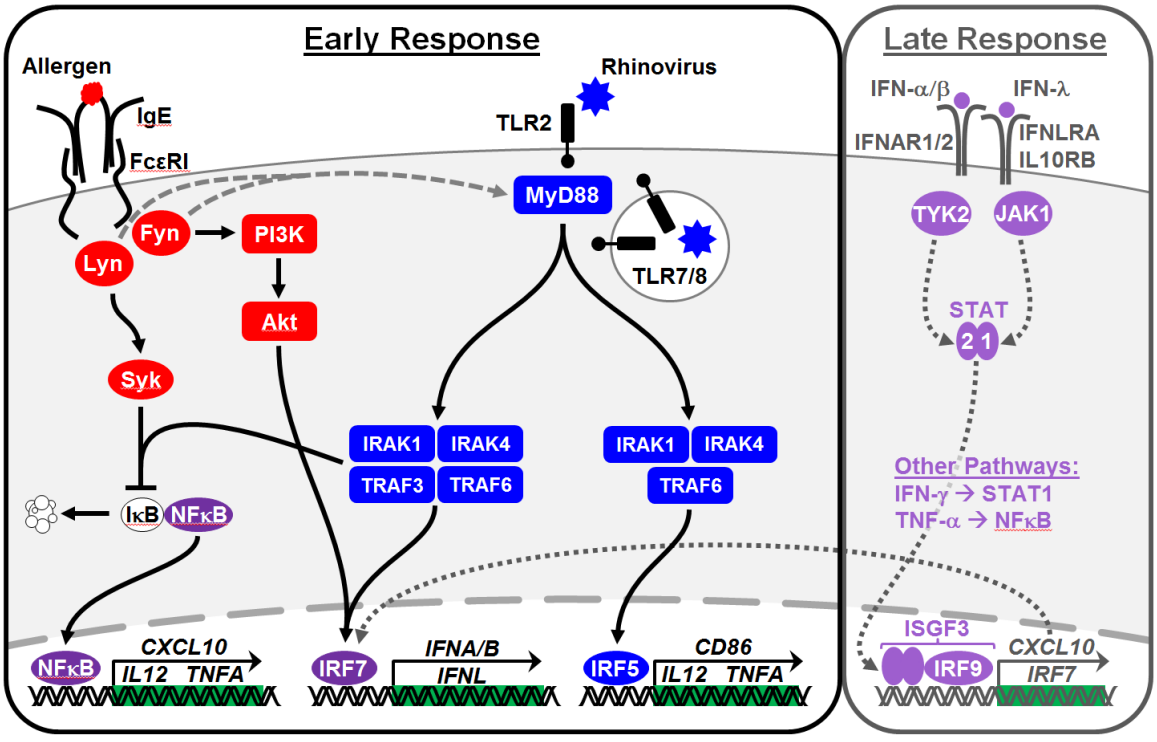


**Figure 5-5. Schematic of the Potential Intersection of IgE and TLR Signaling Pathways in DCs**

Signaling components in red are associated with allergen/IgE signaling pathways, while blue components are associated with virus/TLR signaling pathways. Potential points of intersection are shown in purple.

## Conclusions and Clinical Implications

In this work, we have extensively characterized the $CD4^+$ T cell response to RV infection, both in health and within the context of allergic asthma. We have identified immunodominant T cell epitopes of RV capsid proteins, demonstrated their conservation across RV strains, and provided proof-of-concept for cross-strain proliferation and cytokine production in responses to these epitopes *in vitro*. Furthermore, we utilized novel tetramer reagents to identify and monitor RV-specific $CD4^+$ T cells during RV infection. This strategy identified a role for $CCR5^+$ $T_H1$ cells specific for conserved capsid epitopes in regulating RV infection in healthy subjects. Taken together, these data suggest that peptide epitopes could provide ideal vaccine candidates for a cross-protective T cell-based vaccine against the common cold. Such an advance, if successful, could significantly improve human health.

We also demonstrate a paradoxical amplification of anti-viral $T_H1$ responses in allergic asthmatics infected with RV, and present evidence to support a pathogenic role for RV-specific $T_H1$ responses in asthma. This represents a major shift in the field. The majority of drugs for allergic asthma that are in development target type 2 inflammation or else aim to boost anti-viral responses. However, the data from our work suggest that attenuating $T_H1$ responses or else redressing the $T_H1/T_H2$ "balance" might be of benefit for virus-induced asthma. Indeed, our data call into question whether treatment strategies focused on enhancing anti-viral immunity in asthmatics might instead promote disease pathogenesis. Although anti-IgE treatment may enhance IFN-$\alpha$ in allergic asthmatics, given that interferons are not deficient in asthmatic with high IgE, the benefits of such an increase are questionable. Our findings support a model wherein repeated "hits" with RV promote $T_H1$-driven processes in allergic asthma that raise the inflammatory set point. By shifting the

spotlight to $T_H1$ cells, this work presents new opportunities for research and treatment. From a broader perspective, this body of work represents a significant advance in the field of RV immunity be revealing for the first time the characteristics of RV-specific $CD4^+$ T cells in health and disease.

*This chapter includes data from: J Wisniewski*, L Muehling*, J Eccles, B Capaldo, R Agrawal, D Shirley, J Patrie, L Workman, A Schuyler, M Lawrence, W Teague, J Woodfolk. "$T_H1$ signatures are present in the lower airways of children with severe asthma, regardless of allergic status." J Allergy Clin Immunol (2018). *Equal contribution.*

# Appendix I — Experimental Rhinovirus Challenge for the Study of Allergic Asthma and the Role of IgE

## Introduction

Respiratory viral infections, including rhinovirus, are important triggers of allergic asthma exacerbations [218,219]. Although the mechanisms of virus-induced asthma require further elucidation, a clear link to allergic sensitization has been established. Previous studies have shown that simultaneous allergen and viral exposure results in enhanced symptom severity [222,223]. Additionally, increased levels of IgE have been linked to worse symptom severity during rhinovirus infection, and dust mite allergen-specific IgE is associated with increased risk of wheeze in children infected with RV [231,232]. In this study, we performed experimental RV challenge in asthmatics, including those receiving anti-IgE treatment, in order to assess the interaction between RV and asthma, as well as to probe the ability for anti-IgE treatment to reduce RV-induced asthma symptom severity.

## Methods

### *Subject Screening and Inclusion/Exclusion Criteria*

Subjects with mild physician-diagnosed allergic asthma were recruited for participation in these studies. Airway hyperreactivity was confirmed by methacholine challenge (≥20% fall in $FEV_1$ at a methacholine concentration of ≤8 mg/mL). Allergic status was confirmed by a positive skin prick test to one or more allergens (*Alternaria*, dust mite, and/or ragweed for fall challenges; grass and/or tree pollens for spring challenges), as well as a determination of total and allergen-specific serum IgE levels by ImmunoCAP. Those subjects with no history of allergic disease were enrolled in the RV challenge if their serum IgE was less than 50 IU/mL.

Subjects who received omalizumab and/or allergen immunotherapy within the past 3 years were excluded from the study, as well as those who had used inhaled corticosteroids, inhaled cromolyn or nedocromil, long-acting beta agonists, inhaled ipratropium bromide, systemic leukotriene modifiers, or nasal corticosteroids within four weeks of the study. In the interest of safety, only mild asthmatics were enrolled into the study, excluding those who required hospitalization or emergency department care for asthma-related reasons in the previous three years, and those who required intubation or intensive care unit treatment for asthma at any time previously. In addition, subjects with an $FEV_1$<70% predicted at time of enrollment were excluded from the study. In order to accommodate subjects with lower lung volumes (FVC≤88% predicted), an alternate exclusion factor of $FEV_1$/FVC<80% was used.

### *Omalizumab Randomization, Dosing, and Administration*

Omalizumab dosing of allergic asthmatic subjects was determined according to subject serum IgE and weight (**Tables I-1** & **I-2**). Those subjects with total IgE and weight outside of the dosing range were enrolled into the RV challenge only. Those subjects eligible to receive omalizumab treatment were administered either drug or placebo (sterile water) by study personnel every two or four weeks according to the dosing schedule, and subjects were monitored following drug administration according to safety recommendations (2 hours for visits 1-3; 30 minutes thereafter) (**Tables I-1** & **I-2**)[359]. Treatment was initiated eight weeks prior to RV challenge, and continued until completion of the study. Subjects who were not enrolled in the omalizumab trial had a shorter seven-day run-in period. The treatment randomization code was not broken until all challenges were completed, and the code was not revealed to the researchers until the completion of all tetramer experiments.

**Table I-1. Omalizumab Dosing (Milligrams) For Administration Every Four Weeks in Adults and Adolescents Over 12 Years of Age**

| Pre-treatment Serum IgE (IU/mL) | Body Weight (kg) | | | |
|---|---|---|---|---|
| | 30-60 | >60-70 | >70-90 | >90-150 |
| ≥30-100 | 150 | 150 | 150 | 300 |
| >100-200 | 300 | 300 | 300 | See Table I-2 |
| >200-300 | 300 | See Table I-2 | See Table I-2 | See Table I-2 |
| >300-400 | See Table I-2 | See Table I-2 | See Table I-2 | See Table I-2 |
| >400-500 | See Table I-2 | See Table I-2 | See Table I-2 | See Table I-2 |
| >500-600 | See Table I-2 | See Table I-2 | See Table I-2 | See Table I-2 |
| >600-700 | See Table I-2 | See Table I-2 | See Table I-2 | See Table I-2 |

**Table I-2. Omalizumab Dosing (Milligrams) For Administration Every Two Weeks in Adults and Adolescents Over 12 Years of Age**

| Pre-treatment Serum IgE (IU/mL) | Body Weight (kg) | | | |
|---|---|---|---|---|
| | 30-60 | >60-70 | >70-90 | >90-150 |
| ≥30-100 | See Table I-1 | See Table I-1 | See Table I-1 | See Table I-1 |
| >100-200 | See Table I-1 | See Table I-1 | See Table I-1 | 225 |
| >200-300 | See Table I-1 | 225 | 225 | 300 |
| >300-400 | 225 | 225 | 300 | DO NOT DOSE |
| >400-500 | 300 | 300 | 375 | DO NOT DOSE |
| >500-600 | 300 | 375 | DO NOT DOSE | DO NOT DOSE |
| >600-700 | 375 | DO NOT DOSE | DO NOT DOSE | DO NOT DOSE |

### *Experimental RV-A16 Inoculation and Clinical Assessments*

The RV-A16 challenge pool was produced under GMP conditions (IND #15162 & 010510). All subjects were inoculated in the evening of day 0. RV-A16 inoculum suspended in HANK's balanced salt solution (0.25 mL, 300-500 $TCID_{50}$) was placed into each nostril. After 5-10 minutes, a second viral inoculum was administered. Subjects remained in hotel rooms under supervision through the morning of study day 4, and returned for outpatient visits thereafter. Neutralizing antibodies were measured using a standard microtiter assay [51]. Viral load in nasal wash specimens was assessed by qPCR using pan-RV primers as previously described, as well as by a semi-quantitative culture assay [51,257]. Subjects were considered infected if they had evidence of RV in nasal wash at any day following inoculation by either culture or qPCR and/or if they seroconverted by day 21 post-inoculation (≥4 fold increase in RV-A16 serum neutralizing antibody titer).

Study personnel performed clinical assessments twice daily while subjects remained under supervision at the hotel, as well as at outpatient visits during the run-in period and the post-inoculation periods. These procedures included lung function assessments, nasal specimen collection, and blood draws for complete blood count (CBC) and serology. A schematic depicting the schedule of all clinical procedures is given in **Figure I-1**. Subjects performed self-assessments throughout the course of the study, including symptom scoring and peak flow monitoring.

### *Nasal Wash and Nasal Lining Specimen Collection*

In order to assess viral load and inflammatory mediator profiles, nasal wash was performed in all subjects over the course of infection. Two mL of phosphate buffered saline (PBS) was instilled in each nostril with a mucosal atomization device (Wolfe Tory Medical,

Inc., Salt Lake City, UT) while the subject held their breath. The specimen was then retrieved by suction using a BBG Nasal Aspirator (Codan, US Corp., Santa Ana, CA). Nasal wash was performed according to the schedule in **Figure I-1**.

In addition, nasal lining fluid was obtained from a subset of subjects, in order to obtain a more concentrated specimen for analysis of inflammatory mediators. Nasal lining fluid was collected prior to performing nasal wash, and was obtained on day 0, during acute infection (day 4), and during convalescence (either day 14 or 21). Surgicel cellulose gauze (Ethicon, Inc., Somerville, NJ) was cut into strips and applied to the inferior turbinate of each nostril for five minutes, during which time the nostrils were held closed by nose clips. After removing the Surgicel with forceps, the strips were placed into a Costar® Spin-X® centrifuge tube insert with no membrane (Corning, Inc., Corning, NY) and was centrifuged at 2000 rpm for 4 minutes in order to extract the specimen. Specimens were diluted 1:4 with nasal lining fluid buffer (PBS with 0.3% human serum albumin [HSA], 0.01% sodium azide, 0.002% Tween20) prior to storage at -80°C.

### *Symptom Severity and Lung Function Assessment*

Upper and lower respiratory tract symptom severity was determined using the modified Jackson criteria [233]. Subjects filled out symptom diary cards in the morning and evening for the duration of the study, denoting medication use as applicable. In addition, subjects monitored peak flow twice daily with a personal PF100 asthma monitor (Microlife USA, Inc., Dunedin, FL). An additional self-assessment, the Asthma Control Test (ACT), was completed prior to study initiation and after study completion [360]. In addition to peak expiratory flow monitoring, numerous lung function assessments were performed in order to determine disease severity. Spirometry was performed by study personnel, in order to

assess numerous aspects of lung function, including lung forced vital capacity (FVC), forced expiratory volume in one second ($FEV_1$), and the forced expiratory flow between 25-75% of FVC ($FEF_{25-75}$), which can be indicative of small airway obstruction. Airway reactivity in asthmatic subjects was assessed by methacholine challenge according to standard procedures, and airway inflammation was assessed by fractional expired nitric oxide ($F_{ENO}$), which was measured using a NioxMino® Nitric Oxide analyzer (Aerocrine AB, Solna, Sweden).

### *Statistical Methods*

The clinical study primary outcome measures were upper and lower respiratory symptom scores, which were compared using the Kruskal-Wallis test and negative binomial models with correction for symptoms during the run-in period. Between-group comparisons of clinical parameters at baseline were performed using the Kruskal-Wallis test. Between-group comparisons over time were performed using repeated measures models for spirometry, and 2-way ANOVA with Sidak's multiple comparisons correction for viral titer, methacholine challenge, $F_{ENO}$, peak flow, and complete blood counts. Within-group comparisons over time were performed using the Wilcoxon test for ACT scores, and the Freidman test for IgE.

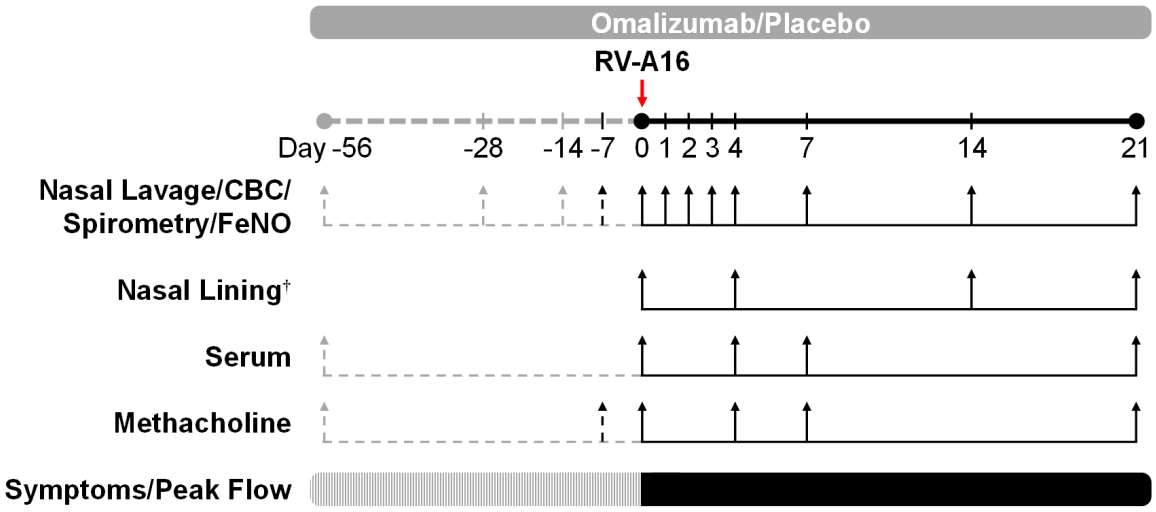


**Figure I-1. RV Challenge Study Design and Clinical Procedures**

Study design schematic depicting clinical assessments and procedures. Pre-infection procedures are denoted with dashed lines, and gray symbols denote procedures performed in the omalizumab study only. An eight-week run-in period was employed for subjects enrolled in the anti-IgE trial, whereas a seven day run-in period was employed for those subjects receiving RV challenge only. †Nasal lining was obtained for either day 14 or 21, but not both.

## Results

### *Subject Screening and Infection Profiles*

A total of 777 subjects were assessed for eligibility to enter this study (**Figure I-2**). Overall, 31 asthmatic and 13 healthy control subjects completed the study and became infected following inoculation. Subject demographics are listed in **Tables I-3** & **I-4**. As shown in **Chapter 4**, asthmatic subjects were divided into those with moderate IgE levels within the omalizumab dosing range who entered the anti-IgE trial, and those with high IgE who received RV challenge only. Asthmatic subjects had allergen-specific IgE directed against numerous common indoor and outdoor allergens, including those for which pMHCII tetramers were available (**Figure I-3**). The most common sensitizing allergen was dust mite (65% of asthmatics), which also had the highest titers of allergen-specific IgE.

One healthy control subject remained uninfected following inoculation, as evidenced by a lack of viral positivity by either qPCR or culture, as well as a lack of seroconversion (**Figure I-2**). Additionally, three subjects were excluded during *post hoc* analysis due to the presence of a confounding RV infection within six weeks prior to inoculation (high IgE: 1 subject; mid IgE [Tx]: 2 subjects) (**Figure I-2**). Although not statistically significant, rates of RV-A16 seroconversion were increased in asthmatic subjects, with the highest rates observed in those with high IgE (**Tables I-3** & **I-4**). In contrast, viral titers were not statistically different between groups, regardless of whether assessed by qPCR or culture methods (**Figure I-4**). Interestingly, viral titers were highest among asthmatics with moderate IgE levels, with virus positivity persisting the longest in those subjects that received anti-IgE (**Figure I-4**). Thus, anti-IgE treatment does not enhance viral clearance, but may instead inhibit clearance, perhaps through modulation of the immune response.

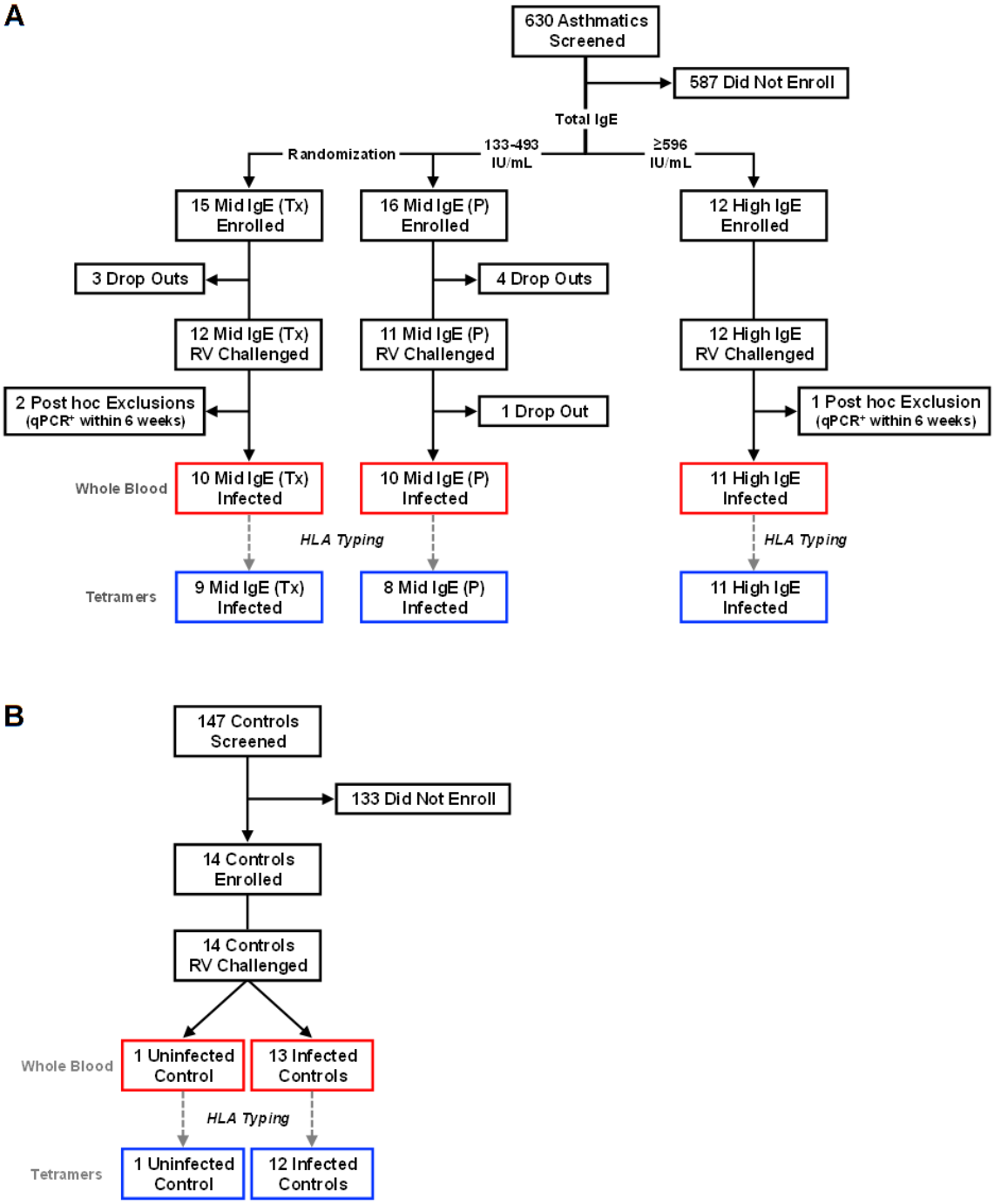


**Figure I-2. Subject Screening and Enrollment**

Screening and enrollment of **(A)** asthmatic, and **(B)** healthy control subjects. Red boxes denote all subjects who completed the challenge study, and blue boxes denote subjects with appropriate HLA types for the tetramer studies described in **Chapter 4**.

**Table I-3. Subject Demographic Data, RV Challenge Only**

| | **Controls (n=13)** | **High IgE (n=11)** | **P Value** |
|---|---|---|---|
| Female Gender [n (%)] | 10 (77%) | 8 (73%) | >0.99 |
| Race [n (%)] | | | 0.20 |
| Black | 0 (0%) | 2 (18%) | |
| White | 13 (100%) | 9 (82%) | |
| Ethnicity [n (%)] | | | >0.99 |
| Non-Hispanic | 13 (100%) | 11 (100%) | |
| Age [yrs, mean (SD)] | 22.1 (20.3-23.9) | 24.5 (19-39) | 0.99 |
| Total IgE [Geo. Mean (range)]* | 13.5 (2.4-42.5) | 1239 (596-4692) | **<0.001** |
| Seroconversion [n (%)] | 8 (62%) | 10 (91%) | 0.16 |

**Table I-4. Subject Demographic Data, Omalizumab Trial**

| | **Mid IgE [Tx] (n=10)** | **Mid IgE [P] (n=10)** | **P Value** |
|---|---|---|---|
| Female Gender [n (%)] | 7 (70%) | 9 (90%) | 0.58 |
| Race [n (%)] | | | 0.40 |
| Black | 1 (10%) | 2 (20%) | |
| White | 8 (80%) | 8 (80%) | |
| Other | 1 (10%) | 0 (0%) | |
| Ethnicity [n (%)] | | | >0.99 |
| Hispanic | 0 (0%) | 1 (10%) | |
| Non-Hispanic | 10 (100%) | 9 (90%) | |
| Age [yrs, mean (SD)] | 21 (17.8-24.2) | 24.3 (19.4-29.2) | 0.16 |
| Total IgE [Geo. Mean (range)]* | 238 (133-493) | 225 (140-473) | 0.97 |
| Seroconversion [n (%)] | 7 (70%) | 7 (70%) | >0.99 |

*IU/mL. Bolded values denote significance ($p \leq 0.05$).

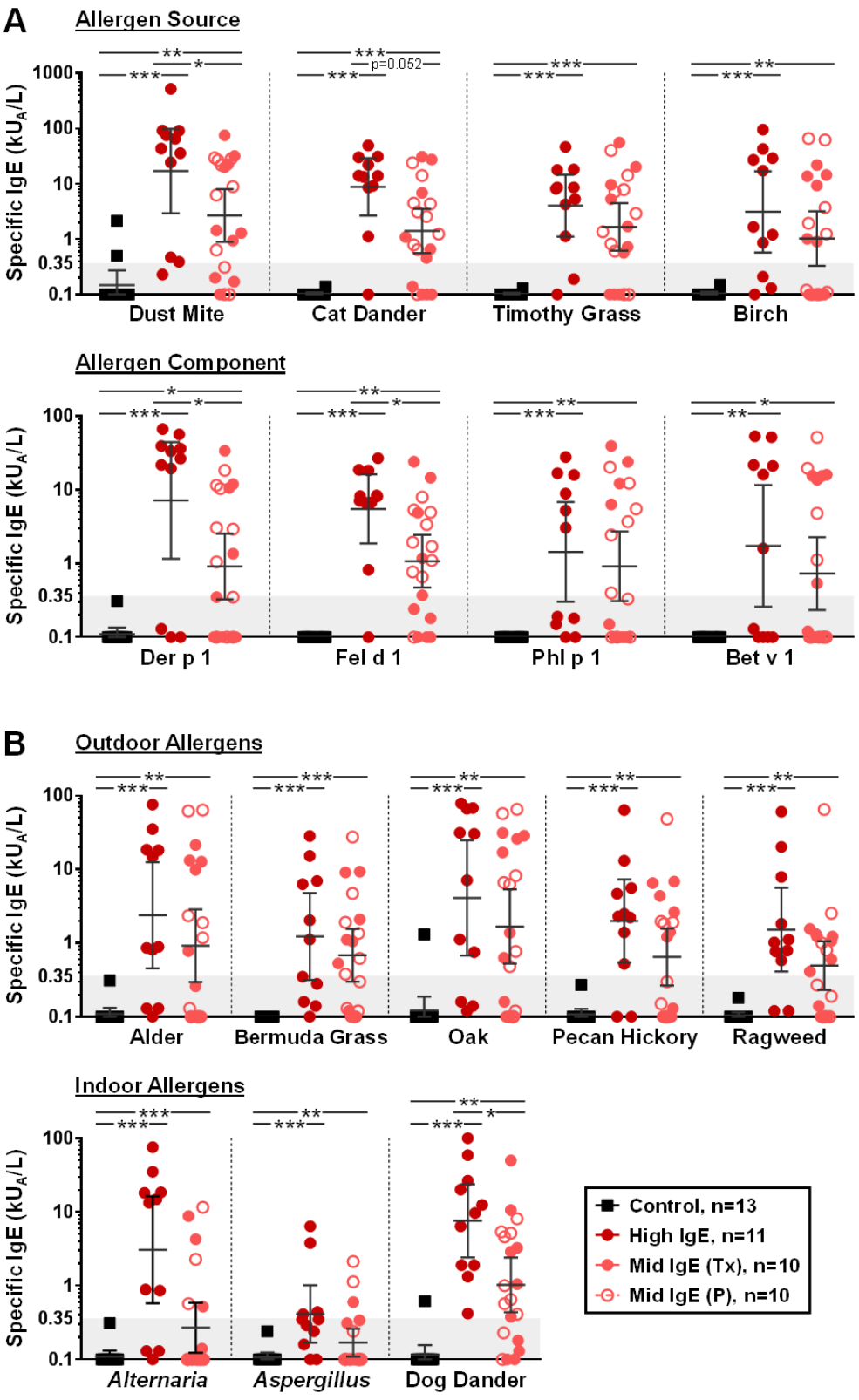
A
Allergen Source
Specific IgE (kUA/L)
1000
100
10
1
0.35
0.1
**
***
*
***
***
p=0.052
***
***
***
**
***
Dust Mite
Cat Dander
Timothy Grass
Birch
Allergen Component
Specific IgE (kUA/L)
100
10
1
0.35
0.1
*
***
*
**
***
*
**
***
*
**
Der p 1
Fel d 1
Phl p 1
Bet v 1
B
Outdoor Allergens
Specific IgE (kUA/L)
100
10
1
0.35
0.1
**
***
***
***
**
***
**
***
**
***
Alder
Bermuda Grass
Oak
Pecan Hickory
Ragweed
Indoor Allergens
Specific IgE (kUA/L)
100
10
1
0.35
0.1
***
***
**
***
**
*
***
Alternaria
Aspergillus
Dog Dander
Control, n=13
High IgE, n=11
Mid IgE (Tx), n=10
Mid IgE (P), n=10

**[Previous] Figure I-3. Allergen-Specific IgE Profiles at Study Initiation**

Allergen-specific IgE to whole allergen and relevant components **(A)** for which tetramer reagents were available, and **(B)** for additional common outdoor and indoor allergens. Shaded regions denote a class 0 IgE range. The assay limit of detection is 0.1 $kU_A/L$. Bars denote geometric means ± 95% CI. *p≤0.05, **p≤0.01, ***p≤0.001.

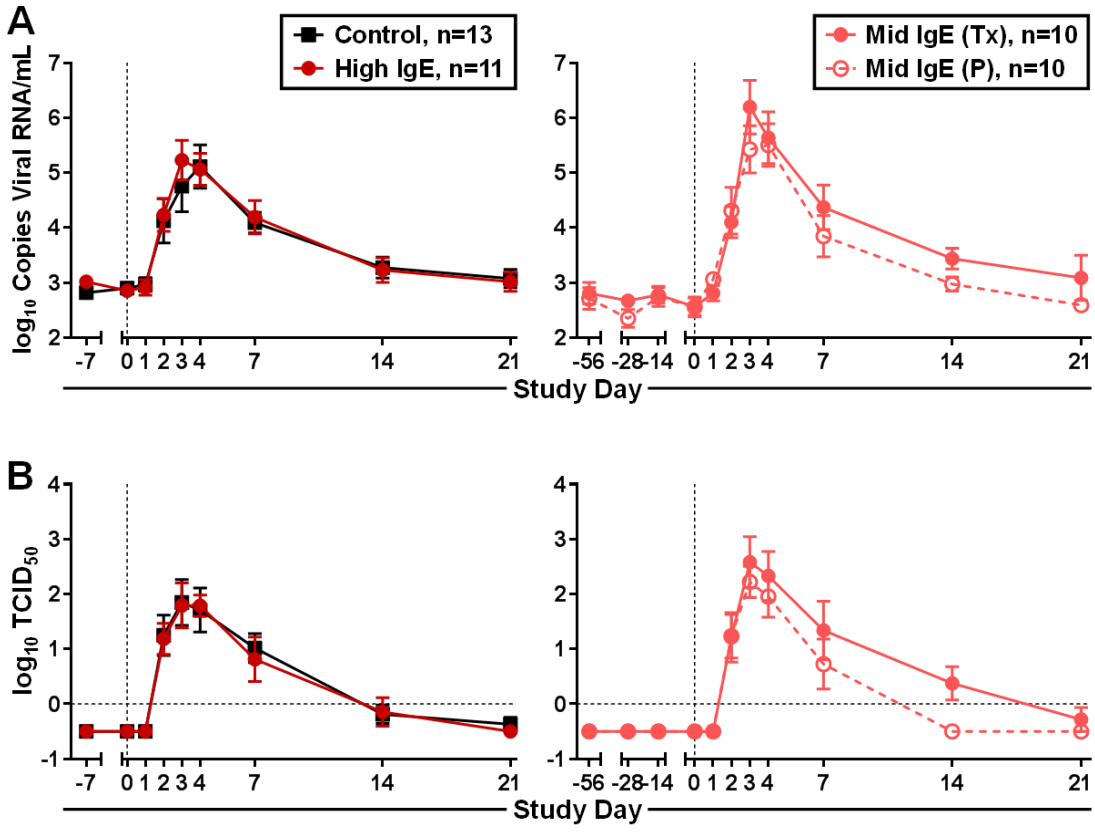


**Figure I-4. Similar Viral Titers in Asthmatic and Control Subjects**

Viral titer in nasal lavage as determined by **(A)** qPCR and **(B)** culture methods. Negative cultures were assigned a value of -0.5. Symbols denote means ± SEM.

### *RV Modulation of Subject Symptoms and Lung Function*

There were no significant differences in symptom scores between subjects receiving anti-IgE and placebo during the pre-treatment phase (**Figure I-5**). In all subjects, RV challenge induced both upper and lower respiratory tract symptoms, although lower respiratory tract symptoms were negligible in control subjects and consisted mainly of cough alone (**Figure I-5**, *data not shown*). Both upper and lower respiratory tract symptoms were enhanced in high IgE asthmatic subjects versus controls during early infection (days 1-4), although this was not significant for upper respiratory symptoms (**Figure I-5**). There was also a trend toward decreased upper respiratory symptoms in anti-IgE treated subjects versus placebo during the first week of infection ($p=0.08$), and lower respiratory symptoms were reduced during the early phase (**Figure I-5**). During the late phase (days 15-21) there was a trend toward increased upper respiratory symptoms in high IgE asthmatics versus controls ($p=0.09$), and symptoms remained elevated at 21 days in those asthmatics with lower levels of IgE, regardless of treatment group. Overall, only a modest reduction in symptoms was observed in subjects receiving anti-IgE.

In addition, subjects completed the Asthma Control Test both at study entry and 28 days after RV infection. At baseline, all asthmatic subjects had reduced asthma control as compared with healthy subjects regardless of study group (**Figure I-6**). Following RV infection, loss of asthma control was most pronounced in those asthmatics with high IgE. There was no significant difference in the post-infection ACT scores of asthmatics receiving anti-IgE and placebo, although subjects receiving placebo did have significantly worse asthma control than healthy subjects, whereas those receiving anti-IgE did not (**Figure I-6**).

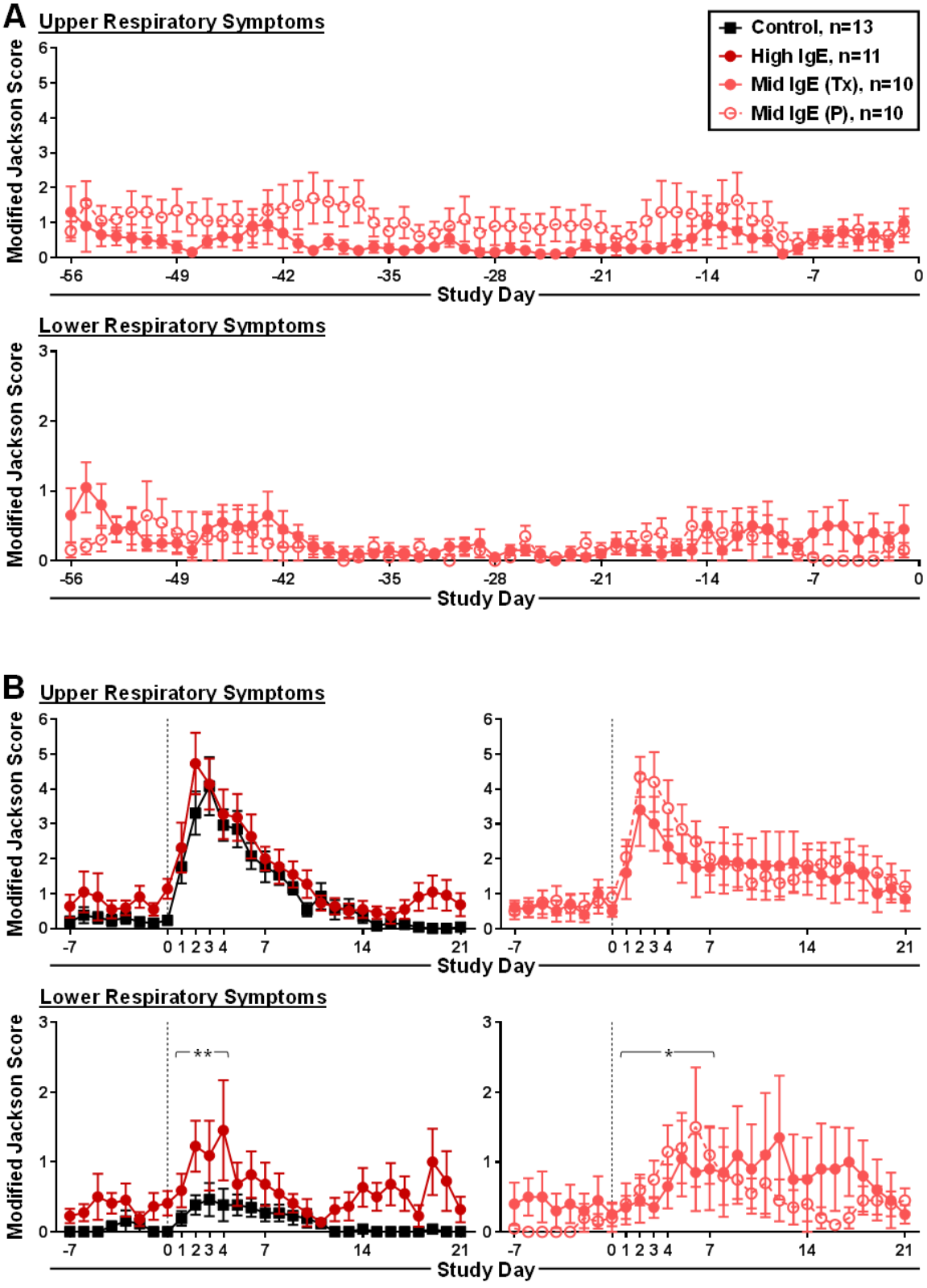
A
Upper Respiratory Symptoms
Control, n=13
High IgE, n=11
Mid IgE (Tx), n=10
Mid IgE (P), n=10
Modified Jackson Score
Study Day
Lower Respiratory Symptoms
B
Upper Respiratory Symptoms
Lower Respiratory Symptoms
**
*

**[Previous] Figure I-5. Increased Symptom Profiles in Allergic Asthmatics Versus Healthy Controls During RV Infection**

**(A & B)** Upper, and lower respiratory tract symptoms as reported by subjects using the modified Jackson criteria, for both **(A)** the pre-treatment phase in the omalizumab trial, and **(B)** the infection phase, including run-in period (days -7 to 0) for all subjects. Values reflect the average of morning and evening symptom scores. Symbols denote means ± SEM. *denote differences in lower respiratory tract symptoms without cough. *p≤0.05, **p≤0.01.

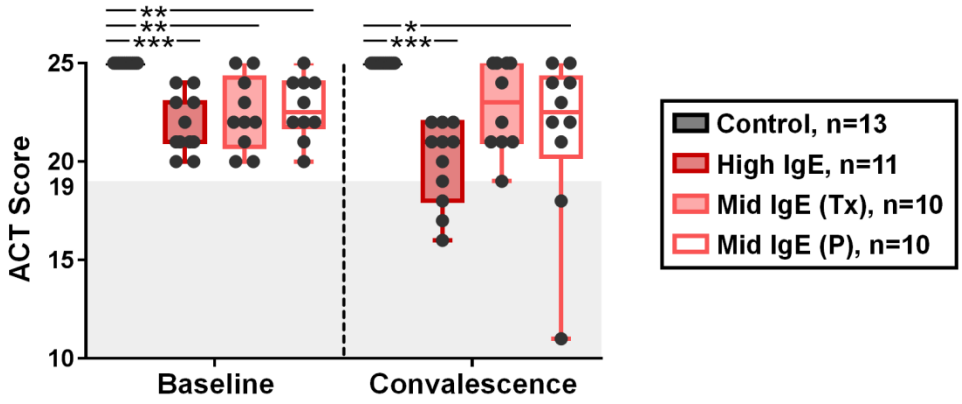


**Figure I-6. Loss of Asthma Control During RV Infection**

Asthma Control Test score, as reported by subjects at baseline. The maximum score is 25. Shaded regions denote a loss of asthma control (score of 19 or below). *between-group comparisons; #within-group comparisons. *p≤0.05; **p≤0.01, ***p≤0.001.

As discussed in **Chapter 4**, baseline assessments of lung function by spirometry revealed heterogeneity among asthmatic subjects (**Figure I-7**). Healthy controls exhibited the highest lung function, while asthmatics with high IgE had reduced lung function, including low expiration over one second ($FEV_1$), low lung capacity (FVC), reduced small airway function ($FEF_{25-75}$), and an $FEV_1$/FVC ratio indicative of airway obstruction (**Figure I-7**)[337]. Interestingly, among asthmatics enrolled in the anti-IgE trial there were noticeable differences in spirometry prior to study initiation. At baseline, those subjects randomized to receive anti-IgE had an increased lung capacity as compared with those randomized to receive placebo; however, overall lung function as assessed by $FEV_1$/FVC was significantly reduced in subjects randomized to receive anti-IgE, resembling the values of the high IgE asthmatics (**Figure I-7**). In contrast, subjects randomized to receive placebo more closely resembled healthy controls (**Figure I-7**). Taken together, this indicates increased disease severity among the anti-IgE group prior to study initiation.

During acute infection, $FEV_1$, $FEV_1$/FVC, and $FEF_{25-75}$ measurements generally dropped, whereas lung capacity remained largely consistent (**Figure I-7**). These changes were most pronounced in high IgE asthmatics and mid IgE asthmatics receiving placebo, whereas these measures did not drop in those receiving anti-IgE; however, there were no statistically significant differences in spirometry responses between those receiving anti-IgE and placebo (**Figure I-7**). Thus, although subjects receiving anti-IgE demonstrated less of a reduction in lung function during RV infection, their spirometry responses were not significantly improved compared with placebo. This is further complicated by their increased severity prior to study initiation.

In addition to spirometry, several additional assessments of lung function and airway inflammation were performed. Methacholine was used to assess airway hyperreactivity in asthmatics. There was no significant difference in the concentration of methacholine triggering a 20% fall in $FEV_1$ ($PC_{20}$) between asthma groups at baseline; however, during RV infection, asthmatics receiving placebo had an elevated $PC_{20}$ versus those receiving anti-IgE and those with high IgE indicating reduced airway responsiveness, although this did not reach statistical significance (**Figure I-8**). Fractional exhaled nitric oxide is a biomarker of airway inflammation, perhaps due to increased activity of the cytokine-inducible NO synthase in asthmatic lungs [361]. At screening, asthmatics with high IgE had the highest $F_{ENO}$, followed by asthmatics randomized to receive anti-IgE, although this was not significantly elevated compared to those receiving placebo (**Figure I-8**). $F_{ENO}$ remained largely constant over the course of the study, regardless of study group, and there were no significant differences between those receiving anti-IgE and placebo; however, there was a non-significant decrease in $F_{ENO}$ during the treatment phase among subjects receiving anti-IgE (**Figure I-8**). Subjects were given peak flow monitors to perform self-assessments twice daily. There were no differences in baseline peak flow measurements between study groups at study initiation, and there were limited changes in peak flow over the course of the study (*data not shown*). Overall, these measurements of lung function and inflammation are reflective of more severe disease in high IgE asthmatics and mid IgE asthmatics receiving anti-IgE prior to study initiation, with modest treatment effects during infection.

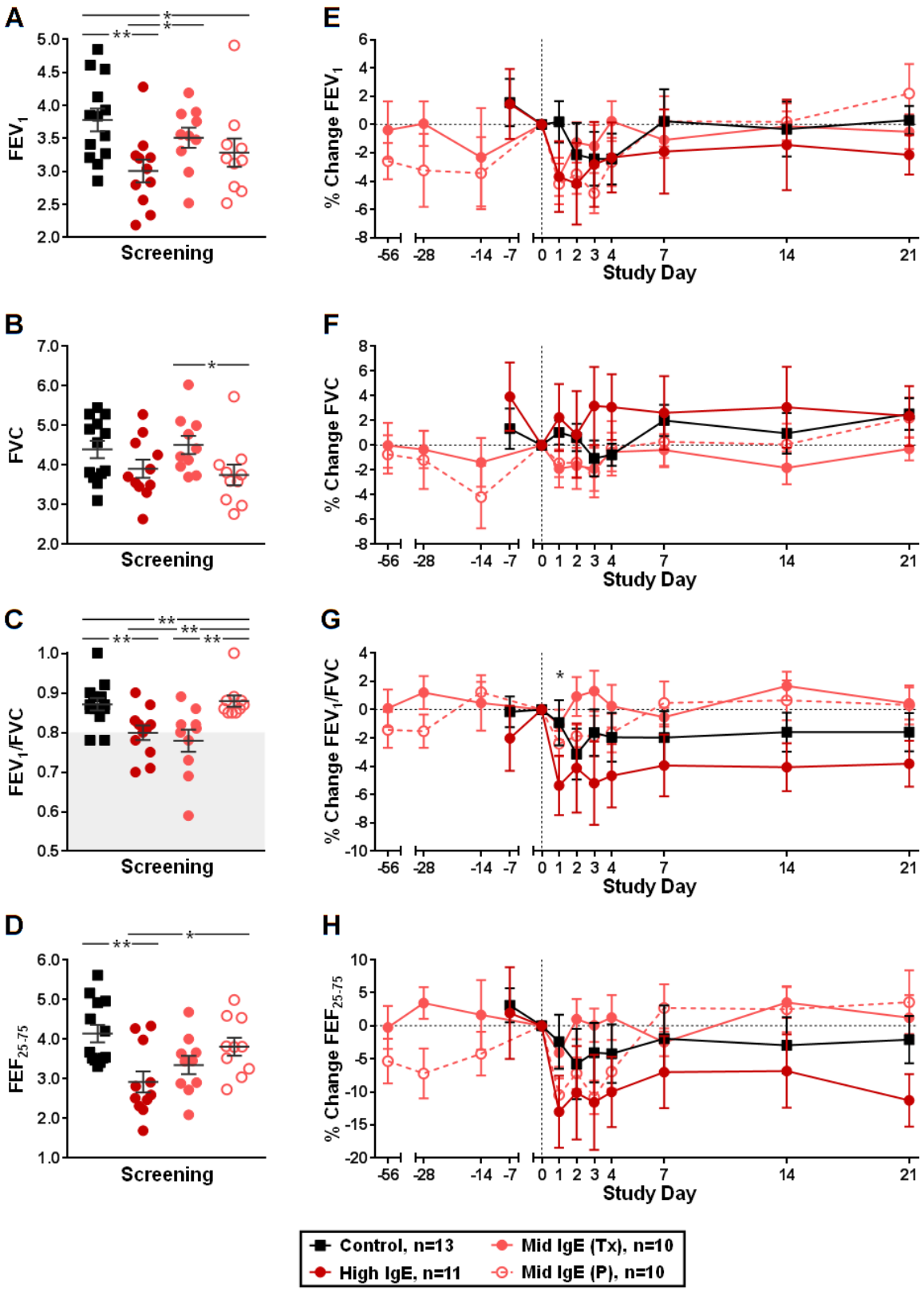
A
B
C
D
E
F
G
H
FEV1
FVC
FEV1/FVC
FEF25-75
Screening
% Change FEV1
% Change FVC
% Change FEV1/FVC
% Change FEF25-75
-56 -28 -14 -7 0 1 2 3 4 7 14 21
Study Day
Control, n=13
High IgE, n=11
Mid IgE (Tx), n=10
Mid IgE (P), n=10

**[Previous] Figure I-7. Spirometry Assessments During RV Challenge**

Between-group comparisons of spirometry measurements, both **(A-D)** at screening, and **(E-H)** during RV infection (percent change from day 0). Grey shaded regions denote reduced lung function according to established guidelines ($FEV_1/FVC<0.80$)[337]. Symbols and bars denote means ± SEM. For **(E-H)**, *represents differences between controls and high IgE asthmatics, as there were no significant differences between mid IgE groups. *p≤0.05, **p≤0.01.

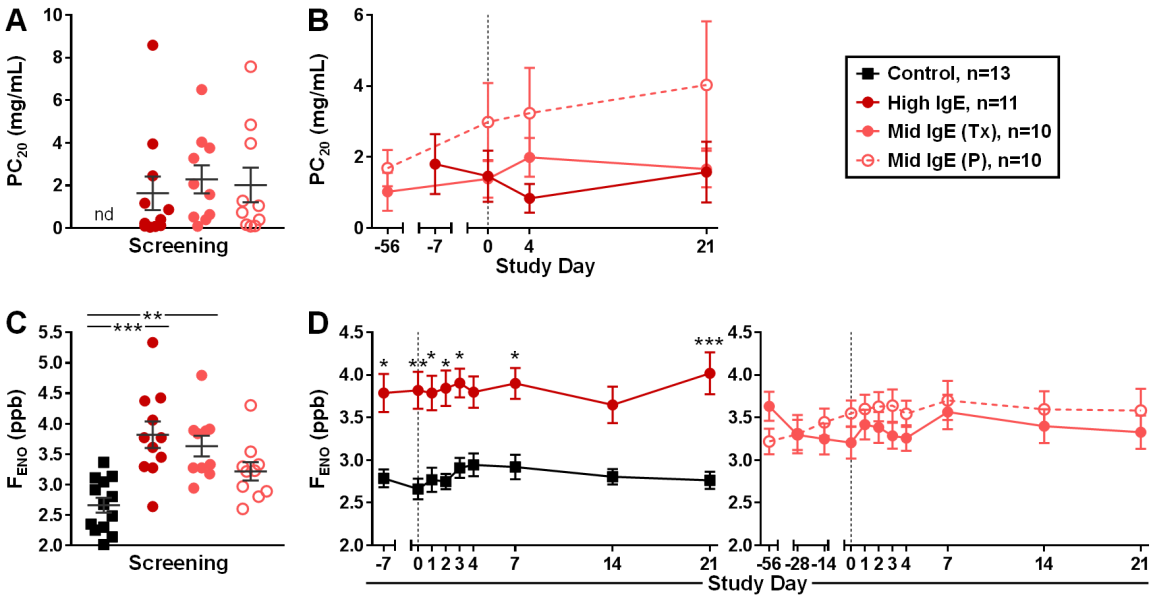


**Figure I-8. Additional Measurements of Airway Reactivity and Inflammation**

**(A & B)** Methacholine challenge ($PC_{20}$), and **(C & D)** $F_{ENO}$, performed at screening **(A & C)**, and during RV infection **(B & D)**. $F_{ENO}$ values are Ln-transformed. Symbols denote means ± SEM. *p≤0.05, **p≤0.01, ***p≤0.001.

### *Peripheral Immune Responses to RV Infection*

In order to monitor global immune responses in the periphery, complete blood counts were performed over the course of the study. Cellular responses generally peaked during acute infection on days 3 to 4 (**Figure I-9**). During acute infection, peripheral basophil, lymphocyte, and eosinophil responses were significantly increased in high IgE asthmatics as compared with controls (**Figure I-9**). As expected, there was a significant reduction in eosinophils during RV infection in subjects receiving anti-IgE versus placebo, including suppression of late eosinophil responses during convalescence; in contrast, there was a non-significant increase in total peripheral white blood cells and neutrophils during convalescence in subjects receiving anti-IgE (**Figure I-9**). Taken together, we observed effective suppression of $T_H2$-associated eosinophil responses by anti-IgE during infection.

In addition, serum total and dust mite-specific IgE were monitored over the course of the study in asthmatics and controls. These measurements were not feasible in subjects receiving anti-IgE treatment due to the formation of IgE aggregate complexes. These complexes are indistinguishable from free IgE by conventional IgE measurements, and the slow clearance of these complexes results in an increase in measured IgE levels during treatment [362]. Interestingly, we observed a transient increase in both total and dust mite-specific IgE during acute infection in asthmatic and control subjects, potentially due to an adjuvant effect of viral infection (**Figure I-10**)[363]. It will be important to determine whether this boost in IgE production compromises the efficacy of anti-IgE treatment.

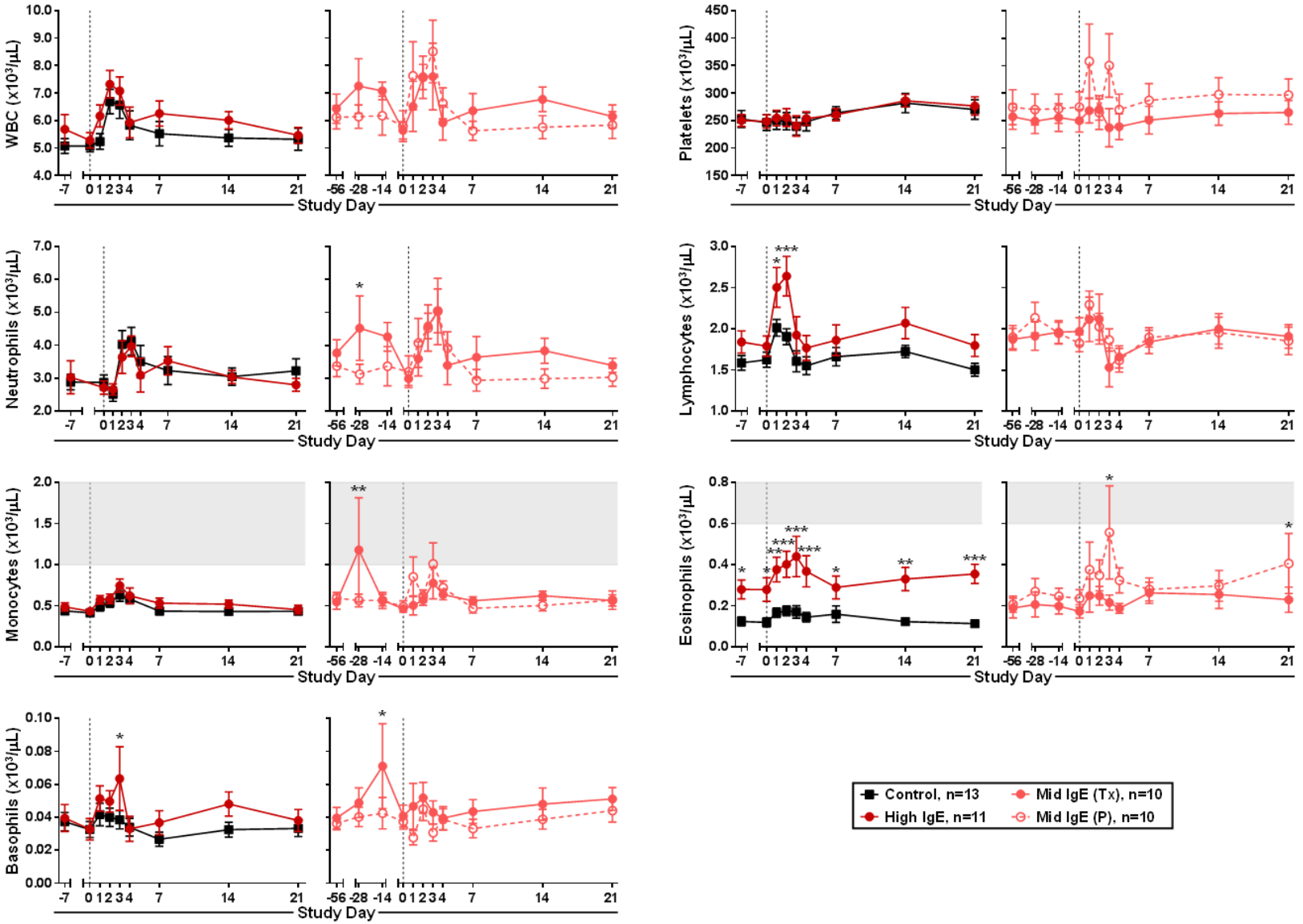
WBC (x10³/µL)
Platelets (x10³/µL)
Neutrophils (x10³/µL)
Lymphocytes (x10³/µL)
Monocytes (x10³/µL)
Eosinophils (x10³/µL)
Basophils (x10³/µL)
Study Day
Control, n=13
High IgE, n=11
Mid IgE (Tx), n=10
Mid IgE (P), n=10

**Figure I-9. Complete Blood Counts (CBCs) During the Course of Experimental Rhinovirus Challenge**

Sequential CBCs from allergic asthmatic and healthy control subjects. Shaded gray areas denote values falling outside of the reference age for healthy adults ≥18 years. Symbols denote means ± SEM. *denotes between-group differences. *p≤0.05, **p≤0.01, ***p≤0.001.

WBC, white blood cell.

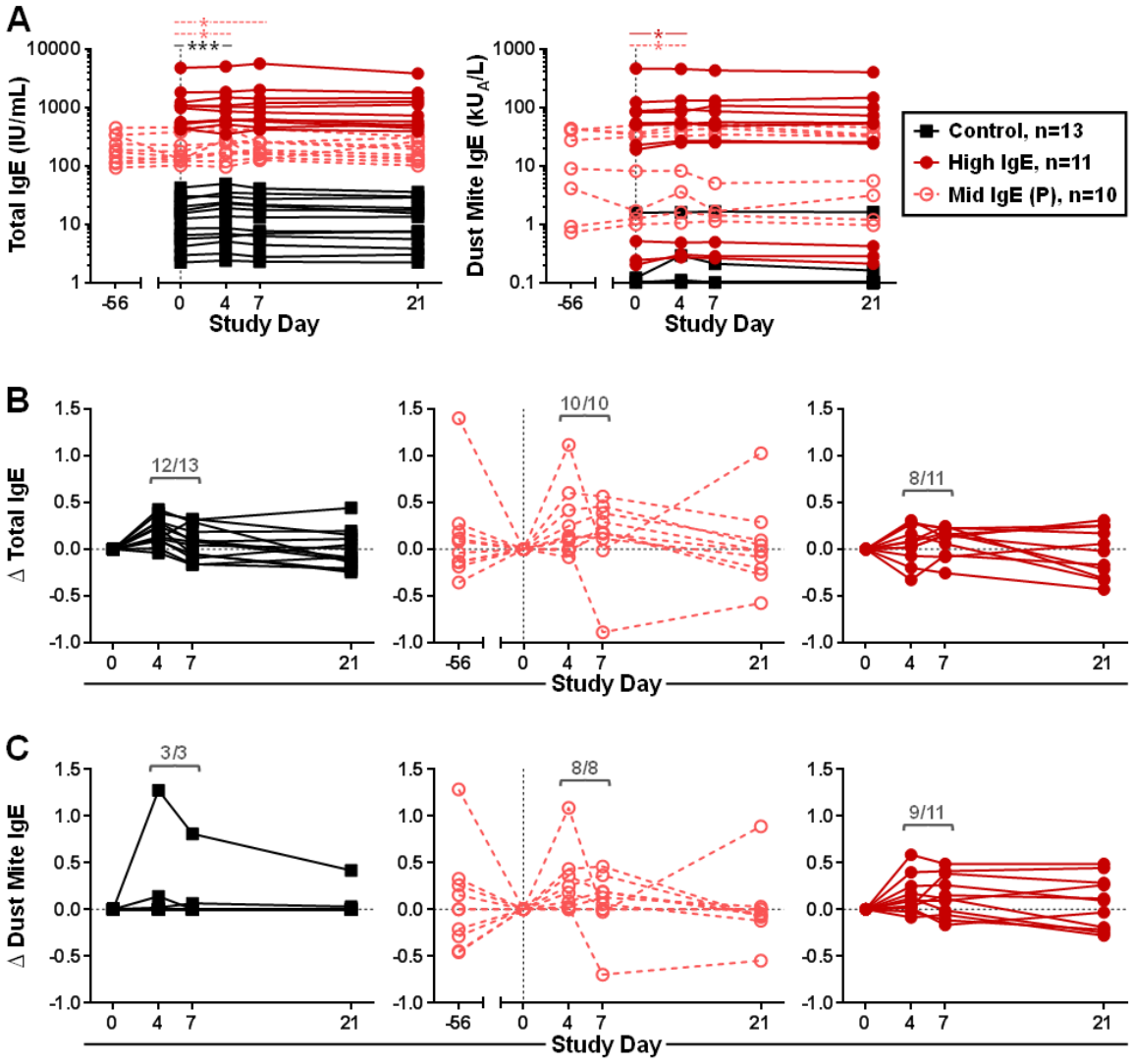


**Figure I-10. Transient Increase in Serum IgE Following RV Infection**

**(A)** Time course of total and dust mite-specific IgE. **(B & C)** Change in **(B)** total, and **(C)** dust mite-specific IgE from day 0. Dust-mite specific IgE over time was only assessed in those subjects with values above the limit of detection (0.1 $kU_A/L$). Graphs depict Log2-transformed fold changes from day 0. Numbers denote the proportion of subjects with increased IgE titers relative to day 0 during infection (day 4 and/or 7). *p≤0.05, ***p≤0.001.

## Discussion

Overall, anti-IgE treatment modestly reduced RV-induced disease exacerbations in mild allergic asthmatics. However, analysis of anti-IgE effects is complicated by baseline differences between subjects receiving anti-IgE and placebo. In particular, subjects randomized to receive anti-IgE had reduced lung function and increased airway inflammation at baseline, whereas those randomized to receive placebo had lung function similar to that of healthy controls. Despite this, we did observe modest reduction in reported symptoms during acute infection in subjects receiving anti-IgE, although symptoms remained elevated for several weeks following inoculation. In addition, subjects receiving anti-IgE experienced less of a drop in lung function than those receiving placebo, and demonstrated reduced peripheral eosinophil responses.

Interestingly, RV infection induced production of IgE in both asthmatics and controls, although the formation of IgE aggregates precluded the assessment of samples from subjects receiving anti-IgE. It will be important to determine whether RV infection does induce an adjuvant effect and boost IgE, and to assess the precise mechanisms through which RV modulates B cell antibody production. Furthermore, it remains to be determined whether a RV-induced boost in IgE would be sufficient to overcome anti-IgE treatment, particularly if the drug has not been administered for several weeks.

Taken together, there appears to be a modest protective effect of anti-IgE treatment with RV challenge; however, analysis of anti-IgE efficacy is complicated by increased inflammation and disease severity prior to study initiation in those subjects that received anti-IgE treatment. As such, follow up studies with larger cohorts are necessary to draw firm conclusions regarding the use of omalizumab for the prevention of RV-induced asthma.

*This appendix was adapted from: "Using the experimental virus infection model and the administration of omalizumab to evaluate the asthmatic response to rhinovirus" (Manuscript in preparation).*

*&*

*L Muehling, R Agrawal, P Wright, H Carper, D Murphy, L Workman, J Eccles, S Ratcliffe, B Capaldo, R Turner, TAE Platts-Mills, P Heymann, W Kwok, J Woodfolk. "Rhinovirus infection in allergic asthmatics induces a paradoxical boost in anti-viral $T_H1$ responses that drives chronic inflammation" (Manuscript in preparation).*

# Appendix II — Statistical Comparisons of Antigen-Specific CD4+ T Cells

## Table II-1. RV-Specific CD4+ T Cell Frequencies

| Comparisons | Unadjusted P Value | Adjusted P Value |
|---|---|---|
| **Between-Group Comparisons** | | |
| **Baseline** | | |
| Control vs. High IgE | 0.583 | 1.000 |
| Mid IgE [Tx] vs. [P] | **0.019** | 0.381 |
| Control vs. Mid IgE [P] | 0.531 | 0.999 |
| Mid IgE [P] vs. High IgE | 0.902 | 0.999 |
| Control vs. Mid IgE [Tx] | **≤0.001** | **0.032** |
| Mid IgE [Tx] vs High IgE | **0.008** | 0.195 |
| **Day -56** | | |
| Mid IgE [Tx] vs. [P] | **0.010** | 0.230 |
| **Day 0** | | |
| Control vs. High IgE | 0.282 | 0.995 |
| Mid IgE [Tx] vs. [P] | 0.131 | 0.931 |
| Control vs. Mid IgE [P] | 0.300 | 0.993 |
| Mid IgE [P] vs. High IgE | 0.919 | 0.993 |
| **Day 4** | | |
| Control vs. High IgE | **≤0.001** | **≤0.001** |
| Mid IgE [Tx] vs. [P] | 0.709 | 0.999 |
| Control vs. Mid IgE [P] | **0.045** | 0.620 |
| Mid IgE [P] vs. High IgE | 0.786 | 1.000 |
| **Day 7** | | |
| Control vs. High IgE | **0.003** | 0.086 |
| Mid IgE [Tx] vs. [P] | **0.005** | 0.135 |
| Control vs. Mid IgE [P] | 0.608 | 0.999 |
| Mid IgE [P] vs. High IgE | **0.028** | 0.494 |
| **Day 21** | | |
| Control vs. High IgE | 0.370 | 0.998 |
| Mid IgE [Tx] vs. [P] | 0.292 | 0.994 |
| Control vs. Mid IgE [P] | 0.488 | 0.999 |
| Mid IgE [P] vs. High IgE | 0.830 | 0.999 |

**Within-Group Comparisons**

| | | |
|---|---|---|
| **Control** | | |
| Day 0 vs. 4 | **0.002** | 0.062 |
| Day 0 vs. 7 | **0.035** | 0.559 |
| Day 0 vs. 21 | **≤0.001** | **≤0.001** |
| **High IgE** | | |
| Day 0 vs. 4 | **0.005** | 0.135 |
| Day 0 vs. 7 | **0.002** | 0.062 |
| Day 0 vs. 21 | **0.043** | 0.620 |
| **Mid IgE [Tx]** | | |
| Day -56 vs. 0 | 0.163 | 0.959 |
| Day 0 vs. 4 | 0.955 | 0.955 |
| Day 0 vs. 7 | **≤0.001** | **≤0.001** |
| Day 0 vs. 21 | 0.373 | 0.996 |
| **Mid IgE [P]** | | |
| Day -56 vs. 0 | 0.702 | 1.000 |
| Day 0 vs. 4 | 0.120 | 0.922 |
| Day 0 vs. 7 | 0.182 | 0.967 |
| Day 0 vs. 21 | **≤0.001** | **≤0.001** |

Baseline data were analyzed using a generalized linear model. Both between- and within-group comparisons over time were analyzed using generalized estimating equations. Multiple comparisons corrections were performed using the Holm-Sidak method for 37 comparisons. Significant values ($p \leq 0.05$) are shown in bold.

## Table II-2. Allergen-Specific $CD4^+$ T Cell Frequencies

| Comparisons | Unadjusted P Value | Adjusted P Value |
|---|---|---|
| **Between-Group Comparisons** | | |
| **Baseline** | | |
| Control vs. High IgE | 0.103 | 0.947 |
| Mid IgE [Tx] vs. [P] | 0.657 | 0.999 |
| Control vs. Mid IgE [P] | 0.458 | 1.000 |
| Mid IgE [P] vs. High IgE | 0.449 | 1.000 |
| Control vs. Mid IgE [Tx] | 0.208 | 0.994 |
| Mid IgE [Tx] vs High IgE | 0.756 | 0.985 |
| **Day -56** | | |
| Mid IgE [Tx] vs. [P] | 0.496 | 0.999 |
| **Day 0** | | |
| Control vs. High IgE | **0.017** | 0.422 |
| Mid IgE [Tx] vs. [P] | 0.757 | 0.941 |
| Control vs. Mid IgE [P] | **0.020** | 0.465 |
| Mid IgE [P] vs. High IgE | 0.489 | 0.999 |
| **Day 4** | | |
| Control vs. High IgE | **≤0.001** | **≤0.001** |
| Mid IgE [Tx] vs. [P] | 0.694 | 0.999 |
| Control vs. Mid IgE [P] | **≤0.001** | **≤0.001** |
| Mid IgE [P] vs. High IgE | 0.585 | 1.000 |
| **Day 7** | | |
| Control vs. High IgE | **≤0.001** | **≤0.001** |
| Mid IgE [Tx] vs. [P] | 0.429 | 1.000 |
| Control vs. Mid IgE [P] | **0.004** | 0.124 |
| Mid IgE [P] vs. High IgE | 0.083 | 0.912 |
| **Day 21** | | |
| Control vs. High IgE | 0.221 | 0.995 |
| Mid IgE [Tx] vs. [P] | 0.642 | 1.000 |
| Control vs. Mid IgE [P] | 0.432 | 1.000 |
| Mid IgE [P] vs. High IgE | 0.477 | 1.000 |

**Within-Group Comparisons**

| | | |
|---|---|---|
| **Control** | | |
| Day 0 vs. 4 | **0.048** | 0.771 |
| Day 0 vs. 7 | 0.290 | 0.999 |
| Day 0 vs. 21 | 0.176 | 0.992 |
| **High IgE** | | |
| Day 0 vs. 4 | **≤0.001** | **≤0.001** |
| Day 0 vs. 7 | 0.146 | 0.983 |
| Day 0 vs. 21 | 0.337 | 0.999 |
| **Mid IgE [Tx]** | | |
| Day -56 vs. 0 | 0.402 | 1.000 |
| Day 0 vs. 4 | 0.182 | 0.992 |
| Day 0 vs. 7 | 0.222 | 0.993 |
| Day 0 vs. 21 | 0.876 | 0.876 |
| **Mid IgE [P]** | | |
| Day -56 vs. 0 | 0.735 | 0.995 |
| Day 0 vs. 4 | 0.061 | 0.839 |
| Day 0 vs. 7 | 0.719 | 0.998 |
| Day 0 vs. 21 | 0.191 | 0.992 |

Baseline data were analyzed using a generalized linear model. Both between- and within-group comparisons over time were analyzed using generalized estimating equations. Multiple comparisons corrections were performed using the Holm-Sidak method for 37 comparisons. Significant values ($p \leq 0.05$) are shown in bold.

*This appendix was adapted from: L Muehling, R Agrawal, P Wright, H Carper, D Murphy, L Workman, J Eccles, S Ratcliffe, B Capaldo, R Turner, TAE Platts-Mills, P Heymann, W Kwok, J Woodfolk. "Rhinovirus infection in allergic asthmatics induces a paradoxical boost in anti-viral $T_H1$ responses that drives chronic inflammation" (Manuscript in preparation).*

## Works Cited


1. Bertino JS. Cost burden of viral respiratory infections: Issues for formulary decision makers. Am J Med. **2002**; 112(6A):42S–49S.
2. Fendrick AM, Monto AS, Nightengale B, Sarnes M. The economic burden of non-influenza-related viral respiratory tract infection in the United States. Arch Intern Med. **2003**; 163:487–494.
3. Heikkinen T, Järvinen A. The common cold. Lancet. **2003**; 361:51–59.
4. Greenberg SB. Respiratory consequences of rhinovirus infection. Arch Intern Med. **2003**; 163:278–284.
5. Gern JE, Calhoun W, Swenson C, Shen G, Busse WW. Rhinovirus infection preferentially increases lower airway responsiveness in allergic subjects. Am J Respir Crit Care Med. **1997**; 155:1872–1876.
6. Cox DW, Bizzintino J, Ferrari G, et al. Human rhinovirus species C infection in young children with acute wheeze is associated with increased acute respiratory hospital admissions. Am J Respir Crit Care Med. **2013**; 188(11):1358–1364.
7. Iwane MK, Prill MM, Lu X, et al. Human rhinovirus species associated with hospitalizations for acute respiratory illness in young US children. J Infect Dis. **2011**; 204:1702–1710.
8. Nicholson KG, Kent J, Hammersley V, Cancio E. Acute viral infections of upper respiratory tract in elderly people living in the community: Comparative, prospective, population based study of disease burden. BMJ. **1997**; 315:1060–1064.
9. McManus TE, Marley A-M, Baxter N, et al. Respiratory viral infection in exacerbations of COPD. Respir Med. **2008**; 102:1575–1580.
10. Kieninger E, Singer F, Tapparel C, et al. High rhinovirus burden in lower airways of children with cystic fibrosis. Chest. **2013**; 143(3):782–790.
11. Jansen RR, Wieringa J, Koekkoek SM, et al. Frequent detection of respiratory viruses without symptoms: Toward defining clinically relevant cutoff values. J Clin Microbiol. **2011**; 49:2631–2636.
12. van Benten I, Koopman L, Niesters B, et al. Predominance of rhinovirus in the nose of symptomatic and asymptomatic infants. Pediatr Allergy Immunol. **2003**; 14:363–370.
13. van der Zalm MM, van Ewijk BE, Wilbrink B, Uiterwaal CSPM, Wolfs TFW, van der Ent CK. Respiratory pathogens in children with and without respiratory symptoms. J Pediatr. **2009**; 154:396–400.
14. Jacobs SE, Lamson DM, St George K, Walsh TJ. Human rhinoviruses. Clin Microbiol Rev. **2013**; 26(1):135–162.
15. Corne JM, Marshall C, Smith S, et al. Frequency, severity, and duration of rhinovirus infections in asthmatic and non-asthmatic individuals: A longitudinal cohort study. Lancet. **2002**; 359:831–834.

16. Gwaltney JM, Hendley JO, Simon G, et al. Rhinovirus infections in an industrial population: I. The occurrence of illness. N Engl J Med. **1966**; 275(23):1261–1268.

17. Winther B, Hayden FG, Hendley JO. Picornavirus infections in children diagnosed by RT-PCR during longitudinal surveillance with weekly sampling: Association with symptomatic illness and effect of season. J Med Virol. **2006**; 78:644–650.

18. Johnston SL, Pattemore PK, Sanderson G, et al. The relationship between upper respiratory infections and hospital admissions for asthma: A time-trend analysis. Am J Respir Crit Care Med. **1996**; 154:654–660.

19. Hendley JO, Gwaltney JM. Mechansisms of transmission of rhinovirus infections. Epidemiol Rev. **1988**; 10:243–258.

20. Hendley JO, Wenzel RP, Gwaltney JM. Transmission of rhinovirus colds by self-inoculation. N Engl J Med. **1973**; 288(26):1361–1364.

21. Palmenberg AC, Spiro D, Kuzmickas R, et al. Sequencing and analyses of all known human rhinovirus genomes reveal structure and evolution. Science. **2009**; 324:55–59.

22. Palmenberg AC, Rathe JA, Liggett SB. Analysis of the complete genome sequences of human rhinovirus. J Allergy Clin Immunol. **2010**; 125(6):1190–1201.

23. Bochkov YA, Gern JE. Clinical and molecular features of human rhinovirus C. Microbes Infect. **2012**; 14:485–494.

24. Conant RM, Vincent ND. Rhinoviruses: Basis for a numbering system I. HeLa cells for propagation and serologic procedures. J Immunol. **1968**; 100(1):107–113.

25. Andries K, Dewindt B, Snoeks J, et al. Two groups of rhinoviruses revealed by a panel of antiviral compounds present divergence and differential pathogenicity. J Virol. **1990**; 64:1117–1123.

26. Lamson D, Renwick N, Kapoor V, et al. MassTag polymerase-chain-reaction detection of respiratory pathogens, including a new rhinovirus genotype, that caused influenza-like illness in New York State during 2004-2005. J Infect Dis. **2006**; 194:1398–1402.

27. Greve JM, Davis G, Meyer AM, et al. The major human rhinovirus receptor is ICAM-1. Cell. **1989**; 56:839–847.

28. Vlasak M, Blomqvist S, Hovi T, Hewat E, Blaas D. Sequence and structure of human rhinoviruses reveal the basis of receptor discrimination. J Virol. **2003**; 77:6923–6930.

29. Vlasak M, Roivainen M, Reithmayer M, et al. The minor receptor group of human rhinovirus (HRV) includes HRV23 and HRV25, but the presence of a lysine in the VP1 HI loop is not sufficient for receptor binding. J Virol. **2005**; 79:7389–7395.

30. Bochkov YA, Watters K, Ashraf S, et al. Cadherin-related family member 3, a childhood asthma susceptibility gene product, mediates rhinovirus C binding and replication. PNAS. **2015**; 112(17):5485–5490.

31. Stein MM, Thompson EE, Schoettler N, et al. A decade of research on the 17q12-21 asthma locus: Piecing together the puzzle. J Allergy Clin Immunol. **2018**; 142(3):749–764.

32. Arruda E, Boyle TR, Winther B, Pevear DC, Gwaltney JM, Hayden FG. Localization of human rhinovirus replication in the upper respiratory tract by in situ hybridization. J Infect Dis. **1995**; 171:1329–1333.

33. Papadopoulos NG, Bates PJ, Bardin PG, et al. Rhinoviruses infect the lower airways. J Infect Dis. **2000**; 181:1875–1884.

34. Papadopoulos NG, Sanderson G, Hunter J, Johnston SL. Rhinoviruses replicate effectively at lower airway temperatures. J Med Virol. **1999**; 58:100–104.

35. Gern JE, Dick EC, Lee WM, et al. Rhinovirus enters but does not replicate inside monocytes and airway macrophages. J Immunol. **1996**; 156:621–627.

36. Handzel ZT, Busse WW, Sedgwick JB, et al. Eosinophils bind rhinovirus and activate virus-specific T cells. J Immunol. **1998**; 160:1279–1284.

37. Ilarraza R, Wu Y, Skappak CD, Ajamian F, Proud D, Adamko DJ. Rhinovirus has the unique ability to directly activate human T cells *in vitro*. J Allergy Clin Immunol. **2013**; 131(2):395–404.

38. Aab A, Wirz O, van de Veen W, et al. Human rhinoviruses enter and induce proliferation of B lymphocytes. Allergy. **2017**; 72:232–243.

39. Gern JE, Vrtis R, Kelly EAB, Dick EC, Busse WW. Rhinovirus produces nonspecific activation of lymphocytes through a monocyte-dependent mechanism. J Immunol. **1996**; 157:1605–1612.

40. Mosser AG, Vrtis R, Burchell L, et al. Quantitative and qualitative analysis of rhinovirus infection in bronchial tissues. Am J Respir Crit Care Med. **2005**; 171:645–651.

41. Iwasaki J, Smith W-A, Khoo S-K, et al. Comparison of rhinovirus antibody titers in children with asthma exacerbations and species-specific rhinovirus infection. J Allergy Clin Immunol. **2014**; 134(1):25–32.

42. McLean GR, Walton RP, Shetty S, et al. Rhinovirus infections and immunisation induce cross-serotype reactive antibodies to VP1. Antiviral Res. **2012**; 95:193–201.

43. Niespodziana K, Cabauatan CR, Jackson DJ, et al. Rhinovirus-induced VP1-specific antibodies are group-specific and associated with severity of respiratory symptoms. EBioMedicine. **2015**; 2:64–70.

44. Bella J, Rossmann MG. ICAM-1 receptors and cold viruses. Pharm Acta Helv. **2000**; 74:291–297.

45. Hadfield AT, Oliveira MA, Kim KH, et al. Structural studies on human rhinovirus 14 drug-resistant compensation mutants. J Mol Biol. **1995**; 253:61–73.

46. Hewat EA, Blaas D. Cryoelectron microscopy analysis of the structural changes associated with human rhinovirus type 14 uncoating. **2004**; 78(6):2935–2942.

47. Barclay WS, Al-Nakib W, Higgins PG, Tyrrell DA. The time course of the humoral immune response to rhinovirus infection. Epidemiol Infect. **1989**; 103:659–669.

48. Alper CM, Doyle WJ, Skoner DP, et al. Prechallenge antibodies: Moderators of infection rate, signs, and symptoms in adults experimentally challenged with rhinovirus type 39. Laryngoscope. **1996**; 106:1298–1305.

49. Alper CM, Doyle WJ, Skoner DP, Buchman CA, Cohen S, Gwaltney JM. Prechallenge antibodies moderate disease expression in adults experimentally exposed to rhinovirus strain Hanks. Clin Infect Dis. **1998**; 27:119–128.

50. Fleet WF, Couch RB, Cate TR, Knight V. Homologous and heterologous resistance to rhinovirus common cold. Am J Epidemiol. **1965**; 82(2):185–196.

51. Gwaltney JM, Colonno RJ, Hamparian V, Turner RB. Rhinovirus. Diagnostic Procedures for Viral, Rickettsial, and Chlamydial Infections. p. 579–614.

52. Glanville N, McLean GR, Guy B, et al. Cross-serotype immunity induced by immunization with a conserved rhinovirus capsid protein. PLOS Pathog. **2013**; 9(9):e1003669.

53. Iwasaki J, Smith W-A, Stone SR, Thomas WR, Hales BJ. Species-specific and cross-reactive IgG1 antibody binding to viral capsid protein 1 (VP1) antigens of human rhinovirus species A, B and C. PLOS One. **2013**; 8(8):e70552.

54. Zhu Z, Tang W, Gwaltney JM, Wu Y, Elias JA. Rhinovirus stimulation of interleukin-8 *in vivo* and *in vitro*: Role of NF-*κ*B. Am J Physiol. **1997**; 273:L814–L824.

55. Zhu Z, Tang W, Ray A, et al. Rhinovirus stimulation of interleukin-6 *in vivo* and *in vitro*: Evidence for nuclear factor *κ*B-dependent transcriptional activation. J Clin Invest. **1996**; 97:421–430.

56. Spurrell JCL, Wiehler S, Zaheer RS, Sanders SP, Proud D, etal. Human airway epithelial cells produce IP-10 (CXCL10) *in vitro* and *in vivo* upon rhinovirus infections. Am J Physiol Lung Cell Mol Physiol. **2005**; 289:L85–L95.

57. Slater L, Bartlett NW, Haas JJ, et al. Co-ordinated role of TLR3, RIG-I and MDA5 in the innate response to rhinovirus in bronchial epithelium. PLOS Pathog. **2010**; 6(11):e1001178.

58. Gern JE, French DA, Grindle KA, Brockman-Schneider RA, Konno S-II, Busse WW. Double-stranded RNA induces the synthesis of specific chemokines by bronchial epithelial cells. Am J Respir Cell Mol Biol. **2003**; 28:731–773.

59. Schroth MK, Grimm E, Frindt P, et al. Rhinovirus replication causes RANTES production in primary bronchial epithelial cells. Am J Respir Cell Mol Biol. **1999**; 20:1220–1228.

60. Naclerio RM, Proud D, Lichtenstein LM, et al. Kinins are generated during experimental rhinovirus colds. J Infect Dis. **1988**; 157(1):133–142.

61. Fraenkel DJ, Bardin PG, Sanderson G, Lampe F, Johnston SL, Holgate ST. Lower airways inflammation during rhinovirus colds in normal and in asthmatic subjects. Am J Respir Crit Care Med. **1995**; 151:879–886.

62. Levandowski RA, Ou DW, Jackson GG. Acute-phase decrease of T lymphocyte subsets in rhinovirus infection. J Infect Dis. **1986**; 153(4):743–748.

63. Wimalasundera SS, Katz DR, Chain BM. Characterization of the T cell response to human rhinovirus in children: Implications for understanding the immunopathology of the common cold. J Infect Dis. **1997**; 176:755–759.

64. Parry DE, Busse WW, Sukow KA, Dick CR, Swenson C, Gern JE. Rhinovirus-induced PBMC responses and outcome of experimental infection in allergic subjects. J Allergy Clin Immunol. **2000**; 105(4):692–698.

65. Gern JE, Dick EC, Kelly EA, Vrtis R, Klein B. Rhinovirus-specific T cells recognize both shared and serotype-restricted viral epitopes. J Infect Dis. **1997**; 175:1108–1114.

66. Kim TS, Sun J, Braciale TJ. T cell responses during influenza infection: Getting and keeping control. Trends Immunol. **2011**; 32(5):225–231.

67. Wilkinson TMA, Li CK. F, Chui CSCC, et al. Preexisting influenza-specific $CD4^+$ T cells correlate with disease protection against influenza challenge in humans. Nat Med. **2012**; 18(2):274–280.

68. Palmenberg AC, Gern JE. Classification and evolution of human rhinoviruses. Rhinoviruses: Methods and protocols. p. 1–10.

69. The Scientific Committee on Common Cold Vaccines. Prevention of colds by vaccination against a rhinovirus. BMJ. **1965**; 1:1344–1349.

70. Perkins JC, Tucker DN, Knopf HLS, et al. Evidence for protective effect of an inactivated rhinovirus vaccine administered by the nasal route. Am J Epidemiol. **1969**; 90(4):319–326.

71. Buscho RF, Perkins JC, Knopf HLS, Kapikian AZ, Chanock RM. Further characterization of the local respiratory tract antibody response induced by intranasal instillation of inactivated rhinovirus 13 vaccine. J Immunol. **1972**; 108(1):169–177.

72. Hamory BH, Hamparian V V, Conant RM, Gwaltney Jr. JM. Human responses to two decavalent rhinovirus vaccines. J Infect Dis. **1975**; 132(6):623–629.

73. Doggett JE, Bynoe ML, Tyrrell DAJ. Some attempts to produce an experimental vaccine with rhinoviruses. BMJ. **1963**; 1:34–36.

74. Lee S, Nguyen MT, Currier MG, et al. A polyvalent inactivated rhinovirus vaccine is broadly immunogenic in rhesus macaques. Nat Commun. **2016**; 7:12838.

75. Niespodziana K, Napora K, Cabauatan C, et al. Misdirected antibody responses against an N-terminal epitope on human rhinovirus VP1 as explanation for recurrent RV infections. FASEB J. **2012**; 26:1001–1008.

76. Papi A, Contoli M. Rhinovirus vaccination: The case against. Eur Respir J. **2011**; 37:5–7.

77. Baggen J, Thibaut HJ, Strating JRPM, van Kuppeveld FJM. The life cycle of non-polio enteroviruses and how to target it. Nat Rev Microbiol. **2018**; 16:368–381.

78. Senior K. FDA panel rejects common cold treatment. Lancet Infect Dis. **2002**; 2:264.

79. Hayden FG, Hipskind GJ, Woerner DH, et al. Intranasal pirodavir (R77,975) treatment of rhinovirus colds. Antimicrob Agents Chemother. **1995**; 39(2):290–294.

80. Benschop KSM, van der Avoort HG, Duizer E, Koopmans MPG. Antivirals against enteroviruses: A critical review from a public-health perspective. Antivir Ther. **2015**; 20:121–130.

81. Hayden FG, Turner RB, Gwaltney JM, et al. Phase II, randomized, double-blind, placebo-controlled studies of ruprintrivir nasal spray 2-percent suspension for prevention and treatment of experimentally induced rhinovirus colds in healthy volunteers. Antimicrob Agents Chemother. **2003**; 47(12):3907–3916.

82. Djukanović R, Harrison T, Johnston SL, et al. The effect of inhaled IFN-β on worsening of asthma symptoms caused by viral infections: A randomized trial. Am J Respir Crit Care Med. **2014**; 190(2):145–154.

83. Silkoff PE, Flavin S, Gordon R, et al. Toll-like receptor 3 blockade in rhinovirus-induced experimental asthma exacerbations: A randomized controlled study. J Allergy Clin Immunol. **2018**; 141(4):1220–1230.

84. Turner R, Bauer R, Woelkart K, Hulsey TC, Gangemi JD. An evaluation of *Echinacea angustifolia* in experimental rhinovirus infections. N Engl J Med. **2005**; 353(4):341–348.

85. Hao Q, Dong B, Wu T. Probiotics for preventing acute upper respiratory tract infections. The Cochrane Library.

86. Kang E-J, Kim SY, Hwang I-H, Ji Y-J. The effect of probiotics on prevention of common cold: A meta-analysis of randomized controlled trial studies. Korean J Fam Med. **2013**; 34:2–10.

87. Martineau AR, Jolliffe DA, Hooper RL, et al. Vitamin D supplementation to prevent acute respiratory tract infections: systematic review and meta-analysis of individual participant data. BMJ. **2017**; 356:i6583.

88. Mainardi T, Kapoor S, Bielory L. Complementary and alternative medicine: Herbs, phytochemicals and vitamins and their immunologic effects. J Allergy Clin Immunol. **2009**; 123(2):283–294.

89. Lambrecht BN, Hammad H. The immunology of asthma. Nat Immunol. **2014**; 16(1):45–56.

90. Asthma's Impact on the Nation: Data from the CDC National Asthma Control Program [Internet]. Available from: http://www.cdc.gov/asthma/impacts_nation/asthmafactsheet.pdf

91. Chung KF, Wenzel SE, Brozek JL, et al. International ERS/ATS guidelines on definition, evaluation and treatment of severe asthma. Eur Respir J. **2014**; 43:343–373.

92. Platts-Mills TAE. The allergy epidemics: 1870-2010. J Allergy Clin Immunol. **2015**; 136(1):3–13.

93. Croisant S. Epidemiology of asthma: Prevalence and burden of disease. Heterogeneity in Asthma. p. 233–254.

94. Hammad H, Lambrecht BN. Barrier Epithelial Cells and the Control of Type 2 Immunity. Immunity. **2015**; 43:29–40.

95. Nakayama T, Hirahara K, Onodera A, et al. $T_H2$ Cells in Health and Disease. Annu Rev Immunol. **2017**; 35:53–84.

96. Wernersson S, Pejler G. Mast cell secretory granules: Armed for battle. Nat Rev Immunol. **2014**; 14:478–494.

97. Chevigné A, Jacquet A. Emerging roles of the protease allergen Der p 1 in house dust mite–induced airway inflammation. J Allergy Clin Immunol. **2018**; 142(2):398–400.

98. Pothoven KL, Norton JE, Hulse KE, et al. Oncostatin M promotes mucosal epithelial barrier dysfunction, and its expression is increased in patients with eosinophilic mucosal disease. J Allergy Clin Immunol. **2015**; 136(3):737–746.

99. Lai T, Wu D, Li W, et al. Interleukin-31 expression and relation to disease severity in human asthma. Sci Rep. **2016**; 6:22835.

100. Stott B, Lavender P, Lehmann S, Pennino D, Durham S, Schmidt-Weber CB. Human IL-31 is induced by IL-4 and promotes $T_H2$-driven inflammation. J Allergy Clin Immunol. **2013**; 132(2):446–454.

101. Hänel KH, Pfaff CM, Cornelissen C, et al. Control of the physical and antimicrobial skin barrier by an IL-31–IL-1 signaling network. J. Immunol.

102. Bell BD, Kitajima M, Larson RP, et al. The transcription factor STAT5 is critical in dendritic cells for the development of $T_H2$ but not $T_H1$ responses. Nat Immunol. **2013**; 14(4):364–371.

103. Headley MB, Zhou B, Shih WX, Aye T, Comeau MR, Ziegler SF. TSLP conditions the lung immune environment for the generation of pathogenic innate and antigen-specific adaptive immune responses. J Immunol. **2009**; 182:1641–1647.

104. Ito T, Wang Y-H, Duramad O, et al. TSLP-activated dendritic cells induce an inflammatory T helper type 2 cell response through OX40 ligand. J Exp Med. **2005**; 202(9):1213–1223.

105. Makrinioti H, Toussaint M, Jackson DJ, Walton RP, Johnston SL. Role of interleukin 33 in respiratory allergy and asthma. Lancet Respir Med. **2014**; 2(3):226–237.

106. Murakami-Satsutani N, Ito T, Nakanishi T, et al. IL-33 promotes the induction and maintenance of $T_H2$ immune responses by enhancing the function of OX40 ligand. Allergol Int. **2014**; 63(3):443–455.

107. Halim TYF, Hwang YY, Scanlon ST, et al. Group 2 innate lymphoid cells license dendritic cells to potentiate memory $T_H2$ cell responses. Nat Immunol. **2015**; 17(1):57–64.

108. Halim TYF, Steer CA, Mathä L, et al. Group 2 innate lymphoid cells are critical for the initiation of adaptive T helper 2 cell-mediated allergic lung inflammation. Immunity. **2014**; 40:425–435.

109. Wawrzyniak P, Wawrzyniak M, Wanke K, et al. Regulation of bronchial epithelial barrier integrity by type 2 cytokines and histone deacetylases in asthmatic patients. J Allergy Clin Immunol. **2017**; 139(1):93–103.

110. Hui CCK, Murphy DM, Neighbour H, et al. T cell-mediated induction of thymic stromal lymphopoietin in differentiated human primary bronchial epithelial cells. Clin Exp Allergy. **2014**; 44(7):953–964.

111. Mirchandani AS, Besnard A-G, Yip E, et al. Type 2 innate lymphoid cells drive $CD4^+$ $T_H2$ cell responses. J Immunol. **2014**; 192(5):2442–2448.

112. De Grove KC, Provoost S, Hendriks RW, et al. Dysregulation of type 2 innate lymphoid cells and $T_H2$ cells impairs pollutant-induced allergic airway responses. J Allergy Clin Immunol. **2017**; 139(1):246–257.

113. Ho IC, Tai TS, Pai SY. GATA3 and the T-cell lineage: Essential functions before and after T-helper-2-cell differentiation. Nat Rev Immunol. **2009**; 9:125–135.

114. van Helden MJ, Lambrecht BN. Dendritic cells in asthma. Curr Opin Immunol. **2013**; 25:745–754.

115. Ebert LM, Schaerli P, Moser B. Chemokine-mediated control of T cell traffic in lymphoid and peripheral tissues. Mol Immunol. **2005**; 42:799–809.

116. Crapster-Pregont M, Yeo J, Sanchez RL, Kuperman DA. Dendritic cells and alveolar macrophages mediate IL-13-induced airway inflammation and chemokine production. J Allergy Clin Immunol. **2012**; 129(6):1621–1627.

117. Kast JI, Wanke K, Soyka MB, et al. The broad spectrum of interepithelial junctions in skin and lung. J Allergy Clin Immunol. **2012**; 130(2):544–547.

118. Steelant B, Farré R, Wawrzyniak P, et al. Impaired barrier function in patients with house dust mite-induced allergic rhinitis is accompanied by decreased occludin and zonula occludens-1 expression. J Allergy Clin Immunol. **2016**; 137(4):1043–1053.

119. Tjota MY, Sperling AI. Distinct dendritic cell subsets actively induce $T_H2$ polarization. Curr Opin Immunol. **2014**; 31:44–50.

120. Tjota MY, Hrusch CL, Blaine KM, Williams JW, Barrett NA, Sperling AI. Signaling through FcRγ-associated receptors on dendritic cells drives IL-33-dependent $T_H2$-type responses. J Allergy Clin Immunol. **2014**; 134(3):706–713.

121. Janss T, Mesnil C, Pirottin D, et al. Interferon response factor-3 promotes the pro-$T_H2$ activity of mouse lung $CD11b^+$ conventional dendritic cells in response to house dust mite allergens. Eur J Immunol. **2016**; 46:2614–2628.

122. Williams JW, Tjota MY, Clay BS, et al. Transcription factor IRF4 drives dendritic cells to promote $T_H2$ differentiation. Nat Commun. **2013**; 4:2990.

123. Akbari M, Honma K, Kimura D, et al. IRF4 in dendritic cells inhibits IL-12 production and controls $T_H1$ immune responses against *Leishmania major*. J Immunol. **2014**; 192:2271–2279.

124. Nouri-Shirazi M, Kahlden C, Nishino P, Guinet E. Nicotine exposure alters the mRNA expression of Notch ligands in dendritic cells and their response to $T_H1$-/$T_H2$-promoting stimuli. Scand J Immunol. **2015**; 81:110–120.

125. Gueguen C, Bouley J, Moussu H, et al. Changes in markers associated with dendritic cells driving the differentiation of either $T_H2$ cells or regulatory T cells correlate with clinical benefit during allergen immunotherapy. J Allergy Clin Immunol. **2016**; 137(2):545–558.

126. van der Heijden FL, van Neerven RJJ, van Katwijk M, Bos JD, Kapsenberg ML. Serum-IgE-facilitated allergen presentation in atopic disease. J Immunol. **1993**; 150:3643–8650.

127. Zheng W-P, Flavell RA. The transcription factor GATA-3 is necessary and sufficient for $T_H2$ cytokine gene expression in CD4 T cells. Cell. **1997**; 89:587–596.

128. Wang Y, Misumi I, Gu A Di, et al. GATA-3 controls the maintenance and proliferation of T cells downstream of TCR and cytokine signaling. Nat Immunol. **2013**; 14(7):714–722.

129. Bruchard M, Rebé C, Derangère V, et al. The receptor NLRP3 is a transcriptional regulator of $T_H2$ differentiation. Nat Immunol. **2015**; 16(8):859–870.

130. Yu Q, Sharma A, Oh SY, et al. T cell factor 1 initiates the T helper type 2 fate by inducing the transcription factor GATA-3 and repressing interferon-γ. Nat Immunol. **2009**; 10(9):992–999.

131. Kuwahara M, Yamashita M, Shinoda K, et al. The transcription factor Sox4 is a downstream target of signaling by the cytokine TGF-β and suppresses $T_H2$ differentiation. Nat Immunol. **2012**; 13(8):778–786.

132. Sahoo A, Alekseev A, Obertas L, Nurieva R. Grail controls $T_H2$ cell development by targeting STAT6 for degradation. Nat Commun. **2014**; 5:4732.

133. Mitson-Salazar A, Prussin C. Pathogenic effector $T_H2$ cells in allergic eosinophilic inflammatory disease. Front Med. **2017**; 4:165.

134. Endo Y, Hirahara K, Yagi R, Tumes DJ, Nakayama T. Pathogenic memory type $T_H2$ cells in allergic inflammation. Trends Immunol. **2014**; 35(2):69–78.

135. Upadhyaya B, Yin Y, Hill BJ, Douek DC, Prussin C. Hierarchical IL-5 expression defines a subpopulation of highly differentiated human $T_H2$ cells. J Immunol. **2011**; 187(6):3111–3120.

136. Prussin C, Lee J, Foster B. Eosinophilic gastrointestinal disease and peanut allergy are alternatively associated with IL-$5^+$ and IL-$5^-$ $T_H2$ responses. J Allergy Clin Immunol. **2009**; 124(6):1326–1332.

137. Hirahara K, Shinoda K, Endo Y, Ichikawa T, Nakayama T. Maintenance of memory-type pathogenic $T_H2$ cells in the pathophysiology of chronic airway inflammation. Inflammation and Regeneration. **2017**; 38(10).

138. Mitson-Salazar A, Yin Y, Wansley DL, et al. Hematopoietic prostaglandin D synthase defines a proeosinophilic pathogenic effector human $T_H2$ cell subpopulation with enhanced function. J Allergy Clin Immunol. **2016**; 137(3):907–918.

139. Wilson RH, Whitehead GS, Nakano H, Free ME, Kolls JK, Cook DN. Allergic sensitization through the airway primes $T_H17$-dependent neutrophilia and airway hyperresponsiveness. Am J Respir Crit Care Med. **2009**; 180:720–730.

140. Bullens DMA, Truyen E, Coteur L, et al. IL-17 mRNA in sputum of asthmatic patients: Linking T cell driven inflammation and granulocytic influx? Respir Res. **2006**; 7:135.

141. Al-Ramli W, Préfontaine D, Chouiali F, et al. $T_H17$-associated cytokines (IL-17A and IL-17F) in severe asthma. J Allergy Clin Immunol. **2009**; 123(5):1185–1187.

142. Molet S, Hamid Q, Davoine F, et al. IL-17 is increased in asthmatic airways and induces human bronchial fibroblasts to produce cytokines. J Allergy Clin Immunol. **2001**; 108(3):430–438.

143. Chakir J, Shannon J, Molet S, et al. Airway remodeling-associated mediators in moderate to severe asthma: Effect of steroids on TGF-β, IL-11, IL-17, and type I and type III collagen expression. J Allergy Clin Immunol. **2003**; 111(6):1293–1298.

144. Wakashin H, Hirose K, Maezawa Y, et al. IL-23 and $T_H17$ cells enhance $T_H2$-cell-mediated eosinophilic airway inflammation in mice. Am J Respir Crit Care Med. **2008**; 178:1023–1032.

145. Zhao J, Lloyd CM, Noble A. $T_H17$ responses in chronic allergic airway inflammation abrogate regulatory T-cell-mediated tolerance and contribute to airway remodeling. Mucosal Immunol. **2013**; 6(2):335–346.

146. Irvin C, Zafar I, Good J, et al. Increased frequency of dual-positive $T_H2/T_H17$ cells in bronchoalveolar lavage fluid characterizes a population of patients with severe asthma. J Allergy Clin Immunol. **2014**; 134(5):1175–1186.

147. Hastie AT, Moore WC, Meyers DA, et al. Analyses of asthma severity phenotypes and inflammatory proteins in subjects stratified by sputum granulocytes. J Allergy Clin Immunol. **2010**; 125(5):1028–1036.

148. Moore WC, Hastie AT, Li X, et al. Sputum neutrophil counts are associated with more severe asthma phenotypes using cluster analysis. J Allergy Clin Immunol. **2014**; 133(6):1557–1563.

149. Peine M, Rausch S, Helmstetter C, et al. Stable T-bet$^+$GATA-3$^+$ $T_H1/T_H2$ hybrid cells arise *in vivo*, can develop directly from naïve precursors, and limit immunopathologic inflammation. PLOS Biol. **2013**; 11(8):e1001633.

150. Mamessier E, Nieves A, Lorec A-M, et al. T-cell activation during exacerbations: A longitudinal study in refractory asthma. Allergy. **2008**; 63:1202–1210.

151. Raundhal M, Morse C, Khare A, et al. High IFN-γ and low SLPI mark severe asthma in mice and humans. J Clin Invest. **2015**; 125(8):3037–3050.

152. Truyen E, Coteur L, Dilissen E, et al. Evaluation of airway inflammation by quantitative $T_H1/T_H2$ cytokine mRNA measurement in sputum of asthma patients. Thorax. **2006**; 61:202–208.

153. Shannon J, Ernst P, Yamauchi Y, et al. Differences in airway cytokine profile in severe asthma compared to moderate asthma. Chest. **2008**; 133:420–426.

154. Krug N, Madden J, Redington AE, et al. T-cell cytokine profile evaluated at the single cell level in BAL and blood in allergic asthma. Am J Respir Cell Mol Biol. **1996**; 14:319–326.

155. Heaton T, Rowe J, Turner S, et al. An immunoepidemiological approach to asthma: Identification of *in vitro* T-cell response patterns associated with different wheezing phenotypes in children. Lancet. **2005**; 365:142–149.

156. Pene J, Chevalier S, Preisser L, et al. Chronically inflamed human tissues are infiltrated by highly differentiated $T_H17$ lymphocytes. J Immunol. **2008**; 180:7423–7430.

157. Cembrzyñska-Nowak M, Szklarz E, Inglot AD, Teodorczyk-Injeyan JA. Elevated release of tumor necrosis factor-α and interferon-γ by bronchoalveolar leukocytes from patients with bronchial asthma. Am Rev Respir Dis. **1993**; 147:291–295.

158. ten Hacken NHT, Oosterhoff Y, Kauffman HF, et al. Elevated serum interferon-γ in atopic asthma correlates with increased airways responsiveness and circadian peak expiratory flow variation. Eur Respir J. **1998**; 11:312–316.

159. Finotto S, Neurath MF, Glickman JN, et al. Development of spontaneous airway changes consistent with human asthma in mice lacking T-bet. Science. **2010**; 295:336–339.

160. Cohn L, Homer RJ, Niu N, Bottomly K. T helper 1 cells and interferon γ regulate allergic airway inflammation and mucus production. J Exp Med. **1999**; 190(9):1309–1318.

161. Irifune K, Yokoyama A, Sakai K, et al. Adoptive transfer of T-helper cell type 1 clones attenuates an asthmatic phenotype in mice. Eur Respir J. **2005**; 25(4):653–659.

162. Huang T-J, MacAry PA, Eynott P, et al. Allergen-specific $T_H1$ cells counteract efferent $T_H2$ cell-dependent bronchial hyperresponsiveness and eosinophilic inflammation partly via IFN-γ. J Immunol. **2001**; 166:207–217.

163. Cui J, Pazdziorko S, Miyashiro JS, et al. $T_H1$-mediated airway hyperresponsiveness independent of neutrophilic inflammation. J Allergy Clin Immunol. **2005**; 115(2):309–315.

164. Hansen G, Berry G, DeKruyff RH, Umetsu DT. Allergen-specific $T_H1$ cells fail to counterbalance $T_H2$ cell-induced airway hyperreactivity but cause severe airway inflammation. J Clin Invest. **1999**; 103:175–183.

165. Randolph D, Carruthers CJ, Szabo SJ, Murphy KM, Chaplin DD. Modulation of airway inflammation by passive transfer of allergen-specific $T_H1$ and $T_H2$ cells in a mouse model of asthma. J Immunol. **1999**; 162:2375–2383.

166. Randolph DA, Stephens R, Carruthers CJL, Chaplin DD. Cooperation between $T_H1$ and $T_H2$ cells in a murine model of eosinophilic airway inflammation. **1999**; 104:1021–1029.

167. Hayashi N, Yoshimoto T, Izuhara K, Matsui K, Tanaka T, Nakanishi K. T helper 1 cells stimulated with ovalbumin and IL-18 induce airway hyperresponsiveness and lung fibrosis by IFN-γ and IL-13 production. PNAS. **2007**; 104(37):14765–14770.

168. Yang M, Kumar RK, Foster PS. Pathogenesis of steroid-resistant airway hyperresponsiveness: Interaction between IFN-γ and TLR4/MyD88 pathways. J Immunol. **2009**; 182:5107–5115.

169. Sugimoto T, Ishikawa Y, Yoshimoto T, Hayashi N, Fujimoto J, Nakanishi K. Interleukin 18 acts on memory T helper cells type 1 to induce airway inflammation and hyperresponsiveness in a naïve host mouse. J Exp Med. **2004**; 199(4):535–545.

170. Hata H, Yoshimoto T, Hayashi N, Hada T, Nakanishi K. IL-18 together with anti-CD3 antibody induces human $T_H1$ cells to produce $T_H1$- and $T_H2$-cytokines and IL-8. Int Immunol. **2004**; 16(12):1733–1739.

171. Dardalhon V, Awasthi A, Kwon H, et al. IL-4 inhibits TGF-β-induced $Foxp3^+$ T cells and, together with TGF-β, generates $IL\text{-}9^+$ $IL\text{-}10^+$ $Foxp3^-$ effector T cells. Nat Immunol. **2008**; 9(12):1347–1355.

172. Veldhoen M, Uyttenhove C, van Snick J, et al. Transforming growth factor-β "reprograms" the differentiation of T helper 2 cells and promotes an interleukin 9-producing subset. Nat Immunol. **2008**; 9(12):1341–1346.

173. Staudt V, Bothur E, Klein M, et al. Interferon-regulatory factor 4 is essential for the developmental program of T helper 9 cells. Immunity. **2010**; 33:192–202.

174. Goswami R, Jabeen R, Yagi R, et al. STAT6-dependent regulation of $T_H9$ development. J Immunol. **2012**; 188:968–975.

175. Petit-Frere C, Dugas B, Braquet P, Mencia-Huerta JM. Interleukin-9 potentiates the interleukin-4-induced IgE and IgG1 release from murine B lymphocytes. Immunology. **1993**; 79:146–151.

176. Eyerich S, Eyerich K, Pennino D, et al. $T_H22$ represent a distinct human T cell subset involved in epidermal immunity and remodeling. J Clin Invest. **2009**; 119(12):3573–3585.

177. Nograles KE, Zaba LC, Shemer A, et al. IL-22-producing "T22" T cells account for upregulated IL-22 in atopic dermatitis despite reduced IL-17-producing $T_H17$ T cells. J Allergy Clin Immunol. **2009**; 123(6):1244–1252.

178. Lin YL, Shieh CC, Wang JY. The functional insufficiency of human $CD4^+CD25^{high}$ T-regulatory cells in allergic asthma is subjected to TNF-α modulation. Allergy. **2008**; 63:67–74.

179. Hartl D, Koller B, Mehlhorn AT, et al. Quantitative and functional impairment of pulmonary $CD4^+CD25^{hi}$ regulatory T cells in pediatric asthma. J Allergy Clin Immunol. **2007**; 119(5):1258–1266.

180. Maazi H, Shirinbak S, Willart M, et al. Contribution of regulatory T cells to alleviation of experimental allergic asthma after specific immunotherapy. Clin Exp Allergy. **2012**; 42:1519–1528.

181. Ray A, Raundhal M, Oriss TB, Ray P, Wenzel SE. Current concepts of severe asthma. J Clin Invest. **2016**; 126(7):2394–2403.

182. Genentech Inc. Press Release: FDA Approves Xoliar [Internet]. Available from: https://www.gene.com/media/press-releases/6287/2003-06-20/fda-approves-xolair-biotechnology-breakt

183. Genentech Inc. Press Release: FDA Approves Genentech's Xolair (omalizumab) for Allergic Asthma in Children [Internet]. Available from: https://www.gene.com/media/press-releases/14632/2016-07-07/fda-approves-genentechs-xolair-omalizuma

184. Busse W, Corren J, Lanier BQ, et al. Omalizumab, anti-IgE recombinant humanized monoclonal antibody, for the treatment of severe allergic asthma. J Allergy Clin Immunol. **2001**; 108(2):184–190.

185. Lowe PJ, Renard D. Omalizumab decreases IgE production in patients with allergic (IgE-mediated) asthma; PKPD analysis of a biomarker, total IgE. Br J Clin Pharmacol. **2011**; 72(2):306–320.

186. Chan MA, Gigliotti NM, Dotson AL, Rosenwasser LJ. Omalizumab may decrease IgE synthesis by targeting membrane $IgE^+$ human B cells. Clin Transl Allergy. Clinical and Translational Allergy; **2013**; 3:29.

187. MacGlashan D. Loss of receptors and IgE *in vivo* during treatment with anti-IgE antibody. J Allergy Clin Immunol. **2004**; 114(6):1472–1474.

188. MacGlashan D, Macglashan D, Xia HZ, et al. IgE-regulated loss, not IgE-regulated synthesis, controls expression of FcεRI in human basophils. J Leukoc Biol. **2001**; 70:207–218.

189. Djukanović R, Wilson SJ, Kraft M, et al. Effects of treatment with anti-immunoglobulin E antibody omalizumab on airway inflammation in allergic asthma. Am J Respir Crit Care Med. **2004**; 170:583–593.

190. Holgate S, Casale T, Wenzel S, Bousquet J, Deniz Y, Reisner C. The anti-inflammatory effects of omalizumab confirm the central role of IgE in allergic inflammation. J Allergy Clin Immunol. **2005**; 115(3):459–465.

191. Gruchalla RS, Sampson HA, Liu AH, et al. Effects of omalizumab on T lymphocyte function in inner-city children with asthma. Pediatr Allergy Immunol. **2016**; 27:320–332.

192. Bagnasco D, Ferrando M, Varricchi G, Puggioni F, Passalacqua G, Canonica GW. Anti-interleukin 5 (IL-5) and IL-5Rα biological drugs: Efficacy, safety, and future perspectives in severe eosinophilic asthma. Front Med. **2017**; 4:135.

193. Castro M, Corren J, Pavord ID, et al. Dupilumab efficacy and safety in moderate-to-severe uncontrolled asthma. N Engl J Med. **2018**; 378(26):2486–2496.

194. Hanania NA, Korenblat P, Chapman KR, et al. Efficacy and safety of lebrikizumab in patients with uncontrolled asthma (LAVOLTA I and LAVOLTA II): Replicate, phase 3, randomised, double-blind, placebo-controlled trials. Lancet Respir Med. **2016**; 4:781–796.

195. Chung KF. Tralokinumab unsuccessful for management of severe, uncontrolled asthma. Lancet Respir Med. **2018**; 6:480–481.

196. Chen Z-G, Zhang T-T, Li H-T, et al. Neutralization of TSLP inhibits airway remodeling in a murine model of allergic asthma induced by chronic exposure to house dust mite. PLOS One. **2013**; 8(1):e51268.

197. Corren J, Parnes JR, Wang L, et al. Tezepelumab in adults with uncontrolled asthma. N Engl J Med. **2017**; 377(10):936–946.

198. Lee HY, Rhee CK, Kang JY, et al. Blockade of IL-33/ST2 ameliorates airway inflammation in a murine model of allergic asthma. Exp Lung Res. **2014**; 40:66–76.

199. Townley RG, Agrawal S. CRTH2 antagonists in the treatment of allergic responses involving $T_H2$ cells, basophils, and eosinophils. Ann Allergy, Asthma Immunol. **2012**; 109:365–374.

200. Huang T, Hazen M, Shang Y, et al. Depletion of major pathogenic cells in asthma by targeting CRTH2. JCI insight. **2016**; 1(7):e86689.

201. Homburg U, Renz H, Timmer W, et al. Safety and tolerability of a novel inhaled GATA3 mRNA targeting DNAzyme in patients with $T_H2$-driven asthma. J Allergy Clin Immunol. **2015**; 136(3):797–800.

202. Krug N, Hohlfeld JM, Kirsten A-M, et al. Allergen-induced asthmatic responses modified by a GATA3-specific DNAzyme. N Engl J Med. **2015**; 372(21):1987–1995.

203. Maimonides M, Rosner F, Dienstag JI. Moses Maimonides' Treatise on Asthma. Maimonides Research Institute;

204. Rosenthal LA, Avila PC, Heymann PW, et al. Viral respiratory tract infections and asthma: The course ahead. J Allergy Clin Immunol. **2010**; 125(6):1212–1217.

205. Eadie MB, Stott EJ, Grist NR. Virological studies in chronic bronchitis. BMJ. **1966**; 2:671–673.

206. Stott E, Grist N, Eadie M. Rhinovirus infections in chronic bronchitis: Isolation of eight possibly new rhinovirus serotypes. J Med Microbiol. **1968**; 1:109–117.

207. Sigurs N, Bjarnason R, Sigurbergsson F, Kjellman B. Respiratory syncytial virus bronchiolitis in infancy is an important risk factor for asthma and allergy at age 7. Am J Respir Crit Care Med. **2000**; 161:1501–1507.

208. Stein R, Sherrill D, Morgan W, et al. Respiratory syncytial virus in early life and risk of wheeze and allergy by age 13 years. Lancet. **1999**; 354:541–545.

209. Jackson DJ, Gangnon RE, Evans MD, et al. Wheezing rhinovirus illnesses in early life predict asthma development in high-risk children. Am J Respir Crit Care Med. **2008**; 178:667–672.

210. Kusel MMH, de Klerk NH, Kebadze T, et al. Early-life respiratory viral infections, atopic sensitization, and risk of subsequent development of persistent asthma. J Allergy Clin Immunol. **2007**; 119(5):1105–1110.

211. Rakes GP, Arruda E, Ingram JM, et al. Rhinovirus and respiratory syncytial virus in wheezing children requiring emergency care IgE and eosinophil snalyses. Am J Respir Crit Care Med. **1999**; 159:785–790.

212. Kusel MMH, de Klerk NH, Holt PG, Kebadze T, Johnston SL, Sly PD. Role of respiratory viruses in acute upper and lower respiratory tract illness in the first year of life. Pediatr Infect Dis J. **2006**; 25(8):680–686.

213. Rubner FJ, Jackson DJ, Evans MD, et al. Early life rhinovirus wheezing, allergic sensitization, and asthma risk at adolescence. J Allergy Clin Immunol. **2017**; 139(2):501–507.

214. Sly PD, Kusel M, Holt PG. Do early-life viral infections cause asthma? J Allergy Clin Immunol. **2010**; 125(6):1202–1205.

215. Thomsen SF, van der Sluis S, Stensballe LG, et al. Exploring the association between severe respiratory syncytial virus infection and asthma: A registry-based twin study. Am J Respir Crit Care Med. **2009**; 179:1091–1097.

216. Wu P, Dupont WD, Griffin MR, et al. Evidence of a causal role of winter virus infection during infancy in early childhood asthma. Am J Respir Crit Care Med. **2008**; 178:1123–1129.

217. Jartti T, Gern JE. Role of viral infections in the development and exacerbation of asthma in children. J Allergy Clin Immunol. **2017**; 140(4):895–906.

218. Johnston SL, Pattemore PK, Sanderson G, et al. Community study of role of viral infections in exacerbations of asthma in 9-11 year old children. BMJ. **1995**; 310:1225–1229.

219. Nicholson KG, Kent J, Ireland DC. Respiratory viruses and exacerbations of asthma in adults. BMJ. **1993**; 307:982–986.

220. Olenec JP, Kim WK, Lee WM, et al. Weekly monitoring of children with asthma for infections and illness during common cold seasons. J Allergy Clin Immunol. **2010**; 125(5):1001–1006.

221. Nakagome K, Bochkov YA, Ashraf S, et al. Effects of rhinovirus species on viral replication and cytokine production. J Allergy Clin Immunol. **2014**; 134(2):332–341.

222. Murray CS, Poletti G, Kebadze T, et al. Study of modifiable risk factors for asthma exacerbations: Virus infection and allergen exposure increase the risk of asthma hospital admissions in children. Thorax. **2006**; 61:376–382.

223. Green RM, Custovic A, Sanderson G, Hunter J, Johnston SL, Woodcock A. Synergism between allergens and viruses and risk of hospital admission with asthma: Case-control study. BMJ. **2002**; 324:1–5.

224. Calhoun WJ, Dick EC, Schwartz LB, Busse WW. A common cold virus, rhinovirus 16, potentiates airway inflammation after segmental antigen bronchoprovocation in allergic subjects. J Clin Invest. **1994**; 94:2200–2208.

225. Avila PC, Abisheganaden JA, Wong H, et al. Effects of allergic inflammation of the nasal mucosa on the severity of rhinovirus 16 cold. J Allergy Clin Immunol. **2000**; 105(5):923–932.

226. De Kluijver J, Evertse CE, Sont JK, et al. Are rhinovirus-induced airway responses in asthma aggravated by chronic allergen exposure? Am J Respir Crit Care Med. **2003**; 168:1174–1180.

227. Busse WW, Morgan WJ, Gergen PJ, et al. Randomized trial of omalizumab (anti-IgE) for asthma in inner-city children. N Engl J Med. **2011**; (364):1005–1015.

228. Esquivel A, Busse WW, Calatroni A, et al. Effects of omalizumab on rhinovirus infections, illness, and exacerbations of asthma. Am J Respir Crit Care Med. **2017**; 196(8):985–992.

229. Teach SJ, Gill MA, Togias A, et al. Preseasonal treatment with either omalizumab or an inhaled corticosteroid boost to prevent fall asthma exacerbations. J Allergy Clin Immunol. **2015**; 136(6):1476–1485.

230. Duff AL, Pomeranz ES, Gelber LE, et al. Risk factors for acute wheezing in infants and children: Viruses, passive smoke, and IgE antibodies to inhalant allergens. Pediatrics. **1993**; 92(4):535–540.

231. Soto-Quiros M, Avila L, Platts-Mills TAE, et al. High titers of IgE antibody to dust mite allergen and risk for wheezing among asthmatic children infected with rhinovirus. J Allergy Clin Immunol. **2012**; 129(6):1499–1505.

232. Zambrano JC, Carper HT, Rakes GP, et al. Experimental rhinovirus challenges in adults with mild asthma: Response to infection in relation to IgE. J Allergy Clin Immunol. **2003**; 111(5):1008–1016.

233. Jackson GG, Dowling HF. Transmission of the common cold to volunteers under controlled conditions. IV. Specific immunity to the common cold. J Clin Invest. **1959**; 38(5):762–976.

234. Johnston NW, Johnston SL, Norman GR, Dai J, Sears MR. The September epidemic of asthma hospitalization: School children as disease vectors. J Allergy Clin Immunol. **2006**; 117(3):557–562.

235. Chairakaki A-D, Saridaki M-I, Pyrillou K, et al. Plasmacytoid dendritic cells drive acute asthma exacerbations. J Allergy Clin Immunol. **2018**; 142(2):542–556.

236. Hong JY, Bentley JK, Chung Y, et al. Neonatal rhinovirus induces mucous metaplasia and airways hyperresponsiveness through IL-25 and type 2 innate lymphoid cells. J Allergy Clin Immunol. **2014**; 134(2):429–439.

237. Beale J, Jayaraman A, Jackson DJ, et al. Rhinovirus induced IL-25 in asthma exacerbation drives type-2 immunity and allergic pulmonary inflammation. Sci Transl Med. **2014**; 6(256):256ra134.

238. Werder RB, Zhang V, Lynch JP, et al. Chronic IL-33 expression predisposes to virus-induced asthma exacerbations by increasing type 2 inflammation and dampening antiviral immunity. J Allergy Clin Immunol. **2018**; 141(5):1607–1619.

239. Schneider D, Hong JY, Popova AP, et al. Neonatal rhinovirus infection induces mucous metaplasia and airways hyperresponsiveness. J Immunol. **2012**; 188:2894–2904.

240. Wark PA, Johnston SL, Bucchieri F, et al. Asthmatic bronchial epithelial cells have a deficient innate immune response to infection with rhinovirus. J Exp Med. **2005**; 201(6):937–947.

241. Contoli M, Message SD, Laza-Stanca V, et al. Role of deficient type III interferon-λ production in asthma exacerbations. Nat Med. **2006**; 12(9):1023–1026.

242. Bratke K, Prieschenk C, Garbe K, Kuepper M, Lommatzsch M, Virchow JC. Plasmacytoid dendritic cells in allergic asthma and the role of inhaled corticosteroid treatment. Clin Exp Allergy. **2013**; 43:312–321.

243. Papadopoulos NG, Stanciu LA, Papi A, Holgate ST, Johnston SL. A defective type 1 response to rhinovirus in atopic asthma. Thorax. **2002**; 57(4):328–332.

244. Message SD, Laza-Stanca V, Mallia P, et al. Rhinovirus-induced lower respiratory illness is increased in asthma and related to virus load and $T_H1/2$ cytokine and IL-10 production. PNAS. **2008**; 105(36):13562–13567.

245. Lynch JP, Werder RB, Simpson J, et al. Aeroallergen-induced IL-33 predisposes to respiratory virus-induced asthma by dampening anti-viral immunity. J Allergy Clin Immunol. **2016**; 138(5):1326–1337.

246. Duerr CU, McCarthy CDA, Mindt BC, et al. Type I interferon restricts type 2 immunopathology through the regulation of group 2 innate lymphoid cells. Nat Immunol. **2015**; 17(1):65–75.

247. Contoli M, Ito K, Padovani A, et al. $T_H2$ cytokines impair innate immune responses to rhinovirus in respiratory epithelial cells. Allergy. **2015**; 70:910–920.

248. Pritchard AL, Carroll ML, Burel JG, White OJ, Phipps S, Upham JW. Innate IFNs and plasmacytoid dendritic cells constrain $T_H2$ cytokine responses to rhinovirus: A regulatory mechanism with relevance to asthma. J Immunol. **2012**; 188:5898–5905.

249. Pritchard AL, White OJ, Burel JG, Upham JW. Innate interferons inhibit allergen and microbial specific $T_H2$ responses. Immunol Cell Biol. **2012**; 90:974–977.

250. Glanville N, Peel TJ, Schröder A, et al. T-bet deficiency causes T helper cell dependent airways eosinophilia and mucus hypersecretion in response to rhinovirus infection. PLOS Pathog. **2016**; 12(9):e1005913.

251. Gill MA, Bajwa G, George TA, et al. Counterregulation between the FcεRI pathway and antiviral responses in human plasmacytoid dendritic cells. J Immunol. **2010**; 184:5999–6006.

252. Tversky JR, Le T, Bieneman AP, Chichester K, Hamilton RG, Schroeder JT. Human blood dendritic cells from allergic subjects have impaired capacity to produce interferon-α via Toll-like receptor 9. Clin Exp Allergy. **2008**; 38(5):781–788.

253. Rowe RK, Pyle DM, Tomlinson AR, Lv T, Hu Z, Gill MA. IgE cross-linking impairs monocyte antiviral responses and inhibits influenza-driven $T_H1$ differentiation. J Allergy Clin Immunol. **2017**; 140(1):294–298.

254. Gill MA, Liu AH, Calatroni A, et al. Enhanced plasmacytoid dendritic cell antiviral responses after omalizumab. J Allergy Clin Immunol. **2018**; 141(5):1735–1743.

255. Henault J, Riggs JM, Karnell JL, et al. Self-reactive IgE exacerbates interferon responses associated with autoimmunity. Nat Immunol. **2016**; 17(2):196–203.

256. Dallari S, Macal M, Loureiro ME, et al. Src family kinases Fyn and Lyn are constitutively activated and mediate plasmacytoid dendritic cell responses. Nat Commun. **2017**; 8:14830.

257. Kennedy JL, Shaker M, McMeen V, et al. Comparison of viral load in individuals with and without asthma during infections with rhinovirus. Am J Respir Crit Care Med. **2014**; 189(5):532–539.

258. Boguniewicz M, Schneider LC, Milgrom H, et al. Treatment of steroid-dependent asthma with recombinant interferon-γ. Clin Exp Allergy. **1993**; 23:785–790.

259. Boguniewicz M, Martin RJ, Martin D, et al. The effects of nebulized recombinant interferon-γ in asthmatic airways. J Allergy Clin Immunol. **1995**; 95(1):133–135.

260. Patel DA, You Y, Huang G, et al. Interferon response and respiratory virus control are preserved in bronchial epithelial cells in asthma. J Allergy Clin Immunol. **2014**; 134(6):1402–1412.

261. DeMore JP, Weisshaar EH, Vrtis RF, et al. Similar colds in subjects with allergic asthma and nonatopic subjects after inoculation with rhinovirus-16. J Allergy Clin Immunol. **2009**; 124(2):245–252.

262. Fleming HE, Little FF, Schnurr D, et al. Rhinovirus-16 colds in healthy and in asthmatic subjects: Similar changes in upper and lower airways. Am J Respir Crit Care Med. **1999**; 160:100–108.

263. Bullens DMA, Decraene A, Dilissen E, et al. Type III IFN-λ mRNA expression in sputum of adult and school-aged asthmatics. Clin Exp Allergy. **2008**; 38:1459–1467.

264. da Silva J, Hilzendeger C, Moermans C, et al. Raised interferon-β, type III interferon and interferon-stimulated genes: Evidence of innate immune activation in neutrophilic asthma. Clin Exp Allergy. **2016**; 47:313–323.

265. Brown V, Warke TJ, Shields MD, Ennis M. T cell cytokine profiles in childhood asthma. Thorax. **2003**; 58:311–316.

266. Schwantes EA, Manthei DM, Denlinger LC, et al. Interferon gene expression in sputum cells correlates with the Asthma Index Score during virus-induced exacerbations. Clin Exp Allergy. **2014**; 44:813–821.

267. Altman MC, Reeves SR, Parker AR, et al. Interferon response to respiratory syncytial virus by bronchial epithelium from children with asthma is inversely correlated with pulmonary function. J Allergy Clin Immunol. **2018**; 142(2):451–459.

268. Zhu J, Message SD, Mallia P, et al. Bronchial mucosal IFN-α/β and pattern recognition receptor expression in patients with experimental rhinovirus-induced asthma exacerbations. J Allergy Clin Immunol. **2018**; In Press.

269. Hansel TT, Tunstall T, Trujillo-Torralbo M-B, et al. A comprehensive evaluation of nasal and bronchial cytokines and chemokines following experimental rhinovirus infection in allergic asthma: Increased interferons (IFN-γ and IFN-λ) and type 2 inflammation (IL-5 and IL-13). EBioMedicine. **2017**; 19:128–138.

270. Custovic A, Belgrave D, Lin L, et al. Cytokine responses to rhinovirus and development of asthma, allergic sensitization and respiratory infections during childhood. Am J Respir Crit Care Med. **2018**; 197(10):1265–1274.

271. Register RB, Uncapher CR, Naylor AM, Lineberger DW, Colonno RJ. Human-murine chimeras of ICAM-1 identify amino acid residues critical for rhinovirus and antibody binding. J Virol. **1991**; 65(12):6589–6596.

272. Bartlett NW, Singanayagam A, Johnston SL. Mouse models of rhinovirus infection and airways disease. Rhinoviruses: Methods and protocols. p. 181–188.

273. Kumar RK, Herbert C, Foster PS. Mouse models of acute exacerbations of allergic asthma. Respirology. **2016**; 21:842–849.

274. Aun M, Bonamichi-Santos R, Arantes-Costa FM, Kalil J, Giavina-Bianchi P. Animal models of asthma: Utility and limitations. J Asthma Allergy. **2017**; 10:293–301.

275. Cate TR, Couch RB, Johnson KM. Studies with rhinoviruses in volunteers: Production of illness, effect of naturallly acquired antibody, and demonstration of a protective effect not associated with serum antibody. J Clin Invest. **1964**; 43(1):56–67.

276. Douglas Jr RG, Cate TR, Gerone PJ, Couch RB. Quantitative rhinovirus sheddding patterns in volunteers. Am Rev Respir Dis. **1965**; 94(2):159–167.

277. Cate TR, Rossen RD, Douglas Jr RG, Butler WT, Couch RB. The role of nasal secretion and serum antibody in the rhinovirus common cold. Am J Epidemiol. **1966**; 84(2):352–363.

278. Louie JK, Yagi S, Nelson FA, et al. Rhinovirus outbreak in a long term care facility for elderly persons associated with unusually high mortality. Clin Infect Dis. **2005**; 41(2):262–265.

279. Heymann PW, Kennedy JL. Rhinovirus-induced asthma exacerbations during childhood: The importance of understanding the atopic status of the host. J Allergy Clin Immunol. **2012**; 130(6):1315–1316.

280. Glanville N, Johnston SL. Challenges in developing a cross-serotype rhinovirus vaccine. Curr Opin Virol. **2015**; 11:83–88.

281. Conant RM, Hamparian V V. Rhinoviruses: Basis for a numbering system. II. Serologic characterization of prototype strains. J Immunol. **1968**; 100(1):114–119.

282. Hogan RJ, Zhong W, Usherwood EJ, Cookenham T, Roberts AD, Woodland DL. Protection from respiratory virus infections can be mediated by antigen-specific $CD4^+$ T cells that persist in the lungs. J Exp Med. **2001**; 193(8):981–986.

283. Ge X, Tan V, Bollyky PL, Standifer NE, James EA, Kwok WW. Assessment of seasonal influenza A virus-specific CD4 T-cell responses to 2009 pandemic H1N1 swine-origin influenza A virus. J Virol. **2010**; 84(7):3312–3319.

284. The Uniprot Consortium. Activities at the Universal Protein Resource (UniProt). Nucleic Acids Res. **2014**; 42:D191–D198.

285. Novak EJ, Liu AW, Gebe JA, et al. Tetramer-guided epitope mapping: Rapid identification and characterization of immunodominant $CD4^+$ T cell epitopes from complex antigens. J Immunol. **2001**; 166(11):6665–6670.

286. Danke NA, Koelle DM, Yee C, Beheray S, Kwok WW. Autoreactive T cells in healthy individuals. J Immunol. **2004**; 172(10):5967–5972.

287. Kwok WW, Roti M, DeLong JH, et al. Direct *ex vivo* analysis of allergen-specific $CD4^+$ T cells. J Allergy Clin Immunol. **2010**; 125(6):1407–1409.

288. Altschul SF, Gish W, Miller W, Myers EW, Lipman DJ. Basic Local Alignment Search Tool. J Mol Biol. **1990**; 215:403–410.

289. Waterhouse AM, Procter JB, Martin DMA, Clamp M, Barton GJ. Jalview Version 2: A multiple sequence alignment editor and analysis workbench. Bioinformatics. **2009**; 25(9):1189–1191.

290. Wang P, Sidney J, Kim Y, et al. Peptide binding predictions for HLA DR, DP and DQ molecules. BMC Bioinformatics. **2010**; 11:568.

291. Wang P, Sidney J, Dow C, Mothé B, Sette A, Peters B. A systematic assessment of MHC class II peptide binding predictions and evaluation of a consensus approach. PLOS Comput Biol. **2008**; 4(4):e1000048.

292. Nielsen M, Lundegaard C, Lund O. Prediction of MHC class II binding affinity using SMM-align, a novel stabilization matrix alignment method. BMC Bioinformatics. **2007**; 8:238.

293. Nielsen M, Lund O. NN-align. An artificial neural network-based alignment algorithm for MHC class II peptide binding prediction. BMC Bioinformatics. **2009**; 10:296.

294. Sturniolo T, Bono E, Ding J, et al. Generation of tissue-specific and promiscuous HLA ligand databases using DNA microarrays and virtual HLA class II matrices. Nat Biotechnol. **1999**; 17(6):555–561.

295. Zhang GL, DeLuca DS, Keskin DB, et al. MULTIPRED2: A computational system for large-scale identification of peptides predicted to bind to HLA supertypes and alleles. J Immunol Methods. **2011**; 374:53–61.

296. Karosiene E, Rasmussen M, Blicher T, Lund O, Buus S, Nielsen M. NetMHCIIpan-3.0, a common pan-specific MHC class II prediction method including all three human MHC class II isotypes, HLA-DR, HLA-DP and HLA-DQ. Immunogenetics. **2013**; 65(10):711–724.

297. Nielsen M, Lundegaard C, Blicher T, et al. NetMHCpan, a method for quantitative predictions of peptide binding to any HLA-A and -B locus protein of known sequence. PLOS One. **2007**; 2(8):e796.

298. Hoof I, Peters B, Sidney J, et al. NetMHCpan, a method for MHC class I binding prediction beyond humans. Immunogenetics. **2009**; 61:1–13.

299. DeLano W. The PyMOL molecular graphics system. San Carlos, CA: DeLano Scientific; **2002**.

300. Hadfield AT, Lee WM, Zhao R, et al. The refined structure of human rhinovirus 16 at 2.15 A resolution: Implications for the viral life cycle. Structure. **1997**; 5(3):427–441.

301. Roederer M, Nozzi JL, Nason MC. SPICE: Exploration and analysis of post-cytometric complex multivariate datasets. Cytometry A. **2011**; 79A:167–174.

302. McIntyre CL, Knowles NJ, Simmonds P. Proposals for the classification of human rhinovirus species A, B and C into genotypically assigned types. J Gen Virol. **2013**; 94:1791–1806.

303. Colonno RJ, Condra JH, Mizutani S, Callahan PL, Davies ME, Murcko MA. Evidence for the direct involvement of the rhinovirus canyon in receptor binding. PNAS. **1988**; 85:5449–5453.

304. Olson NH, Kolatkar PR, Oliveira MA, et al. Structure of a human rhinovirus complexed with its receptor molecule. PNAS. **1993**; 90:507–511.

305. Oliveira M, Zhao R, Lee W, Kremer M. The structure of human rhinovirus 16. Structure. **1993**; 1(1):51–68.

306. Mahon BP, Katrak K, Nomoto A, Macadam AJ, Minor PD, Mills KHG. Poliovirus-specific $CD4^+$ $T_H1$ clones with both cytotoxic and helper activity mediate protective humoral immunity against a lethal poliovirus infection in transgenic mice expressing the human poliovirus receptor. J Exp Med. **1995**; 181:1285–1292.

307. Morita R, Schmitt N, Bentebibel S-E, et al. Human blood $CXCR5^+CD4^+$ T cells are counterparts of T follicular cells and contain specific subsets that differentially support antibody secretion. Immunity. **2011**; 34:108–121.

308. Crotty S. Follicular helper CD4 T cells ($T_{FH}$). Annu Rev Immunol. **2011**; 29:621–663.

309. Yang J, James EA, Huston L, Danke NA, Liu AW, Kwok WW. Multiplex mapping of CD4 T cell epitopes using class II tetramers. Clin Immunol. **2006**; 120:21–32.

310. Yang J, James EA, Sanda S, Greenbaum C, Kwok WW. $CD4^+$ T cells recognize diverse epitopes within GAD65: Implications for repertoire development and diabetes monitoring. Immunology. **2013**; 138(3):269–279.

311. Woodfolk JA, Sung SS, Benjamin DC, Lee JK, Platts-Mills TAE. Distinct human T cell repertoires mediate immediate and delayed-type hypersensitivity to the Trichophyton antigen, Tri r 2. J Immunol. **2000**; 165:4379–4387.

312. Gaido CM, Stone S, Chopra A, Thomas WR, Le Souëf PN, Hales BJ. Immunodominant T-cell epitopes in the VP1 capsid protein of rhinovirus species A and C. J Virol. **2016**; 90(23):10459–10471.

313. James EA, LaFond RE, Gates TJ, Mai DT, Malhotra U, Kwok WW. Yellow fever vaccination elicits broad functional $CD4^+$ T cell responses that recognize structural and nonstructural proteins. J Virol. **2013**; 87(23):12794–12804.

314. Su LF, Kidd BA, Han A, Kotzin JJ, Davis MM. Virus-specific $CD4^+$ memory-phenotype T cells are abundant in unexposed adults. Immunity. **2013**; 38(2):373–383.

315. Kistler AL, Webster DR, Rouskin S, et al. Genome-wide diversity and selective pressure in the human rhinovirus. Virol J. **2007**; 4:40.

316. Panjwani A, Strauss M, Gold S, et al. Capsid protein VP4 of human rhinovirus induces membrane permeability by the formation of a size-selective multimeric pore. PLOS Pathog. **2014**; 10(8):e1004294.

317. Hastings GZ, Rowlands DJ, Francis MJ. Proliferative responses of T cells primed against human rhinovirus to other rhinovirus serotypes. J Gen Virol. **1991**; 72:2947–2952.

318. West NP, Horn PL, Pyne DB, et al. Probiotic supplementation for respiratory and gastrointestinal illness symptoms in healthy physically active individuals. Clin Nutr. **2014**; 33:581–587.

319. Turner RB, Woodfolk JA, Borish L, et al. Effect of probiotic on innate inflammatory response and viral shedding in experimental rhinovirus infection – A randomised controlled trial. Benef Microbes. **2017**; 8(2):207–215.

320. Shekhar K, Brodin P, Davis MM, Chakraborty AK. Automatic Classification of Cellular Expression by Nonlinear Stochastic Embedding (ACCENSE). PNAS. **2014**; 111(1):202–207.

321. Amir ED, Davis KL, Tadmor MD, et al. viSNE enables visualization of high dimensional single-cell data and reveals phenotypic heterogeneity of leukemia. Nat Biotechnol. **2013**; 31(6):545–552.

322. West NP, Horn PL, Pyne DB, et al. Probiotic supplementation has little effect on peripheral blood regulatory T-cells. J Allergy Clin Immunol. **2016**; 138(6):1749–1752.

323. Kohlmeier JE, Miller SC, Smith J, et al. The chemokine receptor CCR5 plays a key role in the early memory $CD8^+$ T cell response to respiratory virus infections. Immunity. **2008**; 29:101–113.

324. Galkina E, Thatte J, Dabak V, Williams MB, Ley K, Braciale TJ. Preferential migration of effector $CD8^+$ T cells into the interstitium of the normal lung. J Clin Invest. **2005**; 115(12):3473–3483.

325. Booth V, Keizer DW, Kamphuis MB, Clark-Lewis I, Sykes BD. The CXCR3 binding chemokine IP-10/CXCL10: Structure and receptor interactions. Biochemistry. **2002**; 41(33):10418–10425.

326. Loetscher M, Loetscher P, Brass N, Meese E, Moser B. Lymphocyte-specific chemokine receptor CXCR3: Regulation, chemokine binding and gene localization. Eur J Immunol. **1998**; 28:3696–3705.

327. Ukena SN, Velaga S, Goudeva L, et al. Human regulatory T cells of G-CSF mobilized allogeneic stem cell donors qualify for clinical application. PLOS One. **2012**; 7(12):e51644.

328. McLoughlin RM, Jenkins BJ, Grail D, et al. IL-6 trans-signaling via STAT3 directs T cell infiltration in acute inflammation. PNAS. **2005**; 102(27):9589–9594.

329. Blanpain C, Migeotte I, Lee B, et al. CCR5 binds multiple CC-chemokines: MCP-3 acts as a natural antagonist. Blood. **1999**; 94(6):1899–1905.

330. Turner RB, Weingand KW, Yeh CH, Leedy DW. Association between interleukin-8 concentration in nasal secretions and severity of symptoms of experimental rhinovirus colds. Clin Infect Dis. **1998**; 26:840–846.

331. West NP, Horn PL, Barrett S, et al. Supplementation with a single and double strain probiotic on the innate immune system for respiratory illness. ESPEN J. **2014**; 9:e178–e184.

332. Teijaro JR, Verhoeven D, Page CA, Turner D, Farber DL. Memory CD4 T cells direct protective responses to influenza virus in the lungs through helper-independent mechanisms. J Virol. **2010**; 84(18):9217–9226.

333. Uller L, Leino M, Bedke N, et al. Double-stranded RNA induces disproportionate expression of thymic stromal lymphopoietin versus interferon-β in bronchial epithelial cells from donors with asthma. Thorax. **2010**; 65:626–632.

334. Jackson DJ, Makrinioti H, Rana BMJ, et al. IL-33–dependent type 2 inflammation during rhinovirus-induced asthma exacerbations *in vivo*. Am J Respir Crit Care Med. **2014**; 190(12):1373–1382.

335. Yao S, Jiang L, Moser EK, et al. Control of pathogenic effector T-cell activities *in situ* by PD-L1 expression on respiratory inflammatory dendritic cells during respiratory syncytial virus infection. Mucosal Immunol. **2015**; 8(4):746–759.

336. Wisniewski JA, Muehling LM, Eccles JD, et al. $T_H1$ signatures are present in the lower airways of children with severe asthma, regardless of allergic status. J Allergy Clin Immunol. **2018**; 141(6):2048–2060.

337. National Heart Lung and Blood Institution. National Asthma Education and Prevention Program Expert Panel Report 3: Guidelines for the diagnosis and management of asthma. **2007**; 08-5846.

338. Gibson SJ, Lindh JM, Riter TR, et al. Plasmacytoid dendritic cells produce cytokines and mature in response to the TLR7 agonists, imiquimod and resiquimod. Cell Immunol. **2002**; 218:74–86.

339. Jego G, Palucka AK, Blanck J-P, Chalouni C, Pascual V, Banchereau J. Plasmacytoid dendritic cells induce plasma cell differentiation through type I interferon and interleukin 6. Immunity. **2003**; 19:225–234.

340. Cella M, Jarrossay D, Facchetti F, et al. Plasmacytoid monocytes migrate to inflamed lymph nodes and produce large amounts of type I interferon. Nat Med. **1999**; 5(8):919–923.

341. Yeon S, Halim L, Chandele A, et al. IL-7 plays a critical role for the homeostasis of allergen-specific memory CD4 T cells in the lung and airways. Sci Rep. **2017**; 7:11155.

342. Di Genova G, Savelyeva N, Suchacki A, Thirdborough SM, Stevenson FK. Bystander stimulation of activated $CD4^+$ T cells of unrelated specificity following a booster vaccination with tetanus toxoid. Eur J Immunol. **2010**; 40:976–985.

343. Boyman O. Bystander activation of $CD4^+$ T cells. Eur J Immunol. **2010**; 40:936–939.

344. Sallusto F, Lanzavecchia A. Understanding dendritic cell and T-lymphocyte traffic through the analysis of chemokine receptor expression. Immunol Rev. **2000**; 177:134–140.

345. van Panhuys N, Klauschen F, Germain RN. T cell receptor-dependent signal intensity dominantly controls $CD4^+$ T cell polarization *in vivo*. Immunity. **2014**; 41:63–74.

346. Berings M, Gevaert P, De Ruyck N, et al. FcεRI expression and IgE binding by dendritic cells and basophils in allergic rhinitis and upon allergen immunotherapy. Clin Exp Allergy. **2018**; 48:970–980.

347. Baumann C, Bonilla W V., Fröhlich A, et al. T-bet- and STAT4-dependent IL-33 receptor expression directly promotes antiviral $T_H1$ cell responses. PNAS. **2015**; 112(13):4056–4061.

348. Bendall SC, Nolan GP, Roederer M, Chattopadhyay PK. A deep profiler's guide to cytometry. Trends Immunol. **2012**; 33(7):323–332.

349. Rubtsova K, Rubtsov A V, van Dyk LF, Kappler JW, Marrack P. T-box transcription factor T-bet, a key player in a unique type of B-cell activation essential for effective viral clearance. PNAS. **2013**; 110(34):E3216–E3224.

350. Barnett BE, Staupe RP, Odorizzi PM, et al. B cell-intrinsic T-bet expression is required to control chronic viral infection. J Immunol. **2016**; 197:10717–1022.

351. Krug N, Erpenbeck VJ, Balke K, et al. Cytokine profile of bronchoalveolar lavage-derived $CD4^+$, $CD8^+$, and γδ T cells in people with asthma after segmental allergen challenge. Am J Respir Cell Mol Biol. **2001**; 25:125–131.

352. Hamzaoui A, Kahan A, Ayed K, Hamzaoui K. T cells expressing the γδ receptor are essential for $T_H2$-mediated inflammation in patients with acute exacerbation of asthma. Mediat Inflamm. **2002**; 11:113–119.

353. Spinozzi F, Agea E, Bistoni O, et al. Increased allergen-specific, steroid-sensitive γδ T cells in bronchoalveolar lavage fluid from patients with asthma. Ann Intern Med. **1996**; 124:223–227.

354. Murdoch JR, Gregory LG, Lloyd CM. γδT cells regulate chronic airway inflammation and development of airway remodelling. Clin Exp Allergy. **2014**; 44:1386–1398.

355. Glanville N, Message SD, Walton RP, et al. γδT cells suppress inflammation and disease during rhinovirus-induced asthma exacerbations. Mucosal Immunol. **2013**; 6(6):1091–1100.

356. Tamura-Yamashita K, Endo J, Isogai S, Matsuoka K, Yonekawa H, Yoshizawa Y. γδ T cell is essential for allergen-induced late asthmatic response in a murine model of asthma. J Med Dent Sci. **2008**; 55:113–120.

357. Komai-Koma M, Wang E, Kurowska-Stolarska M, Li D, McSharry C, Xu D. Interleukin-33 promoting $T_H1$ lymphocyte differentiation dependents on IL-12. Immunobiology. **2016**; 221:412–417.

358. Smithgall MD, Comeau MR, Park Yoon BR, Kaufman D, Armitage R, Smith DE. IL-33 amplifies both $T_H1$- and $T_H2$-type responses through its activity on human basophils, allergen-reactive $T_H2$ cells, iNKT and NK Cells. Int Immunol. **2008**; 20(8):1019–1030.

359. Cox L, Platts-Mills TAE, Finegold I, Schwartz LB, Simons FER, Wallace D V. American Academy of Allergy, Asthma & Immunology/American College of Allergy, Asthma and Immunology Joint Task Force Report on omalizumab-associated anaphylaxis. J Allergy Clin Immunol. **2007**; 120(6):1373–1377.

360. Nathan RA, Sorkness CA, Kosinski M, et al. Development of the Asthma Control Test: A survey for assessing asthma control. J Allergy Clin Immunol. **2004**; 113(1):59–65.

361. Pendharkar S, Mehta S. The clinical significance of exhaled nitric oxide in asthma. Can Respir J. **2008**; 15(2):99–106.

362. Miller CWT, Krishnaswamy N, Johnston C, Krishnaswamy G. Severe asthma and the omalizumab option. Clin Mol Allergy. **2008**; 6:4.

363. Rose NR. The adjuvant effect in infection and autoimmunity. Clin Rev Allergy Immunol. **2008**; 34:279–282.